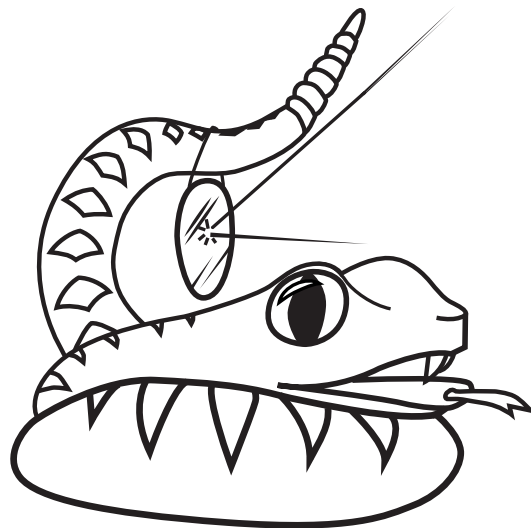


RATTLESNAKE NANOACTUATOR

A PRECISION HIGH SPEED CLOSED LOOP LINEAR
ACTUATOR WITH CAPACITIVE SENSOR

JONATHAN LOCK



Master's Thesis
Department of Microtechnology and Nanoscience
CHALMERS UNIVERSITY OF TECHNOLOGY
SE-412 96 Gothenburg, Sweden August 2011

Jonathan Lock: *Rattlesnake Nanoactuator*, A precision high speed closed loop linear actuator with capacitive sensor, August 2011.

Department of Microtechnology and Nanoscience
Chalmers University of Technology
SE-412 96 Göteborg, Sweden
Telephone 046 (0)31 772 1000

Copyright ©2011 Jonathan Lock. Permission is granted to copy, distribute and/or modify this document under the terms of the GNU Free Documentation License, Version 1.3 or any later version published by the Free Software Foundation; with no Invariant Sections, no Front-Cover Texts, and no Back-Cover Texts. A copy of the license is included in the section entitled "GNU Free Documentation License".

FRONT COVER ILLUSTRATION: The graphic on the cover is a rattlesnake with a suspended mirror, alluding to a device driving a moving payload quickly.

ABSTRACT

This thesis describes the development of a novel linear actuator based on a closed loop tightly integrated magnetic motor and capacitive sensor. Mechanical, electrical and software work has resulted in a device achieving a mechanical range of travel of $\pm 1\text{mm}$ with a steady state RMS error of 62nm at a closed loop bandwidth of 3.5kHz , a typical tracking error of hundreds of nanometers (dependent on the waveform shape) and a maximum error in the range of $1 - 10\mu\text{m}$. The stiffness of the system at 10Hz is $4\text{N}/\mu\text{m}$ and the actuator has a useful range of motion up to $300 - 500\text{Hz}$ with reduced travel at these speeds due to force limitations. This is possibly an area of continued work; minor modifications could lead to an RMS error of $\approx 20\text{nm}$, making it possible to outperform piezoelectric actuators in some applications such as adaptive optics or interferometry.

SAMMANFATTNING

Den här rapporten beskriver utvecklingen av en linjärmotor med ett slutet reglersystem där motorn är nära ihopkopplad med en kapacitiv lägesgivare. Arbete inom mekanik, elektronik och mjukvara har skett och resulterade i en enhet med en mekanisk slaglängd på $\pm 1\text{mm}$ med ett steady-state RMS fel på 62nm vid en sluten bandbredd på 3.5kHz , ett typiskt reglerfel på ett hundratal nanometer (beroende på utformningen av borsvärdevågformen) och ett maximalt fel inom området $1 - 10\mu\text{m}$. Systemets styvhet vid 10Hz är $4\text{mN}/\text{nm}$ och motorn har ett arbetsområde på upp till $300 - 500\text{Hz}$, men då med ett begränsat utslag på grund av kraftbegränsningar. Resultaten ger styrka åt möjligheten till framtida arbete med denna typ av linjärmotor, några kända mindre ändringar skulle uppskattningsvis leda till ett RMS fel på $\approx 20\text{nm}$, vilket möjliggör bättre prestanda än piezoelektriska motorer inom vissa områden som t.ex. adaptiv optik eller interferometri.

PREFACE

This thesis is based on studies done during January 2011 to August 2011 at the department of Microtechnology and Nanoscience, Chalmers University of Technology, Gothenburg Sweden.

My greatest thanks go out to Magnus Karlsson, my Professor at Chalmers who has been of great help with proofreading the thesis as well as sorting out the requirements from Chalmers; Tomas Lock, my father and supervisor who has helped define the project as well as assistance with several design details and sponsoring component costs; Hans Hjelmgren, head of the Wireless and Photonics Master's program, who helped with getting the thesis accepted and registered with Chalmers; Carl-Magnus Kihlman, who generously granted access to MC2's mechanical workshop and supplied much-needed advice related to precision machining; Mikroponent AB, who generously sponsored the flexures used in the actuator; Max Sikström, without whose help the embedded program code would be nowhere near as effective and clean; Andreas Henriksson and Anton Landberg, for respectively drawing and vectorizing the mascot of the project as seen on the title page; Deitra Sawh and Katie Sharp, who greatly helped with proofreading and editing this document; ETA (Elektrosektionens Teletekniska Avdelning) whose instruments and food provided the measurement capabilities and sustenance needed to work on the implementation of the actuator; on a personal note I would also like to thank Johannes and Berit Lock, my brother and mother for their personal support throughout the process.

Jonathan Lock, August 2011

CONTENTS

I INTRODUCTION	1
1 INTRODUCTION	3
1.1 Introduction	3
1.2 Existing topologies	3
1.3 Key parameters	5
1.4 Possible uses	6
1.5 Scope of thesis	6
1.6 Thesis structure	8
1.7 License	8
II BACKGROUND	9
2 BACKGROUND	11
2.1 Capacitive sensing	11
2.2 Magnetic motors	12
2.3 Mechanical stress	12
III TOPOLOGY	15
3 TOPOLOGY	17
3.1 System-level topology	17
3.2 Mechanical structure	17
3.3 Electrical structure	21
3.4 Software structure	30
IV IMPLEMENTATION	33
4 IMPLEMENTATION	35
4.1 Mechanical implementation	35
4.2 Electrical implementation	37
4.3 Software implementation	54
V RESULTS	57
5 RESULTS	59
5.1 Waveform tests	60
5.2 System characterization	88
VI CONCLUSION	93
6 FUTURE IMPROVEMENTS	95
7 CONCLUSION	97
BIBLIOGRAPHY	99
VII APPENDIX	103
A MECHANICS	105
A.1 Individual parts	105

A.2	Assembled views	116
B	ELECTRICAL	119
B.1	Capacitive sensor	119
B.2	Controller	123
B.3	Demodulator	131
B.4	Digital board	135
B.5	Excitation control	149
B.6	Motor drive	151
B.7	Power supply	155
C	SOFTWARE	161
C.1	Microprocessor software	161
C.2	Matlab demo application	162
D	GNU FREE DOCUMENTATION LICENSE	179
D.1	PREAMBLE	179
D.2	APPLICABILITY AND DEFINITIONS	179
D.3	VERBATIM COPYING	181
D.4	COPYING IN QUANTITY	181
D.5	MODIFICATIONS	182
D.6	COMBINING DOCUMENTS	184
D.7	COLLECTIONS OF DOCUMENTS	185
D.8	AGGREGATION WITH INDEPENDENT WORKS	185
D.9	TRANSLATION	185
D.10	TERMINATION	186
D.11	FUTURE REVISIONS OF THIS LICENSE	186
D.12	RELICENSING	187
D.13	ADDENDUM: How to use this License for your documents	187

LIST OF FIGURES

Figure 1	Common topologies for precision actuators. . .	4
Figure 2	System-level topology of the actuator, illustrating the core blocks in the system and their interconnections.	18
Figure 3	Cutaway view of mechanical structure of actuator with motor and actuator visible, various supporting structures hidden.	18
Figure 4	Simulation of the magnetic current and flux density for various positions in a radial-symmetric 2D representation. In all images the magnet is to the left, the reversed E shape is the magnetic conductor and coils fill the “empty” zones in the magnetic conductor. The four images illustrate from left to right and top to bottom; centered magnet, no current in coil; centered magnet, current in coil; offset magnet, no current in coil; offset magnet, current in coil.	20
Figure 5	Qualitative estimate of the steady-state magnet position as function of coil current for a constant spring load.	20
Figure 6	Stress simulation of the flexure illustrating stress levels, total displacement and a 3D representation of the displacement.	22
Figure 7	Block diagram of sensor electric topology, from excitation to output waveform.	23
Figure 8	Stylized image of a contactless capacitive position sensor using two reference electrodes. The “Sense pickup” block can move relative to the reference blocks, causing the capacitances C_B and C_A to vary linearly with position, as per equation 2.1.	23
Figure 9	Input and output waveform for two different positions from capacitive sensor assuming ideal components and no fringe-fields. Output 1 corresponds to the sensor not being in the center of the travel range, whereas Output 2 corresponds to the sensor being in the middle of the travel range.	25
Figure 10	Effects of stray capacitive coupling and fringe fields on sensor.	26

Figure 11	Adding an active guard to the capacitive sensor reduces the effects of fringing and stray capacitance.	27
Figure 12	Block diagram of the controller electronics, showing the signal pathway from demodulator to motor drive.	29
Figure 13	Block diagram of key parts of the microprocessor structure.	30
Figure 14	Cross section view of the implementation of the actuator with supporting structure visible. . . .	36
Figure 15	Photograph of implementation of actuator, with visible central rod, payload, flexure and supporting structure.	37
Figure 16	Photograph of front side of implementation of controller with connectors to actuator visible and functionality marked.	38
Figure 17	Simplified schematic of capacitive sensor, with some component blocks removed.	39
Figure 18	Motor coil model and relative impedance. . . .	41
Figure 19	Photograph of internals of controller implementation, with printed circuit board (PCB)'s visible and functionality marked.	43
Figure 20	Simplified schematic of the power supply block which supplies power rails and reference voltages for all of the other components.	44
Figure 21	Simplified schematic of the excitation block which generates the reference waveforms for the capacitive sensor.	46
Figure 22	Simplified schematic of the demodulator block which demultiplexes and samples the output from the capacitive sensor.	47
Figure 23	Simplified schematic of part of the digital block, this portion contains the microprocessor, universal serial bus (USB)/recommended standard 232 (RS232) interface and LCD shift register.	49
Figure 24	Simplified schematic of part of the digital block, this portion contains the analog-digital converter (ADC)s and digital-analog converter (DAC) for reading the current position and setting the linear analog controller's setpoint.	50
Figure 25	Simplified schematic of part of the digital block, this portion contains all electronics to do with the user interface, such as the LCD display, rotary input dial and joystick.	51

Figure 26	Simplified schematic of the analog linear controller block which generates the control signal to the motor drive.	52
Figure 27	Simplified schematic of the motor drive block which drives the motor for the actuator.	55
Figure 28	Zero setpoint, showing the RMS error of 62nm and a constant offset.	61
Figure 29	Position measurement for square wave setpoint.	62
Figure 30	Enlargement of position measurement for square wave setpoint and large-scale motion.	63
Figure 31	Velocity measurement for square wave setpoint.	64
Figure 32	Acceleration measurement for square wave setpoint.	65
Figure 33	Position measurement for triangle wave setpoint.	67
Figure 34	Velocity measurement for triangle wave setpoint.	68
Figure 35	Acceleration measurement for triangle wave setpoint.	69
Figure 36	Position measurement for sine wave setpoint. .	71
Figure 37	Velocity measurement for sine wave setpoint. .	72
Figure 38	Acceleration measurement for sine wave setpoint.	73
Figure 39	Position measurement for polynomial 0 wave setpoint.	75
Figure 40	Velocity measurement for polynomial 0 wave setpoint.	76
Figure 41	Acceleration measurement for polynomial 0 wave setpoint.	77
Figure 42	Position measurement for polynomial 0 wave setpoint, clipping, large scale motion.	78
Figure 43	Velocity measurement for polynomial 0 wave setpoint, clipping, large scale motion.	79
Figure 44	Acceleration measurement for polynomial 0 wave setpoint, clipping, large scale motion.	79
Figure 45	Position measurement for polynomial 1 wave setpoint.	81
Figure 46	Velocity measurement for polynomial 1 wave setpoint.	82
Figure 47	Acceleration measurement for polynomial 1 wave setpoint.	83
Figure 48	Position measurement for polynomial 2 wave setpoint.	85
Figure 49	Velocity measurement for polynomial 2 wave setpoint.	86
Figure 50	Acceleration measurement for polynomial 2 wave setpoint.	87

Figure 51	Open loop bode diagram of the system transfer function (measured at the motor drive interface). Sampled frequencies marked with a dot. The transfer function is V_{out}/V_{in}	88
Figure 52	Measured system stiffness over frequency. Sampled frequencies marked with a dot.	89
Figure 53	Capacitive sensor integral nonlinearity (INL) over position.	90
Figure 54	Holds the motor assembly and conducts heat to the outside of the actuator. Constructed from 6061-T6 aluminum.	105
Figure 55	Covers the bottom of the actuator, limits the throw range of the actuator should an error occur. Constructed from 6061-T6 aluminum.	106
Figure 56	Excitation ring for the capacitive sensor. Constructed from brass.	106
Figure 57	Top of Faraday cage around sensor. Constructed from PCB laminate (FR4 with 35 μ m copper and tin plating).	107
Figure 58	Side of Faraday cage around sensor. Constructed from PCB laminate (FR4 with 35 μ m copper and tin plating).	107
Figure 59	Guard ring for capacitive sensor. Constructed from brass.	108
Figure 60	Electrical isolation for excitation rings for capacitive sensor from actuating rod. Constructed from kapton film.	108
Figure 61	Capacitive sensor sensing ring. Constructed from brass.	109
Figure 62	Placeholder for capacitive sensor PCB, see appendix B for actual shape of PCB.	109
Figure 63	Placeholder for coil used in motor. Constructed from 0.15mm copper enamel wire, with approximately 550 turns.	110
Figure 64	Magnetic flux conductor for motor. Constructed from iron powder toroid, of type Amidon T400A-26.	110
Figure 65	Magnetic flux conductor for motor. Constructed from iron powder toroid, of type Amidon T400A-26.	111
Figure 66	Flexure used for suspension of moving parts of actuator. Constructed from AISI-301 hardened stainless steel.	111

Figure 67	Magnet used for generating force on the actuator. Constructed from N35 Neodymium rare-earth magnet, of type N-0221-1 from Svenska Magnetfabriken AB. This magnet has a specification of $B_r = 1.19 \pm 0.02$ [T] and $iH_C > 955$ [kA/m].	112
Figure 68	Outer ring for holding together actuator. Constructed from 6061-T6 aluminum.	112
Figure 69	Outer ring for holding together actuator. Constructed from 6061-T6 aluminum.	113
Figure 70	Outer ring for holding together actuator. Constructed from 6061-T6 aluminum.	113
Figure 71	Isolation ring for electrically isolating the flexures from the rest of the actuator. Constructed from FR4 laminate.	114
Figure 72	Lock-pin used to limit the throw of the actuator. Constructed from mild steel.	114
Figure 73	Central actuating rod for transmitting force. Constructed from brass.	115
Figure 74	Assembled, colored, cross section view of actuator.	116
Figure 75	Assembled crosshatched cross section view with callouts for part names.	117
Figure 76	Schematic for capacitive sensor.	119
Figure 77	Top layer of PCB for capacitive sensor. Multiple layers of PCB are stacked to build the Faraday cage surrounding the sensitive electronics.	120
Figure 78	Bottom layer of PCB for capacitive sensor. Multiple layers of PCB are stacked to build the Faraday cage surrounding the sensitive electronics.	120
Figure 79	Schematic sheet 1 for controller.	123
Figure 80	Schematic sheet 2 for controller.	124
Figure 81	simulation program with integrated circuit emphasis (SPICE) schematic for slew rate limiter.	125
Figure 82	SPICE ramp response and time derivative of ramp response ($\frac{d}{dt}V_{out}$) for slew rate limiter.	125
Figure 83	SPICE ramp response for slew rate limiter.	126
Figure 84	Top layer of PCB for controller.	126
Figure 85	Bottom layer of PCB for controller.	127
Figure 86	Schematic for demodulator.	131
Figure 87	Top layer of PCB for demodulator.	132
Figure 88	Bottom layer of PCB for demodulator.	133
Figure 89	Schematic for sheet 2 of digital board.	135
Figure 90	Schematic for sheet 3 of digital board.	135
Figure 91	Schematic for sheet 1 of digital board.	136
Figure 92	Schematic for sheet 4 of digital board.	137
Figure 93	Schematic for sheet 5 of digital board.	138
Figure 94	Top layer of PCB for digital board.	139

Figure 95	Bottom layer of PCB for digital board.	140
Figure 96	Schematic for excitation control.	149
Figure 97	Top layer of PCB for excitation control.	149
Figure 98	Bottom layer of PCB for excitation.	149
Figure 99	Schematic for motor drive.	151
Figure 100	Top layer of PCB for motor drive.	152
Figure 101	Bottom layer of PCB for motor drive.	153
Figure 102	Schematic for power supply.	155
Figure 103	Top layer of PCB for power supply.	156
Figure 104	Bottom layer of PCB for power supply.	156

LIST OF TABLES

Table 1	Predetermined values and topologies for the actuator.	7
Table 2	Scalar measured parameters of the system.	60
Table 3	Comparison of developed system and existing solutions.	91
Table 4	Errata for capacitive sensor PCB and schematic.	121
Table 5	Errata for controller PCB and schematic.	127
Table 6	Errata for demodulator PCB and schematic.	133
Table 7	Errata for digital board PCB and schematic.	141
Table 8	Errata for motor drive PCB and schematic.	153
Table 9	Errata for motor drive PCB and schematic.	156

ACRONYMS

STM	scanning tunneling microscopy
AF	autofocus
ADC	analog-digital converter
DAC	digital-analog converter
PID	proportional integral derivative
FIFO	first in first out

USB	universal serial bus
RS232	recommended standard 232
PCB	printed circuit board
OPAMP	operational amplifier
MOSFET	metal-oxide-semiconductor field-effect transistor
GBW	gain-bandwidth product
RF	radio-frequency
ESD	electrostatic discharge
RISC	reduced instruction set computing
RAM	random access memory
USART	universal asynchronous receiver/transmitter
IC	integrated circuit
I/O	input/output
SPICE	simulation program with integrated circuit emphasis
NTC	negative temperature coefficient
INL	integral nonlinearity
SNR	signal to noise ratio
FPGA	field-programmable gate array
GCC	GNU C compiler
AVRDUDE	AVR downloader uploader
ISPMKii	in system programmer mark ii

Part I

INTRODUCTION

INTRODUCTION

This section describes the scientific background of this thesis, Rattlesnake Nanoactuator¹, the key parameters for the developed actuator, a brief comparison with existing solutions as well as the scope and structure of the thesis.

1.1 INTRODUCTION

High-precision linear actuators² have a remarkably wide range of applications in both research and industrial environments. Movement and cost scale from scanning tunneling microscopy (STM), with motion in the sub-nanometer range, though with a range of travel often only in the range of hundreds to few thousands of nanometers (DME-SPM [9]) to optical autofocus (AF) and beam deflection systems with wildly ranging accuracies, though often spanning a range of accuracy of hundreds of nanometers and travel in the millimeter scale (eg. Thorlabs AB [16]). The goal of this thesis is to develop and test a new type of linear actuator with a closely integrated motor and sensor that allows for high-speed closed loop operation, with a travel range on the order of millimeters and as high a resolution as possible.

1.2 EXISTING TOPOLOGIES

There exist many different types of actuators in the same order of magnitude of specifications, most can be divided into a number of subgroups (see figure 1 on the following page);

PIEZOELECTRIC A piezoelectric actuator uses a material with a piezoelectric effect which causes a change in mechanical dimensions upon applied electric field. Commonly used materials have a change of length around 0.1% of the total length. Typically several piezoelectric discs are stacked on each other to give a larger travel at lower voltages. There is some residual hysteresis when applying an alternating electric field, necessitating a closed-loop system when high accuracy is required (Choi and Han [8]).

DIRECT DRIVE Direct-drive piezoelectric actuators typically use stacked piezoelectric discs to directly control the position

¹ Named so to create a mental image of a rattlesnake's tail, which rapidly moves back and forth as illustrated on the front page.

² A linear actuator is a mechanical device that, loosely defined, creates a linear motion (i.e. one dimensional) without any type of mechanical transmission - the linear motion is intrinsic to the design of the actuator (Lindström et al. [10]).

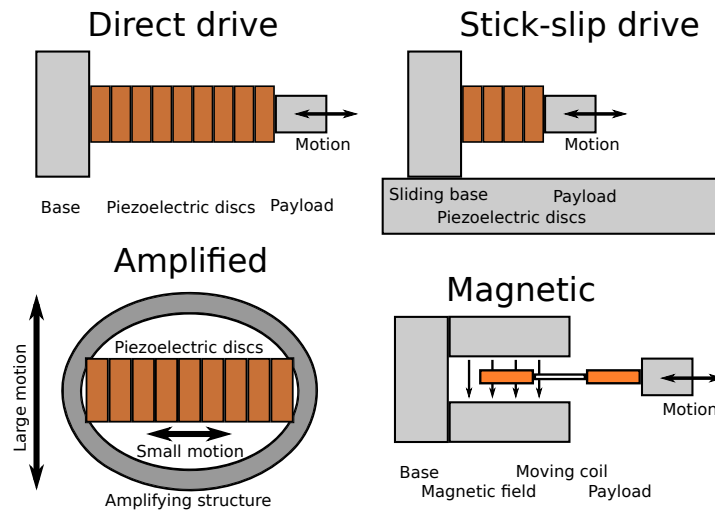


Figure 1: Common topologies for precision actuators.

of the payload. Benefits of this approach are very high resolution (often sub-nanometer) and system stiffness, though at cost of very limited travel (on the range of hundreds of nanometers) (Choi and Han [8]).

SLIP-STICK A slip-stick drive utilizes the difference in static and dynamic friction between two bases and the high acceleration that can be achieved with a piezoelectric actuator to slowly “inchworm” the payload in the desired direction. This reduces the limited travel problem associated with a direct-drive approach, however at cost of very slow rough movement and low maximum applied force (as the payload would simply slide if too large a force is applied) (Choi and Han [8]).

AMPLIFIED STRUCTURE A mechanical structure designed to amplify a small range of motion in one direction to a larger range of motion in another gives the amplified piezoelectric structure large throw and high static force. However the large structure will tend to give a relatively “weak” system, with a low stiffness ($[m/N]$) (Choi and Han [8]).

MAGNETIC DRIVE A magnetic actuator uses changing magnetic fields to apply a force to a magnet or coil in order to move a payload, following Lenz’s law (Cheng [7]). Depending on the structure chosen this allows for a potentially much larger travel range, though as the magnetic actuator can only apply a force some type of closed loop system must be implemented to maintain a desired position (Brauer [5]).

All of these different topologies offer their own strengths and weaknesses. Piezoelectric designs offer great resolution and high stiffness. This is at the cost of low travel and hysteresis in the applied voltage

and resulting position requiring some type of closed loop control for high-accuracy systems. Though various methods exist for increasing the travel of the payload these come at the cost of either reduced system stiffness or slow large-scale motion and low applied force for an amplified and stick-slip topology respectively. A magnetic actuator offers far larger ranges of travel, with force limited only by the permissible magnetic flux. However as the output from the magnetic actuator is force (rather than position) a high-speed controller must be used with some type of sensor to form a closed-loop system to drive the payload to the desired position.

1.3 KEY PARAMETERS

Some key parameters were established before the development of the actuator began, in an attempt to both limit the size of the thesis and scope of the work. Key definitions in the development of the actuator have been;

CLOSED LOOP A closed loop actuator measures its own current position and generates a motor force to counteract any external forces that would otherwise move it. This is of great value, as it compensates for varying internal conditions (such as nonlinearity in the motor stage) and external conditions (such as varying payload or vibration) and achieves a set position.

CAPACITIVE SENSOR The use of a capacitive sensor allows for tight integration of motor and sensor, reducing delays and mechanical deflection that is critical for the small distances that are of interest.

MAGNETIC DRIVE A magnetic motor was specified in order to give a far larger throw than piezoelectric systems. This comes at the cost of increased complexity and reduced stiffness compared to piezoelectrics.

LINEARITY Linearity is critical for a high-precision actuator, the use of a closed-loop design enables the possibility a high precision system as the controller will reduce many of the residual nonlinearities to a large degree. Large weight is placed on developing an inherently linear sensor, which is critical to achieving a high system linearity.

SIZE The size of the actuator developed for the thesis should allow for easy reduction of scale for later versions - allowing for arrays of actuators for eg. adaptive optics.

FRICITIONLESS A (near-)frictionless actuator is of great use as the actuator lifespan can be made practically unlimited, reduces the amount of noise presented to the payload and simplifies the

closed-loop design. For this thesis a frictionless design using flexures will be used.

HIGH SPEED High speed of motion is always of interest, as a quicker movement speed allows for a wider range of applications. Additionally, a high-speed servo will ensure the system stiffness is kept large even at high disturbance frequencies.

1.3.1 *Predetermined values*

Prior to the start of this thesis some parameters/values have been predetermined. The definitions are shown in table 1 on the next page, as well as a short description to motivate the selection.

1.4 POSSIBLE USES

A few of the possible uses of the type of actuator described above are:

- **AF** and beam deflection for optical systems
- Rough positioning for **STM**
- Adaptive optic arrays (if the actuator is made smaller)
- Absolute interferometry - using white light and sweeping reference arm length
- General purpose high-accuracy position or velocity generation

1.5 SCOPE OF THESIS

Several limitations have been placed to control the scope of the thesis:

- A linear control scheme will be implemented, however for future work a nonlinear controller may give better performance in the sense of improved slew rate.
- One actuator and controller will be constructed, as a sufficient proof of concept.
- A moving-magnet design will be chosen, as a moving coil structure would require powering the moving mass and would result in cooling difficulties.
- Only first-order mechanical attributes will be studied, higher order effects such as movement along axes other than the axis of motion will be ignored.

Table 1: Predetermined values and topologies for the actuator.

PARAMETER	VALUE	REASON
Motor type	Magnetic	Large throw, high force and stiffness
Motor force	Approx. 30[N]	Allows for $\sim 150m/s^2$ acceleration of a 20g payload, deemed to be enough
External dimensions	Cylindrical, approx. 30x50[mm, mm]	Easy to manufacture prototype, design to be able to scale down in size
Throw	Approx $\pm 1mm$	Far exceeds travel of long piezoelectric direct drive actuators
Bandwidth	As high as possible, $> 100Hz$	A bandwidth of 100Hz is a lower bound of usefulness, more is better
Sensor	Capacitive	Allows for contactless sensing of position, high accuracy possible
Suspension	Flexure	Can result in a (near) friction-free actuator with a practically unlimited lifespan
Resolution	Preferred $< 20nm$	With better than 20nm resolution the actuator can compete with some piezoelectric systems
Interface	Manual control or RS232 over USB	Manual and computer controlled setpoint of the payload allows for finding results easily

1.6 THESIS STRUCTURE

Section 2 contains the background theory needed for a cursory understanding of the thesis. In section 3 a system-level overview of the logical blocks used in the entire system is given from a mechanical, electrical and software standpoint. These blocks will be described in more detail in section 4, while actual drawings, schematics and program listings will be contained in appendices A,B,C. All measured results and a brief discussion of them can be found in section 5, future work and conclusions can be found in Sections 6 and 7 respectively. Additionally, due to space constraints, not all calculations will be shown. The omitted details are straightforward and not critical to the the core of the work which lie with the performance of the closed-loop system.

1.7 LICENSE

Copyright ©2011 Jonathan Lock. Permission is granted to copy, distribute and/or modify this document under the terms of the GNU Free Documentation License, Version 1.3 or any later version published by the Free Software Foundation; with no Invariant Sections, no Front-Cover Texts, and no Back-Cover Texts. A copy of the license is included in the section entitled "GNU Free Documentation License".

Part II

BACKGROUND

BACKGROUND

This section contains a brief overview of capacitive sensors and magnetic motors.

2.1 CAPACITIVE SENSING

Capacitive sensing uses capacitive coupling between two or more objects to give an output signal. Recall that the capacitance, measured in farad [F], is defined as [C/V] or coulomb per volt. The textbook example of a capacitor is a parallel plate capacitor. If there exist two parallel conductive plates with area A and separation distance d , with a nonconductive medium between the two with a relative dielectric constant of ϵ_r then the capacitance between the two of them is given by

$$C = \epsilon_0 \epsilon_r \frac{A}{d} \quad (2.1)$$

where ϵ_0 is the dielectric constant ($\epsilon_0 \approx 8.854 \cdot 10^{-12}$ [F/m]) and assuming no fringing fields (which is a good approximation when d is small and A is large) (Baxter [4], Cheng [7]).

Capacitive sensing is an attempt to use the variation of capacitance between two or more objects to detect a change in the system parameters by varying one of the parameters in equation (2.1). Some examples of the use of capacitive sensors are:

- Oil level sensor: two parallel plates with a varying level of oil between them can form a capacitive sensor, as oil has a higher relative dielectric constant than air. If the plate area and separation distance are kept constant the capacitance will vary with the level of oil.
- Distance sensor: two parallel plates with a varying distance between them will function as a capacitive sensor. As the distance varies so too will the capacitance between them.
- Size sensor: one reference plate's capacitive coupling to a measured plate with unknown area can be used to determine the size of the unknown plate by measuring the capacitance.

Capacitive sensors are quite attractive as they offer an easy measurement method for many possible scenarios, often work in a contactless fashion which ensures there is no mechanical wear, are robust and can be simple to implement. However, some care must be taken when designing them to ensure that higher-order effects are kept small

enough, such as variations of undesired parameters e.g. ϵ_r varying over temperature, as well as limiting the effects of fringing fields and capacitance to other undesired bodies.

2.2 MAGNETIC MOTORS

A magnetic motor is a device that uses magnetic fields to perform mechanical work. Typically a magnetic motor's power is supplied electrically and is then converted to a magnetic field which then exerts a force and motion on some other part in the magnetic field. Commonly used magnetic motors include;

- DC and AC rotary motors,
- loudspeakers,
- head positioning for computer harddisk drives.

A magnetic motor converts electrical power to a magnetic field. Most often this is expressed with Ampère's law;

$$\oint_{\mathbf{C}} \mathbf{B} \cdot d\mathbf{l} = \mu_0 \iint_{\mathbf{S}} \mathbf{J} \cdot d\mathbf{S} = \mu_0 I_{enc}$$

where the left hand side of the equation is the closed line integral around some curve \mathbf{C} , and \mathbf{B} is the magnetic field. The first right hand side μ_0 is the magnetic constant, the integral over the surface \mathbf{S} spanned by \mathbf{C} , and \mathbf{J} is the total current density through the surface \mathbf{S} . The second right hand side I_{enc} is the total net current that flows through \mathbf{S} .

A magnetic field causes a force to be applied to charges as described by

$$\mathbf{F} = q(\mathbf{v} \times \mathbf{B})$$

where \mathbf{F} is the net force, q is the charge, \mathbf{v} is the velocity of the charge and \mathbf{B} is the magnetic field (Cheng [7], Nordling and Österman [12]). This shows the desired effect - that in some circumstances an electric current can cause a force to be applied. With careful design an effective motor can be built to maximize the force and reduce losses due to ohmic heating and eddy losses in the electric and magnetic conductors respectively.

2.3 MECHANICAL STRESS

Accurately describing the stresses in a solid body is critical when designing a reliable mechanical structure. The von Mises Criterion can be used to estimate the yield strength of a ductile material. The condition states that plastic deformation at a point in the material

occurs when the total distortion energy reaches the energy level of distortion for uniaxial tension. This is equivalent to

$$\frac{1}{2} \left[(\sigma_1 - \sigma_2)^2 + (\sigma_2 - \sigma_3)^2 + (\sigma_3 - \sigma_1)^2 \right] \leq \sigma_y^2$$

where $\sigma_{1,2,3}$ is the strain along three orthogonal planes at a point and σ_y is the yield strength for uniaxial tension. This is in contrast to the slightly less conservative estimate, the maximum shear stress condition, which limits the principle stress difference and the principle stresses to be less than the yield shear stress

$$|\sigma_1| \leq \sigma_y, |\sigma_2| \leq \sigma_y, |\sigma_1 - \sigma_2| \leq \sigma_y.$$

As the maximum shear stress condition is typically used for more brittle materials, and as a flexure is intended to flex over a large range and not shatter on transients exceeding the specified travel range a relatively ductile material is desired, leading to the use of the von Mises criterion (Young and Budynas [17], Nordling and Österman [12]). See section 3.2.2 for simulations performed on a mechanical flexure structure using the von Mises stress critereon.

Part III

TOPOLOGY

TOPOLOGY

This section illustrates the general topology of the actuator for the implementation chosen (described in more detail in section 4). The total system wide topology is divided into three subsections: mechanical, electrical, and software. More details involving implementation-specific parameters can be found in section 4 and appendices A,B,C.

Note that the topologies discussed below represent one particular choice. Some motivation for the design choices performed will be given, nevertheless design choices made only represent one possible design.

3.1 SYSTEM-LEVEL TOPOLOGY

The entire system-level topology uses two hardware blocks, an actuator and a controller. The actuator houses a motor which generates force and a sensor which measures the current position. The controller demodulates the measured position, feeds it as the current process variable to a linear controller which outputs a control current. This is amplified with a power amplifier and fed back to the motor, driving the actuator to the desired position. Additionally, a microprocessor samples the position with an ADC continuously, can control the set-point with a DAC to the controller and receives and transmits data over an external communication interface. A simple block diagram can be seen in figure 2 on the following page which illustrates the system-level topology. The reason for the discrimination between the actuator block and the controller block is primarily due to size - the current controller block is physically large in order to more easily develop and test the entire system.

3.2 MECHANICAL STRUCTURE

A diagram of the mechanical actuator design chosen is shown in figure 3 on the next page. Important factors taken into account have been;

STIFFNESS High stiffness is important, both between the actuator and the payload and internally between the motor and sensor. If the stiffness of the driving structure between the actuator and the payload is insufficient then external forces and acceleration will cause errors in the set position. In particular, if the stiffness between the motor and sensor inside the actuator is insufficient,

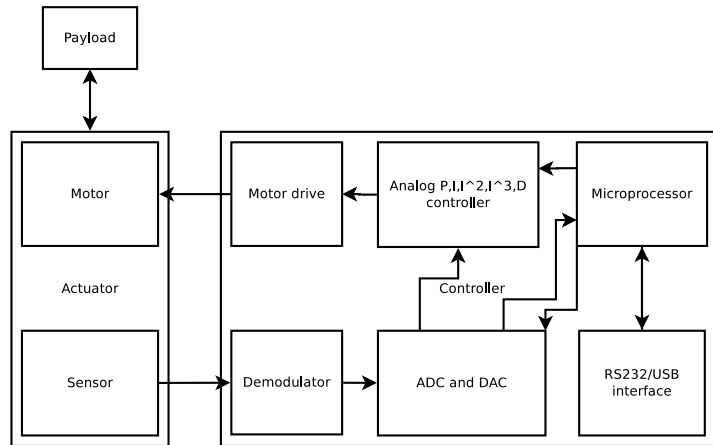


Figure 2: System-level topology of the actuator, illustrating the core blocks in the system and their interconnections.

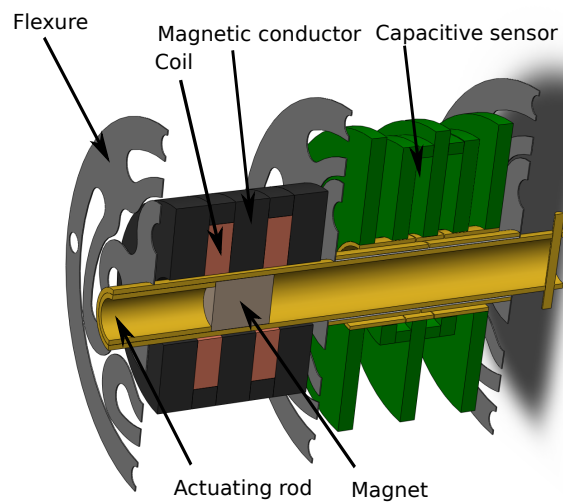


Figure 3: Cutaway view of mechanical structure of actuator with motor and actuator visible, various supporting structures hidden.

oscillatory and/or unstable behavior may be exhibited due to the added pole in the closed loop system.

MASS A small moving mass is critical to high dynamic performance, ie. rapid acceleration. The force required to achieve a desired acceleration is linearly proportional to the mass, by Newton's second law $F = ma$ (Nordling and Österman [12]).

FRICTION A near-frictionless actuator is of great value as it allows for a near unlimited lifespan and ease of control. Additionally, friction causes great changes in the linear description of a system potentially leading to instability.

These main parameters can be achieved through the actuator design in figure 3 on the facing page. The capacitive sensor and the motor are the two main parts, separated by a flexure suspension that suspend the moving parts. The motor is a moving magnet type, as described in section 1.2, with two coils to direct the magnetic flux and a magnetic conductor to concentrate the flow through the coils to maximize the resulting force for a given current (see simulations in appendix A). The capacitive sensor's hardware consists of two moving reference cylinders attached to the moving actuating rod and one non-moving sense cylinder surrounded by two non-moving guard cylinders, shown in figure 3 on the preceding page as the brass-colored sections of the sensor. These cylinders are held in place by a PCB with electronics for the sensor, shown in the figure as the green-colored sections.

The moving mass is kept low by ensuring only the lightweight parts of the motor and sensor move. Stiffness is kept high between the sensor and actuator by using a short cylindrical structure. Friction is kept to a minimum by using a flexure suspension which also allows for applying electrical voltages to the moving parts of the capacitive sensor.

3.2.1 Motor design

The motor has been designed to apply a maximum of force at a reasonable voltage and current (roughly 4Ω DC resistance) and saturating the magnetic conductor roughly at the same time around the coils. See figure 4 on the following page for a simulation of the magnetic current and flux density for various magnet positions and coil currents. The magnetic conductor tends to concentrate the magnetic flux (as seen by the black field lines) and when there is current in the coil the magnetic field lines shift, which places a force on the magnet. Simulations assuming the size of components as in the drawings in appendix C predict a force of $30N \pm 5N$ over the travel of the magnet at a current of 3A. Figure 5 on the next page illustrates a qualitative estimate of the normalized steady-state motor position over normalized current for a constant spring load. A limited range of motion in the center

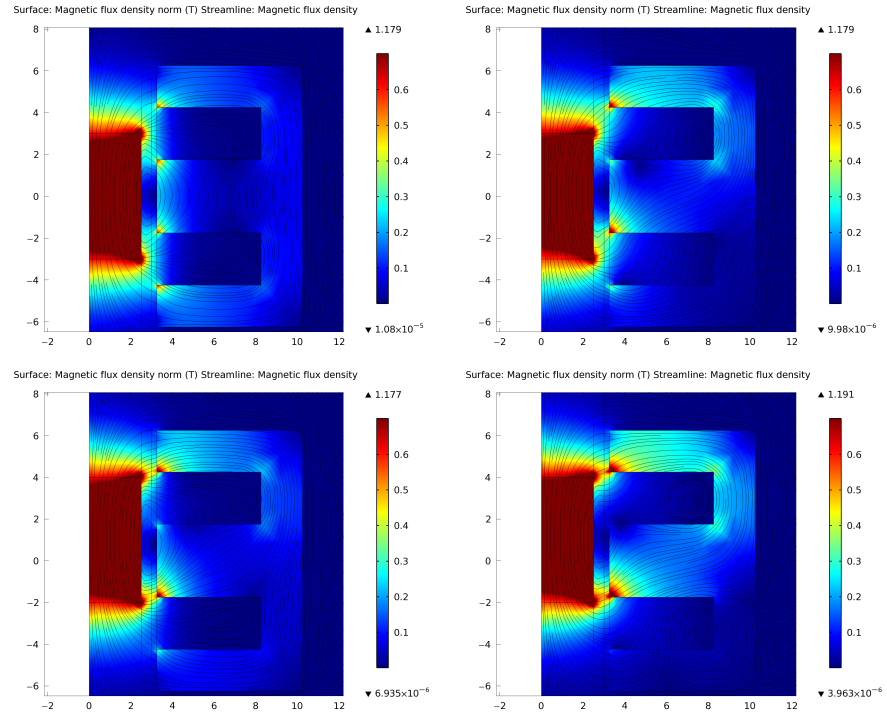


Figure 4: Simulation of the magnetic current and flux density for various positions in a radial-symmetric 2D representation. In all images the magnet is to the left, the reversed E shape is the magnetic conductor and coils fill the “empty” zones in the magnetic conductor. The four images illustrate from left to right and top to bottom; centered magnet, no current in coil; centered magnet, current in coil; offset magnet, no current in coil; offset magnet, current in coil.

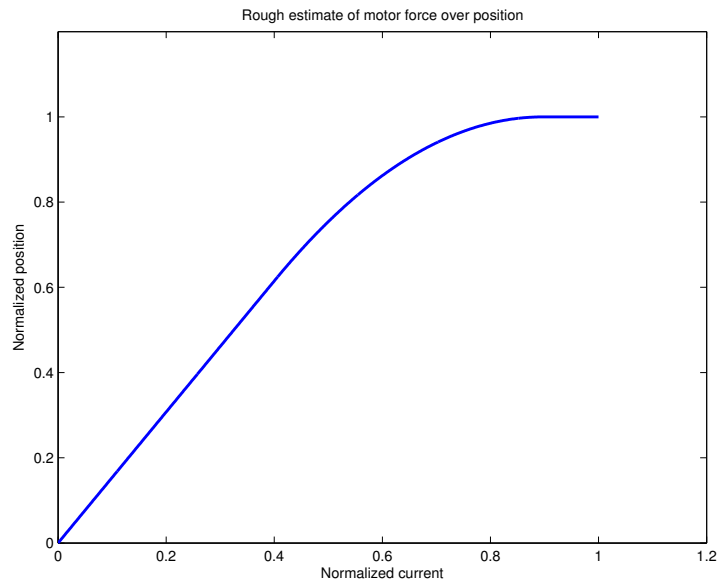


Figure 5: Qualitative estimate of the steady-state magnet position as function of coil current for a constant spring load.

is relatively linear, but as the excursion increases the force decreases (leading to a reduced change in position) and finally reaches an equilibrium point, after which no increase in current will cause any more force to be applied, leading to a constant position (Brauer [5]).

3.2.2 Flexure design

The flexures used to suspend the structure are critical for the performance of the actuator. Ideally the flexure would be infinitely weak along the direction of travel and infinitely stiff along all axes of rotation and the remaining axes of translation. Additionally, in order to achieve a high lifespan for the flexure the stress in the material must be limited. For a flexure to sustain a lifespan of 10^{10} or more flexing cycles the strain in the material, assuming a hardened stainless steel material, must be limited to around 50% of the tensile yield strength (Young and Budynas [17]). The flexure illustrated in figure 6 on the following page is an approximation of both of these ideals. The von Mises stress (which gives an overall measure of the stresses in the system, covering tensile, compression and shear stresses) is limited to 145MPa , which is just below $1/2$ of the rated tensile strength of 300MPa . When designing the shape of the flexure arms primary targets are;

- keeping the size of the radii large which helps to reduce the stress that is concentrated in the corners,
- ensuring that the straight sections are as long and wide as possible to maximize and minimize the stiffness along and perpendicular to the axis of motion respectively.

Simulations assuming a homogeneous source material and an outer radius of 36mm (as per the sizes and material specified in appendix A) give a stiffness along the axis of translation of 0.105N/mm , and minimum stiffness perpendicular to the axis of translation of 289N/mm .

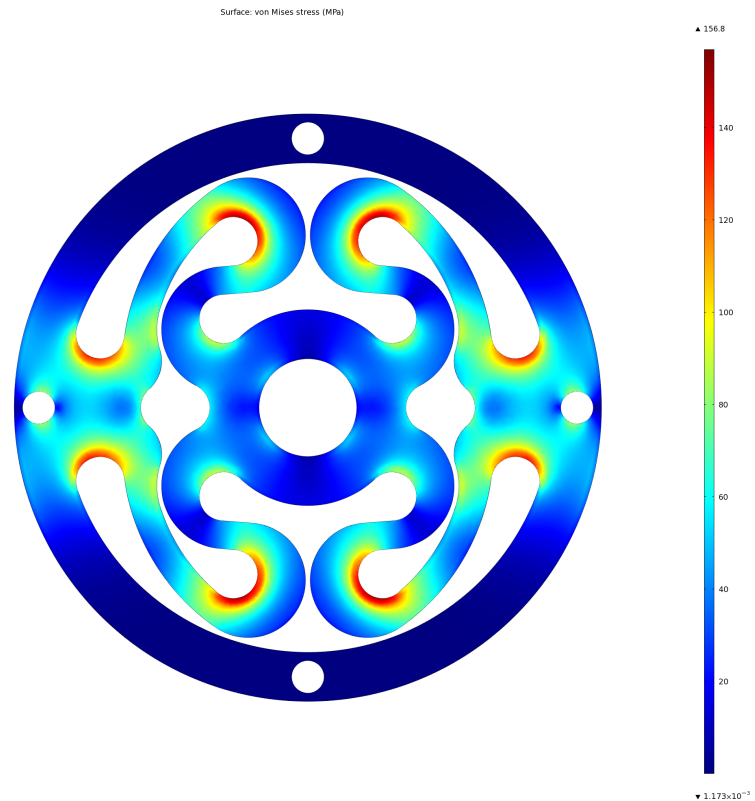
Also, as the range of travel is limited to $\pm 1\text{mm}$, in comparison with the length of the arms which is around 20mm , and there is no plastic deformation over the typical travel range the flexure acts to a good approximation as a linear spring, that is to say that the force becomes

$$F = -kx$$

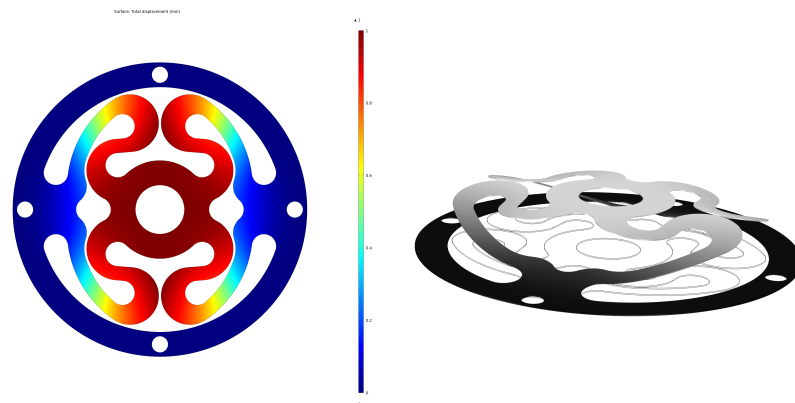
where k is denoted the spring constant and x is the position of the spring relative to its neutral position.

3.3 ELECTRICAL STRUCTURE

The electrical structure of the entire system involves with two logical blocks: one being the electronics that deal entirely with the sensor, the other with all the remaining electronics.



(a) Total Von-Mises stress for the flexure assuming a 1mm displacement along the axis of movement.



(b) Total displacement for the flexure assuming a 1mm displacement along the axis of movement.

Figure 6: Stress simulation of the flexure illustrating stress levels, total displacement and a 3D representation of the displacement.

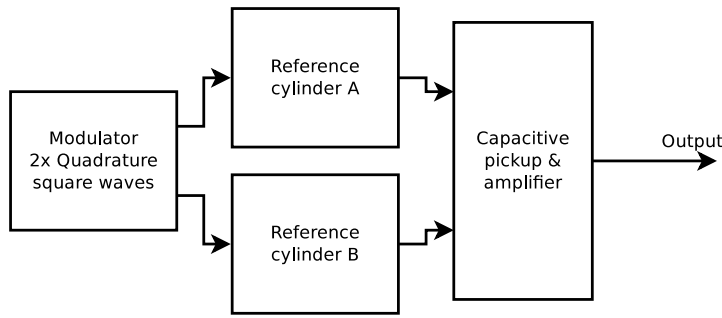


Figure 7: Block diagram of sensor electrics topology, from excitation to output waveform.

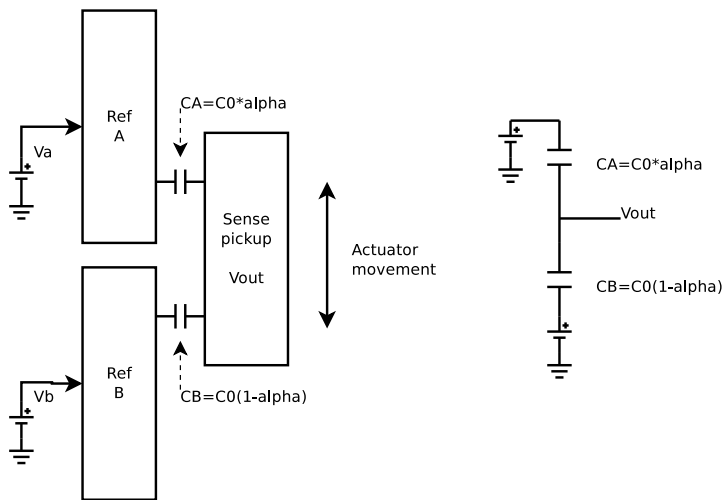


Figure 8: Stylized image of a contactless capacitive position sensor using two reference electrodes. The “Sense pickup” block can move relative to the reference blocks, causing the capacitances C_B and C_A to vary linearly with position, as per equation 2.1.

3.3.1 Sensor electrics

The electrics related to the sensor are everything contained in the “sensor” block in figure 2 on page 18. This single block can be expanded into a group of logical sub-blocks, as shown in figure 7. Some important parameters to take into account for the design of the sensor are;

LINEARITY Linearity of the sensor is critical as this is the only source for position measurement. Any nonlinearities over the range of travel will directly translate to nonlinearities in the output position. As described in section 2 certain types of capacitive sensors can be made to have a very linear output, limited primarily by fringing fields.

NOISE Low noise in the sensor is important, as with the rest of the system, as high noise will result in position inaccuracy.

RESOLUTION The sensor must be able to resolve a small enough change in position to be able to achieve the desired performance.

Due to various implementation effects described in section 4 and appendix B an effective sensor design should try to minimize the effects of parameters other than position affecting the output. Figure 3 on page 18 and figure 8 on the preceding page show a solution to this, where two reference electrodes are driven to known voltages and the voltage of a high-impedance sensor electrode is measured. The voltage on the sensor will then be a capacitive voltage division of the two reference electrodes and a function of its position. If the fringe fields are ignored the total capacitance between the pickup electrode and the two reference electrodes is constant (per equation (2.1), the area and separation distance are constant). However the relative capacitance between each electrode, C_A and C_B will vary linearly with position as the area between the sensor and the reference electrode will vary as:

$$\begin{aligned} A_A &= A_0\alpha \\ A_B &= A_0(1 - \alpha). \end{aligned}$$

Choosing a suitable carrier frequency must balance the speed of the amplifier chosen and the impedance level of the capacitive divider. A low frequency will not require as fast an amplifier but will require a reduced load on the sensor electrode. If two square waves 90 degrees out of phase with each other are used as the excitation signal for the two reference cylinders a desirable output similar to figure 9 on the next page is achieved, assuming ideal components and no fringe fields. Two different output waveforms are shown, one corresponding to the sensor being in the center position (output 2) and one at some other position (output 1).

When the two excitation waveforms are of opposite polarity a capacitive voltage division over the sensing surface is achieved, corresponding to the position, whereas when the waveforms are of the same polarity a reference output is achieved.

When both waveforms are of the same polarity ($U_A = U_B$) the voltage on the sensing surface ($V_{Out_{ref}}$) will become

$$V_{Out_{ref}} = \frac{\frac{1}{j\omega C_B}}{\frac{1}{j\omega C_B} + \frac{1}{j\omega C_A}} \underbrace{(U_A - U_B)}_{=0} + U_B = U_B = U_A$$

where C_b and C_a are the capacitance between the sensing surface and the drive surfaces A and B respectively. The equation is according to simple voltage division (Nordling and Österman [12]). When the

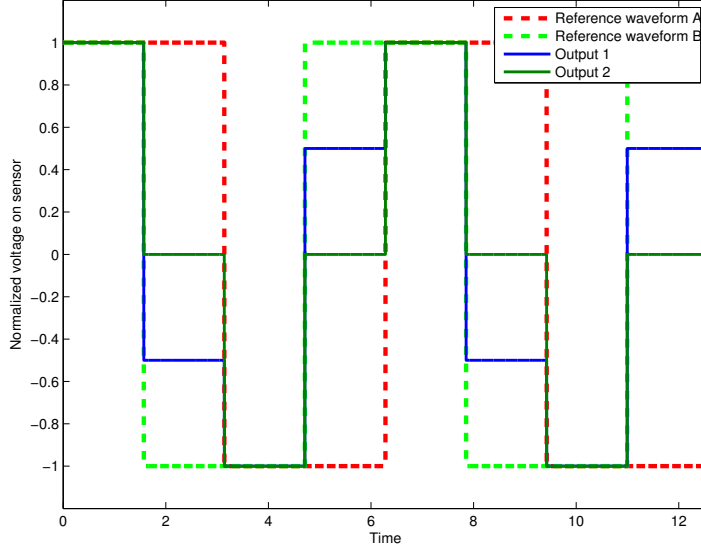


Figure 9: Input and output waveform for two different positions from capacitive sensor assuming ideal components and no fringe-fields. Output 1 corresponds to the sensor not being in the center of the travel range, whereas Output 2 corresponds to the sensor being in the middle of the travel range.

waveforms are of opposite polarity however the voltage on the sensing surface becomes $V_{Out_{meas}}$;

$$\begin{aligned}
 V_{Out_{meas}} &= \frac{\frac{1}{j\omega C_B}}{\frac{1}{j\omega C_B} + \frac{1}{j\omega C_A}} (U_A - U_B) + U_B \\
 &= \frac{\frac{1}{j\omega C_0(1-\alpha)}}{\frac{1}{j\omega C_0(1-\alpha)} + \frac{1}{j\omega C_0\alpha}} (U_A - U_B) + U_B \\
 &= \frac{1-\alpha}{1} U_A \\
 &= U_A (1-\alpha).
 \end{aligned}$$

This gives a very attractive linear output voltage over position ($\alpha \in [0, 1]$, α corresponds to the position from minimum to maximum), where $V_{Out_{meas}}$ is denoted the output from the “measurement” phase and $V_{Out_{ref}}$ is denoted the output from the “reference” phase. The total output then becomes

$$V_{Out_{tot}} = \frac{V_{Out_{meas}}}{V_{Out_{ref}}} = \frac{U_A (1-\alpha)}{U_A} = 1 - \alpha.$$

The output is *preserved without any distortion and independent of the amplitudes of the reference waveforms and the size of the capacitance C_0 , additionally, in the absence of any stray electric fields the output is linear with regards to position of the sensor.* This is very desirable behavior as this reduces the effect of other parameters varying causing an output

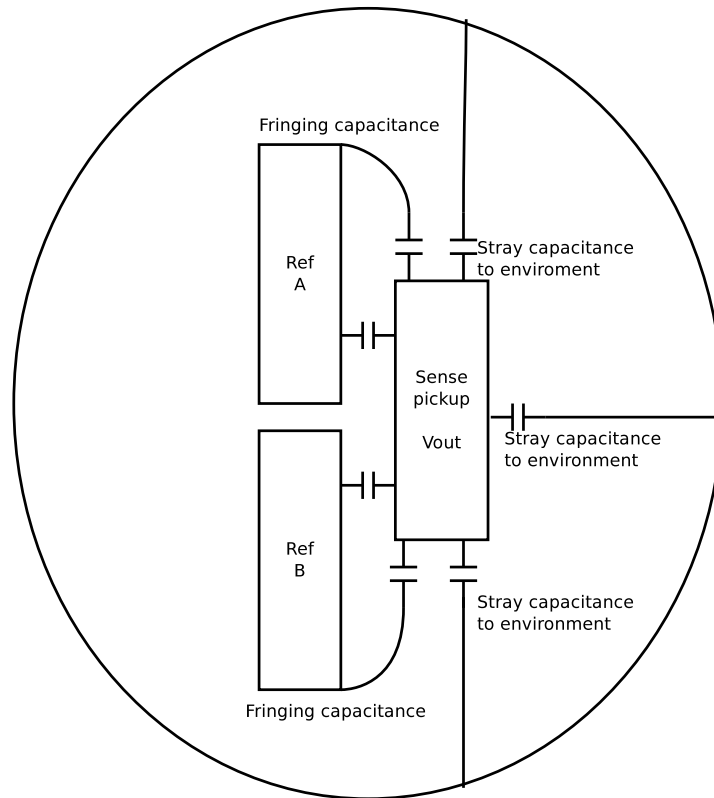


Figure 10: Effects of stray capacitive coupling and fringe fields on sensor.

voltage change (such as for example a varying gain or attenuation in some stage).

However, the described system does not in any way handle capacitive coupling from the sensor to the rest of the environment. See figure 10 for an illustration of the effects of stray capacitance and fringing fields. Fringing fields will increase the effective capacitance and create a nonlinear term as the increase in capacitance due to the fringing fields will vary depending on the position of the actuator. More importantly, the stray capacitance from the sensor to the rest of the environment is completely uncontrolled. If no method of reducing the stray capacitance is implemented the linearity of the sensor will suffer and any external alternating voltage will directly couple into the sensor giving an erroneous reading.

One method for simultaneously reducing the fringing and stray capacitance effects is to use an active guard, shown in figure 11 on the next page. The pickup electrode is surrounded by an active guard box driven to the same potential as the pickup by an amplifier. As the potentials of the pickup and the guard are the same there are no electric fields between the two, nearly completely removing the stray capacitance from the pickup. The only stray fields must go from the pickup, through the narrow gap between the reference electrode and the guard, and then reach the rest of the environment (Baxter [4]).

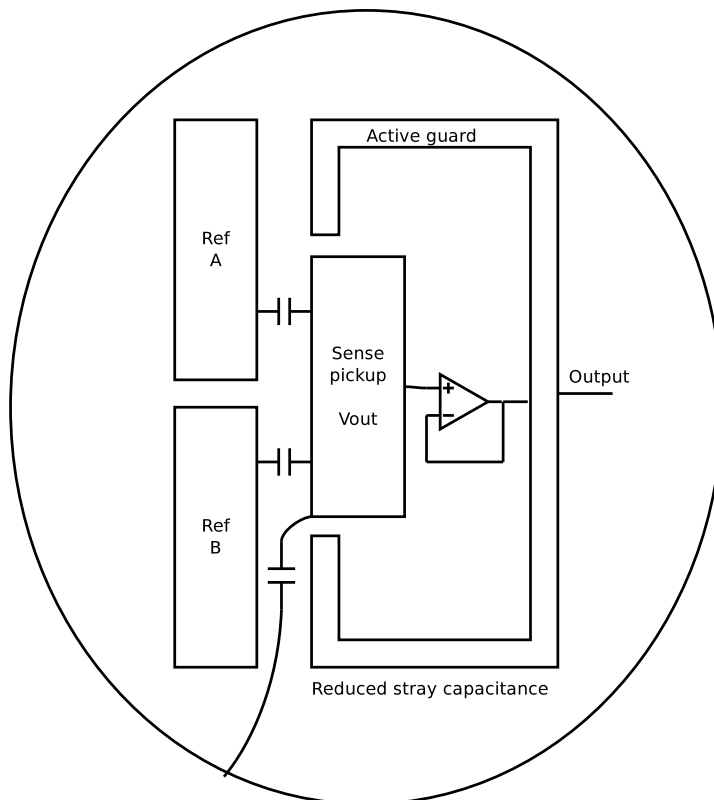


Figure 11: Adding an active guard to the capacitive sensor reduces the effects of fringing and stray capacitance.

See section 5.2 for an estimation of the size of the stray capacitances based on measurements from the implemented sensor. Fringing fields are also nearly completely removed if the guard box extends beyond the pickup far enough. The electric field will be practically entirely horizontal, and the only stray fields will be from the guard to the rest of the environment, which has no effect on the pickup voltage.

3.3.2 Controller electronics

The electronics in the controller relate everything from decoding the output waveform from the sensor to driving the motor coils. A somewhat more detailed block diagram of the controller electronics is shown in figure 12 on the facing page

The signal propagates as follows;

- A multiplexer splits the signal into four different paths depending on the current waveform state illustrated in figure 9 on page 25. The four possible waveform states, denoted $Reference_{pos}$, $Position_{neg}$, $Reference_{neg}$, $Position_{pos}$ (which correspond to $t = (0, \pi/2)$, $t = (\pi/2, \pi)$, $t = (\pi, 3\pi/2)$, $t = (3\pi/2, 2\pi)$ in the figure) are fed into the corresponding sample and hold block, whose output can be viewed as zero-order hold filter (assuming the multiplexer samples signals at $t \leq 0$ and holds at $t > 0$)

$$V_{Out_{S\&H}}(t) = \begin{cases} V_{multiplexer}(t) & t \leq 0 \\ V_{multiplexer}(0) & t > 0. \end{cases}$$

- The output from the sample and hold filter is fed into two ADC's, which are used for measuring the position and reference signals (used for outputting the position to a PC for viewing the data) and a summation block to convert the balanced signal into an unbalanced signal for the controller. A DAC controlled by the microprocessor outputs a setpoint which is subtracted from the current position to give a signal proportional to the error in position.
- The unbalanced signal is fed into an analog linear controller (a proportional integral derivative (PID) controller with several integrators), which outputs a control signal that is proportional to a force to be applied to the actuator in order to bring it to the desired position.
- The output from the controller is fed into a motor driver, which is essentially a high-power transconductance (voltage to current) amplifier. This is desirable as the current through the motor is directly proportional to the resulting force, as per Lenz law (Nordling and Österman [12]).

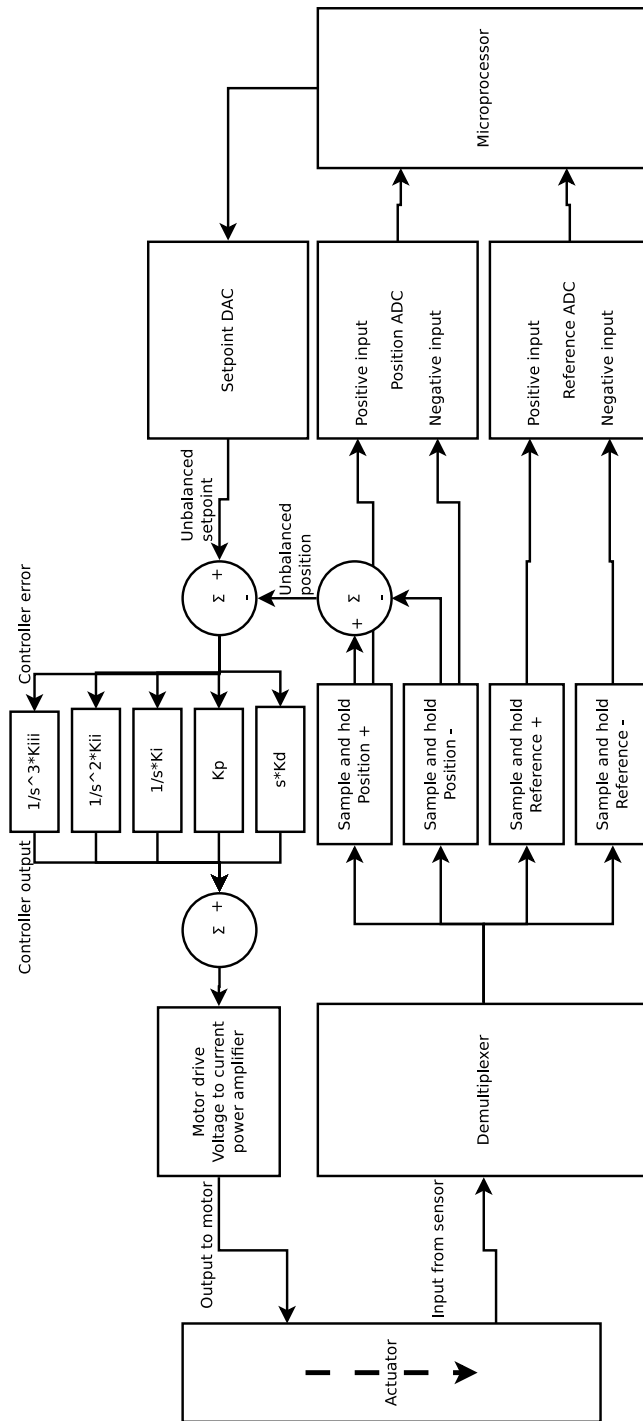


Figure 12: Block diagram of the controller electronics, showing the signal pathway from demodulator to motor drive.

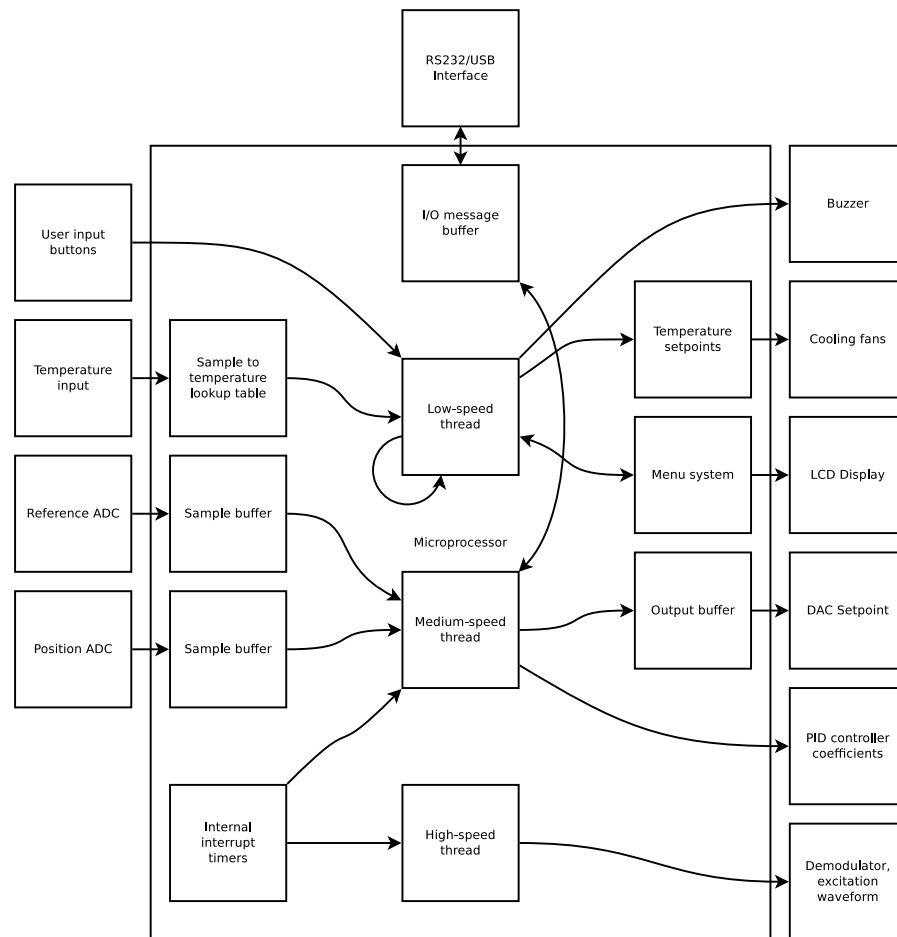


Figure 13: Block diagram of key parts of the microprocessor structure.

As can be seen from the signal propagation path an error in position must be converted to a desired force in the actuator using the linear controller, i.e. K_p will give a constant force in response to an error in position.

3.4 SOFTWARE STRUCTURE

A block diagram of the microprocessor structure is shown in figure 13. It performs operations at four different priority levels;

HIGH The most time-critical operations are excitation waveform (the two square-wave reference signals mentioned in subsection 3.3.1) and demodulator control (the sample and hold filter in subsection 3.3.2). This thread is called at specific time intervals and the corresponding output control signals are set to drive the excitation and demodulator control lines.

MEDIUM-HIGH (*Not shown in block diagram*) When a message is received from the external digital hardware connected to the microprocessor (from the ADC's, DAC, USB/RS232 interface) the message

is stored in a first in first out (FIFO) buffer for later use. Additionally, data from the output buffer to the DAC is sent at a certain time interval.

MEDIUM At a specific time interval, faster than the sampling speed of the ADC's and the external interface, the buffers are read, data is may be sent to the external interface, and PID controller coefficients may be adjusted. This is the main "heartbeat" of the microprocessor and where much of the data shuffling takes place.

LOW This thread is run whenever a higher priority thread is not running, it checks the current button status on the front panel of the controller (used for manually controlling the setpoint etc.), writes data to the LCD data display, checks the temperature of various components, turns cooling fans on and off respectively and controls the system buzzer (used for warnings and other status messages).

Data can be moved around the various parts of the system effectively by performing system operations using these four different priority levels. Note that the microprocessor only has control of the linear controller coefficients, the actual linear PID controller is not implemented in software.

Part IV

IMPLEMENTATION

IMPLEMENTATION

This section will describe implementation-specific information about each block described in section 3. Drawings, schematics and code are contained in appendices A, B, and C respectively. As many of the aspects briefly touched on in section 3 are first-order approximations an effective implementation must take these approximations into account and attempt to reduce the non-ideal effects that present themselves in a real-world implementation. This section is divided into three primary parts, mechanical, electrical, and software.

4.1 MECHANICAL IMPLEMENTATION

4.1.1 *Actuator mechanical implementation*

The mechanical implementation of the actuator is similar to that shown in the section 3, though with an added supporting structure as can be seen in figure 14 on the next page which is the primary difference compared to the view shown in figure 3 on page 18.

Figure 15 on page 37 is a photograph of the real-world implementation of the actuator with visible central actuating rod, flexure, supporting structure and dummy payload. Additionally several electrical wires are visible which transfer both power and signals to and from the capacitive sensor and motor. Full drawings of all the parts of the actuator are included in appendix A.

4.1.2 *Controller mechanical implementation*

The controller's mechanical implementation is shown in figures 16 on page 38 and 19 on page 43, which illustrate the user interface and connectors to the actuator, and the PCB's and their functionality respectively.

The front panel houses several connections that go directly to the actuator. These connections transmit power to the motor and sensor electronics, as well as the reference waveforms and the output signal (as specified in section 3.3.1). A BNC input is available for manually driving a setpoint to the controller. Additionally, an LCD display, rotary dial and multi-directional joystick are present for manually controlling system parameters, a USB port is used for external data communication, and a 230V AC power socket is available on the rear side (not shown).

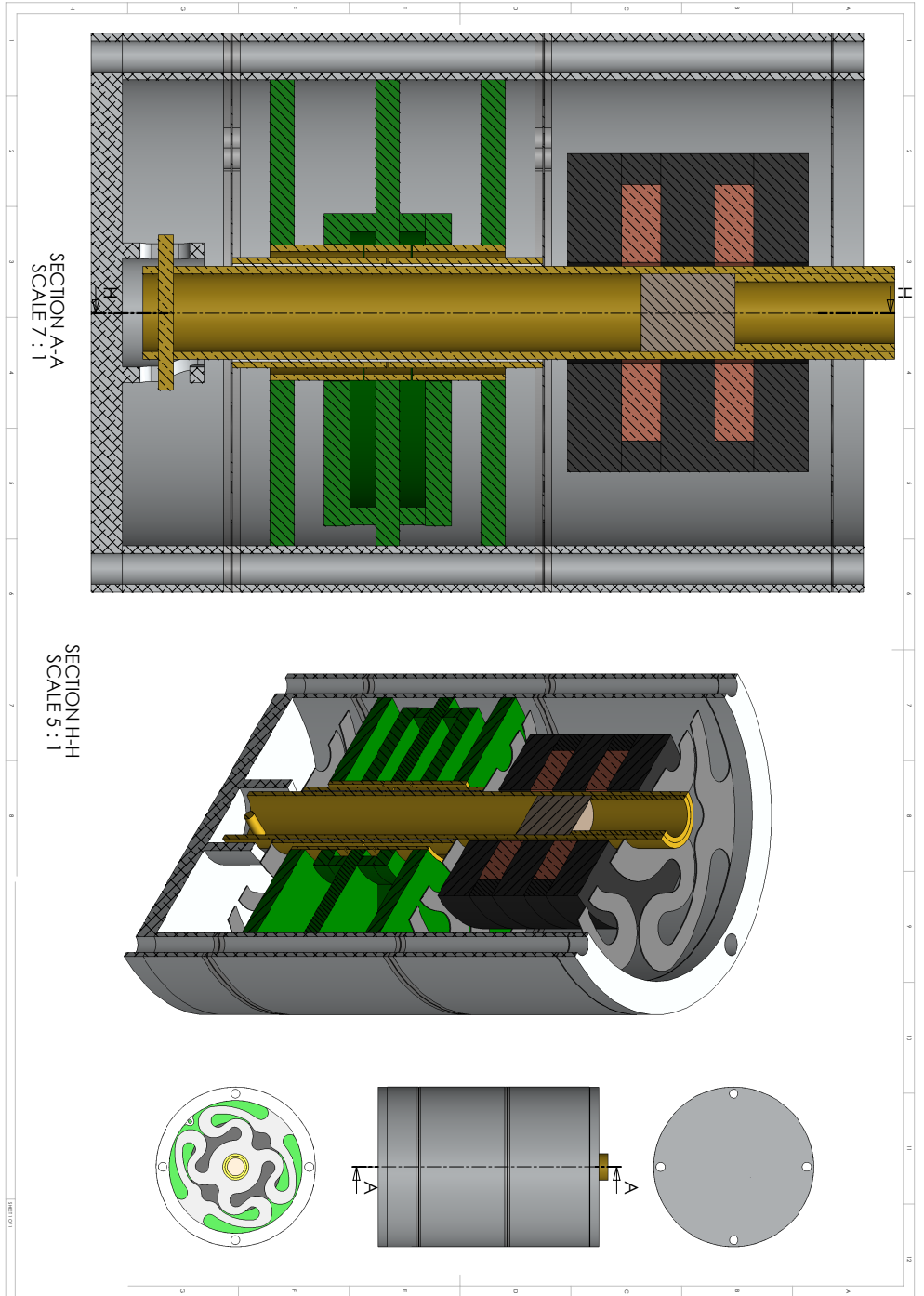


Figure 14: Cross section view of the implementation of the actuator with supporting structure visible.

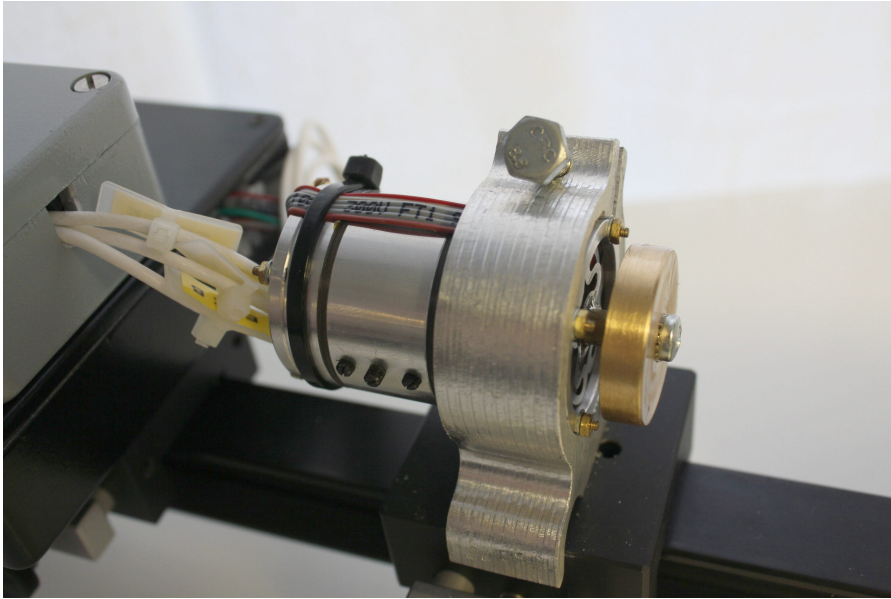


Figure 15: Photograph of implementation of actuator, with visible central rod, payload, flexure and supporting structure.

4.2 ELECTRICAL IMPLEMENTATION

4.2.1 Actuator electrical implementation

The implementation of the electrics in the actuator are primarily focused on the sensor previously described and illustrated in figure 8 on page 23. An assumption made was a method of detecting the voltage on the sensing pad without loading it in any way. The sensor must be loaded in some way to measure it, and ideally this load should be as small as possible.

A simple solution is to use a low bias current operational amplifier (OPAMP) in a non-inverting unity gain configuration and a single resistor to ground, which will ensure that the DC level of the output is reasonably close to ground without loading the sensor pad too much. However, this simple solution does not take into account the variance of input capacitance over input voltage range. The input capacitance of a typical metal-oxide-semiconductor field-effect transistor (MOSFET) input OPAMP is on the order of $5 - 10\text{pF}$ (the amplifier used - OPA827 - has an input capacitance of typically 9pF (Texas Instruments [15])). As this is of the same order of magnitude as the measured capacitance a variation of input capacitance leads to a nonlinear output over position. In order to reduce these effects a multiple-stage setup is used, where the first OPAMP (IC1 in figure 17 on page 39) is enclosed in a Faraday cage driven by the amplifier IC2A to the measured voltage. The supply voltage to IC1 is kept relative to the Faraday cage, so that regardless of the input voltage on the pickup of IC1, all the voltages inside the Faraday cage will be constant (after a transient



Figure 16: Photograph of front side of implementation of controller with connectors to actuator visible and functionality marked.

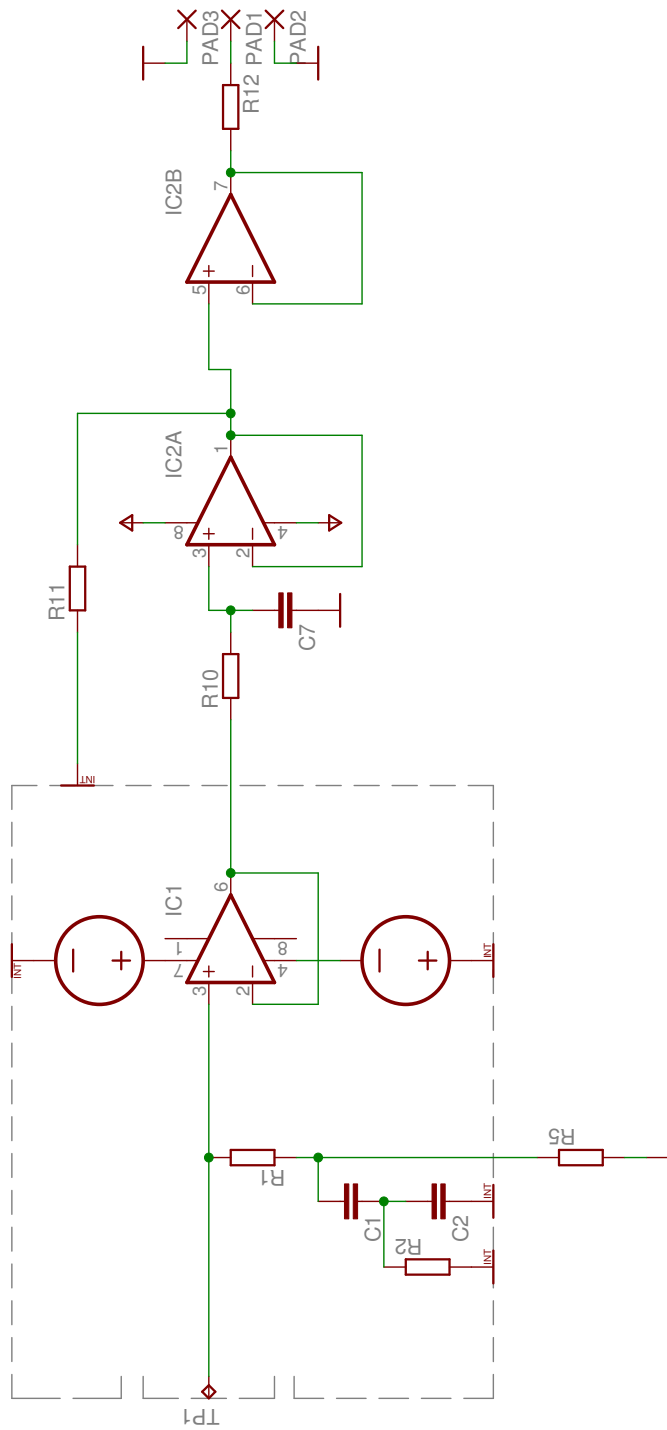


Figure 17: Simplified schematic of capacitive sensor, with some component blocks removed.

settling time). This means that all charges inside the Faraday cage (see figure 11 on page 27) will be constant over varying input voltage. The input capacitance to the Faraday cage will then be very close to zero, so nearly no charge flows into the Faraday cage with varying input voltage.

This is a great improvement over the topology shown in Baxter [4], which only drives the negative power supply rail of the amplifier to a constant offset from the measured voltage. The result of this is a significant residual capacitance inside the amplifier from various parts to the positive supply and its internally generated levels. This is in contrast to the chosen implementation which embeds the amplifier entirely inside a Faraday cage, resulting in a nearly constant positive and negative power supply voltage compared to the amplifier.

There are additional components shown in figure 8 on page 23, which perform the following tasks;

- $R1, R2, C1, C2$ form a filter to ensure that only very low frequency currents go through $R5$, reducing the effect of the Faraday cage moving up and down in voltage causing an error due to currents in the bias resistor $R1$. $R2$ and $C2$ serve to suppress feedback resonance at low frequencies, $C1$ and $C2$ decouple the external and internal voltages and preserve the function of the Faraday cage.
- $R10, C7$ form a lowpass filter to ensure that there is no oscillation between $IC1$ and $IC2A$, which may otherwise occur as there are essentially two operational amplifiers connected in feedback (via the stray capacitance from the Faraday cage to the input of $IC1$). By keeping the bandwidth low enough (slightly below the gain-bandwidth product (GBW) of the amplifiers $IC1$ and $IC2A$), stability is ensured.
- $R11$ stabilizes the output from $IC2A$, which may otherwise oscillate or ring due to excessive capacitive loading.
- $IC2B, R12$ form an output stage to buffer the signal for transmission to the demodulator stage (as shown in figure 12 on page 29).

The motor electrical implementation is relatively simple as it consists of two coils with 500-550 turns of 0.15mm copper enamel wire. This gives approximately 4Ω of DC resistance. A dynamic model is critical in order to design the motor driver, measurements give a coil model and a simulated response as shown in figure 18 on the next page. As can be seen for very low frequencies the impedance is quite low and current is limited solely by the DC resistance. As the frequency increases a more inductive response takes over and the impedance increases significantly. This is valid up to around 1.2MHz where a relatively lossy resonance between the inductance and inter-winding

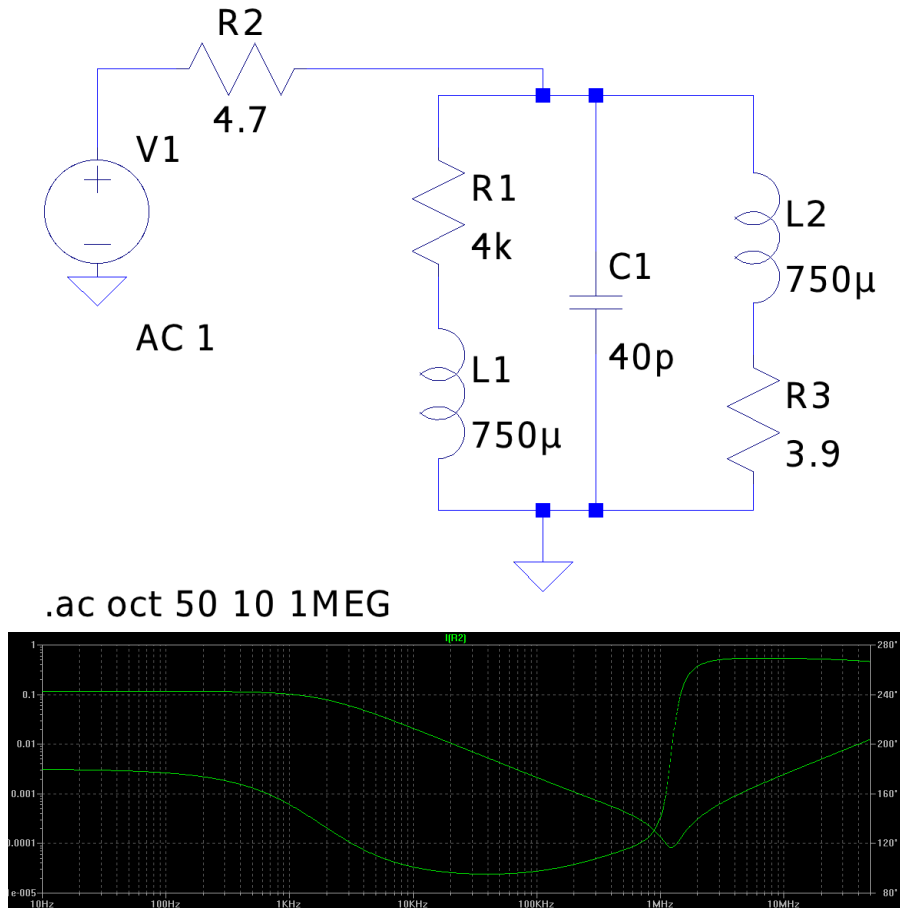


Figure 18: Motor coil model and relative impedance.

capacitance occurs and at higher frequencies the inter-winding shunt capacitance takes over, causing a decrease in system impedance.

The force from the motor is limited primarily by the saturation flux of the magnetic conductor around the coils, when it saturates the coils will apply practically no force to the magnet. The point of saturation has been placed slightly above the maximum current through the motor drive board (by adjusting the thickness of the conductor). Note that high currents come at a very steep cost, as the resistive heating power in the coils is

$$P = R \cdot i^2$$

where R is the resistance of the coil and i is the current. Ie. there is a quadratic increase in developed heat in the coil relative to the current applied (which is proportional to the force). Heat is very detrimental to the performance of the actuator as a change in temperature will result in a significant change in mechanical dimensions.

The dynamic range of the motor is limited by many factors, primarily by the flexure's need to stay within safe strain levels. In the implementation the travel is limited by a hard stop as the locking pin

at the bottom of the actuating rod will reach the top or bottom of a slot in the lower capping plate (see appendix A).

4.2.2 Controller electrical implementation

The functionality of the PCB's are marked out in figure 19 on the facing page which correspond roughly to the blocks shown in section 3.3.2. Each PCB's functionality is described in the following sub-subsections with a simplified schematic and a reduced number of components. Components not shown include those not directly in the signal pathway such as temperature sensors, cooling fans, decoupling capacitors, status indicators, electrostatic discharge (ESD)-clamping diodes, power and signal connections and headers and other components. For all full schematics (as well as PCB artwork) see appendix B.

4.2.2.1 Power supply

Figure 20 on page 44 illustrates a simplified schematic of the power supply section which generates power rails and reference voltages for all the components. The basic power flow is as follows;

- External 230VAC mains enters in the top block and is clamped by varistors to limit power surges, as well as fuses and an negative temperature coefficient (NTC) resistor to limit the inrush current. This is then connected to a 230VAC - 2x15VAC transformer (not shown) with the signals $TW1 - HV$ and $TW2 - HV$ for the primary winding and $TW1P$, GND , GND , $TW2N$ for the secondary windings respectively.
- This is then rectified using $B1$, with a snubber network to limit the radio-frequency (RF) emissions from diode switching. $F3$ and $F4$ are fuses to limit the current in case of a failure.
- The nets VDD and VSS are passed on to the linear regulators $IC4$ and $IC6$ that create a $\pm 15V$ output for driving the motor. This supply is capable of supplying $3A$ of current, deemed to be enough for the motor in the actuator. These nets are also used for generating the $+5V$ and $+2.6V$ supplies with $IC3$ and $IC5$ used for the microprocessor and related hardware.
- $R5, R6, R7, R18, R19, R20$ and $C3, C4, C5, C6, C10, C11, C12, C13$ form a passive RC lowpass network to limit high-frequency signals from passing to the more sensitive power supply sections. The voltage out from this filter is fed to the linear regulators $IC1$ and $IC2$ which generate a $\pm 15V$ power supply for all the sensitive analog electronics.
- $IC10$ is used to generate a highly accurate $4.096V$ reference voltage, which is then inverted and amplified with $IC7$ and $IC8$

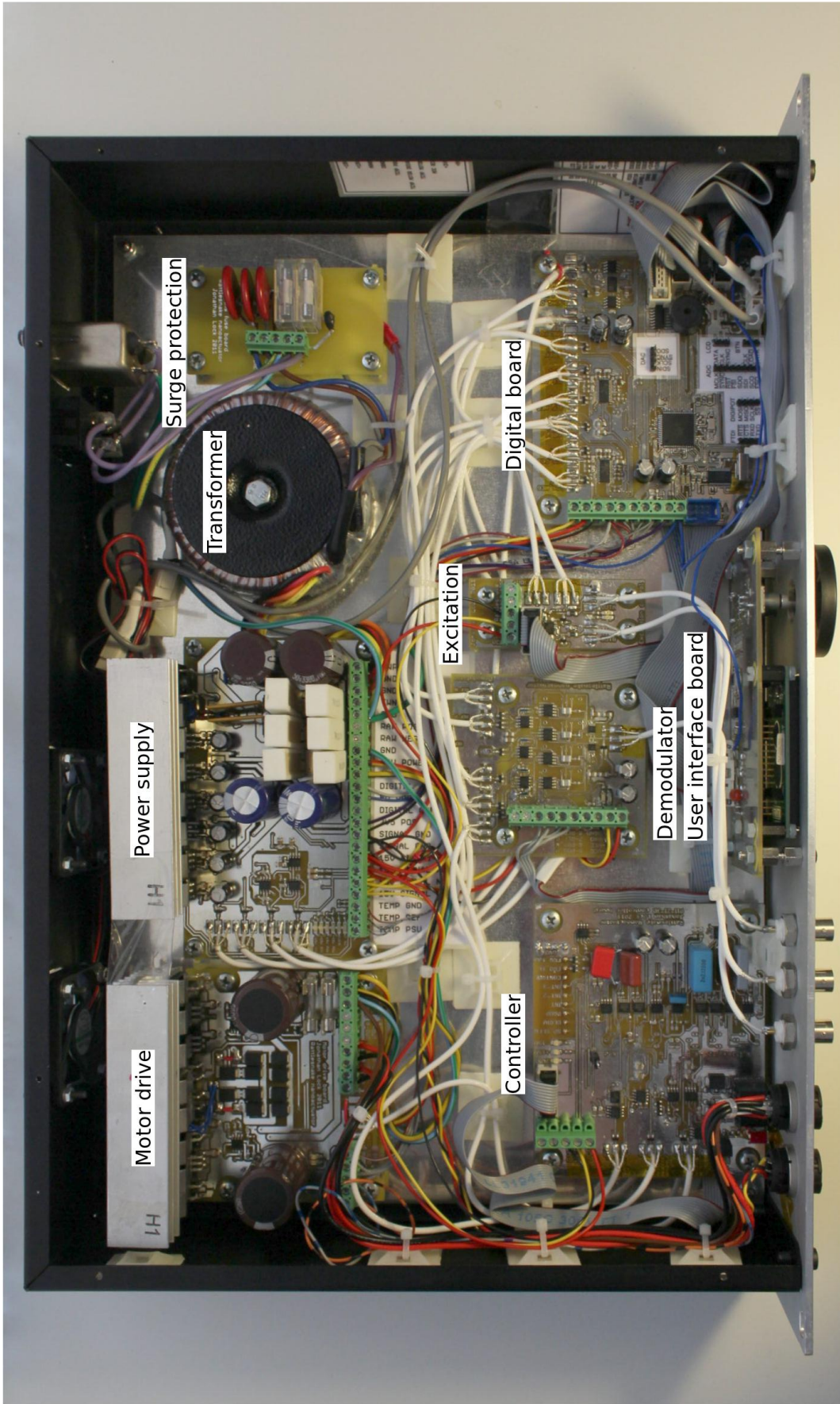


Figure 19: Photograph of internals of controller implementation, with PCB's visible and functionality marked.

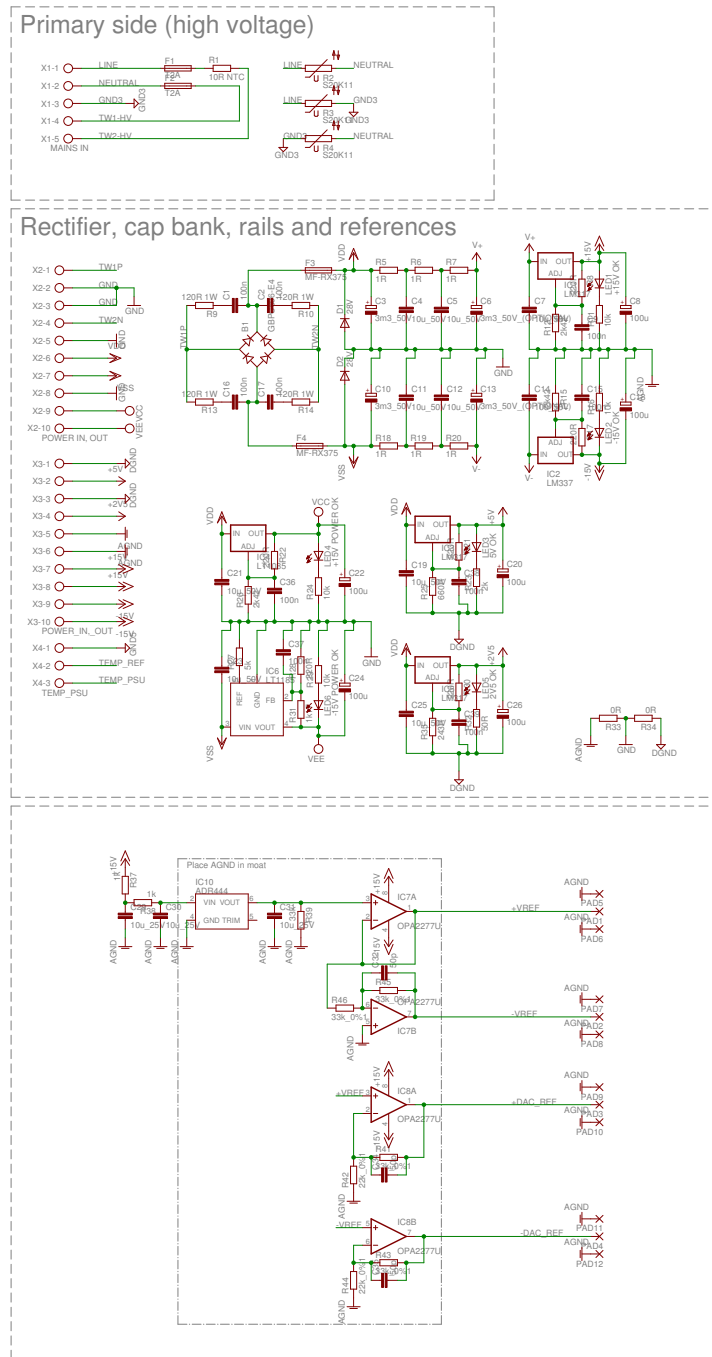


Figure 20: Simplified schematic of the power supply block which supplies power rails and reference voltages for all of the other components.

to generate the four reference voltages $\pm V_{REF}$ and $\pm 2 \cdot V_{REF}$ used for excitation for the sensor and the DAC respectively. Since all four reference voltages are generated from the same source they are all ratiometric to each other, in other words a slowly changing reference voltage will not cause any change in the measurement (if assuming purely linear components that run off the reference voltage). In any case, the ratiometric references increase the robustness of the system with regards to variations in the reference voltage as small changes in the reference voltages will result in negligible changes in the output, which is $V_{signal} / V_{reference}$.

See appendix B for the full schematic and PCB layout which contain more components.

4.2.2.2 Excitation

Figure 21 on the following page illustrates a simplified schematic of the excitation generator used for the capacitive sensor's reference electrodes. $+V_{REF}$ and $-V_{REF}$ (at $\pm 4.096V$) are reference voltages generated from the power supply board and applied to the reference electrodes in the sensor. IC1 is a pair of complementary analog switches that switch between $+V_{REF}$ and $-V_{REF}$ depending on the logic level state of EXC1 and EXC2. R1, R2 and C3, C4 form a passive lowpass circuit to reduce the very highest RF emissions generated by the near-square wave output. Additionally, R1, R2 limit the current flowing out to the sensor, so that a short circuit to ground will not exceed the maximum permissible current through IC1. See appendix B for the full schematic and PCB layout which contain more components.

4.2.2.3 Demodulator

Figure 22 on page 47 illustrates a simplified schematic of the demodulator block which demultiplexes and samples the output from the capacitive sensor. The signal waveform sent out from the sensor, described in section 3.3.1 is received at PAD6 and then split into four different paths via IC2 and IC3, which close SW1 – 4 depending on the waveform state (*Sense+*, *Sense-*, *Reference+*, *Reference-*) which charge C11, C13, C15, C17 through R5, R7, R8, R9 to form a lowpass filter that holds the voltage when SW1 – 4 are open. (i.e. a sample and hold circuit). IC3, IC5, IC7, IC9 are low input bias current operational amplifiers that serve to load the sample and hold capacitors as little as possible. The output from them is both halved¹, buffered and sent to the ADC's on the digital board using RN2, RN4 and IC4, IC8 as well as summed (converted to a single-ended signal) using RN1, RN3 and IC1 which is used for the analog linear controller.

¹ the output voltage from the capacitive sensor is $\pm V_{REF} = \pm 4.096V$, which is greater than the $\pm 2.5V$ range for the ADC's used on the digital board.

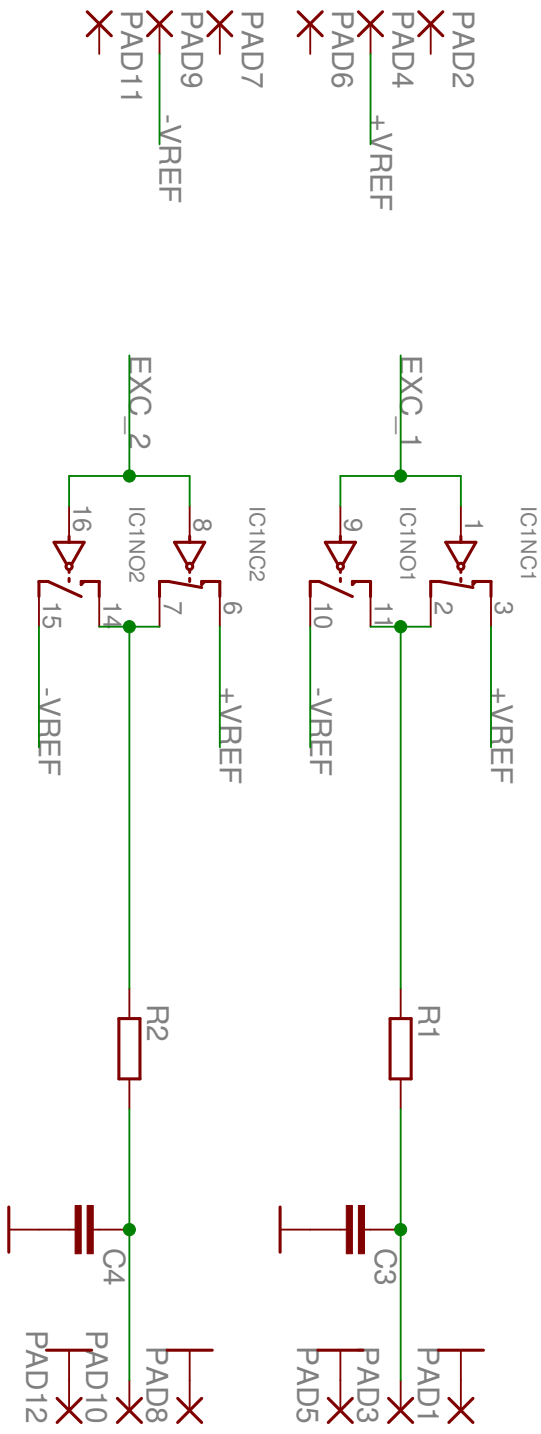


Figure 21: Simplified schematic of the excitation block which generates the reference waveforms for the capacitive sensor.

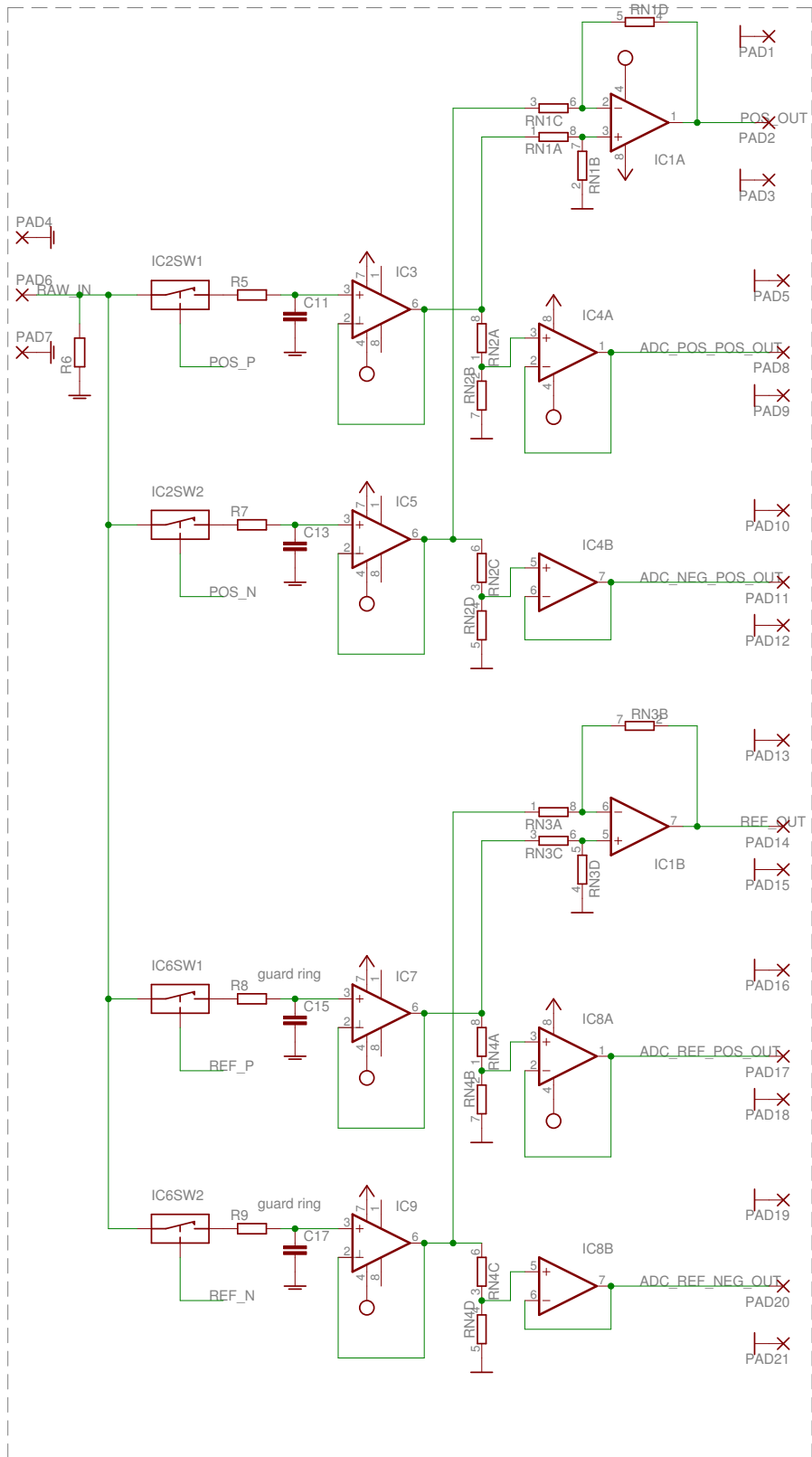


Figure 22: Simplified schematic of the demodulator block which demultiplexes and samples the output from the capacitive sensor.

See appendix B for the full schematic and PCB layout which contain more components.

4.2.2.4 Digital board

Figures 23 on the facing page, 24 on page 50, 25 on page 51 illustrate the simplified schematics of the digital block which handles many aspects of the actuator.

Figure 23 on the next page contains IC102, which is the microprocessor that handles many of the system tasks (among others, excitation and demodulator control, reading ADC's and writing to the DAC, transmitting and receiving data over the external interface) and is an Atmel ATxmega128A3, an 8-bit reduced instruction set computing (RISC) microprocessor with integrated random access memory (RAM) and Flash memories, as well as many other silicon peripherals used in the software described in section 4.3 (Atmel [3]). IC101 is an universal asynchronous receiver/transmitter (USART) to RS232 over USB integrated circuit (IC) that allows for communication between the microprocessor and an external computer. Many of the components in the figure are self-explanatory and/or appear directly in the datasheets for the corresponding components, except for D101 which serves to supply power to IC101 even if the power to the PCB is removed, which ensures that the host operating system does not receive a USB connect/disconnect signal on power cycle, which would quickly become enervating when developing the software. IC103 is a serial-in-parallel-out shift register which is used to drive the LCD display for the user interface. This is done as there was a shortage of input/output (I/O) pins on the microprocessor and the LCD does not require a very fast servicing speed.

Figure 24 on page 50 contains the ADC's and DAC which are used for measuring the current position and writing the setpoint for the analog linear controller. Both the connection to the ADC's and DAC follow the datasheets' recommended connections accordingly (Analog devices [1, 2]). Errors in measurement due to quantization noise and INL are kept low by using high-performance ADC's and DAC's. The ADC has a resolution of 24 bits and a dynamic range of 109dB, the DAC has a resolution of 20 bits and a dynamic range of 120dB. This corresponds to a worst case position quantization error of 1.9nm assuming a travel of $\pm 1mm$, which is deemed to be far enough below the any other sources of error in the system.

Figure 25 on page 51 contains all the components for the user interface, which includes an LCD display, a rotary input dial and a joystick for menu navigation. All inputs are debounced² in hardware with an RC circuit and a Schmitt-input logic inverter. IC502 and IC503. As the number of inputs on the microprocessor is limited a

² "debouncing" is a term for reducing the behavior of a button to oscillate quickly between the on and off state for a limited time when pressed or released.

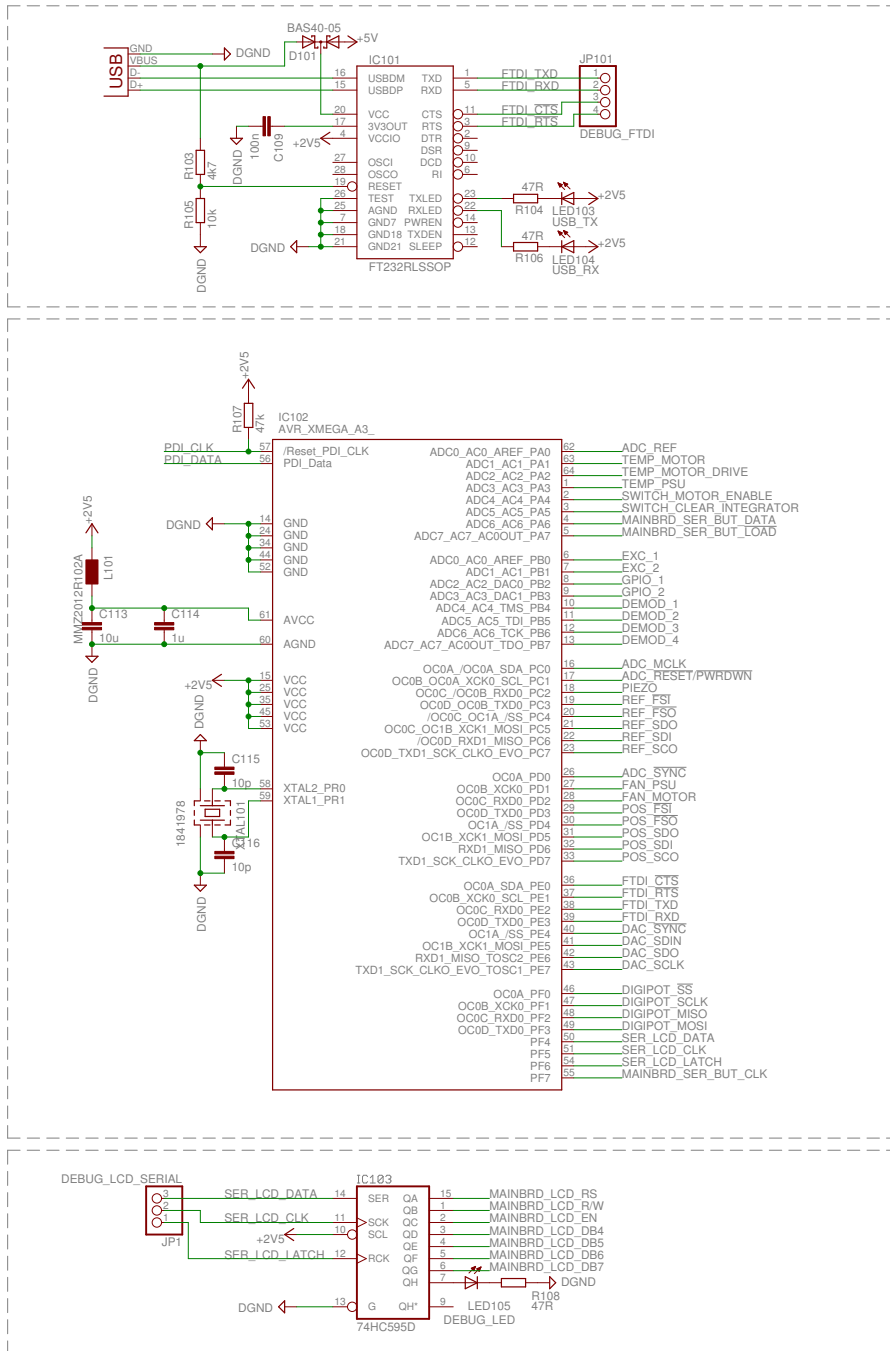


Figure 23: Simplified schematic of part of the digital block, this portion contains the microprocessor, USB/RS232 interface and LCD shift register.

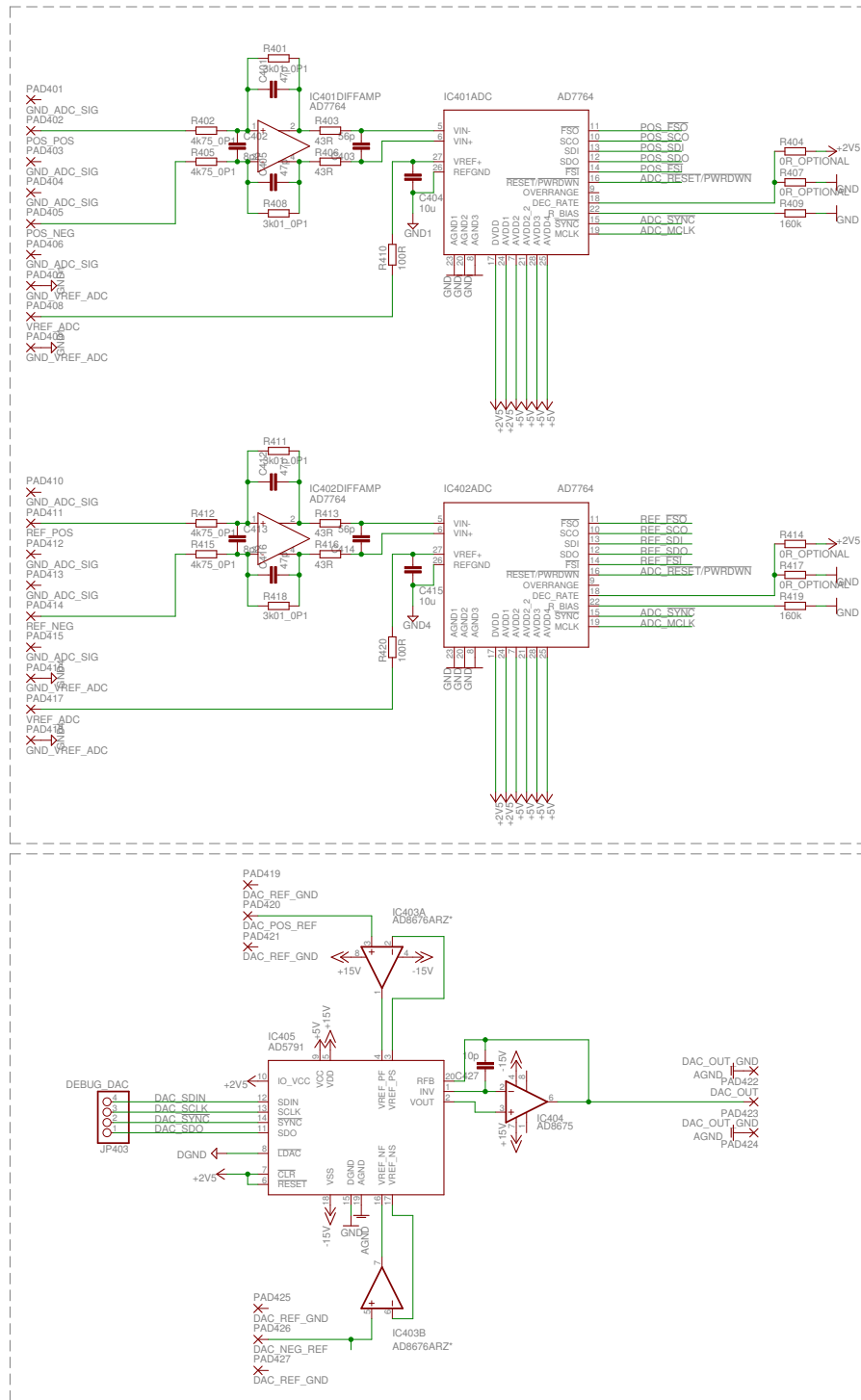


Figure 24: Simplified schematic of part of the digital block, this portion contains the ADCs and DAC for reading the current position and setting the linear analog controller's setpoint.

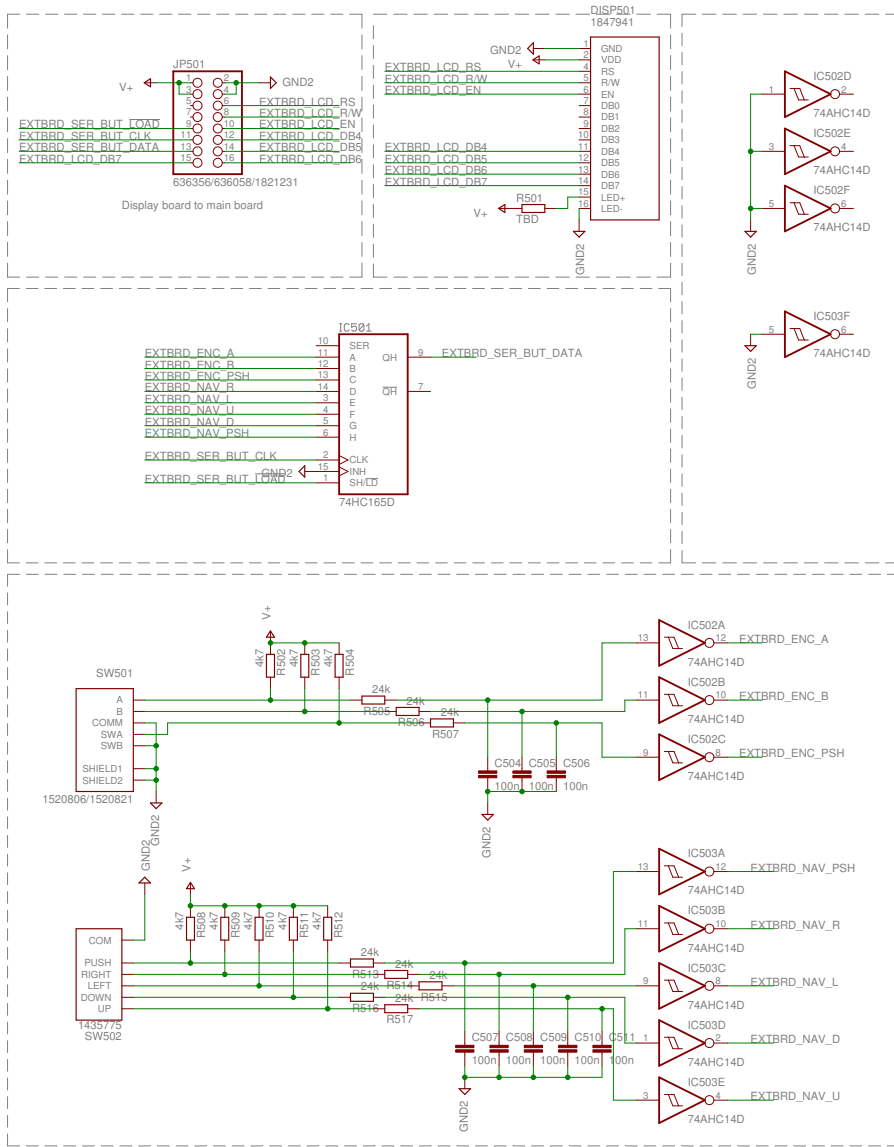


Figure 25: Simplified schematic of part of the digital block, this portion contains all electronics to do with the user interface, such as the LCD display, rotary input dial and joystick.

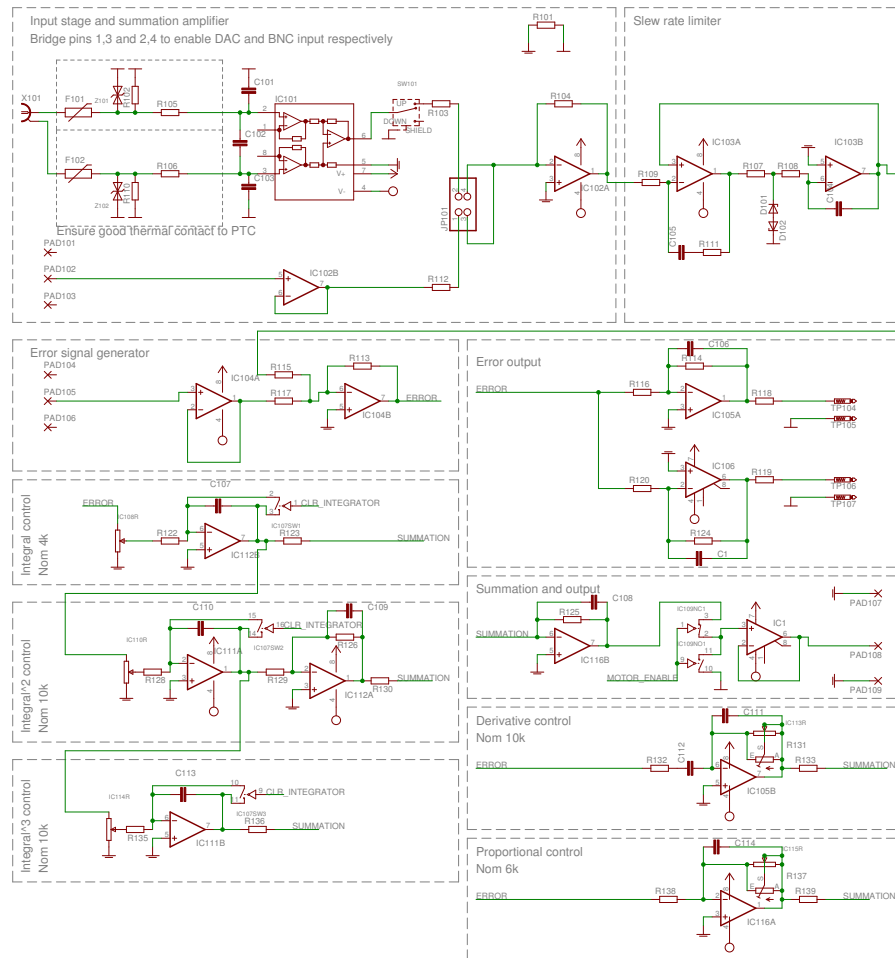


Figure 26: Simplified schematic of the analog linear controller block which generates the control signal to the motor drive.

parallel-in-serial-out shift register (*IC501*) is used to reduce the pins needed. Since the buttons only need to be checked relatively seldom this performance penalty is not important.

See appendix B for the full schematic and PCB layout which contain more components.

4.2.2.5 Controller

Figure 26 illustrates a simplified schematic of the analog linear controller block which generates the control signal to the motor drive. The input to this block is the summed, single-ended output from the demodulator, the output from the DAC on the digital board and an optional BNC input for external analog setpoint control. The output from this board goes directly to the motor drive. The signal flow from input to output is roughly as follows;

- The setpoint is generated using the top two dashed-line blocks, the left block sums the DAC output and the external analog

setpoint, with a fully differential receiver for the external input in order to remove any ground-loops. The right block limits the slew rate of the signal, if too fast a setpoint change is applied $IC103A$'s output will start $D101, D102$ conducting, limiting the voltage on $R108$. This will cause a constant current to travel through $R108$, leading to a constant current through $C104$ and a linearly rising/falling ramp out from $IC103B$. $C105$ and $R111$ form a stabilizing network for $IC103$ to ensure stability, as there is otherwise enough phase delay from the positive feedback from $IC103B$ to cause oscillation. Once the inverting and non-inverting inputs of $IC103A$ are at the same voltage the output from $IC103A$ will be zero, causing $IC103B$ to maintain a constant voltage. Note that in the steady-state the output voltage from $IC103B$ will only differ from the input voltage with the offset voltage of $IC103A$, with the amplifiers chosen this is only $10\mu V$ (Texas Instruments [14]).

- The error ($Process\ variable - Setpoint$) is generated in the block titled "Error signal generator", which is simply a summing amplifier connection. The error is fed into each of the linear blocks that correspond to $K_d, K_p, K_i, K_{ii}, K_{iii}$. Additionally, a test-point for the error outputs is created with 100 and 1000 gain in the block "Error output". This is used primarily for development purposes to measure the error signal.
- The blocks "Integral control", "Integral² control", "Integral³ control", "Derivative control", "Proportional control" are the analog circuit implementations of the desired corresponding linear elements. A digital potentiometer, controlled by the microprocessor, can set the gains of each stage. Additionally, there is an analog switch to disable the integrators ($IC107$) for development purposes.
- The "Summation and output" block sums the output from each of the linear control blocks and outputs a low-impedance output to the motor drive board. There is a switch to disable the output while starting up the system and as a safety if an error state occurs (such as the sensor exceeding the allowed travel range).

Note that there are several lowpass filter stages present, this is to limit the bandwidth, primarily from the derivative output which is particularly sensitive to the process and thermal noise from the previous stages. The bandwidth of the filters must be high enough to give sufficient performance, yet low enough to not feed too much noise through the system.

See appendix B for the full schematic and PCB layout which contain more components, as well as a SPICE simulation of the slew-rate limiting block.

4.2.2.6 Motor drive

Figure 27 on the next page illustrates a simplified schematic of one channel of two of the the motor drive board. The input voltage arrives from the controller board, which corresponds to a desired force. This is a high-power transadmittance converter (i.e. voltage to current). The initial voltage divider $R12, R15$ scales the output voltage from the controller board to a level suited for the motor drive. The amplifier $IC1$ is essentially a non-inverting gain configuration. $R1, R2$ and $Q1, T1$ form a current-boost stage. $R1$ and $R2$ are chosen so that the voltage drop across them due to the quiescent current in $IC1$ causes around a $0.3V$ drop over them. If the current output from $IC1$ rises the voltage drop over $R1$ or $R2$ will increase until $Q1$ or $T1$ start conducting current. As the transistors are connected in a Darlington manner the current amplification is of the order of 10000, boosting the maximum output current from $IC1$ greatly. The signals $LOAD_A_P$ and $LOAD_A_N$ are connections for the motor. $R5$ is a low-inductance resistor for measuring the current through the motor. As this is connected to the inverting input of the amplifier the steady-state output of the amplifier is;

$$I_{out} = \frac{V_{in}}{R5}$$

Note the additional components $C1, C2, R4, R13, C13, R3$ are needed to stabilize the amplifier, which would oscillate without them. ($C1$ and $C2, R4$ act as high-frequency shunts to increase the phase margin, $R13, C13, R3$ lowpass filters the measured current over $R5$ to reduce noise effects). Additionally, $D1, D2, D3, D4, Z1, Z2$ are added to reduce the risk of an inductive voltage spike due to the very high inductance of the load and high slew rates applied.

Note that as the load is mostly inductive a step in voltage input would correspond to a step in desired current, which is not possible due to the continuous nature of current in an inductor. This will cause $IC1$ to rail, feeding a ramping current into the load, until the desired current is achieved.

See appendix B for the full schematic and PCB layout which contain more components, as well as SPICE simulations of a couple of input signal test cases.

4.3 SOFTWARE IMPLEMENTATION

See figure 13 on page 30 for a simple overview of the basic functionality of the microprocessor. As was specified in section 4.2.1 the microprocessor handles much of the sensor, it handles the excitation control and the demodulator. Additionally it also must drive the two ADC's and the DAC, adjust the controller gains, drive the user interface and handle external communications.

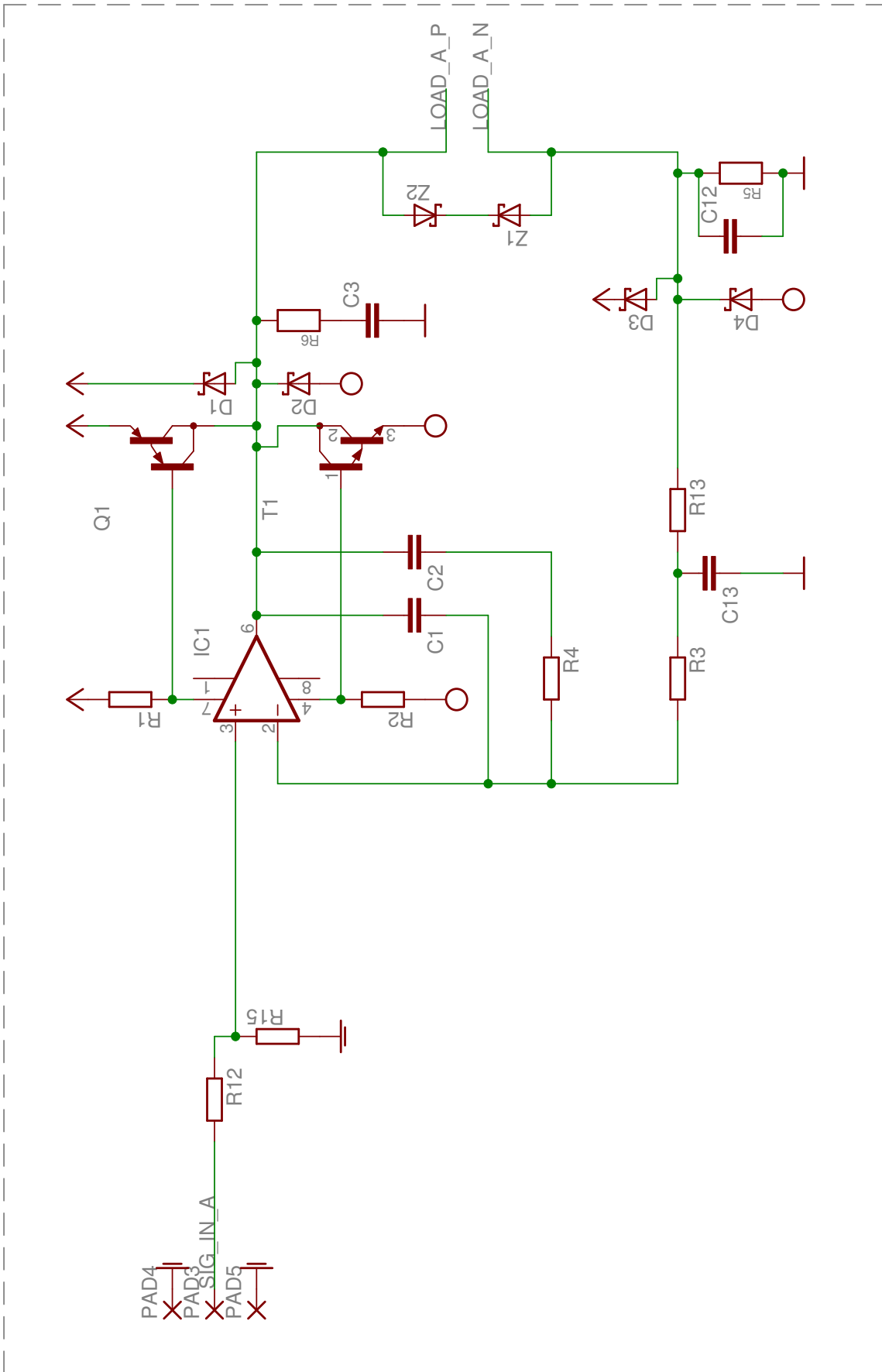


Figure 27: Simplified schematic of the motor drive block which drives the motor for the actuator.

The microprocessor is a RISC based Harvard architecture 8-bit single-chip microprocessor, more specifically an Atmel ATxmega128a3 (Atmel [3]). The software is written in fairly standard C code and can be found in an unpublished paper distributed alongside this thesis (Lock [11]).

The microprocessor has to handle a great number of functions in pseudo-real-time with varying priorities. The priority list is handled by gratuitous use of interrupts of multiple priorities and an infinite main loop, with the following functions performed;

HIGH The most time-critical operations are excitation waveform (the two square-wave reference signals mentioned in subsection 3.3.1) and demodulator control (the sample and hold filter in subsection 3.3.2). This thread is called at specific time intervals and the corresponding output control signals are set to drive the excitation and demodulator control lines.

MEDIUM When a message is received from the external digital hardware connected to the microprocessor (from the ADC's, DAC, USB/RS232 interface) an interrupt is generated and the message is stored in a FIFO buffer for later use. Additionally, data from the output buffer to the DAC is sent at a certain time interval.

LOW At a specific time interval, faster than the sampling speed of the ADC's and the external interface, the buffers are read, data may be sent to the external interface, and linear analog controller coefficients may be adjusted. This is the main "heartbeat" of the microprocessor and where much of the data shuffling takes places.

MAIN The main loop is run continuously whenever another interrupt is not running. It checks the current button status on the front panel of the controller (used for manually controlling the setpoint etc.), writes data to the LCD data display, checks the temperature of various components, turns cooling fans on and off respectively and controls the system buzzer (used for warnings and other status messages).

Part V

RESULTS

RESULTS

This section contains all measured parameters of the system. Several scalar parameters were measured as shown in [Table 2 on the next page](#). Parameters more suited to plots are shown in [section 5.2](#). Additionally, several position setpoint waveforms have been generated and tested to evaluate the performance of the system. These waveforms are:

ZERO A constant (zero) setpoint, for testing the noise level of the system

SQUARE A square-wave setpoint, designed to test the effectiveness of the slew-rate limiter

TRIANGLE Triangle waveform, this should result in a constant-velocity motion

SINE Sine-wave test signal, offers a smoother function than a triangular waveform

POLYNOMIAL Several polynomial waveforms, with 0,1, and 2 continuous derivatives with regards to position to offer various degrees of smoothness

The waveforms are tested at two different amplitudes, one large-scale at a lower speeds and one with a lower amplitude and higher speed. The results of the tests are shown in [figures 28 on page 61](#) through [50 on page 87](#) in this section with plots of the desired, measured, and error in position velocity and acceleration as well as an occasional enlargement of certain regions. Note that in many of the graphs the actuator seems to exhibit non-causal behavior. This is because the position and setpoint waveforms are time-shifted in post-processing to maximize the cross-correlation to make it easier to view the results.

Table 2: Scalar measured parameters of the system.

PARAMETER	VALUE
Throw	+1.159154, -1.030394 [mm]
Force (motor, maximum)	3.36 [N]
Capacitive sensor waveform period	58 [μs]
Analog linear controller bandwidth	Two poles at 3.5 [kHz]
ADC sample rate	1.9531 [kHz]
DAC sample rate	2 [kHz]
RMS error for a zero setpoint	62 [nm]
Motor driver voltage/force relationship	3.86 [V/N]
Net mass (payload and actuator)	44 [g]
Linear controller coefficients ($K_d - K_{\beta}$)	516, 84, 441, 69, 4 [unitless]

5.1 WAVEFORM TESTS

5.1.1 Zero setpoint

Figure 28 on the facing page shows the result of applying a zero setpoint to the controller and measuring the actuator position. As can be seen there is a constant offset of $\approx -150nm$ due do offset voltages in the operational amplifiers and, more importantly, noise in the measured position. Assuming an error of $62nm$ gives a system resolution of one part in 32000, roughly 15 bits of resolution, or a system signal to noise ratio (SNR) of $90.2dB$.

Studying the figure one can see that the noise is primarily of one fundamental frequency with some overtones (speculation on the cause of this in section 6). If these frequencies are ignored or could be removed the noise floor level would become much more flat over frequency and the total noise level would reduced by a factor of roughly 3, which would give an RMS error in the region of $20nm$. This would correspond to a system resolution of one part in 100000, 16.6 bits of resolution, or an SNR of roughly $100dB$.

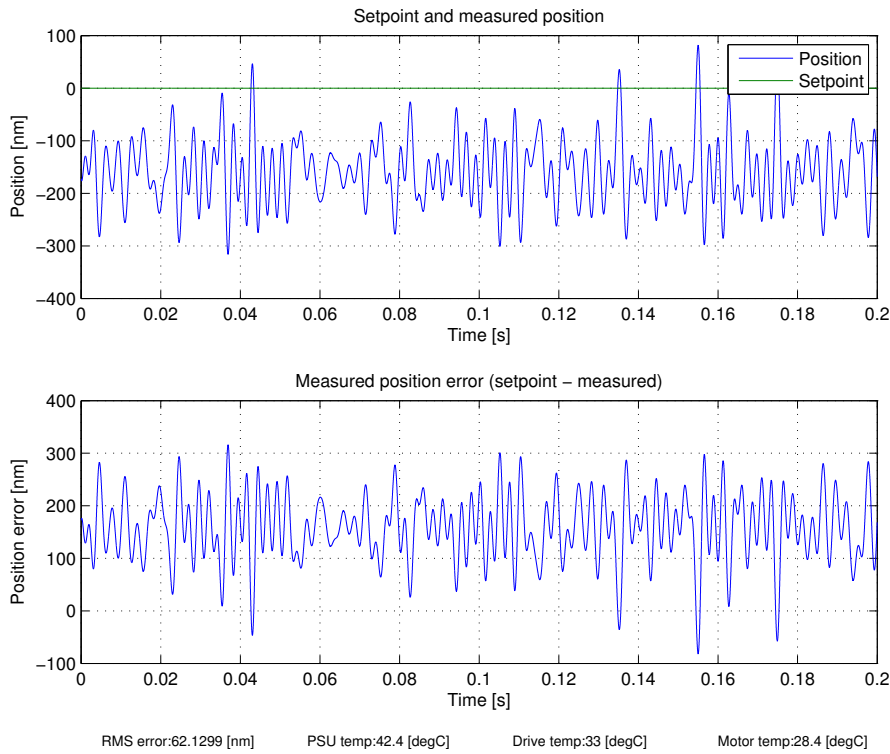
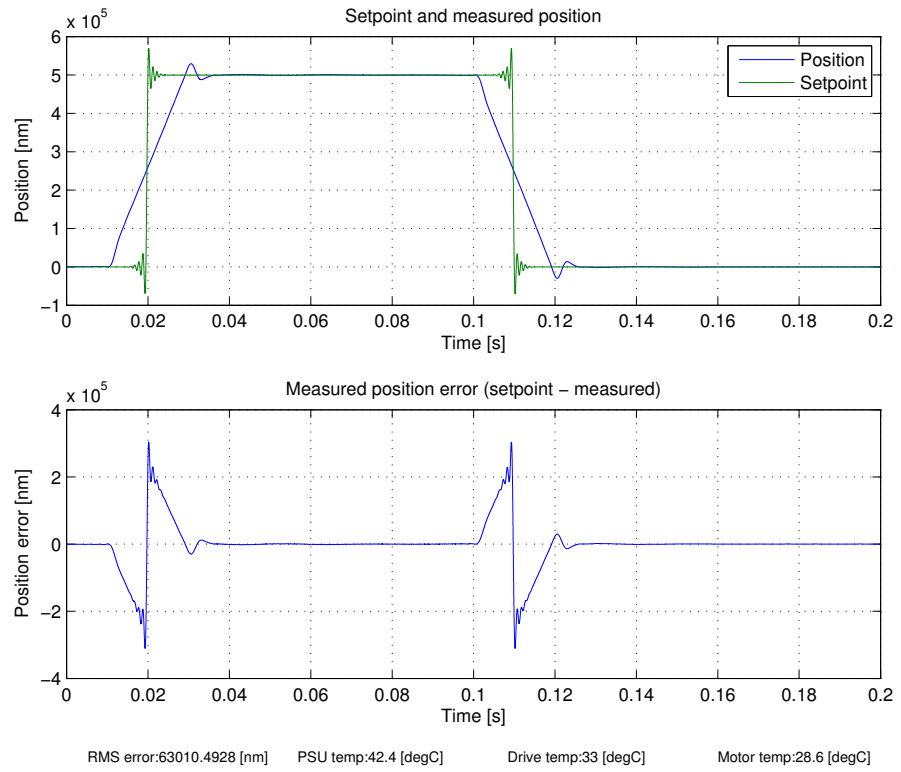


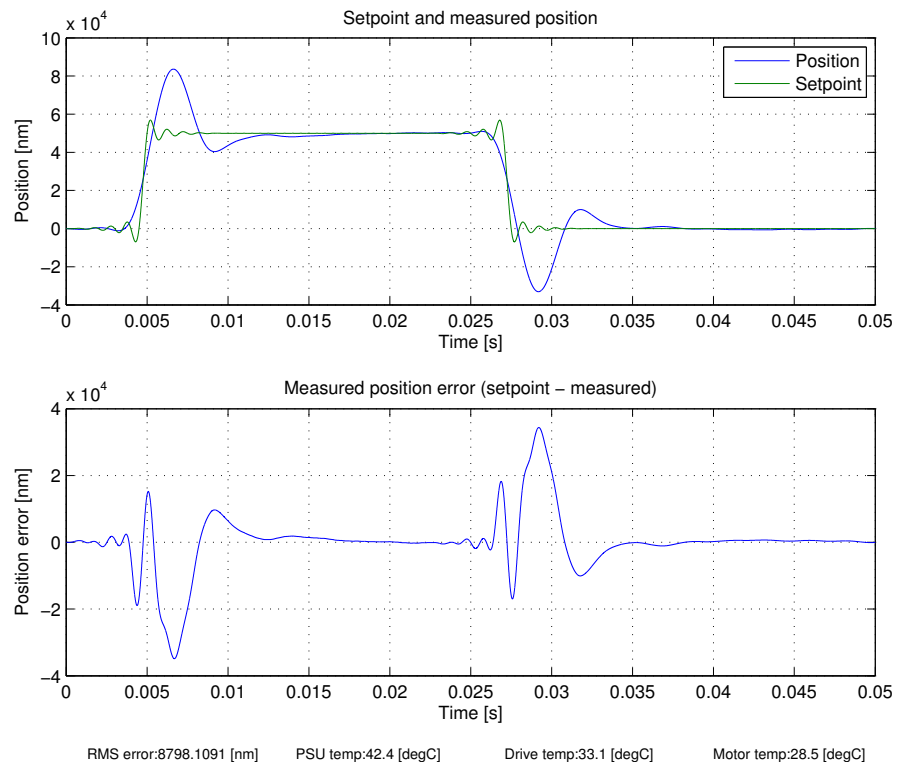
Figure 28: Zero setpoint, showing the RMS error of 62nm and a constant offset.

5.1.2 Square setpoint

A square-wave waveform illustrates the effect of the slew-rate limiter in the system. Shown in figures 29 on the next page through 32 on page 65 are the position through acceleration of a square-wave trajectory. It is particularly apparent in the large-scale motion that the position of the actuator linearly ramps between the two setpoints, with a slight overshoot primarily due to the slew-rate limiter's overshoot (see figure 82 on page 125). However, the position quickly stabilizes towards the desired value as seen in figure 30 on page 63, with a slight oscillation due to the controller. The plots for velocity and acceleration reveal that a square-wave setpoint results in a commanded velocity and acceleration that are very difficult to achieve, with near delta-function like velocity and acceleration. This makes it hard to follow a square wave excitation accurately.



(a) Large-scale motion.



(b) Small-scale motion.

Figure 29: Position measurement for square wave setpoint.

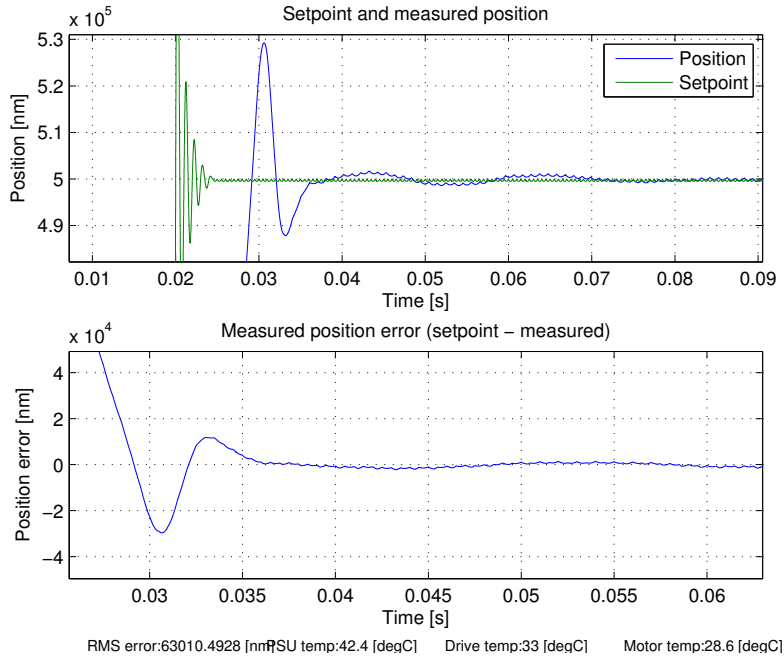
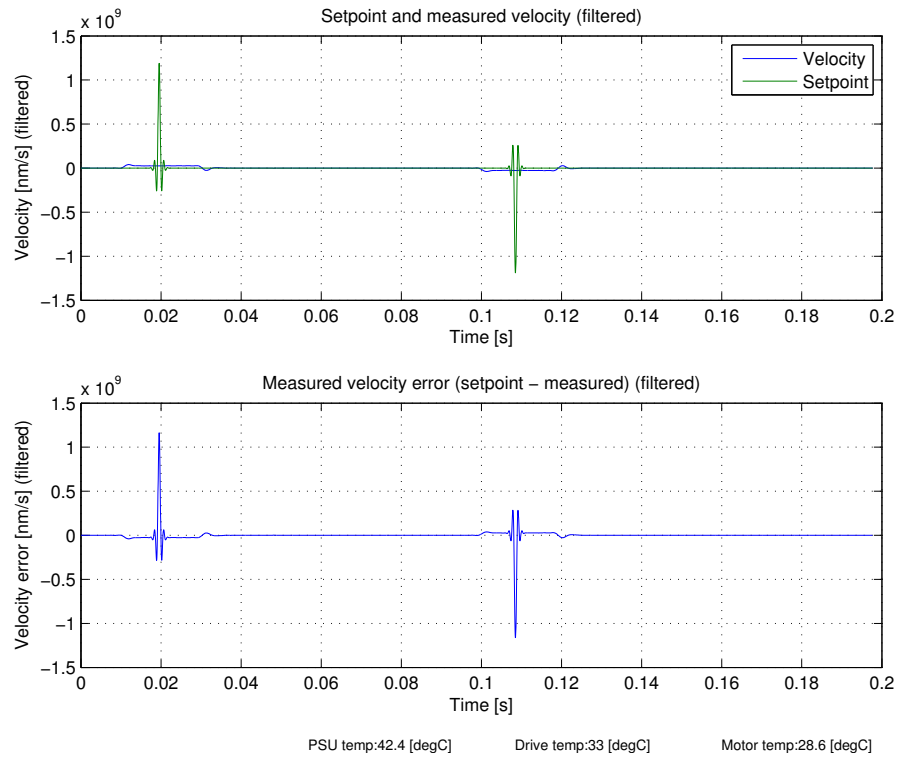
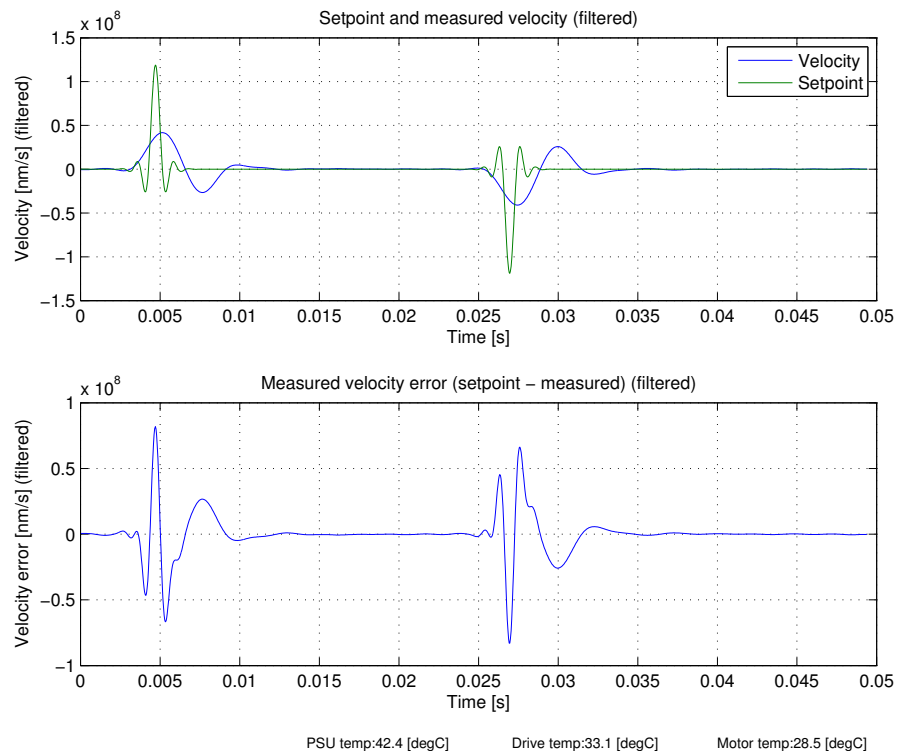


Figure 30: Enlargement of position measurement for square wave setpoint and large-scale motion.

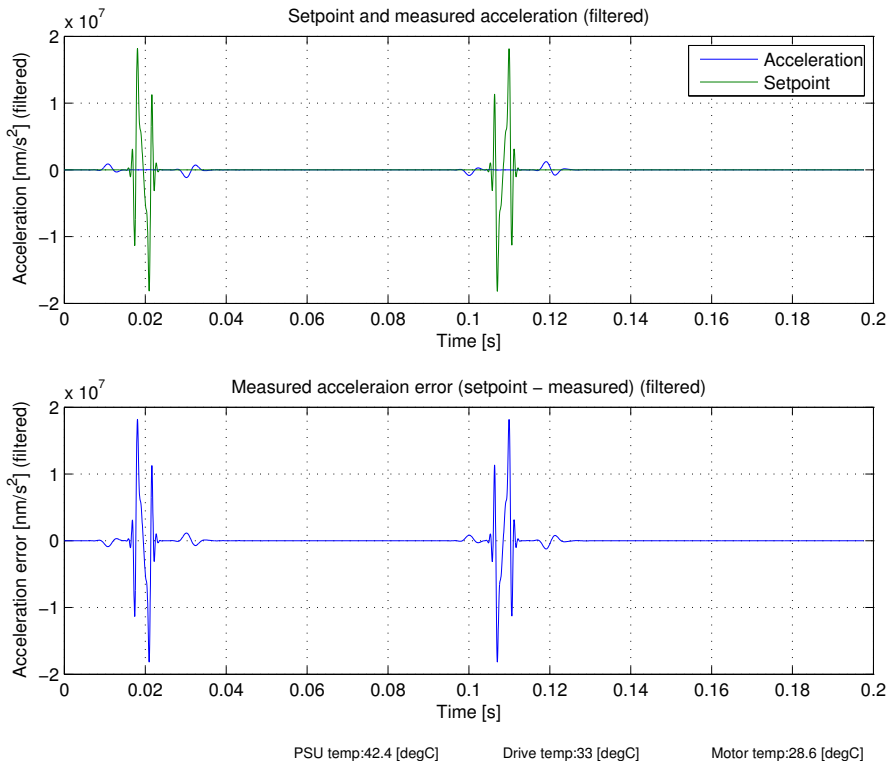


(a) Large-scale motion.

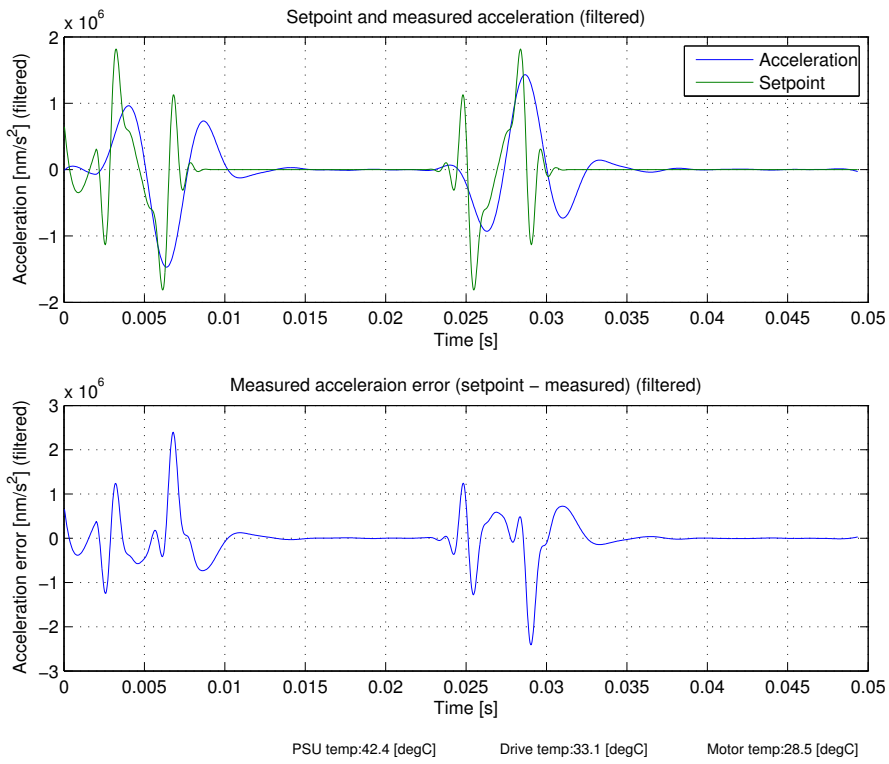


(b) Small-scale motion.

Figure 31: Velocity measurement for square wave setpoint.



(a) Large-scale motion.

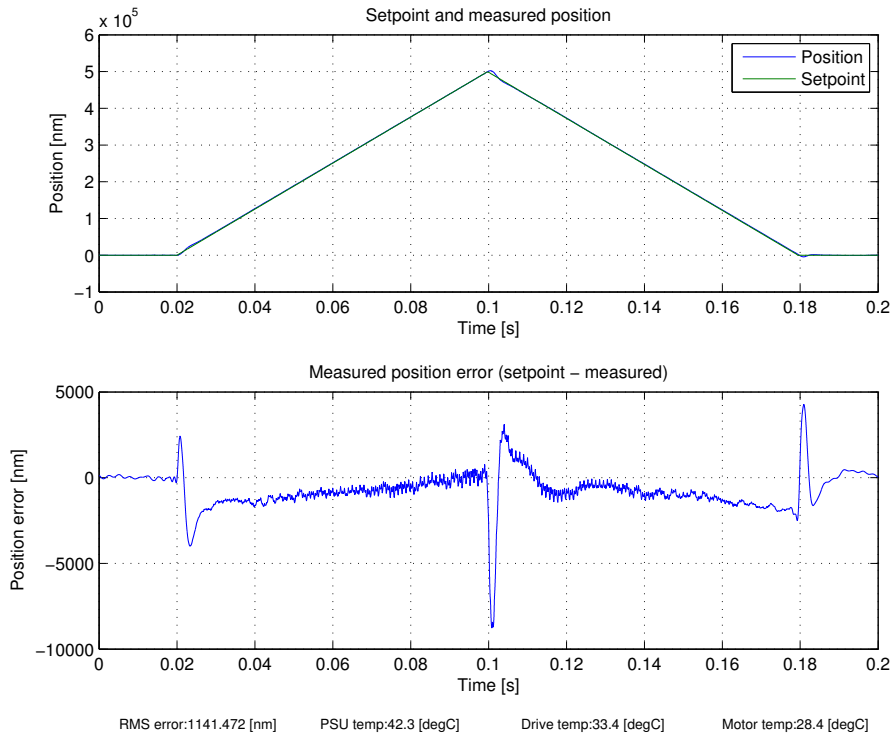


(b) Small-scale motion.

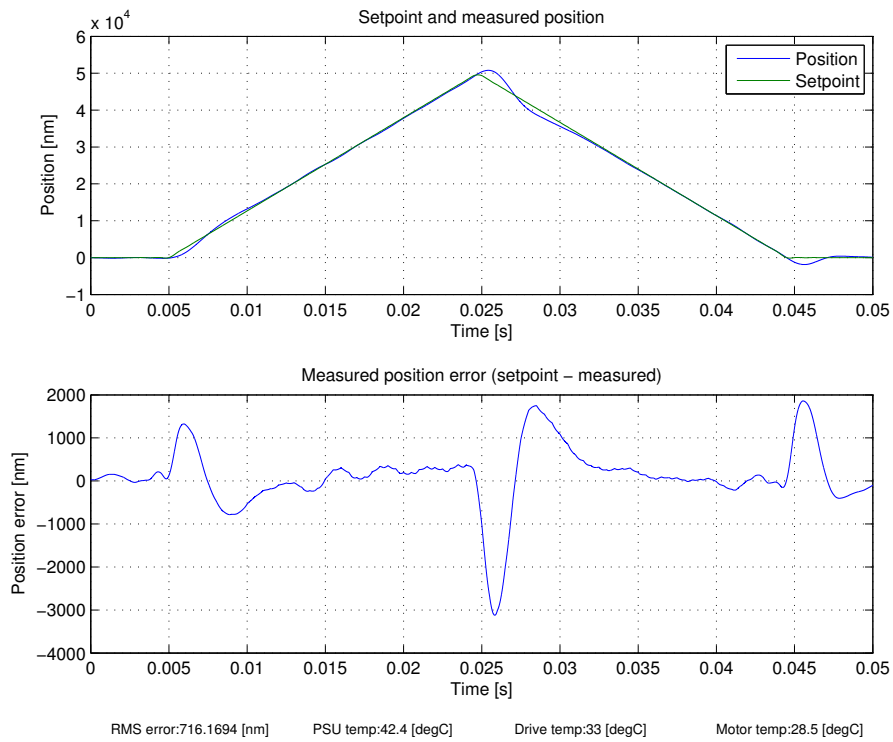
Figure 32: Acceleration measurement for square wave setpoint.

5.1.3 *Triangle setpoint*

The triangle waveform is a more feasible setpoint waveform, in that it does not result in a requested instantaneous change in position. Figures 33 on the next page through 35 on page 69 show the position through acceleration for a triangle setpoint. As can be seen the error is small except for the regions with discontinuous velocity. Note that as the output to the actuator is a force the output required to drive a hypothetical actuator without any springs or friction would be an impulse at each velocity discontinuity and zero otherwise. The actuator coasts at a constant velocity until the next impulse. The real-world actuator however does have some non-ideal behavior, since the motor must push against the flexure suspension. As the motor force is non-linear for a given current over position this is believed to be the main cause of error in the large-scale motion position plot. The plots of velocity and acceleration clearly show similarities to the piecewise constant velocity and delta-function like acceleration profiles that the ideal actuator without flexure would exhibit.

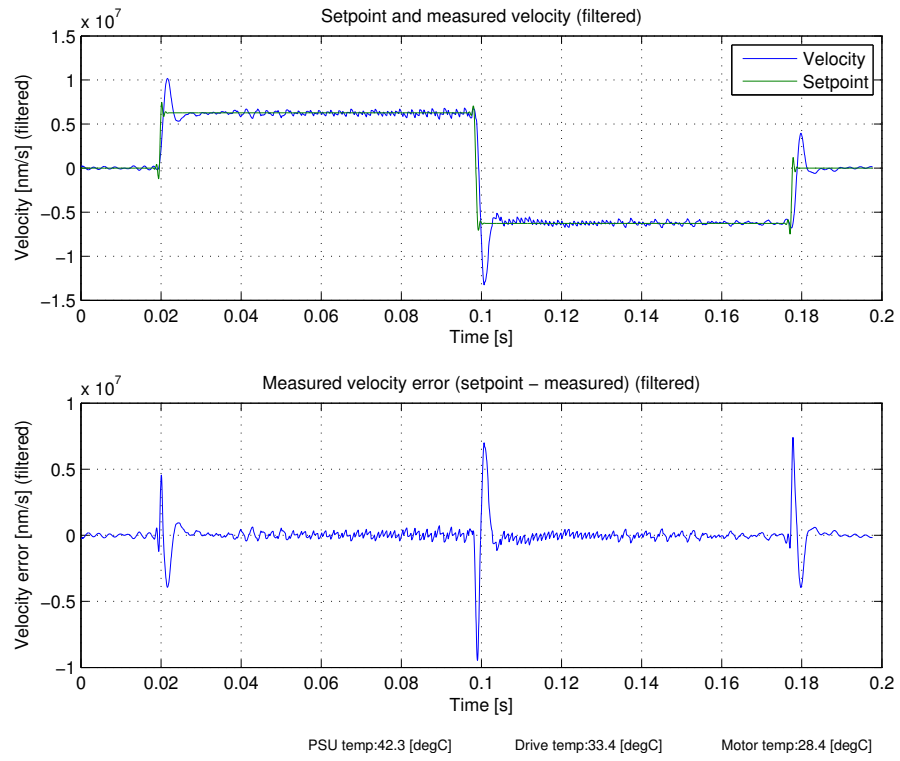


(a) Large-scale motion.

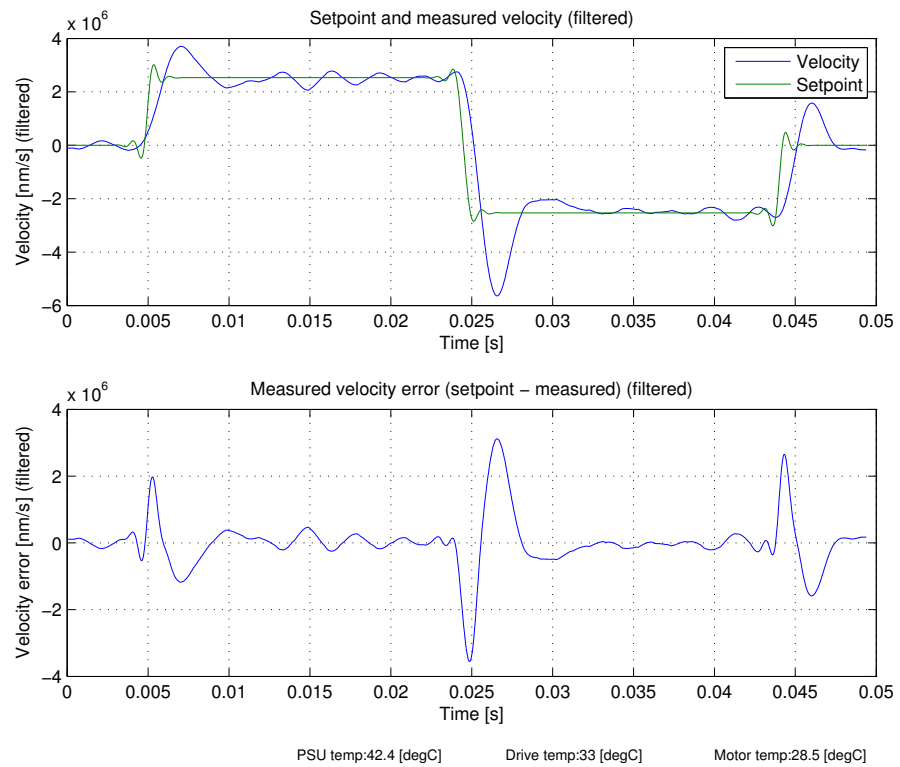


(b) Small-scale motion.

Figure 33: Position measurement for triangle wave setpoint.

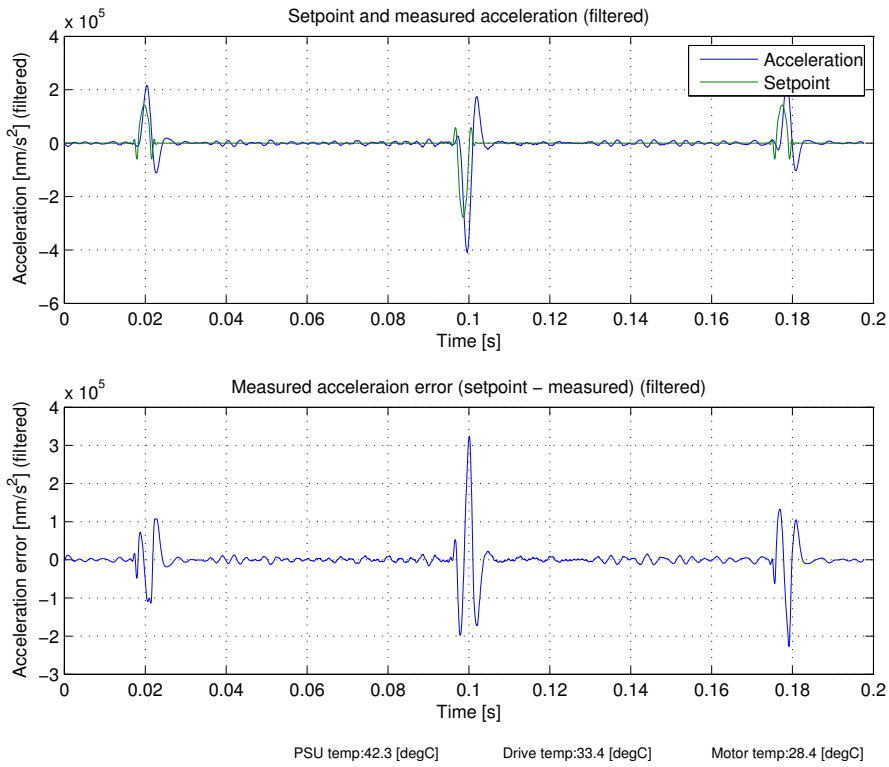


(a) Large-scale motion.

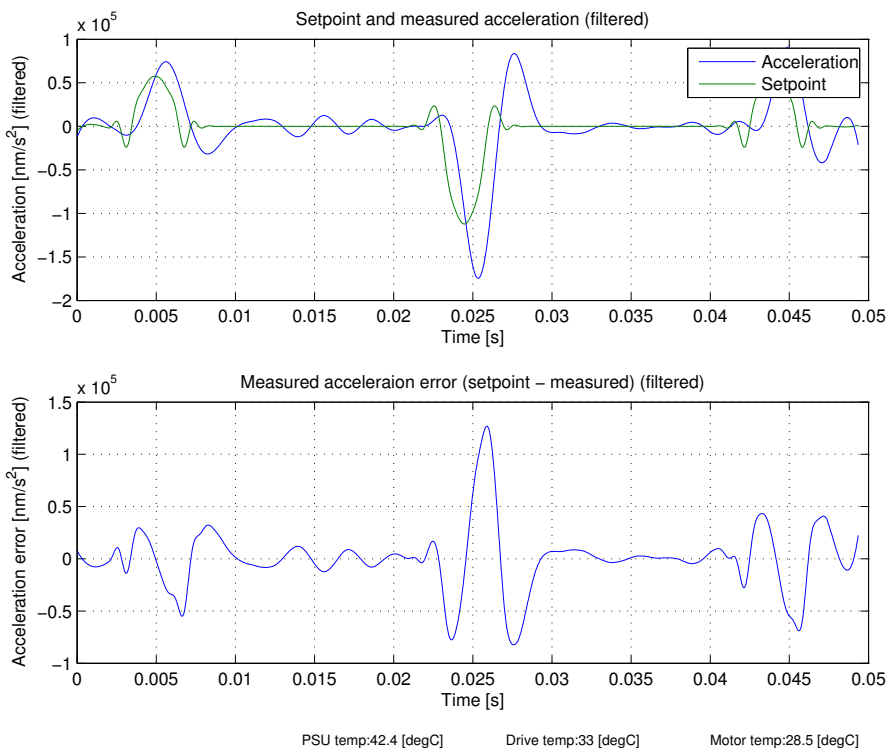


(b) Small-scale motion.

Figure 34: Velocity measurement for triangle wave setpoint.



(a) Large-scale motion.

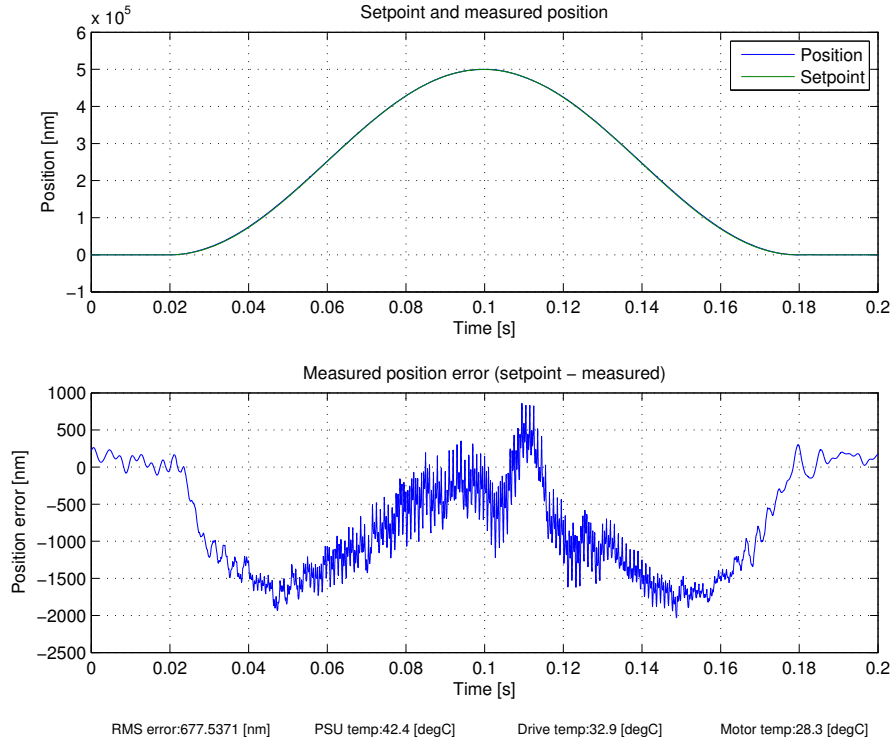


(b) Small-scale motion.

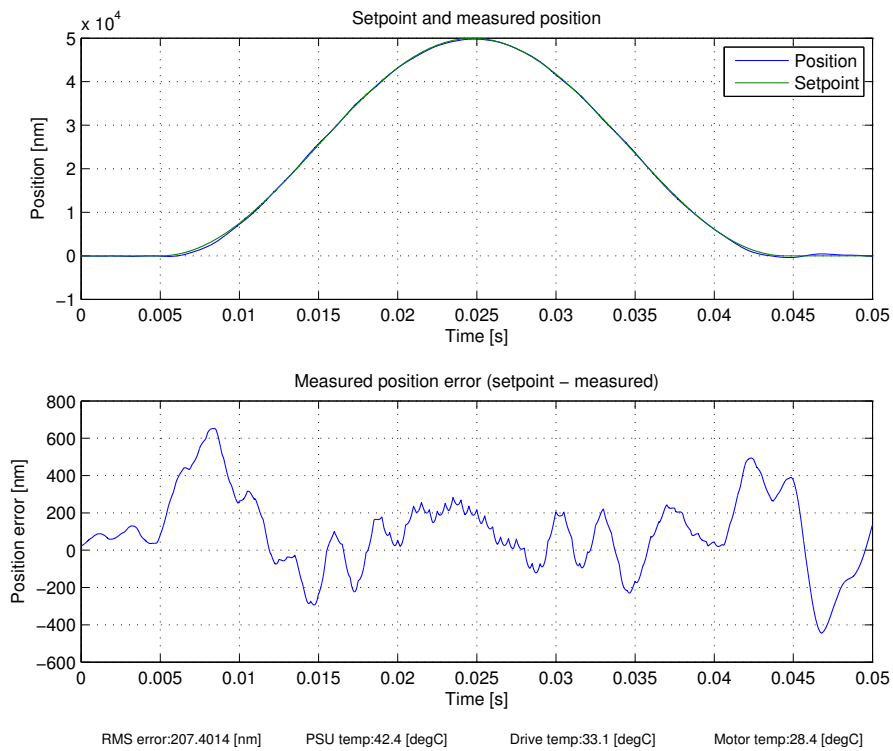
Figure 35: Acceleration measurement for triangle wave setpoint.

5.1.4 *Sine setpoint*

A sine setpoint waveform is an implementation of a smoother trajectory to follow. Figures [36 on the next page](#) through [38 on page 73](#) show the position through acceleration of a sine setpoint. Figure [36a on the next page](#) shows the maximum error is reduced compared to the triangular waveform. The anomaly in the error plot in figure [36a on the facing page](#) at time 105 – 120ms is believed to be caused by a mechanical defect, probably friction between the actuating rod and a static part of the actuator, as a similar anomaly can be seen at this position on the other plots (though not as prominently). While the sine waveform is relatively smooth, it is not perfect as the acceleration is discontinuous at the start and end of the waveform, causing much of the error at the start and end of the sine wave path.

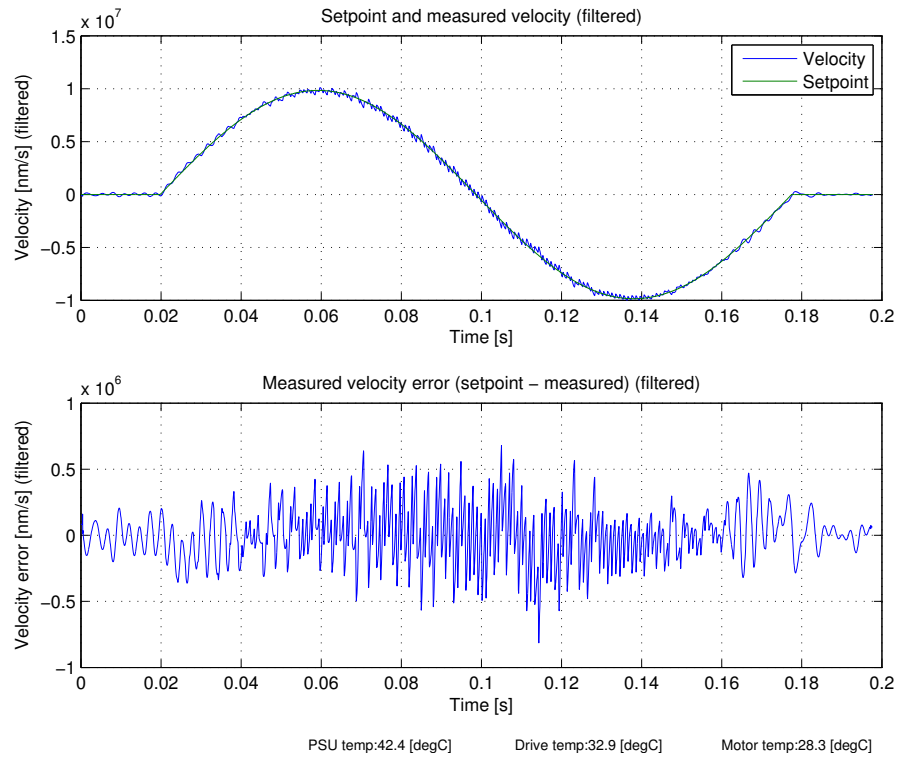


(a) Large-scale motion.

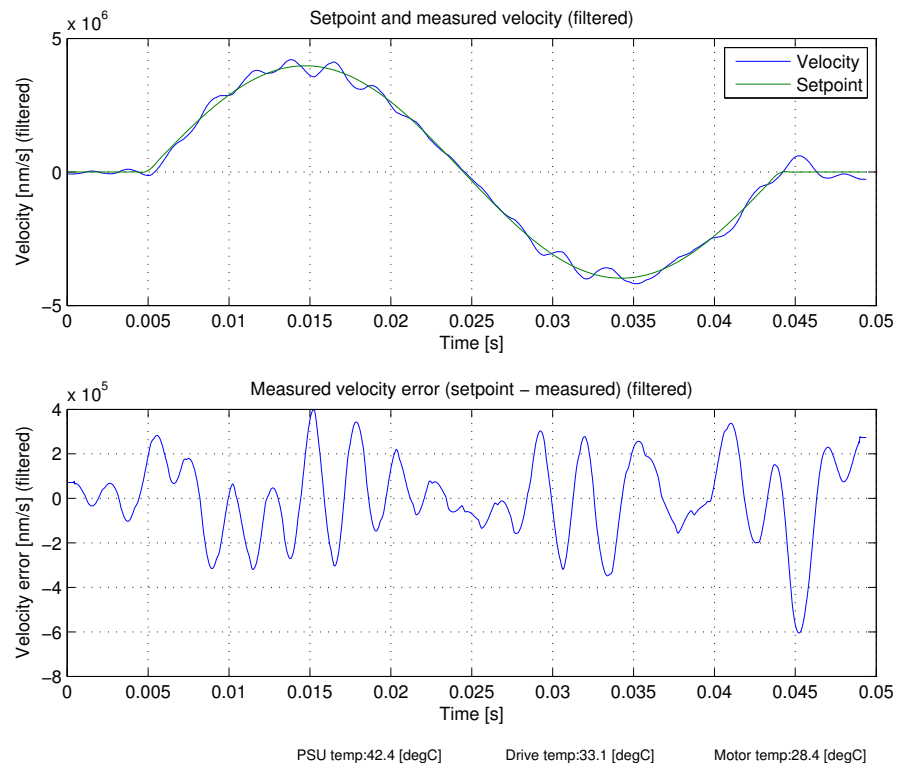


(b) Small-scale motion.

Figure 36: Position measurement for sine wave setpoint.

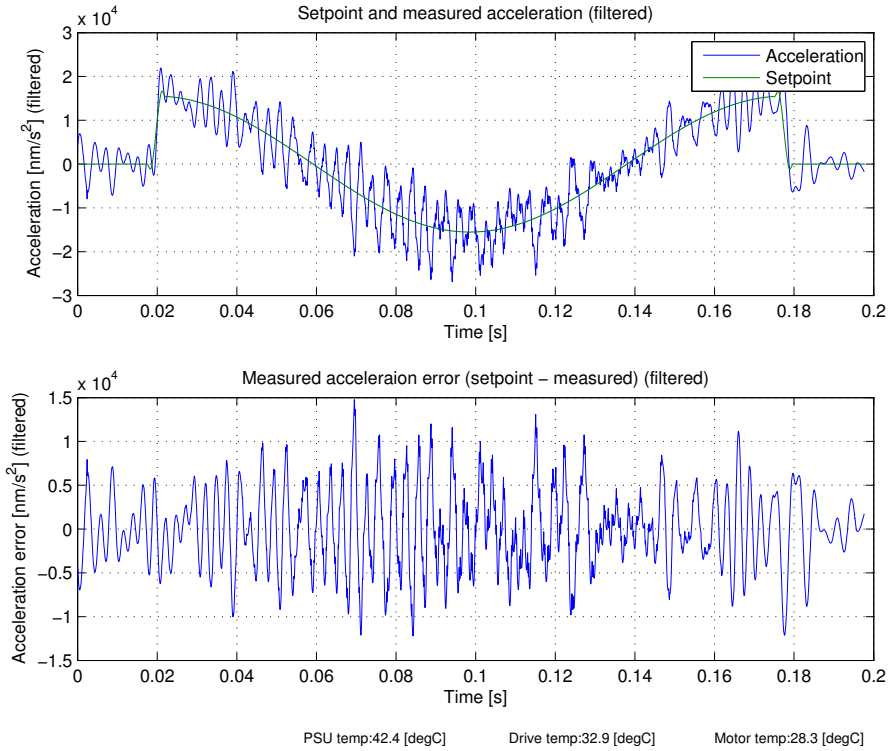


(a) Large-scale motion.

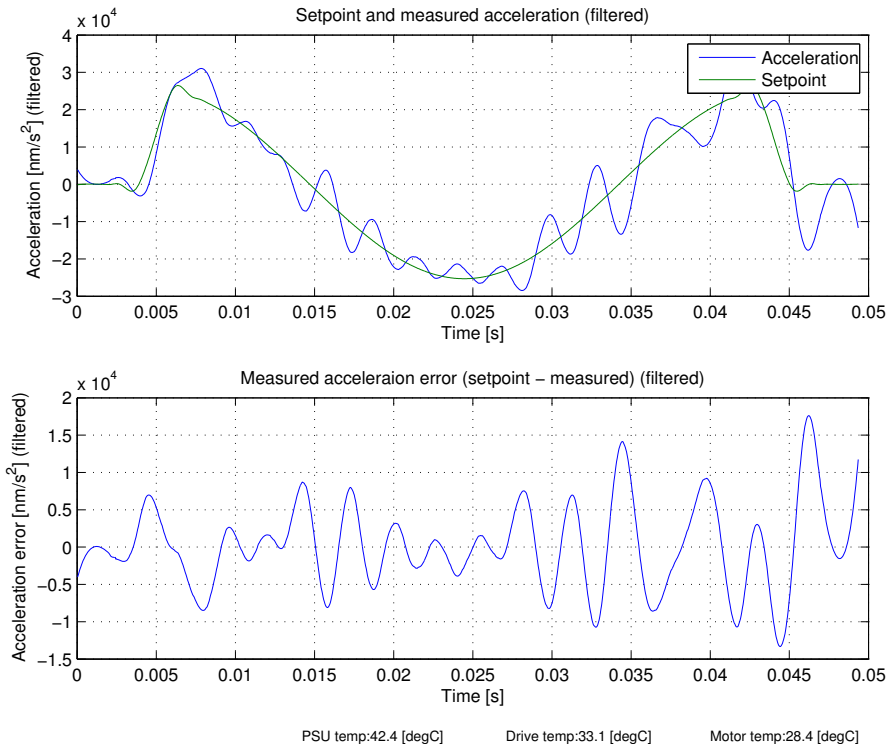


(b) Small-scale motion.

Figure 37: Velocity measurement for sine wave setpoint.



(a) Large-scale motion.



(b) Small-scale motion.

Figure 38: Acceleration measurement for sine wave setpoint.

5.1.5 Polynomial setpoints

The polynomial waveforms are three different waveforms with a varying number of continuous derivatives with respect to position (0,1, or 2). These were created in an attempt to implement a very smooth trajectory that would be easy to follow with a low error.

The three polynomials used are defined as

$$\begin{aligned} p_2(t) &= a_4t^4 + a_3t^3 + a_2t^2 + a_1t \\ p_1(t) &= k_1\dot{p}_2(t) \\ p_0(t) &= k_0\ddot{p}_2(t) \end{aligned}$$

such that

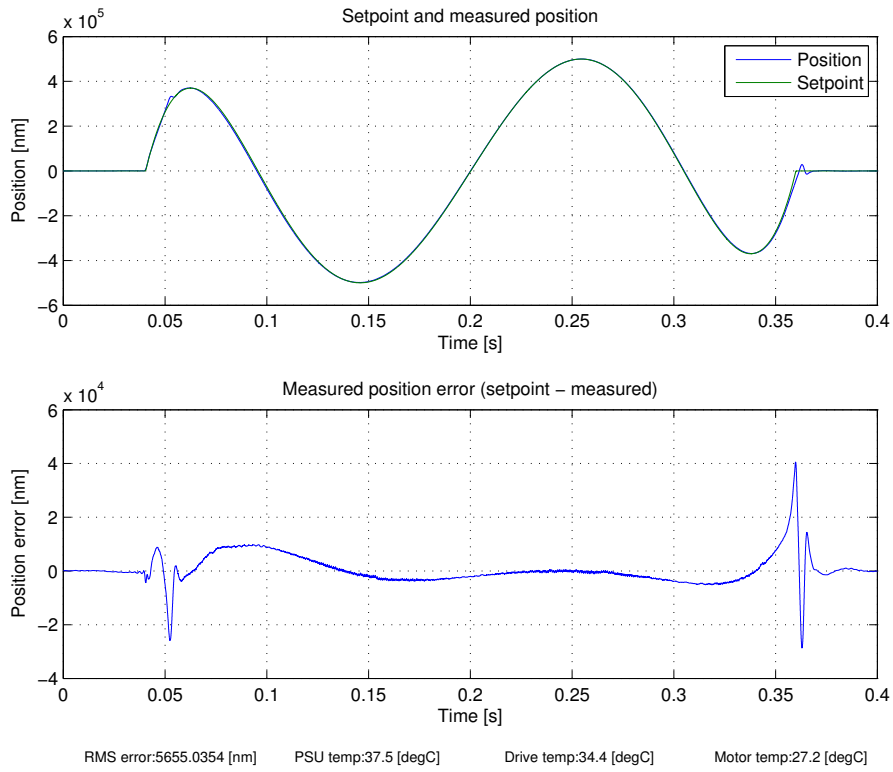
$$\begin{aligned} p_2(0) &= p_2(T) = 0 \\ \dot{p}_2(0) &= \dot{p}_2(T) = 0 \\ \ddot{p}_2(0) &= \ddot{p}_2(T) = 0 \\ \max(p_2(t))_0^T &= A \\ \max(p_1(t))_0^T &= A \\ \max(p_0(t))_0^T &= A. \end{aligned}$$

In other words, polynomial 2 ($p_2(t)$) is defined to have some maximum amplitude $A \neq 0$ and have zero position, velocity and acceleration and time $t = 0$ and $t = T$. Polynomials 1 and 0 ($p_1(t)$, $p_0(t)$ respectively) are generated from polynomial 2 and are scaled after the derivation operator to have an equal amplitude by setting k_1 and k_0 respectively.

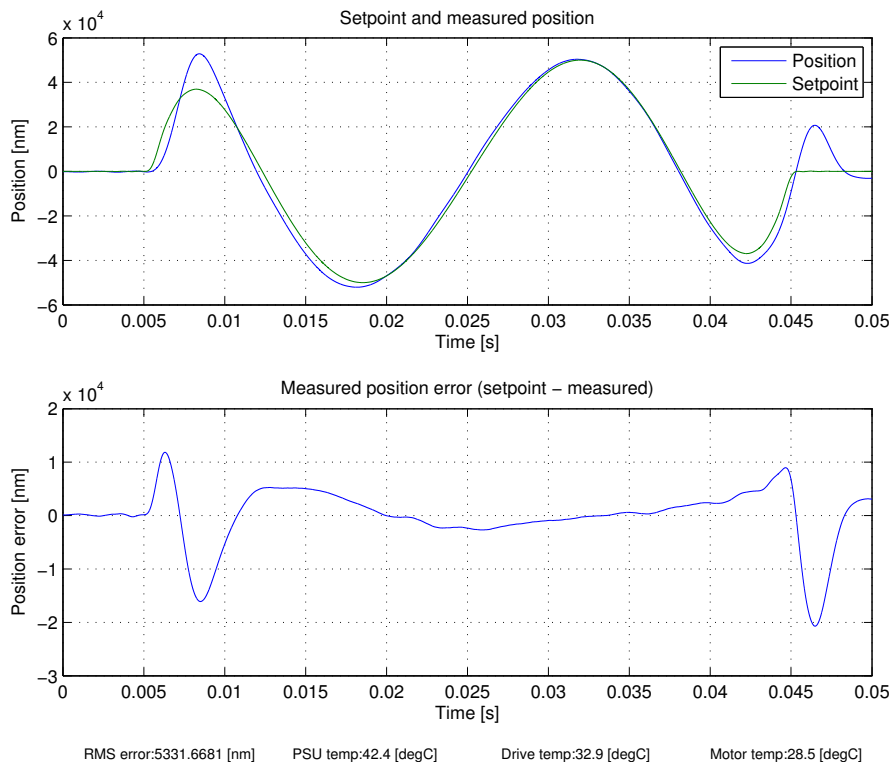
Figure 48a on page 85 shows the result of tracking a polynomial of form $p_2(t)$. Note that this waveform results in twice as far a traveled motion as compared to the previous trajectories (as the previous trajectories traveled over a range $[0, x]$, whereas this trajectory spans $[-x, x]$), meaning that the error shown should be halved. If this is done then the maximum error is roughly 70% of the sine-wave trajectory. There is an anomaly at the same location analogous to the sine-wave trajectory, justifying the possibility that friction causes the error.

5.1.5.1 Polynomial 0 setpoint, no clipping

Figures 39 on the facing page through 41 on page 77 show the results of tracking a polynomial without any continuous velocity or acceleration and without significant setpoint limiting.

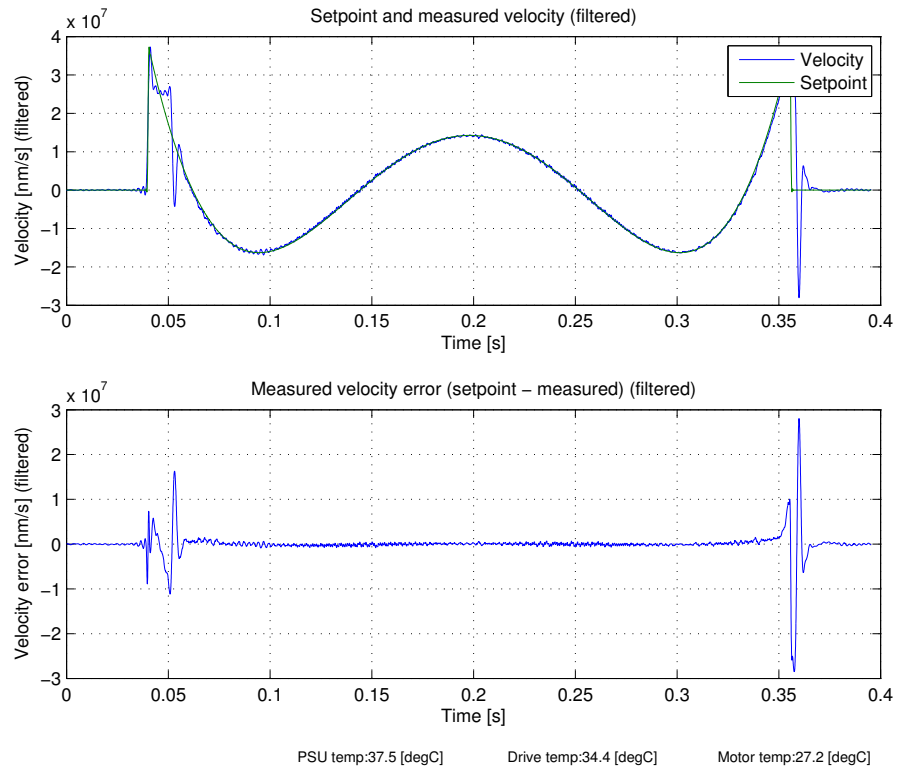


(a) Large-scale motion.

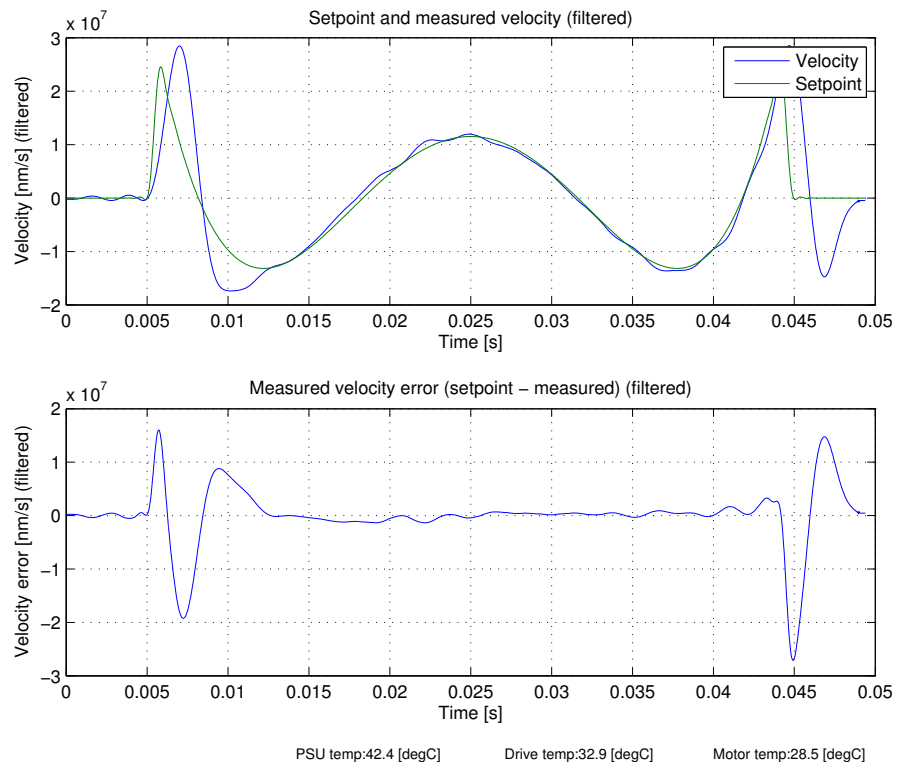


(b) Small-scale motion.

Figure 39: Position measurement for polynomial 0 wave setpoint.

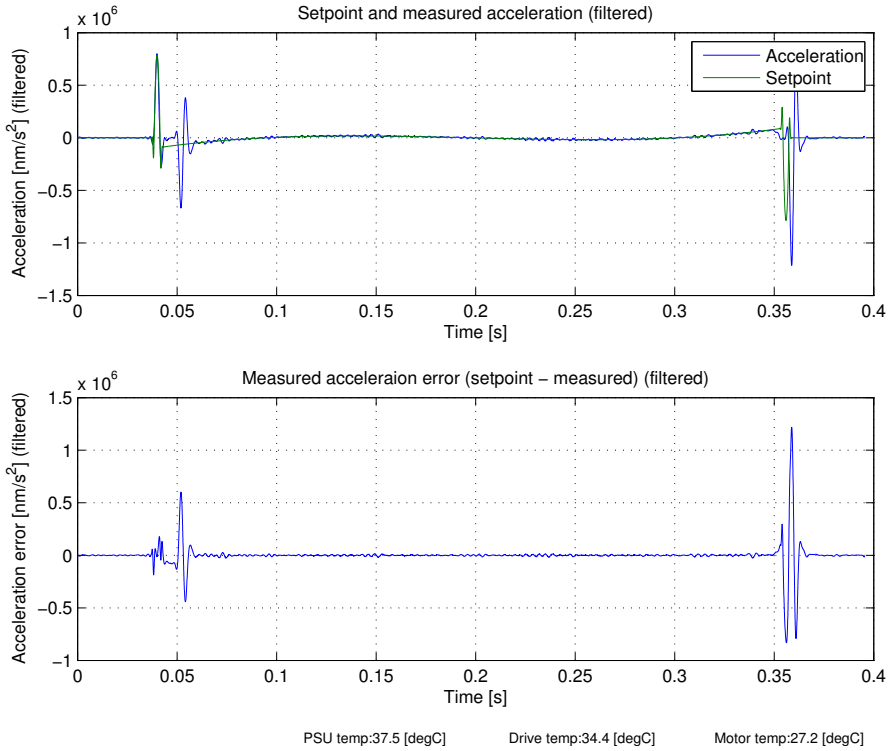


(a) Large-scale motion.

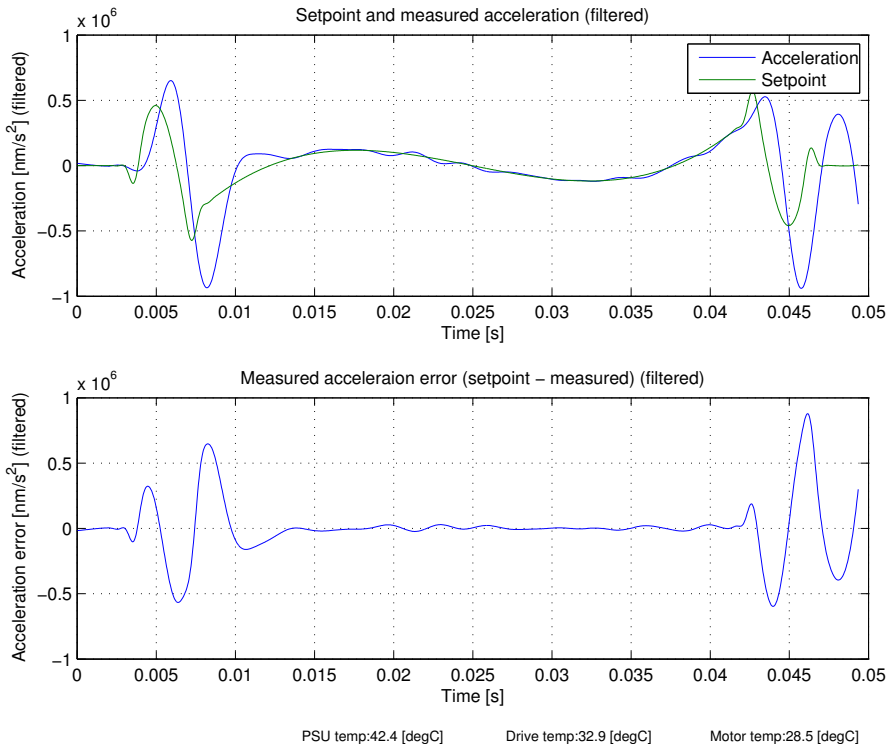


(b) Small-scale motion.

Figure 40: Velocity measurement for polynomial o wave setpoint.



(a) Large-scale motion.



(b) Small-scale motion.

Figure 41: Acceleration measurement for polynomial wave setpoint.

5.1.5.2 Polynomial o setpoint, clipping

Figures 42 through 44 on the next page show the results of tracking a polynomial without any continuous velocity or acceleration with significant setpoint limiting. Figure 43 on the facing page in particular shows the effect that the slew-rate limiter has on the trajectory, as the magnitude of the velocity is clearly clamped to a maximum value. Note that the transition from clamped velocity to tracking the set velocity is not instantaneous. There is some time required to switch from the clamped velocity to following the waveform again.

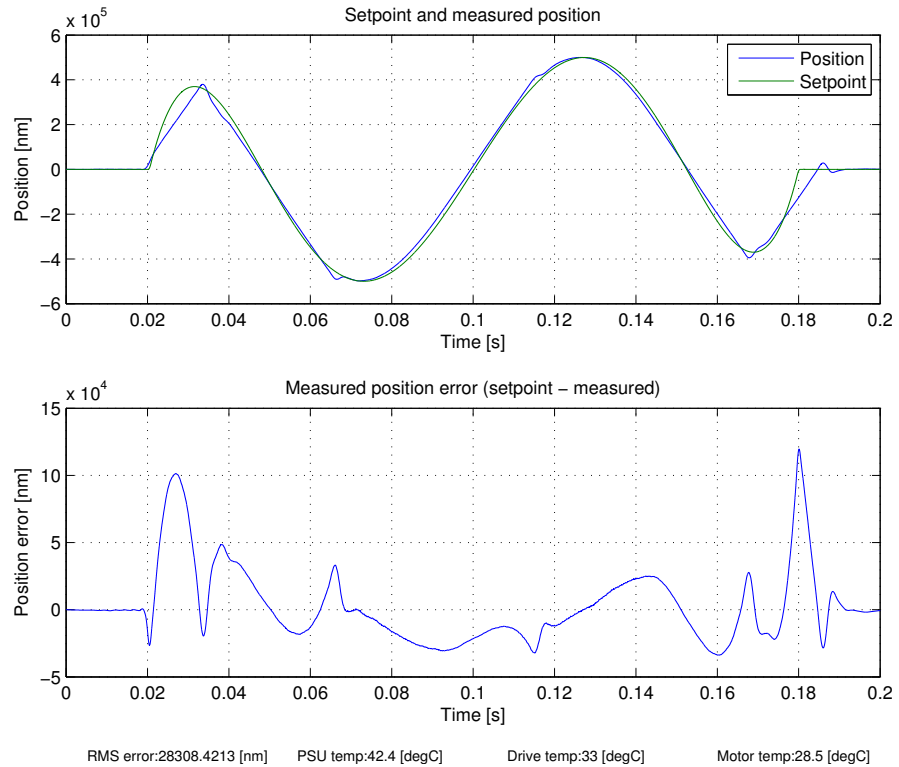


Figure 42: Position measurement for polynomial wave setpoint, clipping, large scale motion.

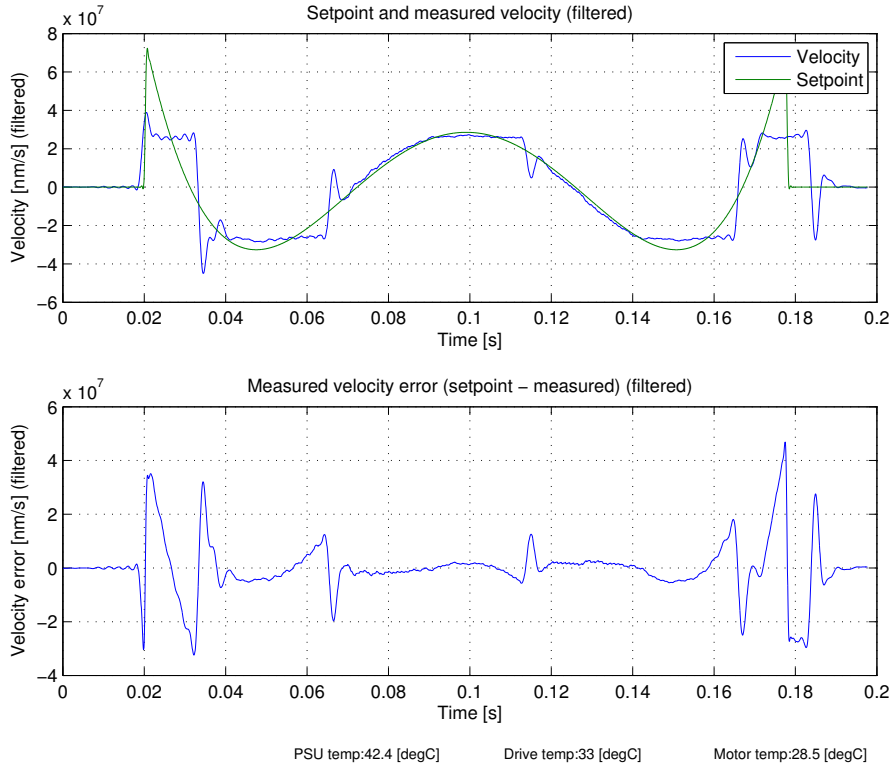


Figure 43: Velocity measurement for polynomial o wave setpoint, clipping, large scale motion.

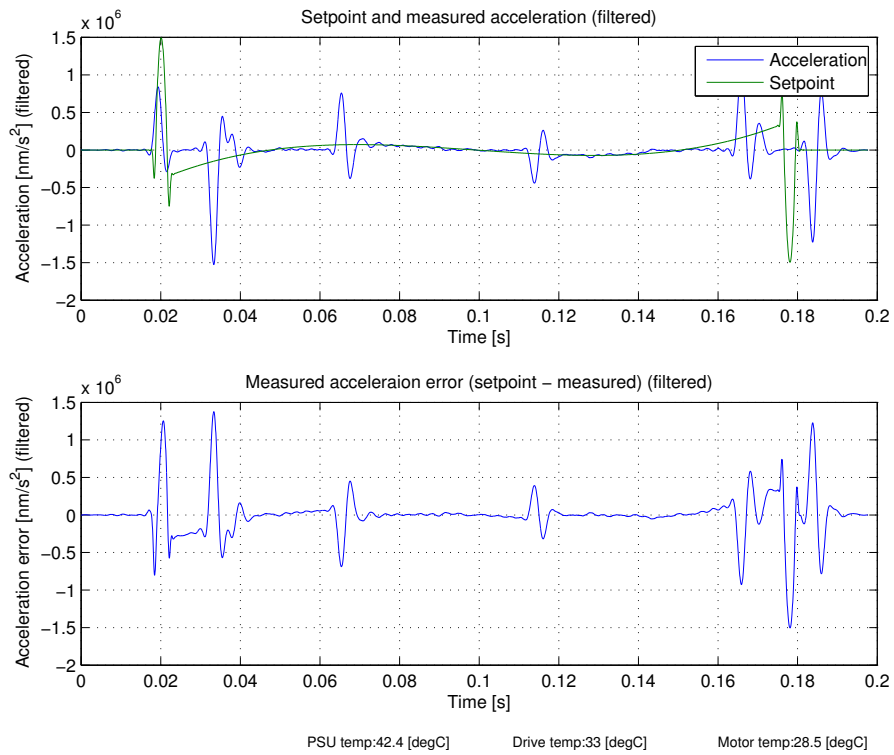
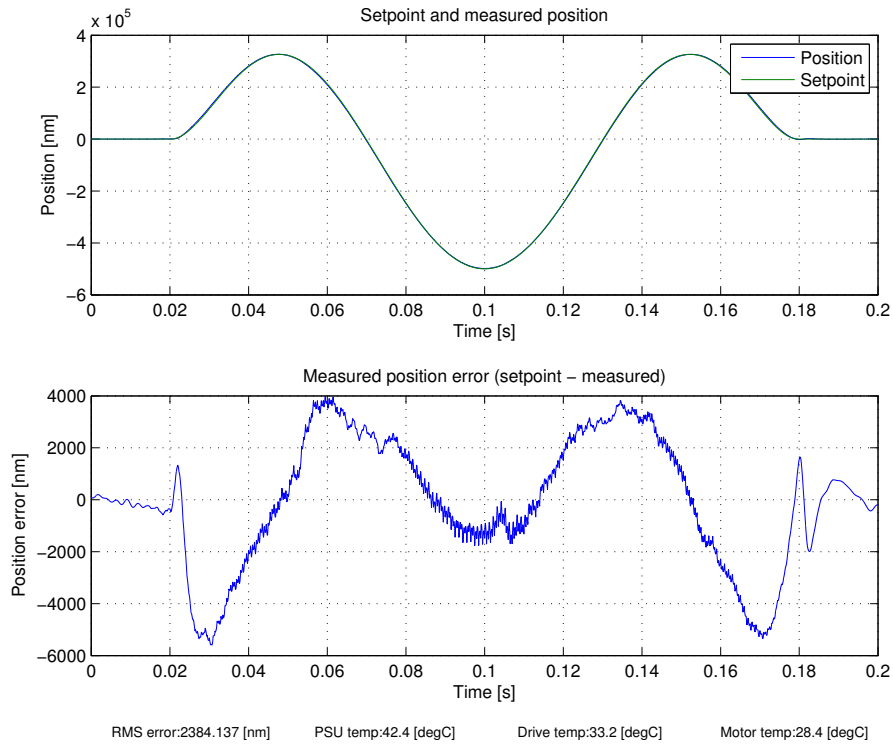


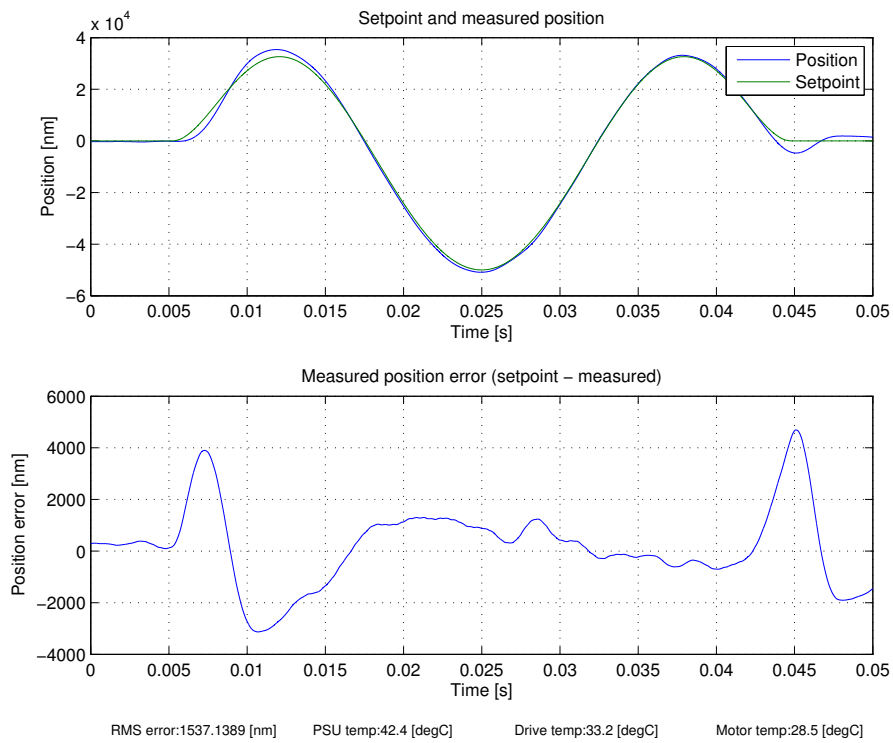
Figure 44: Acceleration measurement for polynomial o wave setpoint, clipping, large scale motion.

5.1.5.3 *Polynomial 1 setpoint*

Figures [45 on the next page](#) through [47 on page 83](#) show the position through acceleration accuracy of tracking a polynomial with continuous velocity but discontinuous acceleration. As can be seen the discontinuous acceleration causes much of the inaccuracy in the waveform tracking.

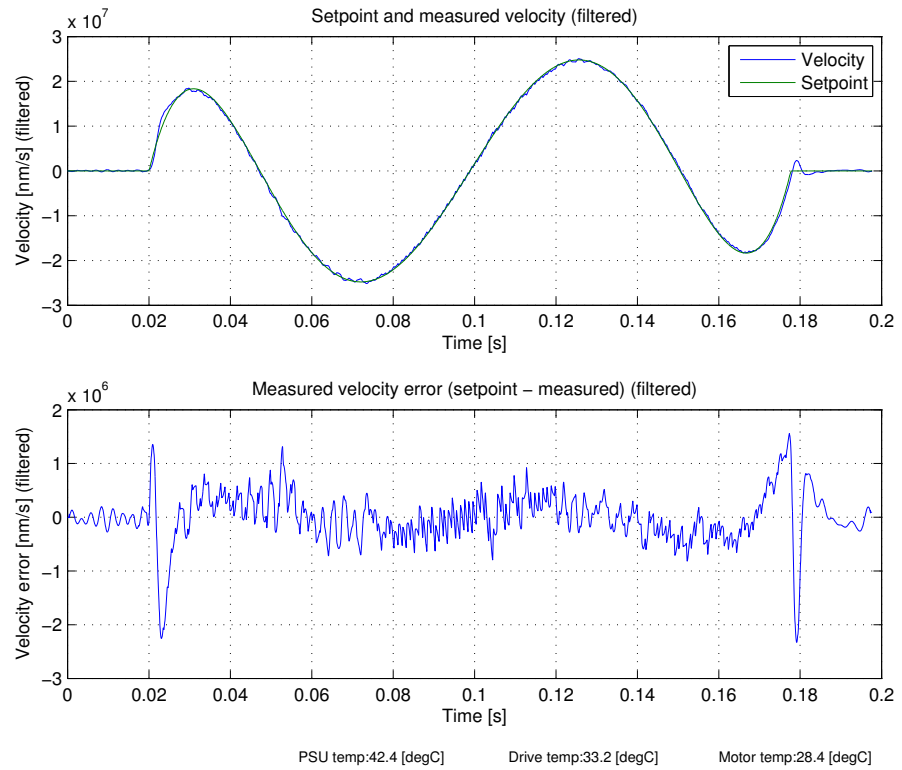


(a) Large-scale motion.

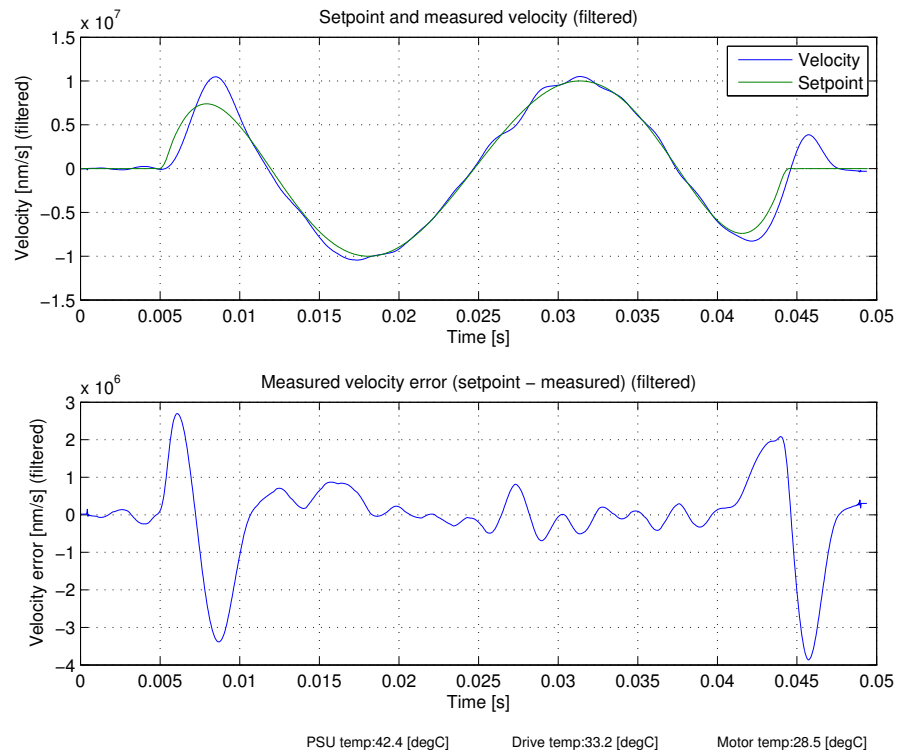


(b) Small-scale motion.

Figure 45: Position measurement for polynomial 1 wave setpoint.

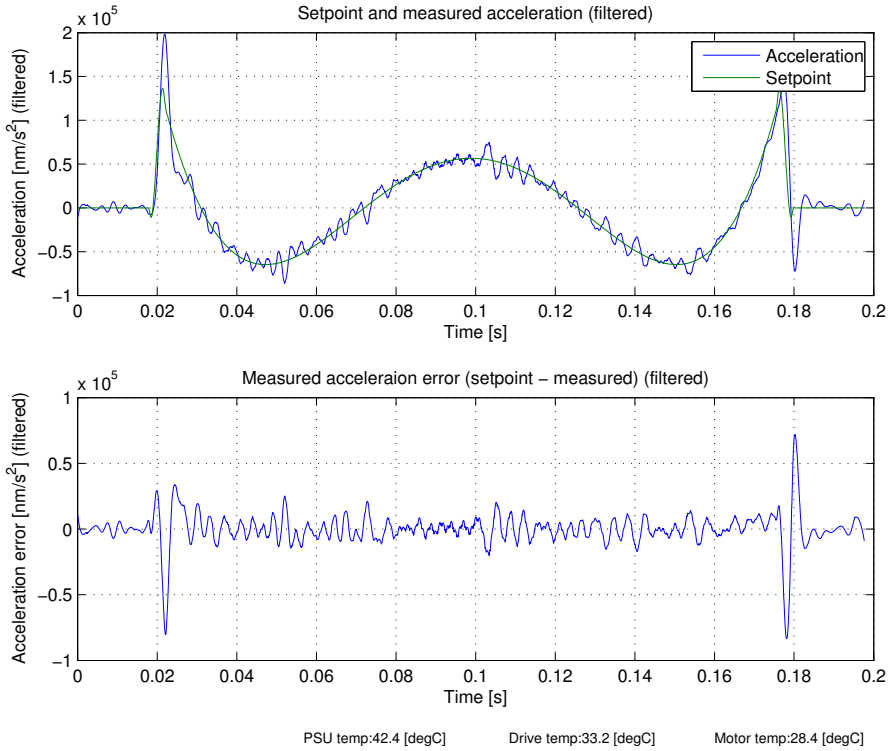


(a) Large-scale motion.

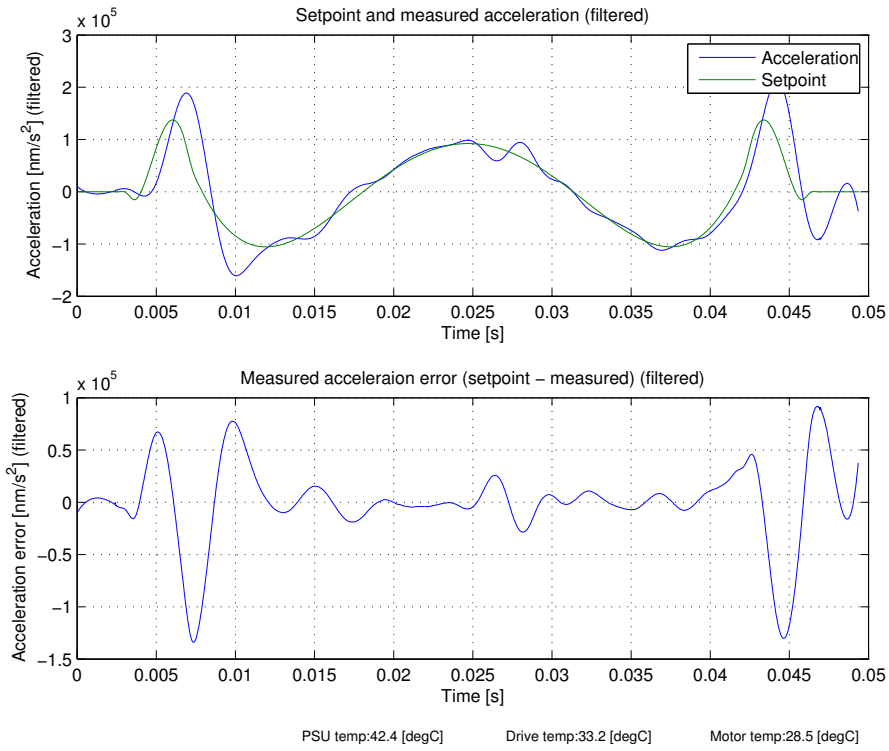


(b) Small-scale motion.

Figure 46: Velocity measurement for polynomial 1 wave setpoint.



(a) Large-scale motion.

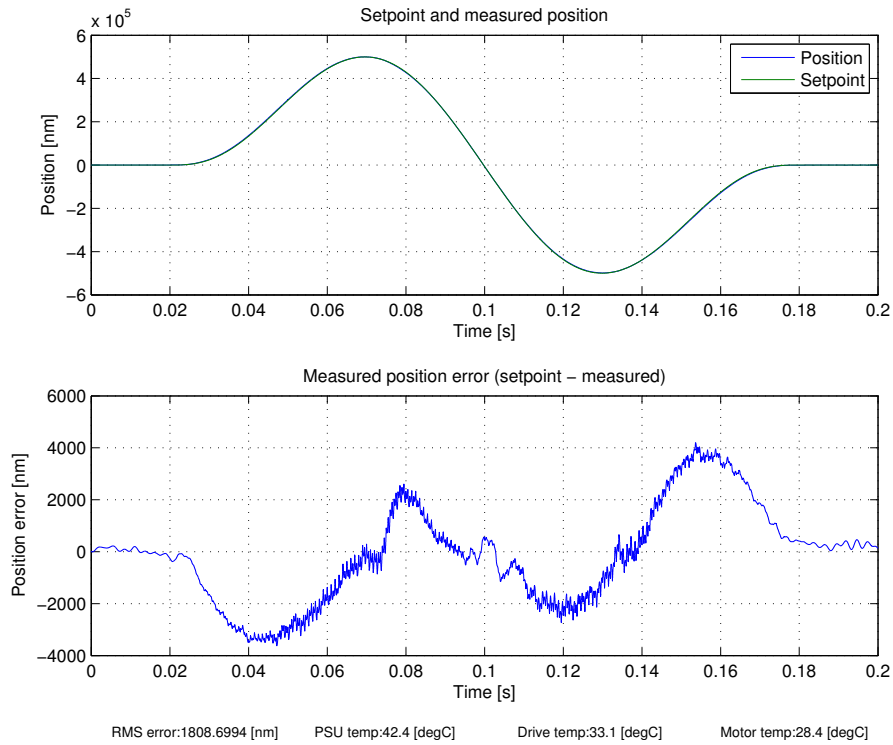


(b) Small-scale motion.

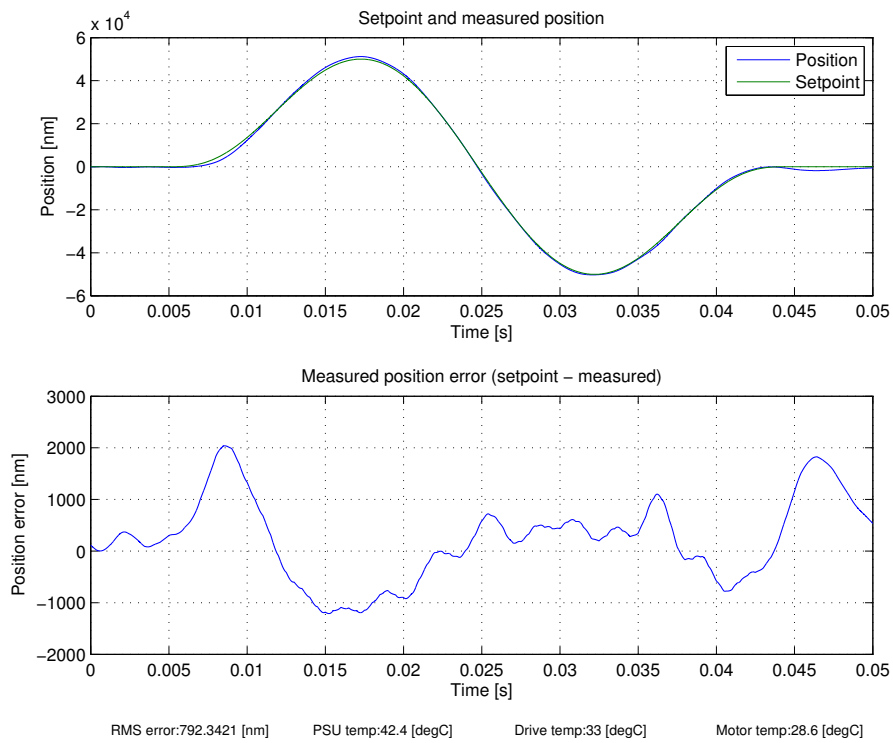
Figure 47: Acceleration measurement for polynomial 1 wave setpoint.

5.1.5.4 *Polynomial 2 setpoint*

Figures [48 on the next page](#) through [50 on page 87](#) show the results of tracking a polynomial with continuous acceleration. This waveform is designed to be very smooth, which will improve the ease of following the trajectory. As can be seen the worst-case error is roughly 70% of the maximum error of the sine waveform, when taking into account the doubled waveform amplitude, which lends credence to the possibility of the waveform being possible to follow with a reduced maximum error.

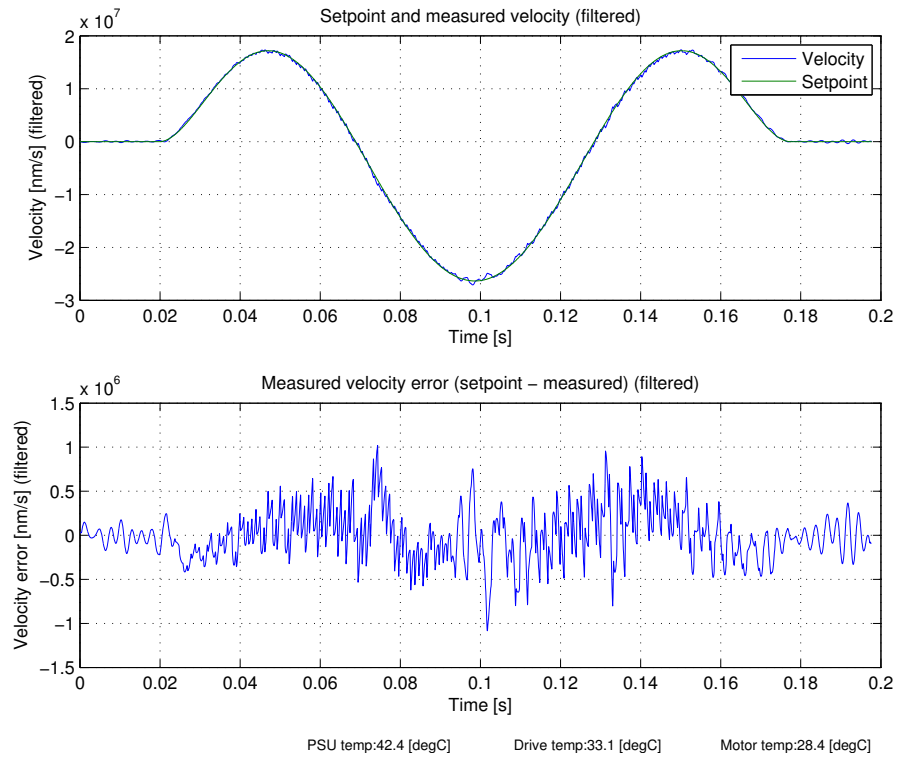


(a) Large-scale motion.

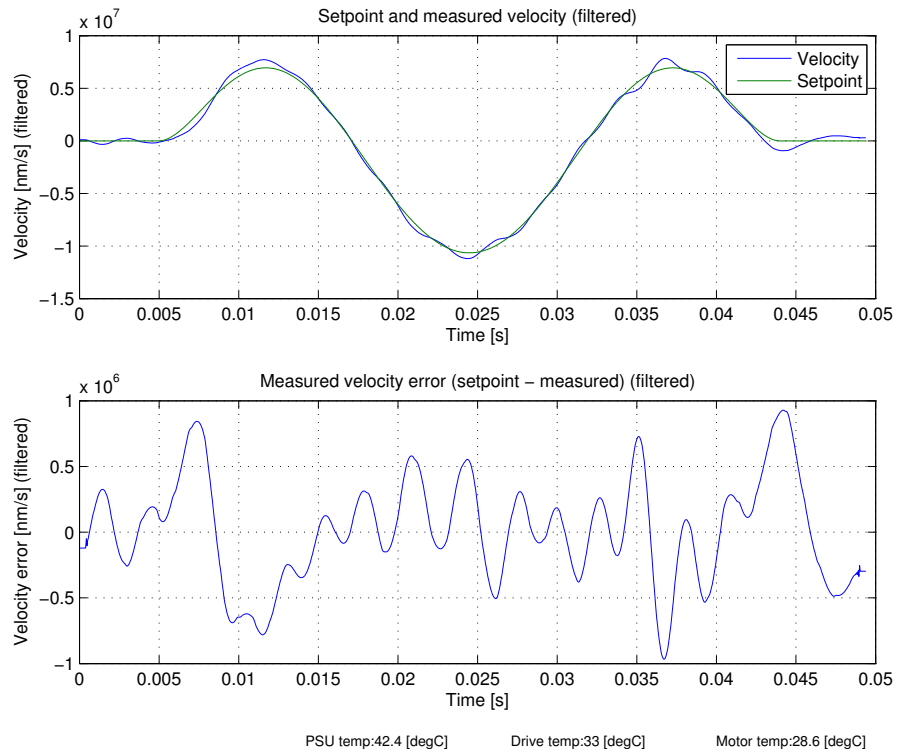


(b) Small-scale motion.

Figure 48: Position measurement for polynomial 2 wave setpoint.

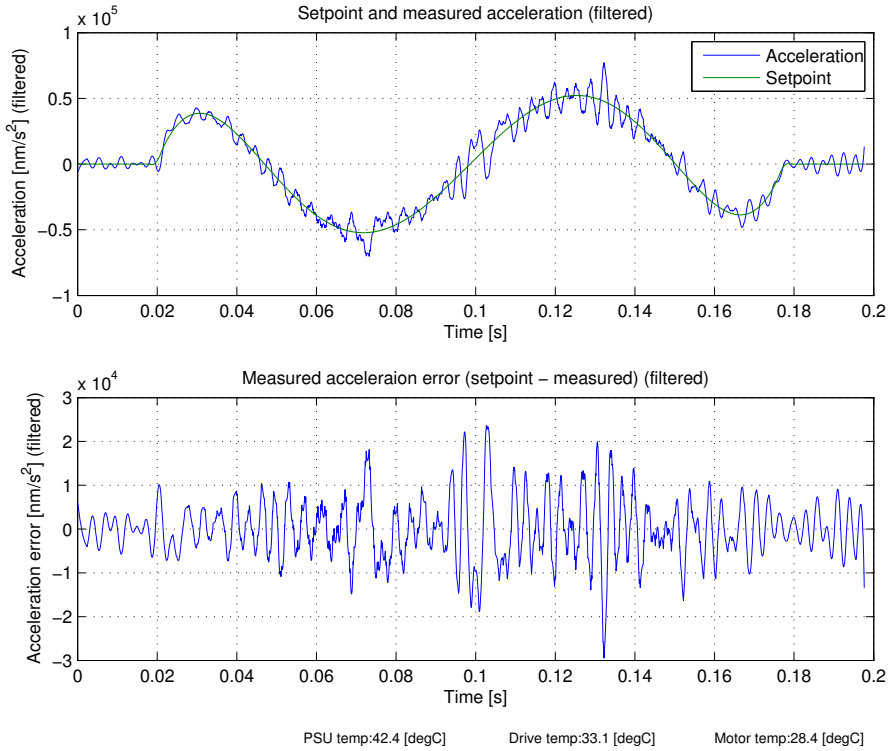


(a) Large-scale motion.

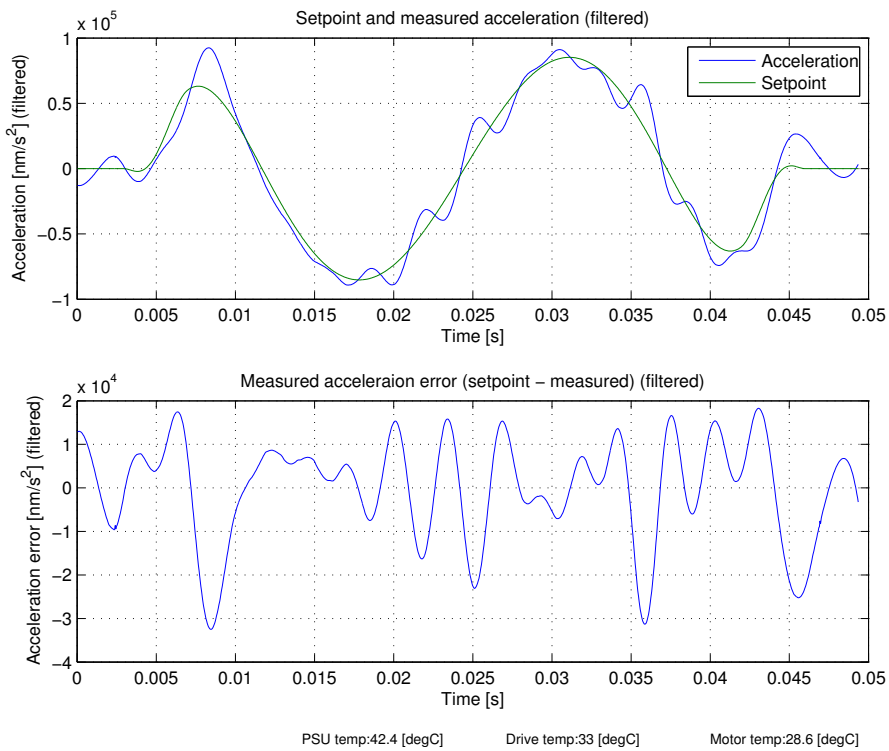


(b) Small-scale motion.

Figure 49: Velocity measurement for polynomial 2 wave setpoint.



(a) Large-scale motion.



(b) Small-scale motion.

Figure 50: Acceleration measurement for polynomial 2 wave setpoint.

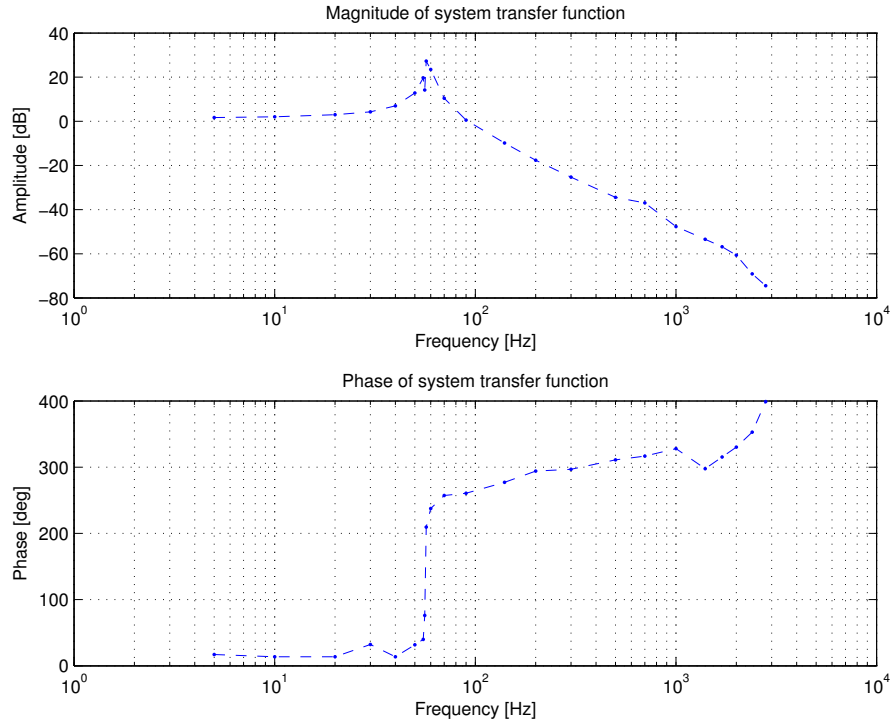


Figure 51: Open loop bode diagram of the system transfer function (measured at the motor drive interface). Sampled frequencies marked with a dot. The transfer function is V_{out}/V_{in} .

5.2 SYSTEM CHARACTERIZATION

Figure 51 shows the results of a manual measurement of the open-loop bode diagram, where the input is sent to the motor driver and the output is measured at the node from the linear controller's output. The transfer function used is defined as

$$H = V_{out}/V_{in}$$

shows an expected response. At low frequencies the excursion for a given force is nearly constant. This excursion then increases and reaches a maximum roughly at 55Hz, which is the resonance frequency of the moving mass and the flexure suspension. Afterwards the excursion decreases at 40 dB/decade. Note that the phase jumps roughly 180 degrees after the resonance as expected.

Figure 52 on the facing page illustrates the measured system stiffness over frequency, where stiffness is defined as the force required to move the payload a certain distance, in this case with the unit $[N/nm]$. The disturbance force is simulated by adding a signal to the motor drive (i.e. the net signal to the motor drive board is $V_{motor\ drive} = V_{linear\ controller} + V_{equivalent\ disturbance\ force}$). As the motor drive generates

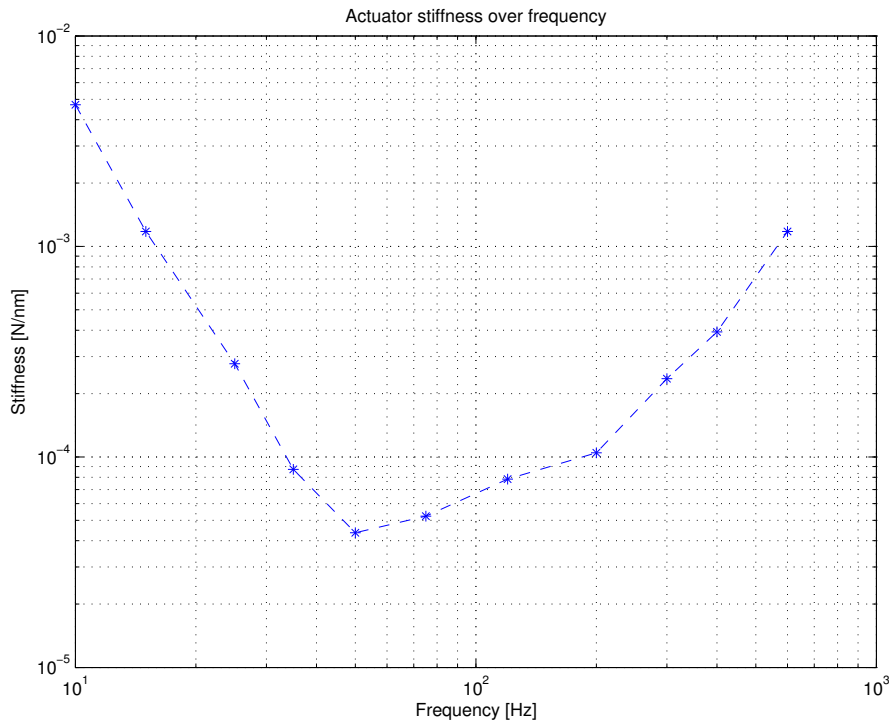


Figure 52: Measured system stiffness over frequency. Sampled frequencies marked with a dot.

a force in the motor proportional to the input voltage this will be equivalent to a disturbance force on the payload¹.

This also shows the expected behavior of a very high stiffness at low frequencies (from the integrators in the linear controller). This stiffness decreases with increasing frequency (as the effect from the integrators decreases) and reaches a minimum at 50 Hz, after which it slowly increases due to the payload mass acting as an inertial damper.

Figure 53 on the next page shows the capacitive sensor INL (that is to say, the maximum total deviation from a linear response) which is limited to $8.5\mu\text{m}$ in the range of $\pm 1\text{mm}$. This is equivalent to a maximum error of 0.425%. As can be seen in the figure the error very quickly increases when the actuator moves beyond 1mm and -1.2mm . This is likely due to fringing fields from the excitation rings no longer being negligible and spilling over onto the guard rings. If a larger travel was desired a longer pickup ring and/or a smaller airgap would have to be used. This is the primary limitation of the useful dynamic range of the sensor, even though the sensor can move much further the nonlinearity makes it next to useless for larger travel ranges. The INL of the sensor was measured by manually driving the payload to several known positions with a micrometer screw and comparing the set position to the reported position.

¹ This is assuming the simulated disturbance force lies within the bandwidth of the motor drive, which is true for the plot shown.

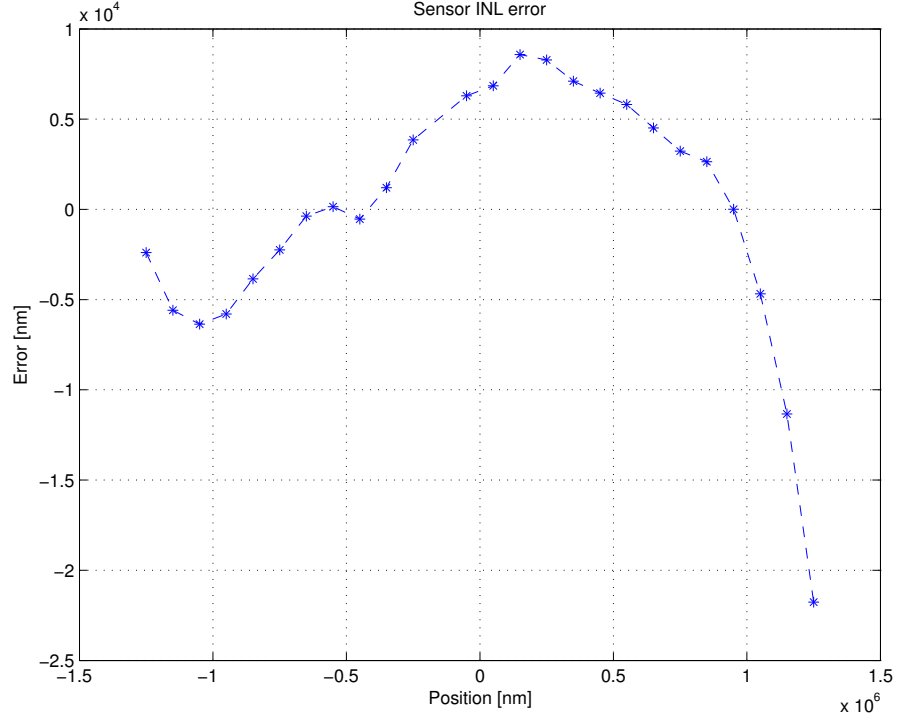


Figure 53: Capacitive sensor **INL** over position.

Assuming all the nonlinearity of the sensor is due to the stray capacitance from the sensor to the ambient environment (which neglects factors such as the actuator's radial motion over the travel range as well as nonidealities in the driven Faraday shield) gives an upper bound to the stray capacitance in the sensor. Thus, $C_{stray} \leq \max(|INL(x)|) \cdot C_{meas-drive}$ where $INL(x)$ is the **INL** for a certain position and $C_{meas-drive}$ is the capacitance between the measurement and drive cylinders respectively. Assuming a simple model for $C_{meas-drive}$ would be a cylindrical capacitance model (Nordling and Österman [12], Cheng [7]) which would result in a nominal capacitance of

$$C_{meas-drive} = \frac{2\pi\epsilon_0\epsilon_r l}{\ln\left(\frac{d_{outer}}{d_{inner}}\right)}$$

where l is the length of the outer and inner cylinders, d_{outer} is the diameter of the outer cylinder and d_{inner} is the diameter of the inner cylinder. Inserting the values of the parts used as shown in appendix A gives $C_{meas-drive} = 1.55pF$. This gives an upper bound to the stray capacitance

$$C_{stray} \leq 6.5fF.$$

Table 3 shows a comparison of the developed system and several existing solutions. As can be seen the dynamic range of the current system is very similar to that available in existing commercial systems, and with proposed changes could exceed the range of existing solutions. Additionally, the actuator travel/length ratio far exceeds that of

PARAMETER	DEVELOPED SYSTEM	EXISTING SYSTEM 1 [13]	EXISTING SYSTEM 2 [16]
Actuator type	Magnetic, closed loop	Piezoelectric, closed loop	Piezoelectric, closed loop
Travel	2000 μm	45 μm	17 μm
Resolution	62nm now, \approx 100000 with improved flexure	0.9nm	0.68nm
Dynamic range (<i>Travel/Resolution</i>)	32000 now, \approx 100000 with improved flexure	50000	25000
Actuator travel/length ratio (<i>travel/length</i> · 1000)	40	0.66	0.85

Table 3: Comparison of developed system and existing solutions.

a piezoelectric system, allowing the use of the developed actuator in space-critical applications.

Part VI

CONCLUSION

FUTURE IMPROVEMENTS

There are several possible amendments to the actuator that have not been implemented due to scope constraints. This section lists a few of these and the impact they may have on the performance of the system.

RMS ERROR As described in section 5 the RMS error consists largely of a certain frequency and its harmonics. Had these been removed the RMS error would be reduced by roughly a factor of three. It is believed that these frequencies arise from resonance in the flexure suspension (the four small arms in figure 6 on page 22), as simulations have shown that they have the same fundamental frequency. As the flexures are constructed from a homogeneous sheet of metal the Q factor of the resonance is very high and acts as an unobservable state to the controller. The unobservable state couples effectively into the actuator rod leading to the observed noise exhibiting a non-flat shape. Could these resonances be reduced in magnitude the total system noise would be greatly reduced and closer to white flat noise. One method of doing this would be to coat them in a highly viscous material that would dampen the resonances.

TRACKING ERROR The tracking error shown in the waveform plots in section 5 could be improved in many ways, such as improving the linearity of the motor, increasing the system bandwidth, or reducing the flexure's stiffness along the axis of motion.

BANDWIDTH Increasing the bandwidth of the system would (in the absence of noise) result in an increase in stiffness performance. This is because raising the total system bandwidth would allow raising the crossover frequencies for the various linear controller coefficients $K_d - K_{i3}$. Increasing the crossover frequencies for the integrators will result in an increase of gain when in a region dominated by the integrators. However this is a system trade-off, since increasing the system bandwidth also increases the amount of noise. Additionally, the design could be changed to reduce the noise (for example by reducing the thermal noise from resistors by decreasing their resistance).

INL The INL of the system can be improved by redesigning the capacitive sensor, which is believed to cause most of the nonlinearity. This is because the sensor functions outside of the control loop, a nonlinearity in the sensor will cause an incorrect process variable to be output (in contrast to the motor, where a nonlinearity

will be compensated by the control loop). The nonlinearity is believed to primarily be caused by stray fields in the sensor, so decreasing the air gap and/or increasing the length of the guard rings would improve the linearity.

SIZE The actuator size can be reduced greatly. The selected size was chosen for ease of construction, however the size can be reduced without any geometric limitations intrinsic to the sensor and motor design chosen.

DIGITAL IMPLEMENTATION A controller that performs more functions in the digital domain could be implemented to reduce the cost and size of the controller. One way of doing this is to use a high-speed **ADC** to directly sample the output from the capacitive sensor and perform demodulation and implement the linear controller in the digital domain. This would require far more processing power than was currently available with the current implementation, though a field-programmable gate array (**FPGA**) may be more suited to perform such a task. This would also allow for ease of dynamically changing the controller coefficients based on the current system parameters, and possibly a controller that is more of an optimal controller rather than a linear controller.

SLEW-RATE LIMITER The current slew-rate limiter clamps the velocity of the actuator. A more ideal way to control the signal slew-rate would be to limit the acceleration, which corresponds to the control signal to the motor driver. This would result in quicker motion when approaching the system power limits. (For example, in figure [32a on page 65](#) the output voltage to the motor is zero for a large portion of the time, whereas an ideal controller would apply maximum positive power for half of the time, and negative maximum power for the other half).

FRICTION As was seen in some of the plots in section [5.1.4](#) an unexpected anomaly is visible at one position which is believed to be caused by friction between the moving and static parts of the actuator. This is definitely not desired, as it causes very large changes in the linear model of the system and may possibly lead to system instability. This is can be rectified by assembling the actuator correctly and/or increasing the gap between the moving and non-moving parts.

TRAVEL By changing the geometry of the actuator and reducing the travel the resolution will be increased (as a change in position will cause an increased change in output voltage from the sensor). This could lead to developments with an actuator capable of nanometer-level resolution with a travel range of hundreds of microns.

CONCLUSION

A new type of precision linear actuator was developed and tested that shows promise and with a few improvements may achieve an SNR of $100dB$. The use of a magnetic drive reduces the hysteresis normally seen in a piezoelectric actuator, though at the cost of active control to maintain a desired position. The range of travel available greatly exceeds that of direct-drive piezoelectric actuators and manages to maintain a high stiffness at low frequencies ($4mN/nm$, $f = 10Hz$) and a high closed-loop bandwidth ($3.5kHz$). Several test waveforms have been evaluated that show the ability of the system to follow a varying setpoint as specified from a host computer, the results of which show a typical maximum error of roughly $2\mu m$ for a $500\mu m$ signal amplitude, which rapidly decreases over time to several hundred nanometers. The steady state RMS noise level is $62nm$ and proposed changes may achieve approximately $20nm$. Additionally, reducing the range of travel would increase the resolution by a roughly equal factor, leading to the possibility of nanometer accurate actuators with a range of travel in the range of hundreds of micrometers.

This new type of actuator shows great promise for future development and may be useful for optics labs in a large range of situations. As has been shown the system has favorable dynamic range as compared with existing solutions, offers a travel/size ratio far exceeding that of a direct-drive piezoelectric system and may be scaled down in travel length to offer similar accuracy to that of a piezoelectric actuator with a far smaller footprint and comparable, if not better, dynamic range.

BIBLIOGRAPHY

- [1] Analog devices. Ad7764 datasheet, . URL www.analog.com/static/imported-files/data_sheets/AD7764.pdf.
- [2] Analog devices. Ad5791 datasheet, . URL www.analog.com/static/imported-files/data_sheets/AD5791.pdf.
- [3] Atmel. Atxmega128a3 summary. URL http://www.atmel.com/dyn/resources/prod_documents/doc8068.pdf.
- [4] Larry K. Baxter. *Capacitive Sensors, Design and Applications*. IEEE Press, 1997.
- [5] John R. Brauer. *Magnetic actuators and sensors*. John Wiley & Sons, Inc., Hoboken, New Jersey, 2006.
- [6] Robert Bringhurst. *The Elements of Typographic Style*. Version 2.5. Hartley & Marks, Publishers, Point Roberts, WA, USA, 2002.
- [7] David K. Cheng. *Field and Wave Electromagnetics*. Addison-Wesley, 2 edition, 1989.
- [8] Seung-Bok Choi and Young-Min Han. *Piezoelectric Actuators: Control Applications of Smart Materials*. CRC Press, 1 edition, 2010.
- [9] DME-SPM. Rasterscope ec stm. URL <http://www.dme-spm.dk/products.html>.
- [10] Prof. Bo Lindström, Prof. Ralph Crafoord, Docent Bengt Rundqvist, and Civiling. Lennar Hågeryd, editors. *Karlebo Handbok*. Liber AB, 15 edition, 2005.
- [11] Jonathan Lock. Rattlesnake nanoactuator firmware. Unpublished document containing source code and function descriptions.
- [12] Carl Nordling and Jonny Österman. *Physics Handbook*. Studentlitteratur, 8 edition, 2006.
- [13] Physik Instrumente. P-841 piezo actuators. URL http://www.physikinstrumente.com/en/pdf/P840_Datasheet.pdf.
- [14] Texas Instruments. Opa277 datasheet. URL <http://focus.ti.com/lit/ds/symlink/opa277.pdf>.
- [15] Texas Instruments. Opa827 datasheet, 2009. URL <http://focus.ti.com/lit/ds/symlink/opa827.pdf>.

- [16] Thorlabs AB. Bpc201, pzs001 controller and actuator. URL http://www.thorlabs.com/_SD-Popup.cfm?partnumber=AE0505D18F; <http://www.thorlabs.com/thorProduct.cfm?partNumber=BPC201>.
- [17] Warren C. Young and Richard G. Budynas. *Roark's Formulas for Stress and Strain*. McGraw-Hill Professional, 7 edition, 2001.

COLOPHON

This thesis was typeset with L^AT_EX 2_ε using Hermann Zapf's *Palatino* and *Euler* type faces (Type 1 PostScript fonts *URW Palladio L* and *FPL* were used). The listings are typeset in *Bera Mono*, originally developed by Bitstream, Inc. as "Bitstream Vera". (Type 1 PostScript fonts were made available by Malte Rosenau and Ulrich Dirr.)

The typographic style was inspired by [Bringhurst](#) as presented in *The Elements of Typographic Style* [6]. It is available for L^AT_EX via CTAN as "[classicthesis](#)".

The graphic on the cover is a rattlesnake with a suspended mirror, alluding to a device driving a moving payload quickly. The graphic was hand drawn by Andreas Henriksson and later vectorized by Anton Landberg.

Block diagrams were created with Dia 0.97.1, electrical schematics and board files with Eagle 5.10.0, mechanical CAD using Solidworks 2009, and plots with Matlab 2010A. All of the development except for mechanical CAD was done on a Linux install, using mostly open-source applications.

Final Version as of September 6, 2011 at 18:28.

Part VII
APPENDIX

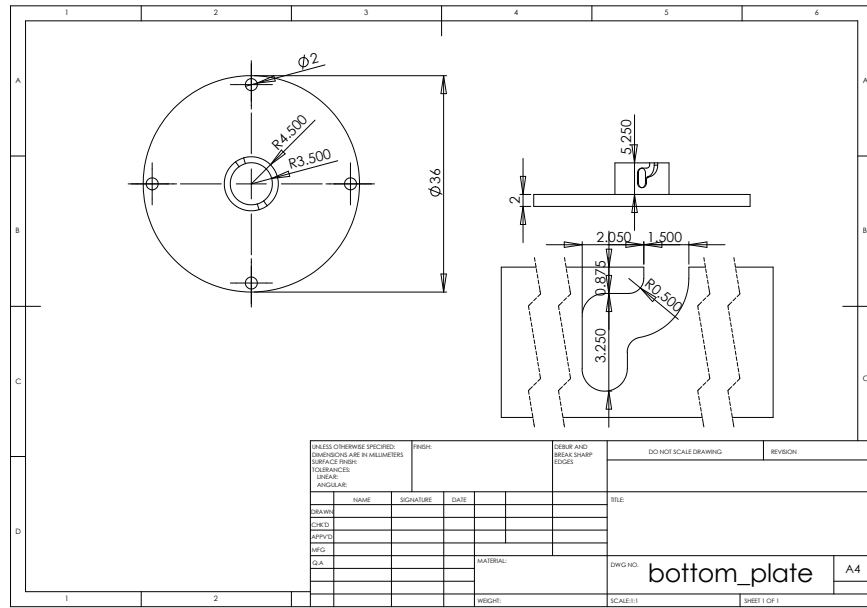


Figure 55: Covers the bottom of the actuator, limits the throw range of the actuator should an error occur. Constructed from 6061-T6 aluminum.

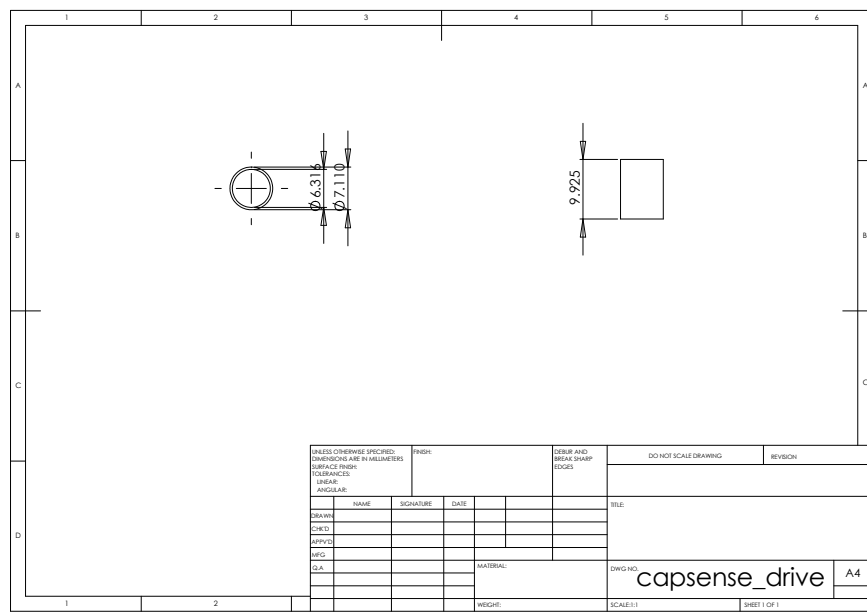


Figure 56: Excitation ring for the capacitive sensor. Constructed from brass.

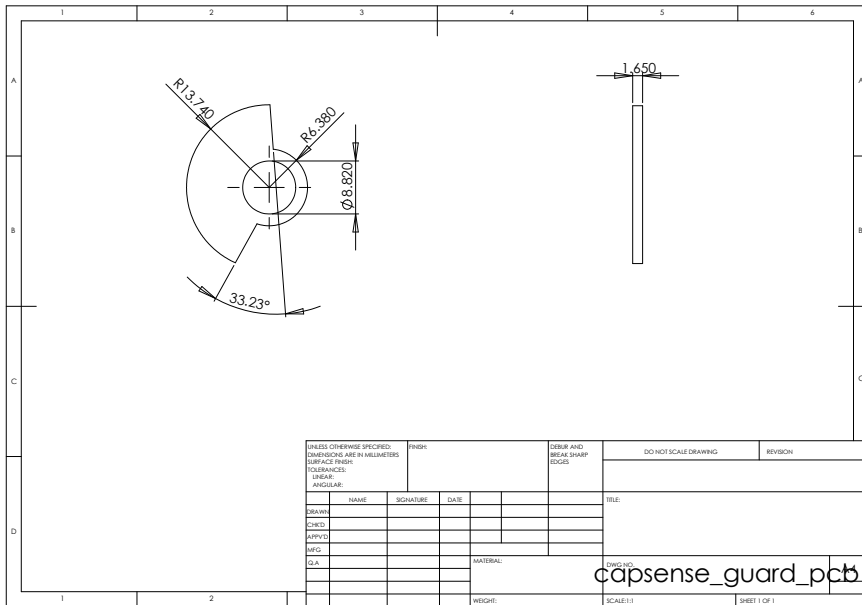


Figure 57: Top of Faraday cage around sensor. Constructed from PCB laminate (FR4 with 35µm copper and tin plating).

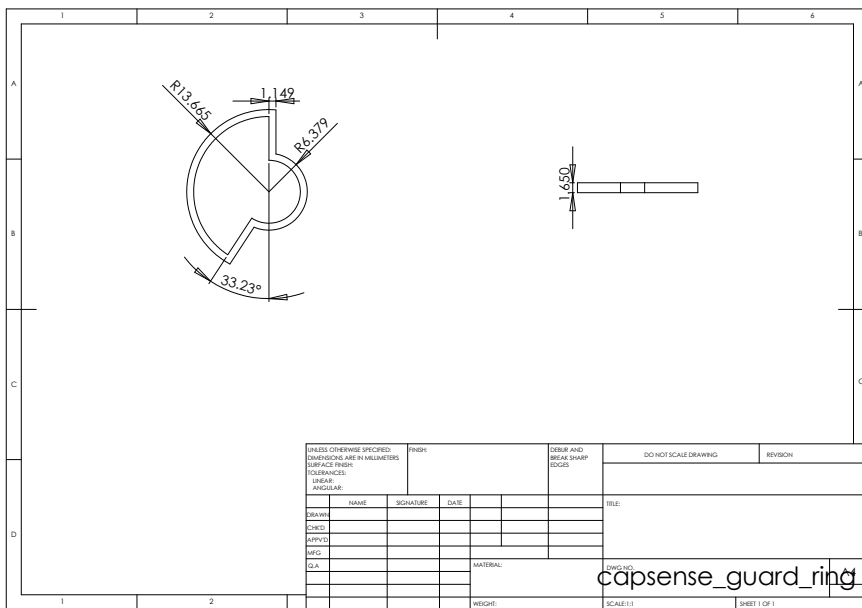


Figure 58: Side of Faraday cage around sensor. Constructed from PCB laminate (FR4 with 35µm copper and tin plating).

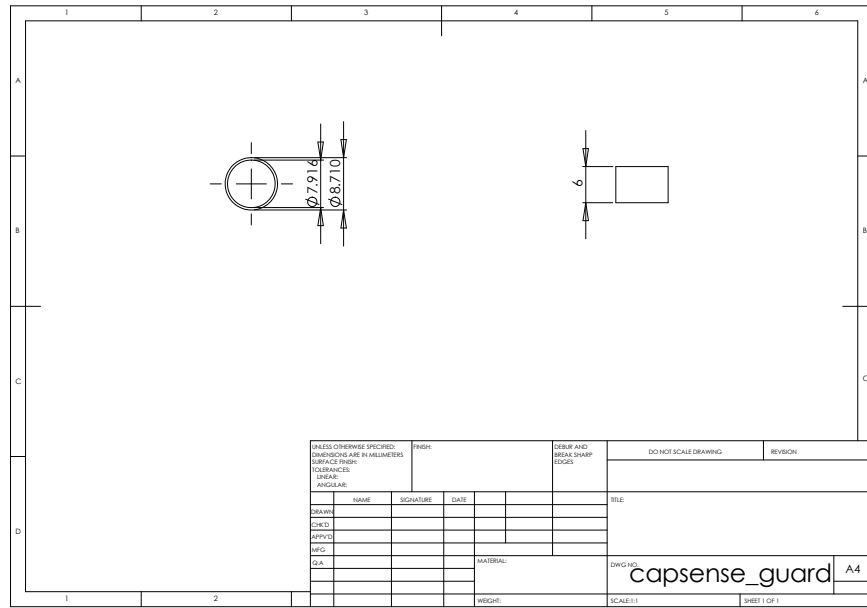


Figure 59: Guard ring for capacitive sensor. Constructed from brass.

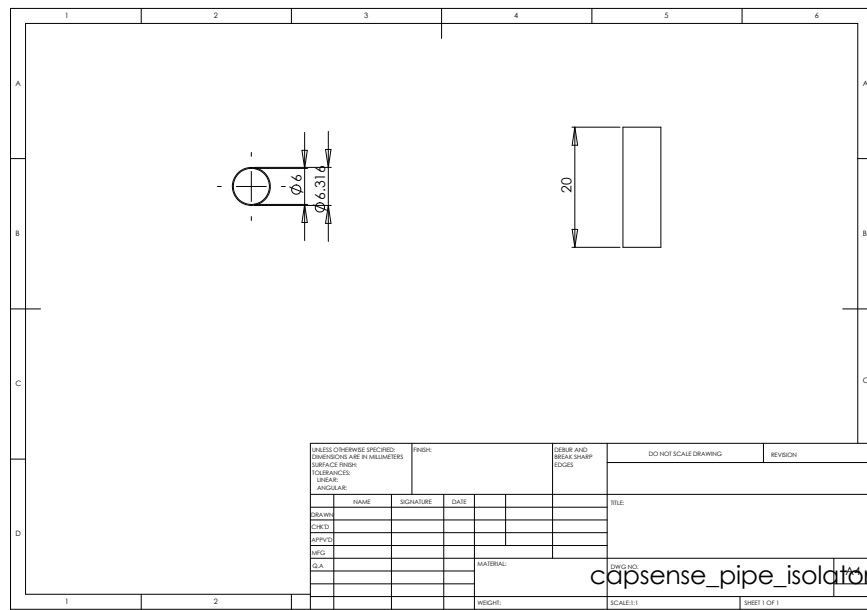


Figure 60: Electrical isolation for excitation rings for capacitive sensor from actuating rod. Constructed from kapton film.

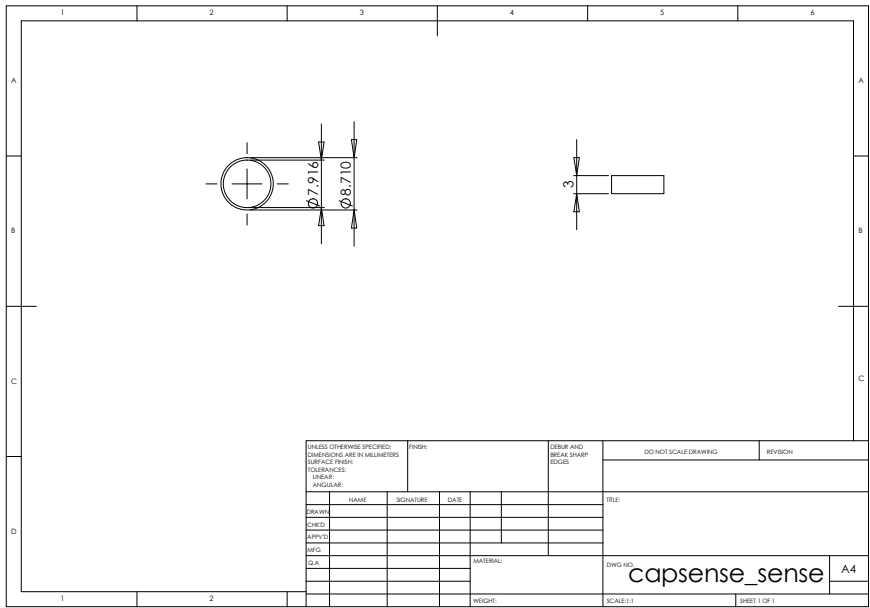


Figure 61: Capacitive sensor sensing ring. Constructed from brass.

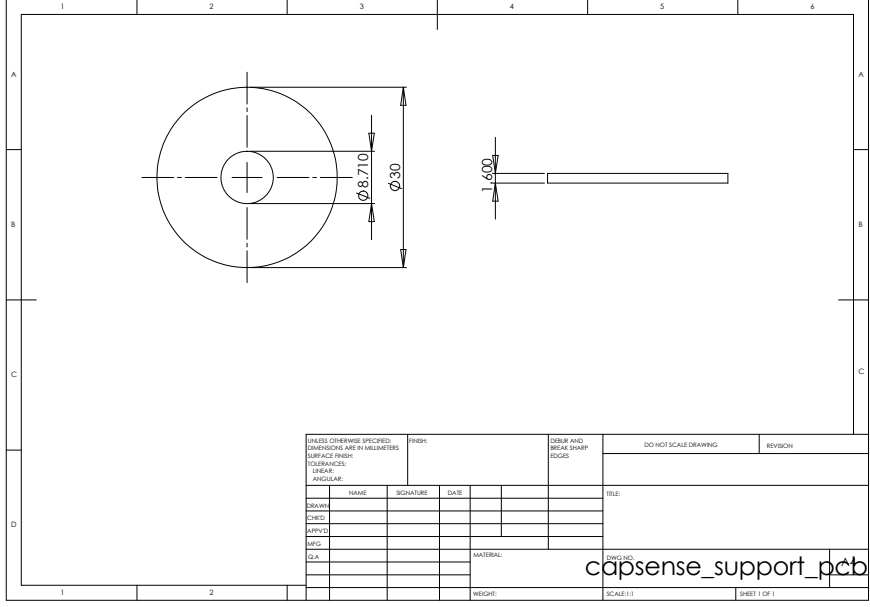


Figure 62: Placeholder for capacitive sensor PCB, see appendix B for actual shape of PCB.

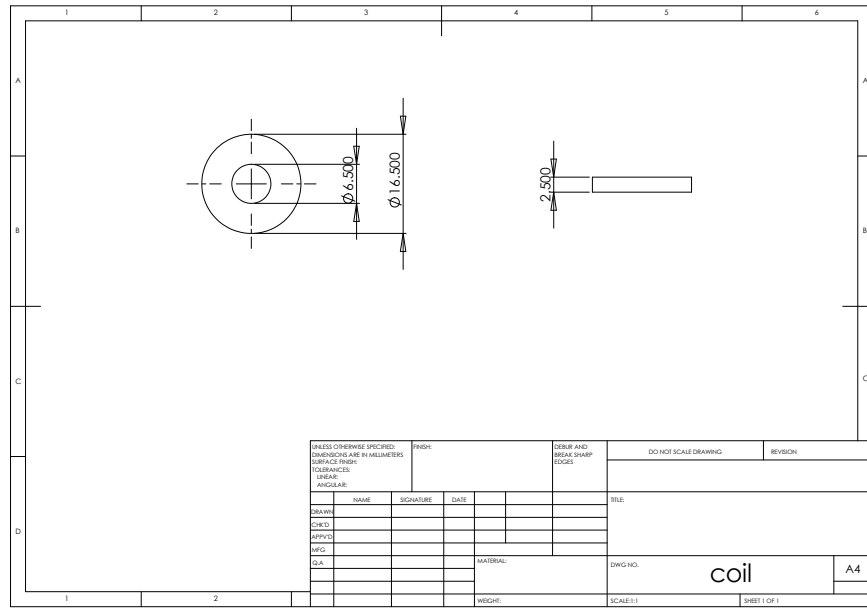


Figure 63: Placeholder for coil used in motor. Constructed from 0.15mm copper enamel wire, with approximately 550 turns.

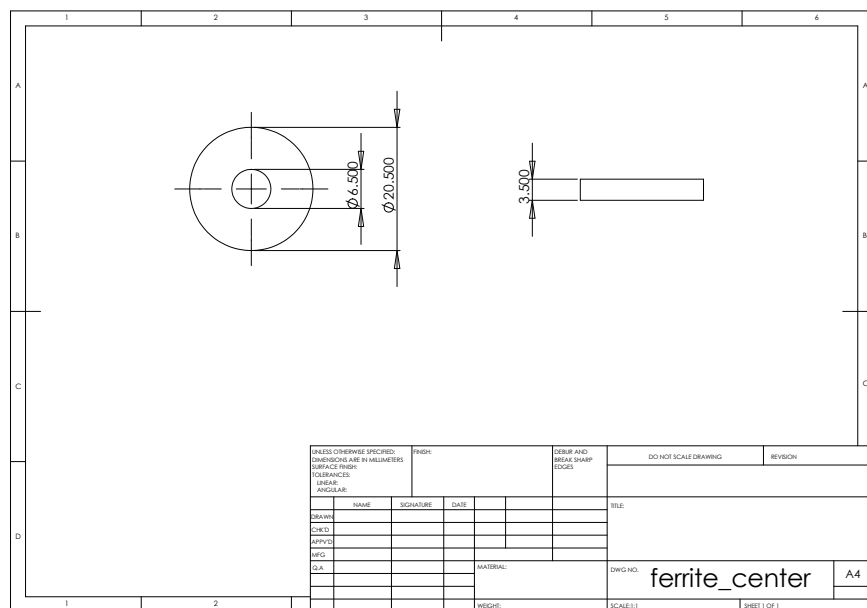


Figure 64: Magnetic flux conductor for motor. Constructed from iron powder toroid, of type Amidon T400A-26.

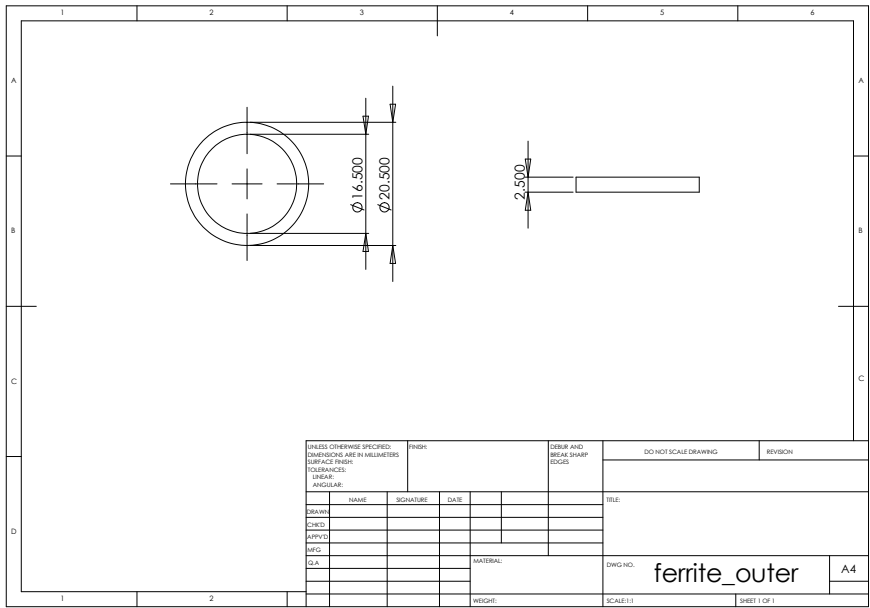


Figure 65: Magnetic flux conductor for motor. Constructed from iron powder toroid, of type Amidon T400A-26.

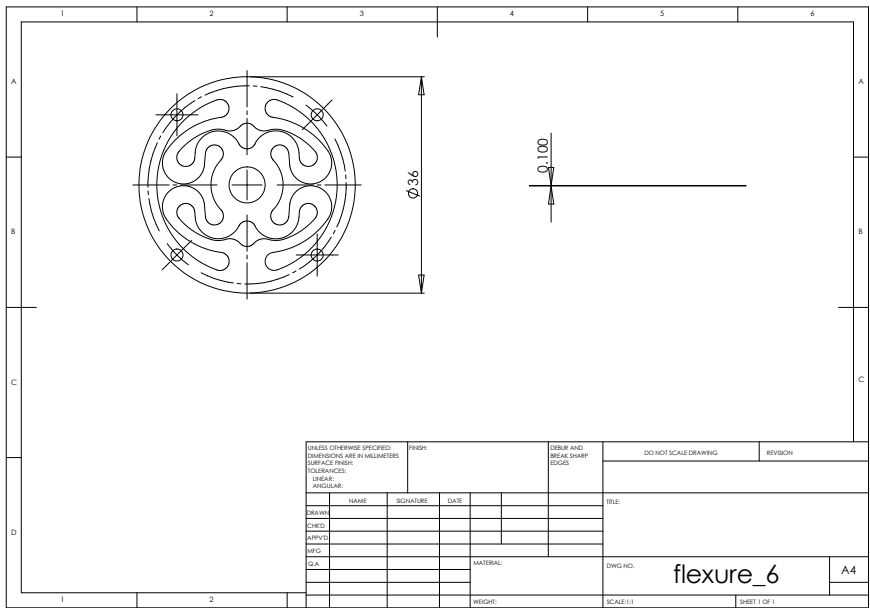


Figure 66: Flexure used for suspension of moving parts of actuator. Constructed from AISI-301 hardened stainless steel.

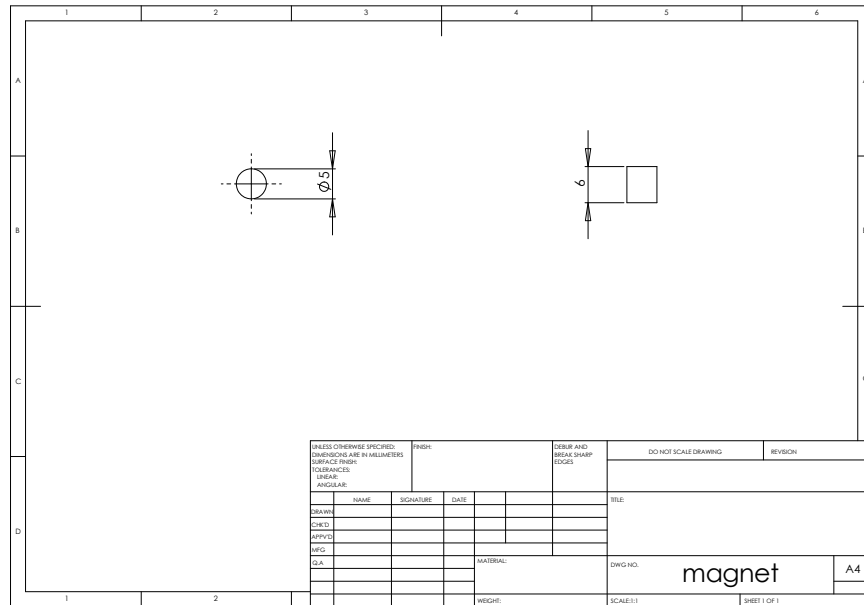


Figure 67: Magnet used for generating force on the actuator. Constructed from N35 Neodymium rare-earth magnet, of type N-0221-1 from Svenska Magnetfabriken AB. This magnet has a specification of $B_r = 1.19 \pm 0.02 [T]$ and $iH_C > 955 [kA/m]$.

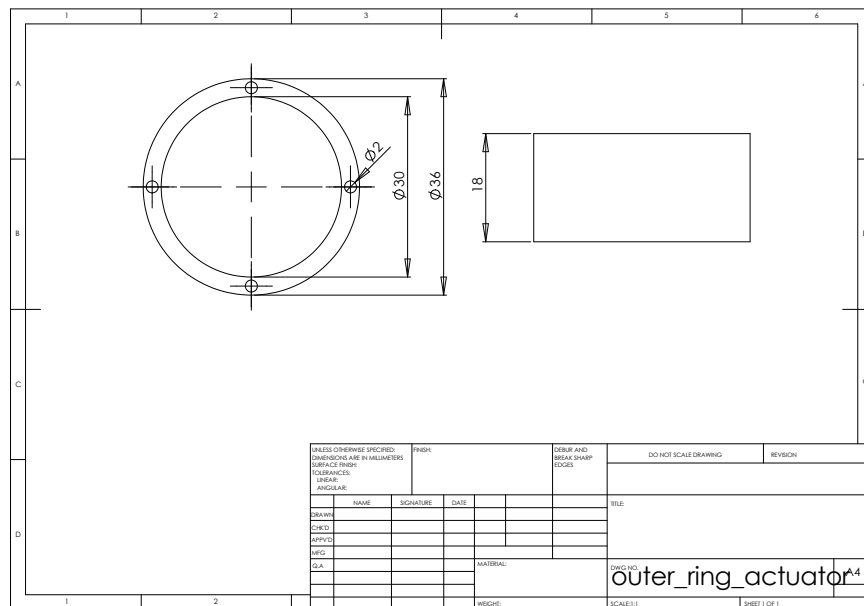


Figure 68: Outer ring for holding together actuator. Constructed from 6061-T6 aluminum.

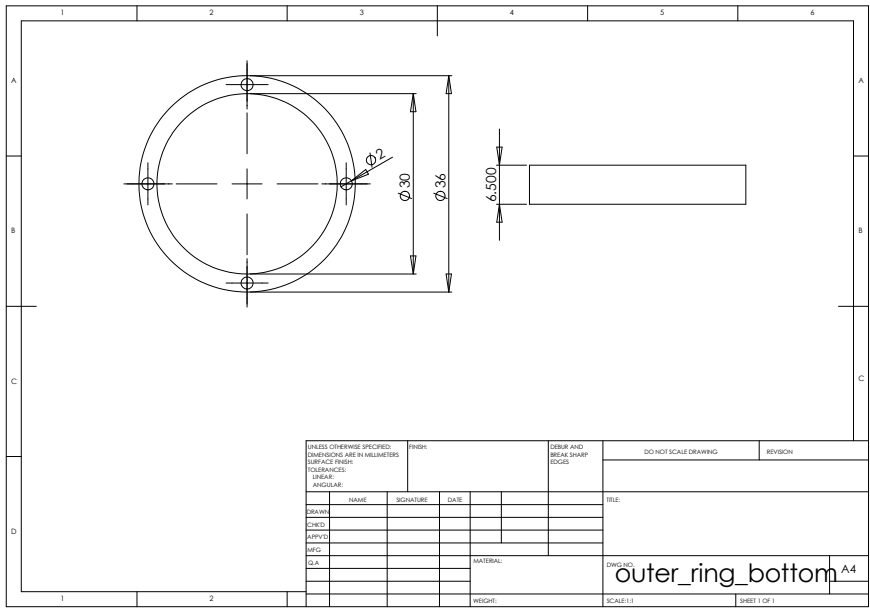


Figure 69: Outer ring for holding together actuator. Constructed from 6061-T6 aluminum.

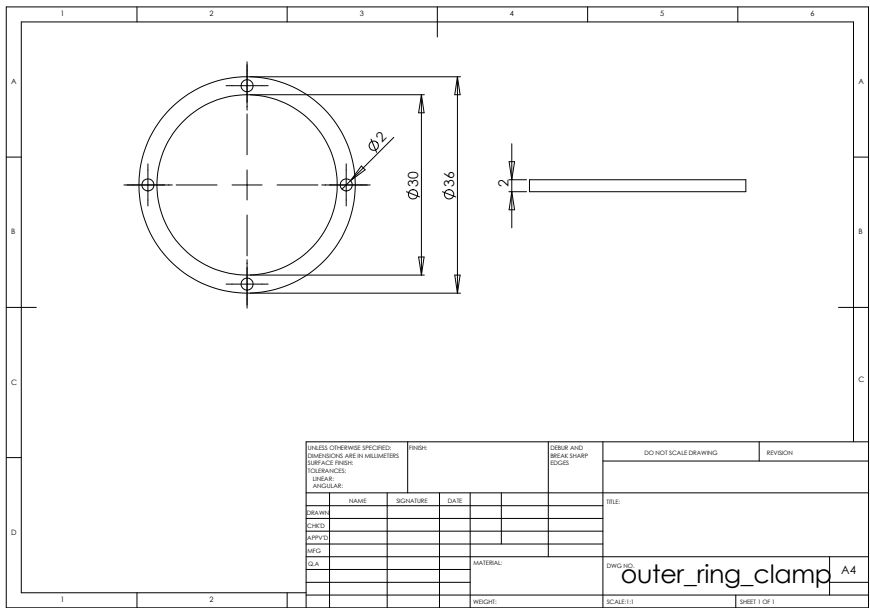


Figure 70: Outer ring for holding together actuator. Constructed from 6061-T6 aluminum.

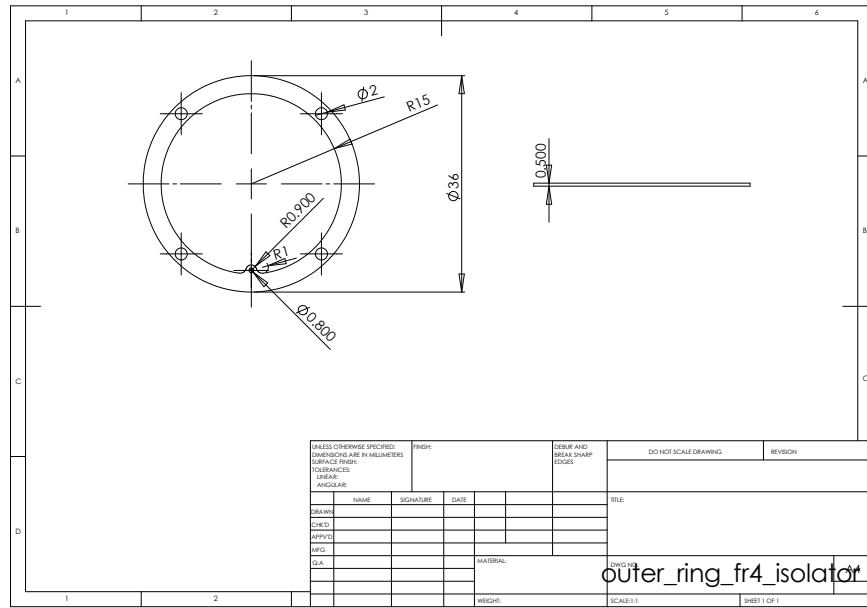


Figure 71: Isolation ring for electrically isolating the flexures from the rest of the actuator. Constructed from FR4 laminate.

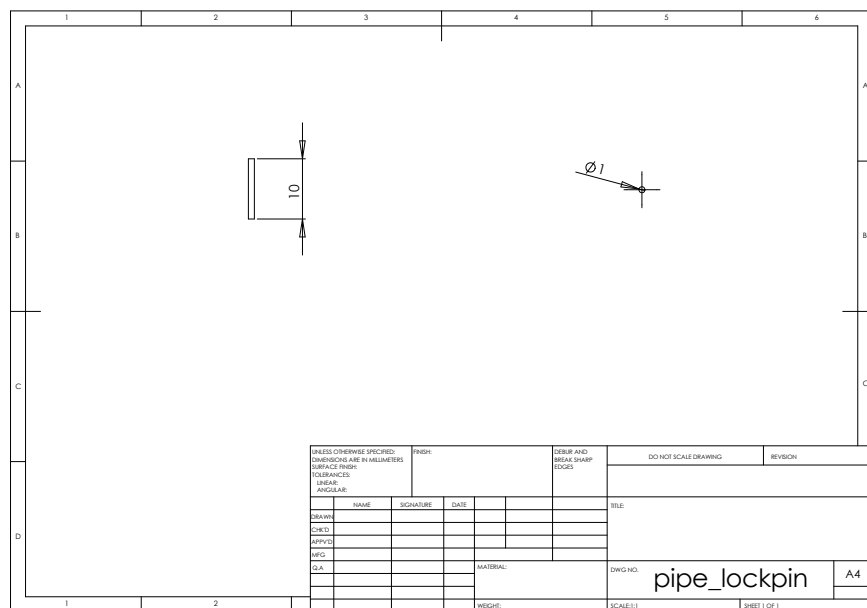


Figure 72: Lock-pin used to limit the throw of the actuator. Constructed from mild steel.

A.2 ASSEMBLED VIEWS

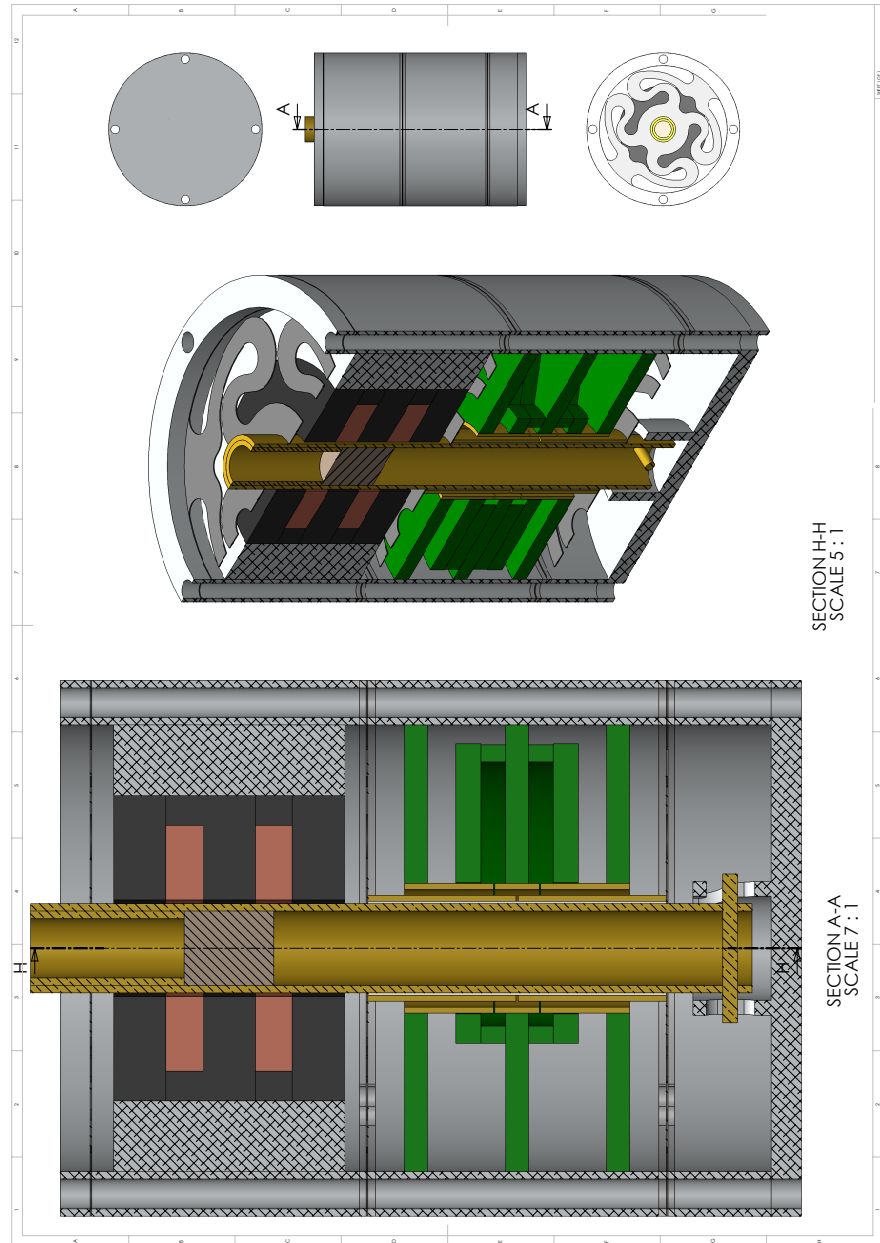


Figure 74: Assembled, colored, cross section view of actuator.

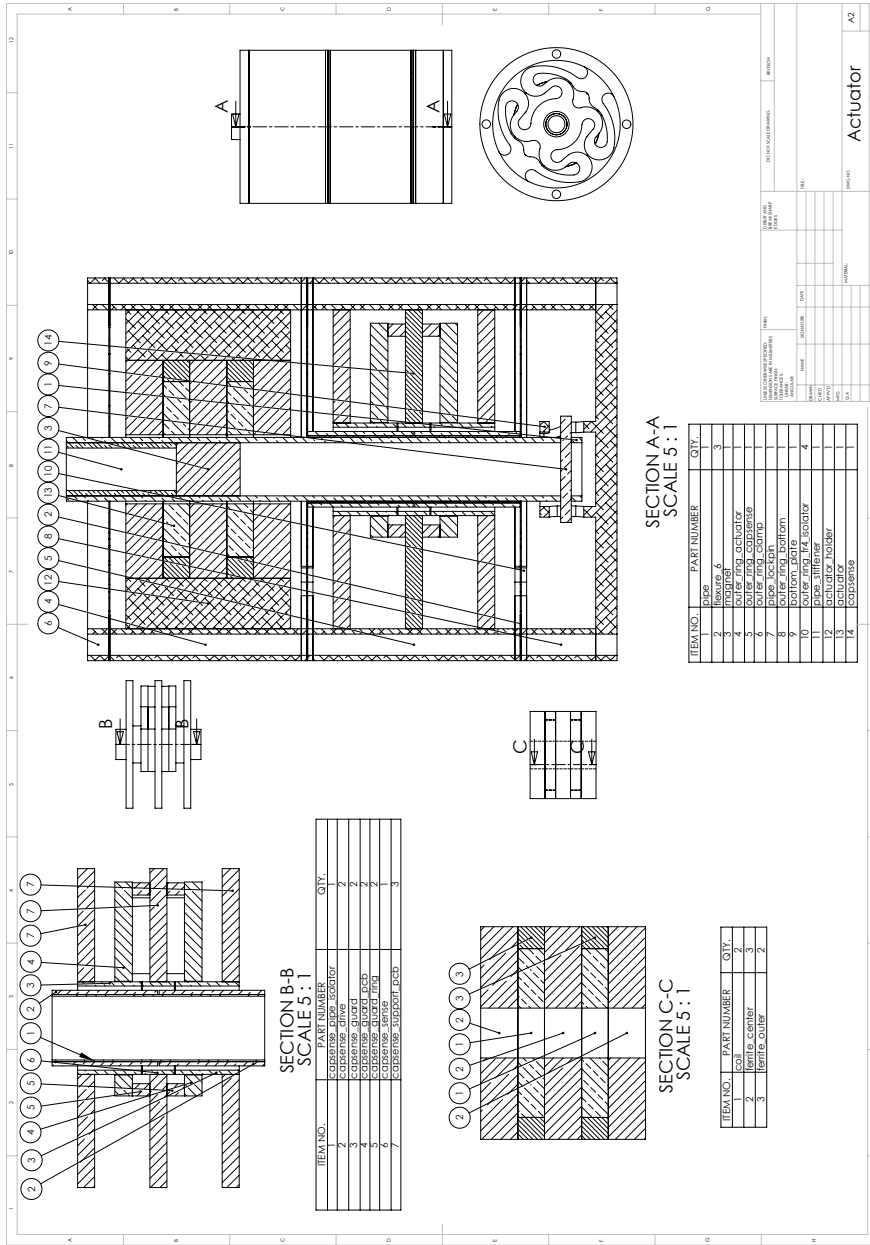


Figure 75: Assembled crosshatched cross section view with callouts for part names.

ELECTRICAL

This section contains electrical schematics, [SPICE](#) simulations, [PCB](#) artwork and part lists for all circuits in the implemented actuator, as well as an errata where applicable.

B.1 CAPACITIVE SENSOR

All schematics, [SPICE](#) simulations, [PCB](#) artwork, part lists and an errata follow.

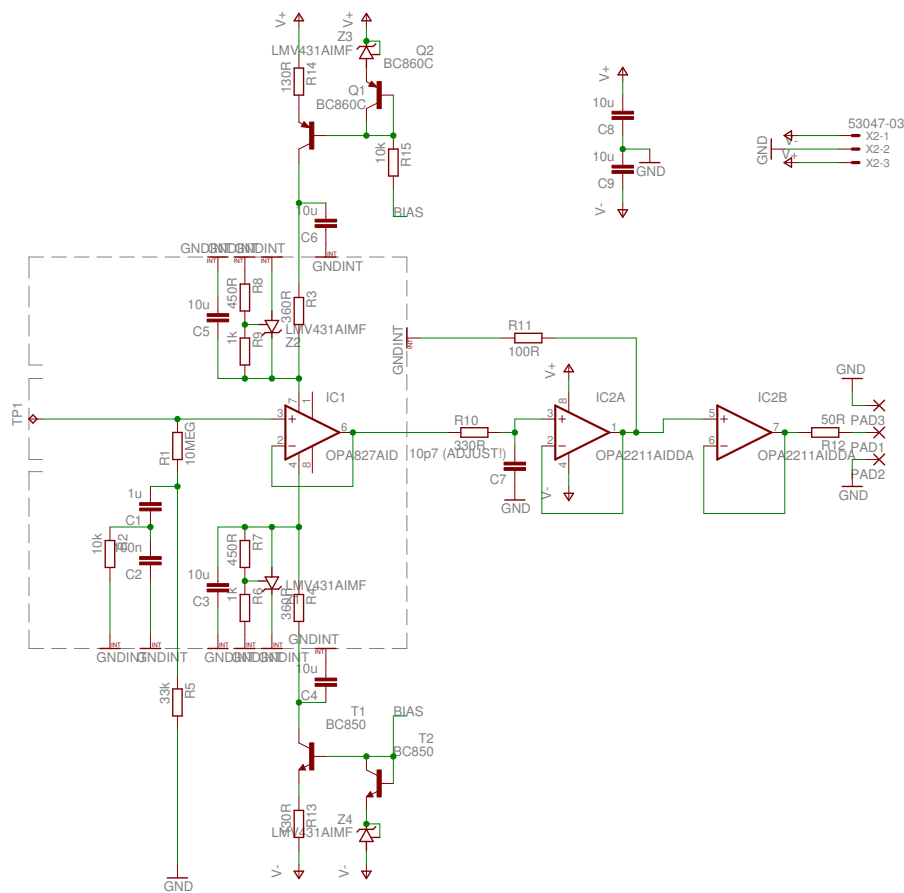


Figure 76: Schematic for capacitive sensor.

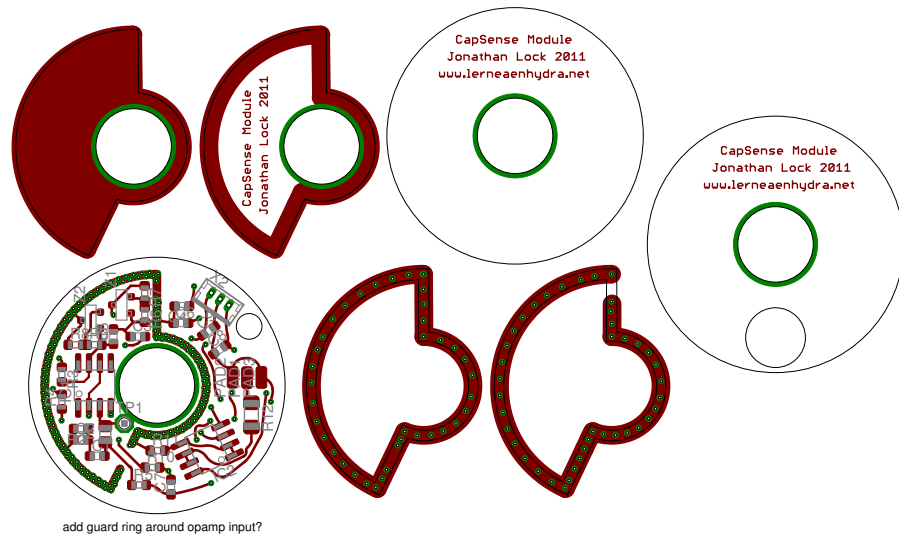


Figure 77: Top layer of **PCB** for capacitive sensor. Multiple layers of **PCB** are stacked to build the Faraday cage surrounding the sensitive electronics.

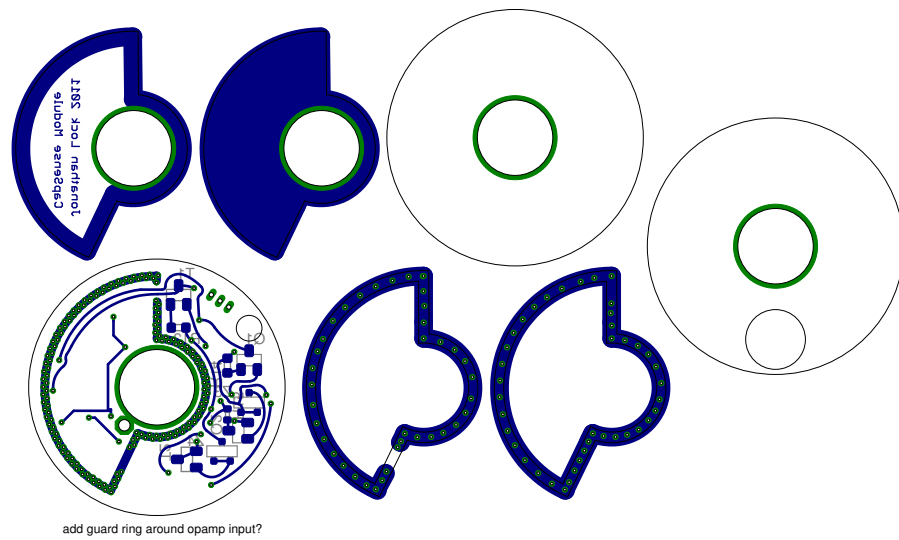


Figure 78: Bottom layer of **PCB** for capacitive sensor. Multiple layers of **PCB** are stacked to build the Faraday cage surrounding the sensitive electronics.

AFFECTED COMPONENT	DESCRIPTION	WORKAROUND
Z1, Z2, Z3, Z4	Footprint for LM431 used	Flip LMV431 upside down, reverse lead bends and mount
IC2	Power-pad on component not taken into account	Solder thin copper tape to IC, electrically connect to correct lead, isolate with kapton film and mount

Table 4: Errata for capacitive sensor PCB and schematic.

Part	Value	Device	Package	Library	Sheet
Partlist					
Exported from capsense.sch at 7/3/11 1:17 PM					
EAGLE Version 5.10.0 Copyright (c) 1988-2010 CadSoft					
C1	1u	C-EUC0603	C0603	rcl	1
C2	100n	C-EUC0603	C0603	rcl	1
C3	10u	C-EUC0603	C0603	rcl	1
C4	10u	C-EUC0603	C0603	rcl	1
C5	10u	C-EUC0603	C0603	rcl	1
C6	10u	C-EUC0603	C0603	rcl	1
C7	10p7 (ADJUST!)	C-EUC0603	C0603	rcl	1
C8	10u	C-EUC0603	C0603	rcl	1
C9	10u	C-EUC0603	C0603	rcl	1
IC1	OPA827AID	OPA134U	S008	burr-brown	1
IC2	OPA2211AIDDA	OPA2134U	S008	burr-brown	1
PAD1		SMD2	SMD1,27-2,54	wirepad	1
PAD2		SMD2	SMD1,27-2,54	wirepad	1
PAD3		SMD2	SMD1,27-2,54	wirepad	1
Q1	BC860C	BC857ALT1SMD	SOT23-BEC	transistor-pnp	1
Q2	BC860C	BC857ALT1SMD	SOT23-BEC	transistor-pnp	1
R1	10MEG	R-EU_R0805	R0805	rcl	1
R2	10k	R-EU_R0603	R0603	rcl	1
R3	360R	R-EU_R0603	R0603	rcl	1
R4	360R	R-EU_R0603	R0603	rcl	1
R5	33k	R-EU_R0603	R0603	rcl	1
R6	1k	R-EU_R0603	R0603	rcl	1
R7	450R	R-EU_R0603	R0603	rcl	1
R8	450R	R-EU_R0603	R0603	rcl	1
R9	1k	R-EU_R0603	R0603	rcl	1
R10	330R	R-EU_R0603	R0603	rcl	1
R11	100R	R-EU_R0603	R0603	rcl	1
R12	50R	R-EU_R1206	R1206	rcl	1
R13	130R	R-EU_R0603	R0603	rcl	1
R14	130R	R-EU_R0603	R0603	rcl	1
R15	10k	R-EU_R0402	R0402	rcl	1
T1	BC850	BC850	SOT23	transistor	1
T2	BC850	BC850	SOT23	transistor	1
TP1	TPPAD1-13	TPPAD1-13	P1-13	testpad	1
X2	53047-03	53047-03	53047-03	con-molex	1
Z1	LMV431AIMF	LM431	SOT-23	LM431	1
Z2	LMV431AIMF	LM431	SOT-23	LM431	1
Z3	LMV431AIMF	LM431	SOT-23	LM431	1
Z4	LMV431AIMF	LM431	SOT-23	LM431	1

B.2 CONTROLLER

All schematics, PCB artwork, part lists and an errata follow.

Figures 81 on page 125, 82 on page 125 and 83 on page 126 illustrate the simulated performance of the slew-rate limiter. As can be seen in the figure the step response exhibits some overshoot, but it is quickly damped. Also note that in figure 82 the output rises linearly for the first $\sim 1.1ms$ (constant derivative), and the output is clamped to a range, that is to say the output is Lipschitz continuous with, assuming the values as shown, a Lipschitz constant of $K \approx 95 [V/\mu s]$. This value is adjustable by changing the values of C2, C3, R4. Additionally, also note the ramp response and error signal, the error for a ramp input approaches zero as time grows, IE. the output from the slew-rate limiter exactly matches any linear input.

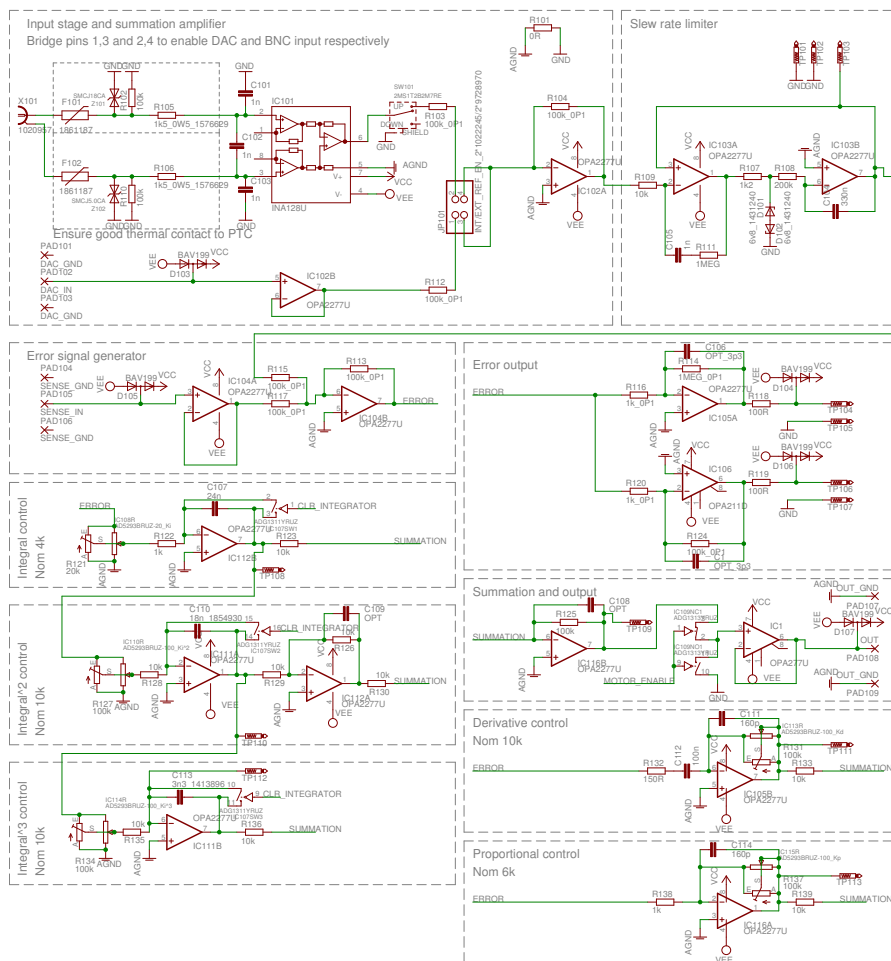


Figure 79: Schematic sheet 1 for controller.

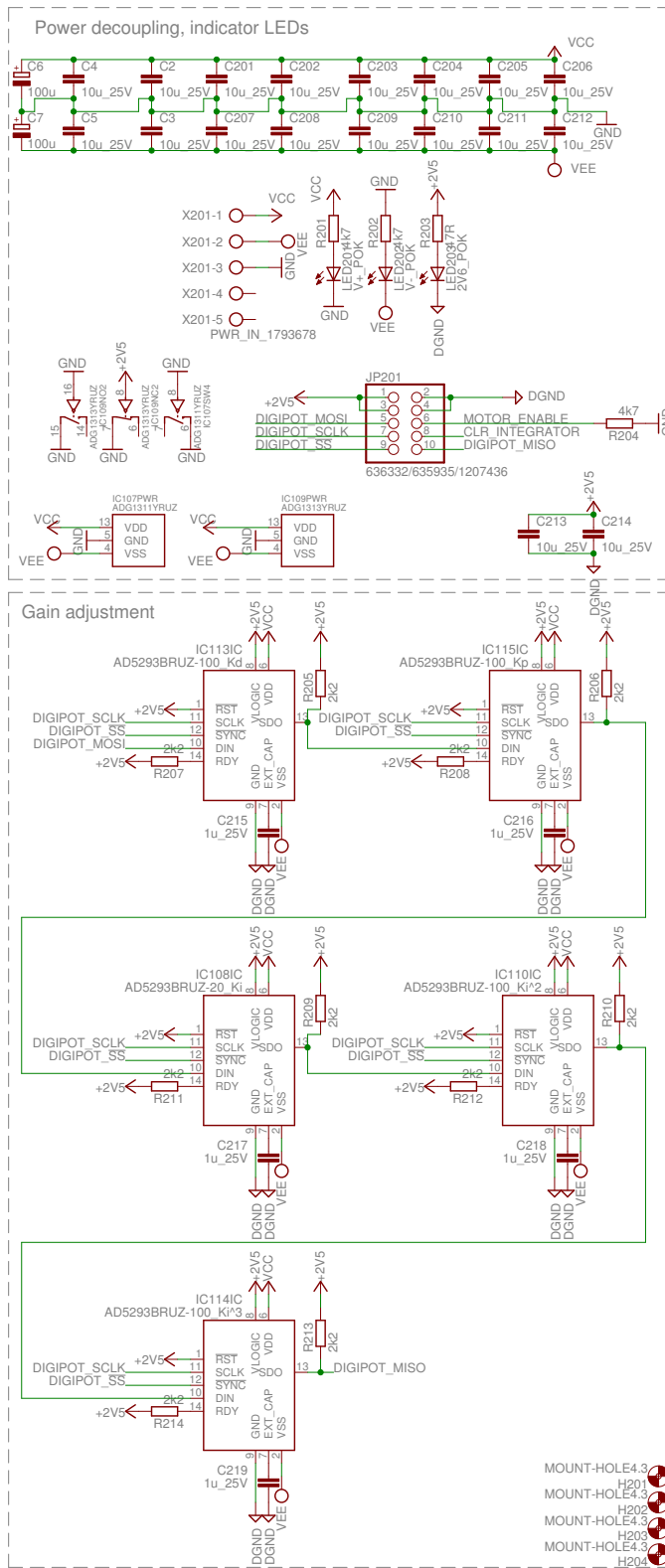


Figure 80: Schematic sheet 2 for controller.

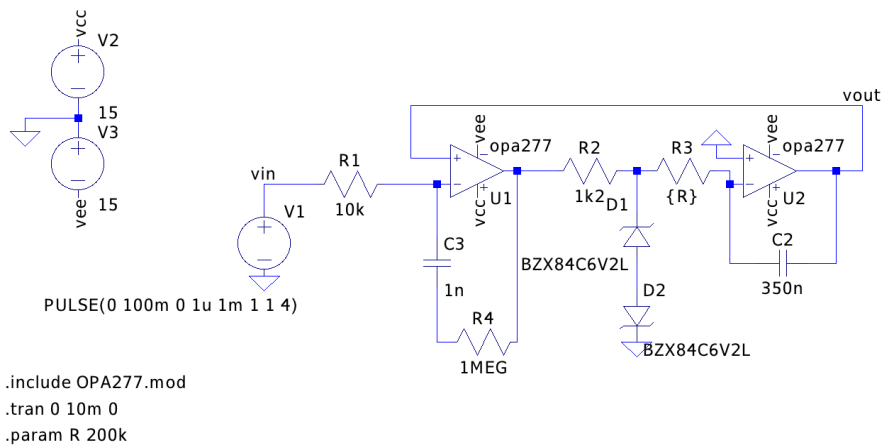


Figure 81: SPICE schematic for slew rate limiter.

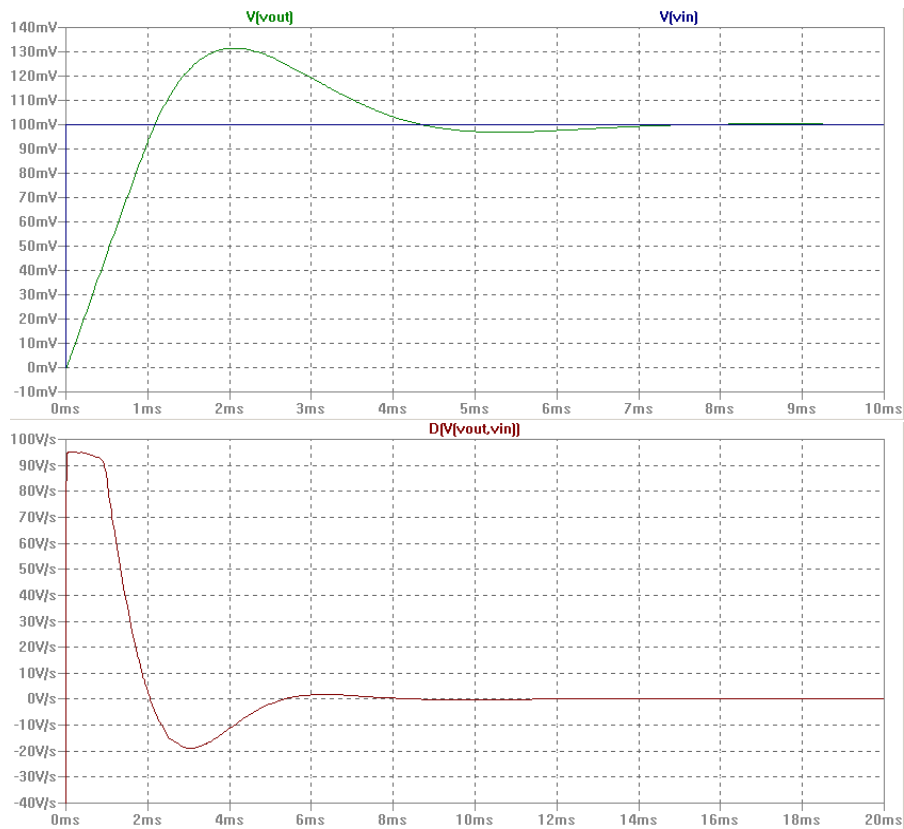


Figure 82: SPICE ramp response and time derivative of ramp response ($\frac{d}{dt}V_{out}$) for slew rate limiter.

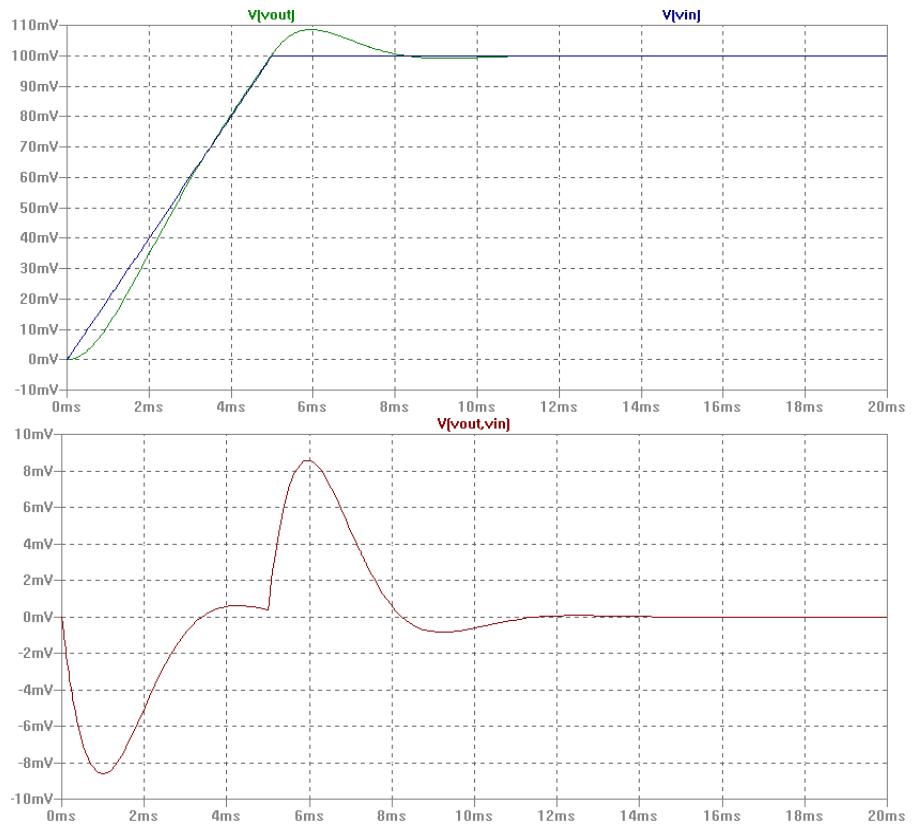


Figure 83: SPICE ramp response for slew rate limiter.

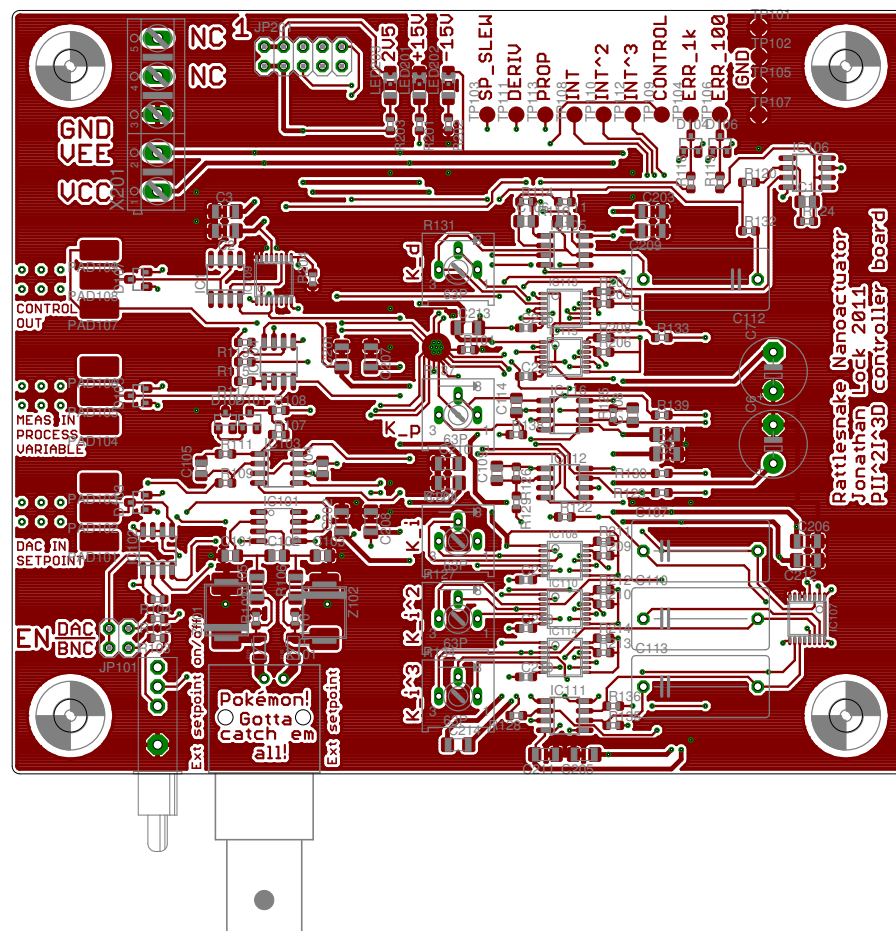


Figure 84: Top layer of PCB for controller.

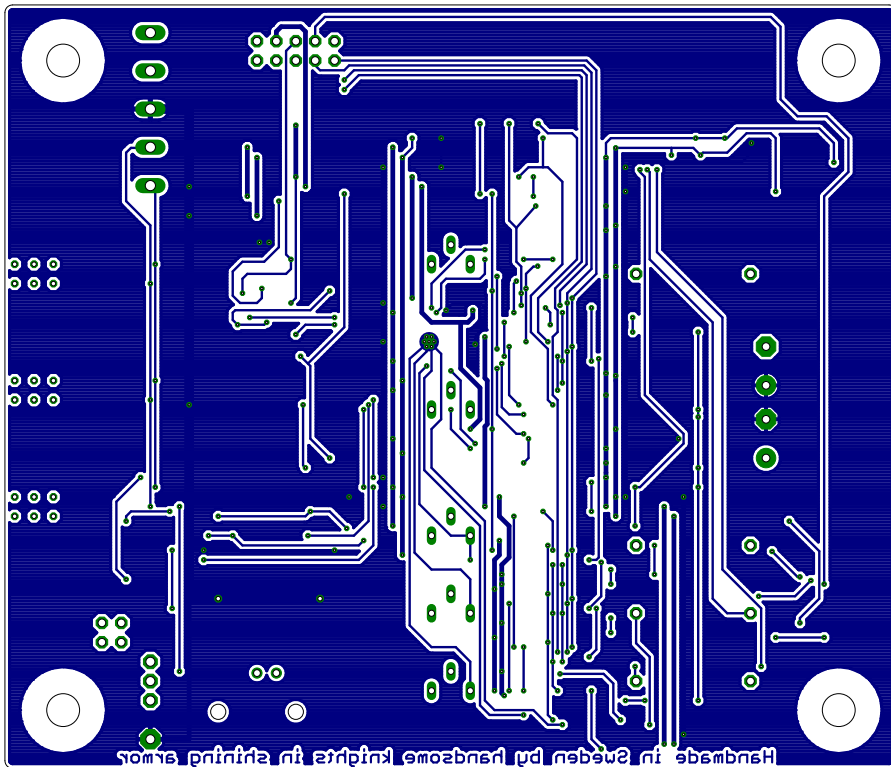


Figure 85: Bottom layer of PCB for controller.

AFFECTED COMPONENT	DESCRIPTION	WORKAROUND
TP112	Incorrect connection	Break trace, connect to other side of C113
R113	Lowpass filtering missing	Place 450p in parallel

Table 5: Errata for controller PCB and schematic.

Partlist					
Exported from controller_2.sch at 7/3/11 1:17 PM					
EAGLE Version 5.10.0 Copyright (c) 1988-2010 CadSoft					
Part	Value	Device	Package	Library	Sheet
C1	OPT_3p3	C-EUC0805	C0805	rcl	1
C2	10u_25V	C-EUC1206	C1206	rcl	2
C3	10u_25V	C-EUC1206	C1206	rcl	2
C4	10u_25V	C-EUC1206	C1206	rcl	2
C5	10u_25V	C-EUC1206	C1206	rcl	2
C6	100u	CPOL-EUES-8.5	E5-8,5	rcl	2
C7	100u	CPOL-EUES-8.5	E5-8,5	rcl	2
C101	1n	C-EUC0805	C0805	rcl	1
C102	1n	C-EUC0805	C0805	rcl	1
C103	1n	C-EUC0805	C0805	rcl	1
C104	330n	C-EUC0805	C0805	rcl	1
C105	1n	C-EUC0805	C0805	rcl	1
C106	OPT_3p3	C-EUC0805	C0805	rcl	1
C107	24n	C-EU150-084X183	C150-084X183	rcl	1

23	C108	OPT	C-EUC0805	C0805	rcl	1
	C109	OPT	C-EUC0805	C0805	rcl	1
	C110	18n_1854930	C-EU150-084X183	C150-084X183	rcl	1
	C111	160p	C-EUC0805	C0805	rcl	1
	C112	100n	C-EU150-084X183	C150-084X183	rcl	1
28	C113	3n3_1413896	C-EU150-084X183	C150-084X183	rcl	1
	C114	160p	C-EUC0805	C0805	rcl	1
	C201	10u_25V	C-EUC1206	C1206	rcl	2
	C202	10u_25V	C-EUC1206	C1206	rcl	2
	C203	10u_25V	C-EUC1206	C1206	rcl	2
33	C204	10u_25V	C-EUC1206	C1206	rcl	2
	C205	10u_25V	C-EUC1206	C1206	rcl	2
	C206	10u_25V	C-EUC1206	C1206	rcl	2
	C207	10u_25V	C-EUC1206	C1206	rcl	2
	C208	10u_25V	C-EUC1206	C1206	rcl	2
38	C209	10u_25V	C-EUC1206	C1206	rcl	2
	C210	10u_25V	C-EUC1206	C1206	rcl	2
	C211	10u_25V	C-EUC1206	C1206	rcl	2
	C212	10u_25V	C-EUC1206	C1206	rcl	2
	C213	10u_25V	C-EUC1206	C1206	rcl	2
43	C214	10u_25V	C-EUC1206	C1206	rcl	2
	C215	1u_25V	C-EUC0603	C0603	rcl	2
	C216	1u_25V	C-EUC0603	C0603	rcl	2
	C217	1u_25V	C-EUC0603	C0603	rcl	2
	C218	1u_25V	C-EUC0603	C0603	rcl	2
48	C219	1u_25V	C-EUC0603	C0603	rcl	2
	D101	6v8_1431240	ZENER-DIODESOT23	SOT23	diode	1
	D102	6v8_1431240	ZENER-DIODESOT23	SOT23	diode	1
	D103	BAV199	BAV199	SOT23	diode	1
	D104	BAV199	BAV199	SOT23	diode	1
53	D105	BAV199	BAV199	SOT23	diode	1
	D106	BAV199	BAV199	SOT23	diode	1
	D107	BAV199	BAV199	SOT23	diode	1
	F101	1861187	PTCSMD	PTC-1206	SparkFun	1
	F102	1861187	PTCSMD	PTC-1206	SparkFun	1
58	IC1	OPA277U	OPA277U	S008	linear	1
	IC101	INA128U	INA128U	S008	burr-brown	1
	IC102	OPA2277U	OPA2277U	S008	linear	1
	IC103	OPA2277U	OPA2277U	S008	linear	1
	IC104	OPA2277U	OPA2277U	S008	linear	1
63	IC105	OPA2277U	OPA2277U	S008	linear	1
	IC106	OPA211D	OPA277U	S008	linear	1
	IC107	ADG1311YRUZ	ADG1311YRUZ	TSS0P16	adg131x	1
	IC108	AD5293BRUZ-20_Ki	AD5293	TSS0P14	ad5293	1
	IC109	ADG1313YRUZ	ADG1313YRUZ	TSS0P16	adg131x	1
68	IC110	AD5293BRUZ-100_Ki^2	AD5293	TSS0P14	ad5293	1
	IC111	OPA2277U	OPA2277U	S008	linear	1
	IC112	OPA2277U	OPA2277U	S008	linear	1
	IC113	AD5293BRUZ-100_Kd	AD5293	TSS0P14	ad5293	1
	IC114	AD5293BRUZ-100_Ki^3	AD5293	TSS0P14	ad5293	1
73	IC115	AD5293BRUZ-100_Kp	AD5293	TSS0P14	ad5293	1
	IC116	OPA2277U	OPA2277U	S008	linear	1
	JP101	INT/EXT_REF_EN_2*1022245/2*9728970	PINHD-2X2	2X02	pinhead	1
	JP201	636332/635935/1207436	PINHD-2X5	2X05	pinhead	2
78	LED201	V+_POK	LEDCHIPLED_1206	CHIPLED_1206	led	2
	LED202	V-_POK	LEDCHIPLED_1206	CHIPLED_1206	led	2
	LED203	2V6_POK	LEDCHIPLED_1206	CHIPLED_1206	led	2
	PAD101	DAC_GND	SMD5	SMD2,54-5,08	wirepad	1
	PAD102	DAC_IN	SMD5	SMD2,54-5,08	wirepad	1
	PAD103	DAC_GND	SMD5	SMD2,54-5,08	wirepad	1
83	PAD104	SENSE_GND	SMD5	SMD2,54-5,08	wirepad	1
	PAD105	SENSE_IN	SMD5	SMD2,54-5,08	wirepad	1
	PAD106	SENSE_GND	SMD5	SMD2,54-5,08	wirepad	1
	PAD107	OUT_GND	SMD5	SMD2,54-5,08	wirepad	1
	PAD108	OUT	SMD5	SMD2,54-5,08	wirepad	1
88	PAD109	OUT_GND	SMD5	SMD2,54-5,08	wirepad	1
	R101	0R	R-EU_R0603	R0603	rcl	1
	R102	100k	R-EU_R0603	R0603	rcl	1
	R103	100k_0P1	R-EU_R0603	R0603	rcl	1
	R104	100k_0P1	R-EU_R0603	R0603	rcl	1
93	R105	1k5_0W5_1576629	R-EU_R1206	R1206	rcl	1
	R106	1k5_0W5_1576629	R-EU_R1206	R1206	rcl	1
	R107	1k2	R-EU_R0603	R0603	rcl	1
	R108	200k	R-EU_R0603	R0603	rcl	1
	R109	10k	R-EU_R0603	R0603	rcl	1
98	R110	100k	R-EU_R0603	R0603	rcl	1
	R111	1MEG	R-EU_R0603	R0603	rcl	1
	R112	100k_0P1	R-EU_R0603	R0603	rcl	1
	R113	100k_0P1	R-EU_R0603	R0603	rcl	1
	R114	1MEG_0P1	R-EU_R0603	R0603	rcl	1
103	R115	100k_0P1	R-EU_R0603	R0603	rcl	1
	R116	1k_0P1	R-EU_R0603	R0603	rcl	1
	R117	100k_0P1	R-EU_R0603	R0603	rcl	1
	R118	100R	R-EU_R0603	R0603	rcl	1
	R119	100R	R-EU_R0603	R0603	rcl	1
108	R120	1k_0P1	R-EU_R0603	R0603	rcl	1
	R121	20k	TRIM_EU-S63P	S63P	pot	1
	R122	1k	R-EU_R0603	R0603	rcl	1
	R123	10k	R-EU_R0603	R0603	rcl	1

	R124	100k_0P1	R-EU_R0603	R0603	rcl	1
113	R125	100k	R-EU_R0603	R0603	rcl	1
	R126	10k	R-EU_R0603	R0603	rcl	1
	R127	100k	TRIM_EU-S63P	S63P	pot	1
	R128	10k	R-EU_R0603	R0603	rcl	1
	R129	10k	R-EU_R0603	R0603	rcl	1
118	R130	10k	R-EU_R0603	R0603	rcl	1
	R131	100k	TRIM_EU-S63P	S63P	pot	1
	R132	150R	R-EU_R0603	R0603	rcl	1
	R133	10k	R-EU_R0603	R0603	rcl	1
	R134	100k	TRIM_EU-S63P	S63P	pot	1
123	R135	10k	R-EU_R0603	R0603	rcl	1
	R136	10k	R-EU_R0603	R0603	rcl	1
	R137	100k	TRIM_EU-S63P	S63P	pot	1
	R138	1k	R-EU_R0603	R0603	rcl	1
	R139	10k	R-EU_R0603	R0603	rcl	1
128	R201	4k7	R-EU_R0603	R0603	rcl	2
	R202	4k7	R-EU_R0603	R0603	rcl	2
	R203	47R	R-EU_R0603	R0603	rcl	2
	R204	4k7	R-EU_R0603	R0603	rcl	2
	R205	2k2	R-EU_R0603	R0603	rcl	2
133	R206	2k2	R-EU_R0603	R0603	rcl	2
	R207	2k2	R-EU_R0603	R0603	rcl	2
	R208	2k2	R-EU_R0603	R0603	rcl	2
	R209	2k2	R-EU_R0603	R0603	rcl	2
	R210	2k2	R-EU_R0603	R0603	rcl	2
138	R211	2k2	R-EU_R0603	R0603	rcl	2
	R212	2k2	R-EU_R0603	R0603	rcl	2
	R213	2k2	R-EU_R0603	R0603	rcl	2
	R214	2k2	R-EU_R0603	R0603	rcl	2
	SW101	2MS1T2B2M7RE	2MS1T2B2M7RE	2MS1T2B2M7RE	2MS1T2B2M7RE	1
143	TP101	GND_1573280	PTR1TP20R	TP20R	testpad	1
	TP102	GND_1573280	PTR1TP20R	TP20R	testpad	1
	TP103	SETPPOINT_SR_LIMITED_1573280	PTR1TP20R	TP20R	testpad	1
	TP104	1k_ERROR_1573280	PTR1TP20R	TP20R	testpad	1
	TP105	GND_1573280	PTR1TP20R	TP20R	testpad	1
148	TP106	100_GAIN_1573280	PTR1TP20R	TP20R	testpad	1
	TP107	GND_1573280	PTR1TP20R	TP20R	testpad	1
	TP108	INTEGRAL_1573280	PTR1TP20R	TP20R	testpad	1
	TP109	CONTROL_OUTPUT_1573280	PTR1TP20R	TP20R	testpad	1
	TP110	INTEGRAL^2_1573280	PTR1TP20R	TP20R	testpad	1
153	TP111	DERIVATIVE_1573280	PTR1TP20R	TP20R	testpad	1
	TP112	INTEGRAL^3_1573280	PTR1TP20R	TP20R	testpad	1
	TP113	PROPORTIONAL_1573280	PTR1TP20R	TP20R	testpad	1
	X101	1020957	1-227161-2	AMP_227161	con-coax	1
	X201	PWR_IN_1793678	AK500/5	AK500/5	con-ptr500	2
158	Z101	SMCJ18CA	TVS_ZENER_BI	SMC	zener-smc	1
	Z102	SMCJ5.0CA	TVS_ZENER_BI	SMC	zener-smc	1

B.3 DEMODULATOR

All schematics, [PCB artwork](#), part lists and an [errata](#) follow.

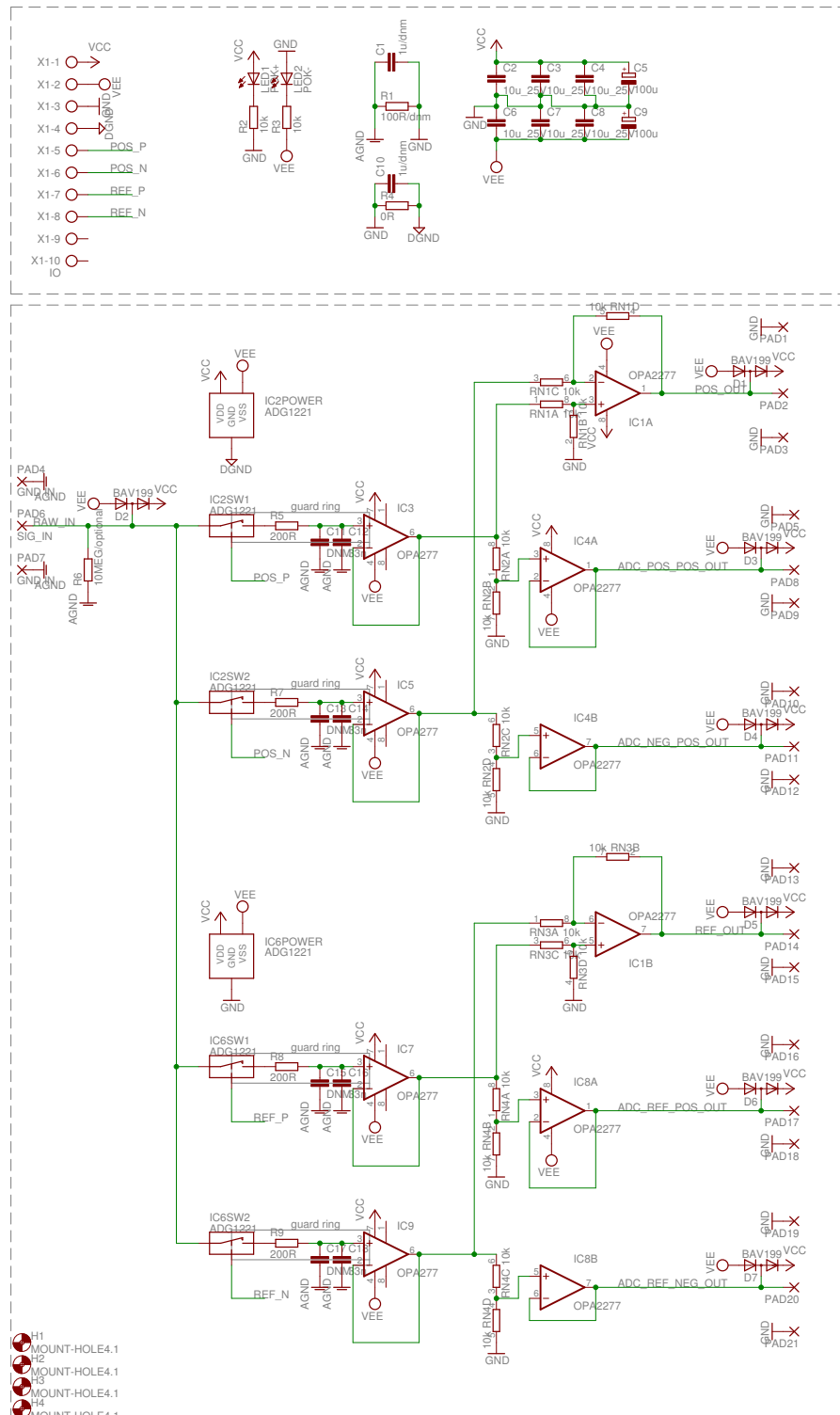


Figure 86: Schematic for demodulator.

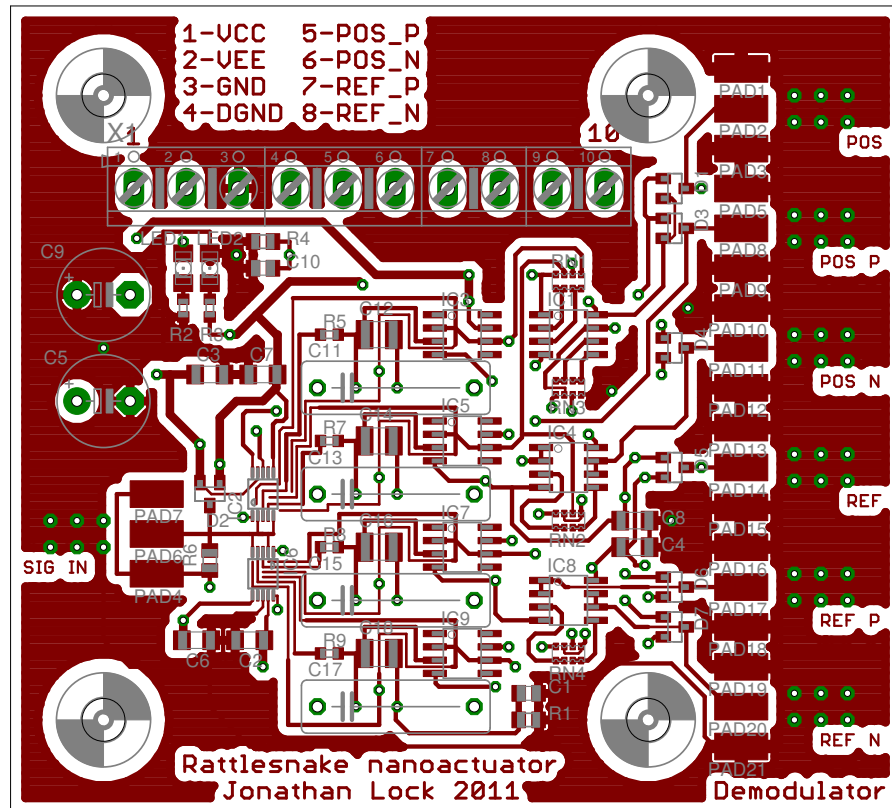


Figure 87: Top layer of PCB for demodulator.

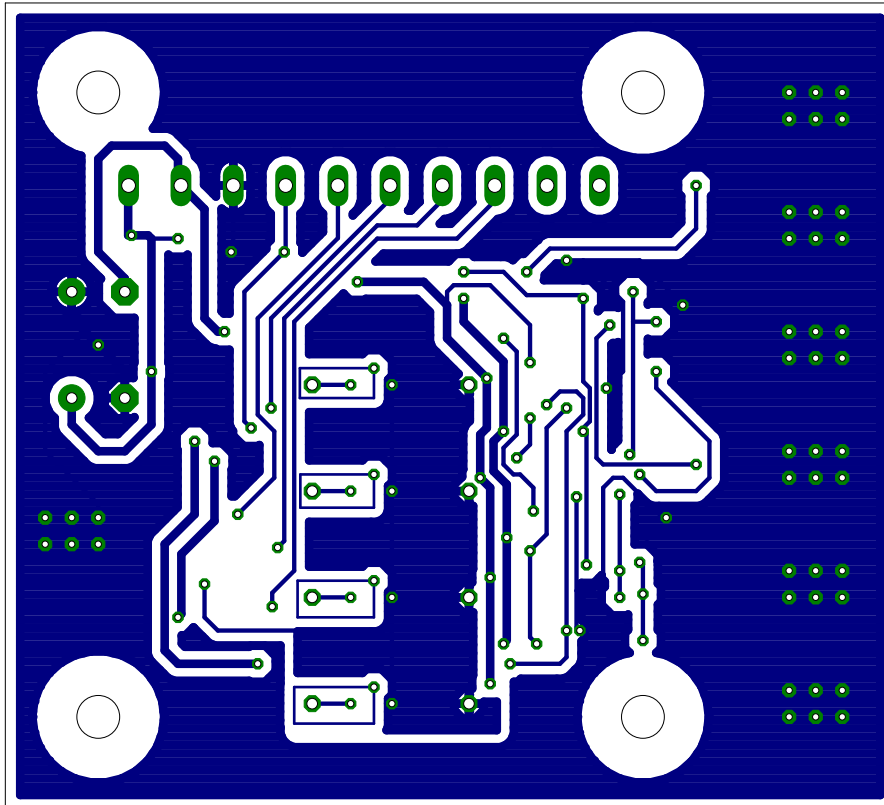


Figure 88: Bottom layer of PCB for demodulator.

AFFECTED COMPONENT	DESCRIPTION	WORKAROUND
IC6	Ground should go to DGND	None, fix board layout
IC1	No lowpass filtering done	Place 4.5n over pins 1-2,3-GND, 6-7,5-GND

Table 6: Errata for demodulator PCB and schematic.

Part	Value	Device	Package	Library	Sheet
C1	1u/dnm	C-EUC0805	C0805	rcl	1
C2	10u_25V	C-EUC1206	C1206	rcl	1
C3	10u_25V	C-EUC1206	C1206	rcl	1
C4	10u_25V	C-EUC1206	C1206	rcl	1
C5	100u	CPOL-EUE5-8.5	E5-8,5	rcl	1
C6	10u_25V	C-EUC1206	C1206	rcl	1
C7	10u_25V	C-EUC1206	C1206	rcl	1

16	C8	10u_25V	C-EUC1206	C1206	rcl	1
	C9	100u	CPOL-EUE5-8.5	E5-8,5	rcl	1
	C10	1u/dnm	C-EUC0805	C0805	rcl	1
	C11	DNM	C-EU150-054X183	C150-054X183	rcl	1
	C12	33n	C-EUC1210	C1210	rcl	1
21	C13	DNM	C-EU150-054X183	C150-054X183	rcl	1
	C14	33n	C-EUC1210	C1210	rcl	1
	C15	DNM	C-EU150-054X183	C150-054X183	rcl	1
	C16	33n	C-EUC1210	C1210	rcl	1
	C17	DNM	C-EU150-054X183	C150-054X183	rcl	1
26	C18	33n	C-EUC1210	C1210	rcl	1
	D1	BAV199	BAV199	SOT23	diode	1
	D2	BAV199	BAV199	SOT23	diode	1
	D3	BAV199	BAV199	SOT23	diode	1
	D4	BAV199	BAV199	SOT23	diode	1
31	D5	BAV199	BAV199	SOT23	diode	1
	D6	BAV199	BAV199	SOT23	diode	1
	D7	BAV199	BAV199	SOT23	diode	1
	IC1	OPA2277	OPA2134U	S008	burr-brown	1
	IC2	ADG1221	ADG1221	MS0P10	ADG1221	1
36	IC3	OPA277	OPA134U	S008	burr-brown	1
	IC4	OPA2277	OPA2134U	S008	burr-brown	1
	IC5	OPA277	OPA134U	S008	burr-brown	1
	IC6	ADG1221	ADG1221	MS0P10	ADG1221	1
	IC7	OPA277	OPA134U	S008	burr-brown	1
41	IC8	OPA2277	OPA2134U	S008	burr-brown	1
	IC9	OPA277	OPA134U	S008	burr-brown	1
	LED1	POK+	LEDSMT1206	1206	led	1
	LED2	POK-	LEDSMT1206	1206	led	1
	PAD1		SMD5	SMD2,54-5,08	wirepad	1
46	PAD2		SMD5	SMD2,54-5,08	wirepad	1
	PAD3		SMD5	SMD2,54-5,08	wirepad	1
	PAD4	GND IN	SMD5	SMD2,54-5,08	wirepad	1
	PAD5		SMD5	SMD2,54-5,08	wirepad	1
	PAD6	SIG IN	SMD5	SMD2,54-5,08	wirepad	1
51	PAD7	GND IN	SMD5	SMD2,54-5,08	wirepad	1
	PAD8		SMD5	SMD2,54-5,08	wirepad	1
	PAD9		SMD5	SMD2,54-5,08	wirepad	1
	PAD10		SMD5	SMD2,54-5,08	wirepad	1
	PAD11		SMD5	SMD2,54-5,08	wirepad	1
56	PAD12		SMD5	SMD2,54-5,08	wirepad	1
	PAD13		SMD5	SMD2,54-5,08	wirepad	1
	PAD14		SMD5	SMD2,54-5,08	wirepad	1
	PAD15		SMD5	SMD2,54-5,08	wirepad	1
	PAD16		SMD5	SMD2,54-5,08	wirepad	1
61	PAD17		SMD5	SMD2,54-5,08	wirepad	1
	PAD18		SMD5	SMD2,54-5,08	wirepad	1
	PAD19		SMD5	SMD2,54-5,08	wirepad	1
	PAD20		SMD5	SMD2,54-5,08	wirepad	1
	PAD21		SMD5	SMD2,54-5,08	wirepad	1
66	R1	100R/dnm	R-EU_R0805	R0805	rcl	1
	R2	10k	R-EU_R0603	R0603	rcl	1
	R3	10k	R-EU_R0603	R0603	rcl	1
	R4	0R	R-EU_R0805	R0805	rcl	1
	R5	200R	R-EU_R0603	R0603	rcl	1
71	R6	10MEG/optional	R-EU_R0805	R0805	rcl	1
	R7	200R	R-EU_R0603	R0603	rcl	1
	R8	200R	R-EU_R0603	R0603	rcl	1
	R9	200R	R-EU_R0603	R0603	rcl	1
	RN1	10k	4R-NCAT16	CAT16	resistor-dil	1
76	RN2	10k	4R-NCAT16	CAT16	resistor-dil	1
	RN3	10k	4R-NCAT16	CAT16	resistor-dil	1
	RN4	10k	4R-NCAT16	CAT16	resistor-dil	1
	X1	I0	AK500/10	AK500/10	con-ptr500	1

B.4 DIGITAL BOARD

All schematics, [PCB artwork](#), part lists and an [errata](#) follow.

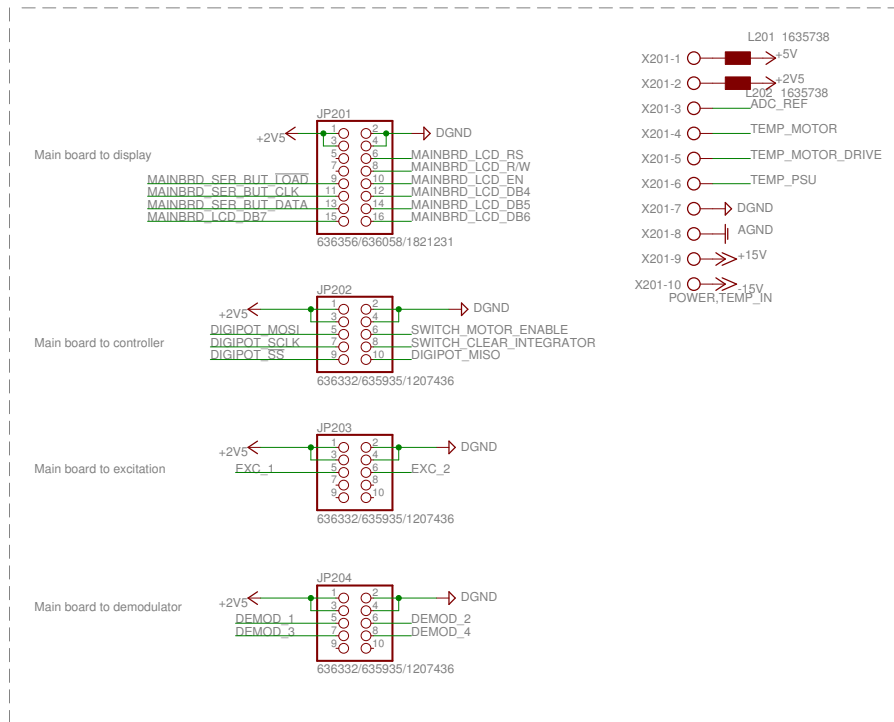


Figure 89: Schematic for sheet 2 of digital board.

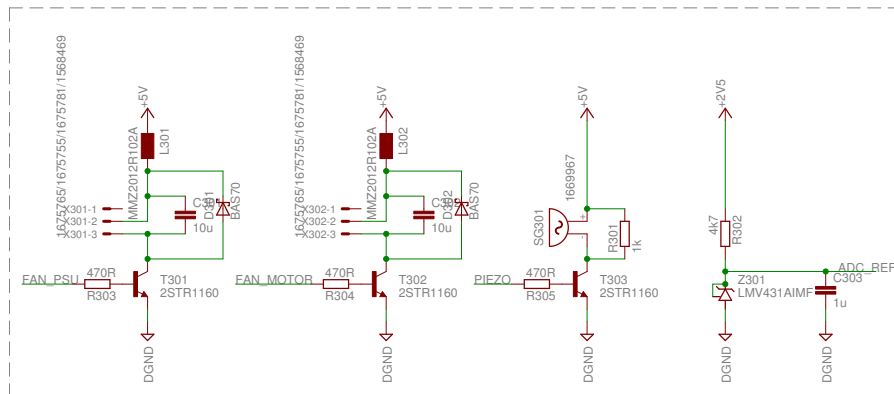
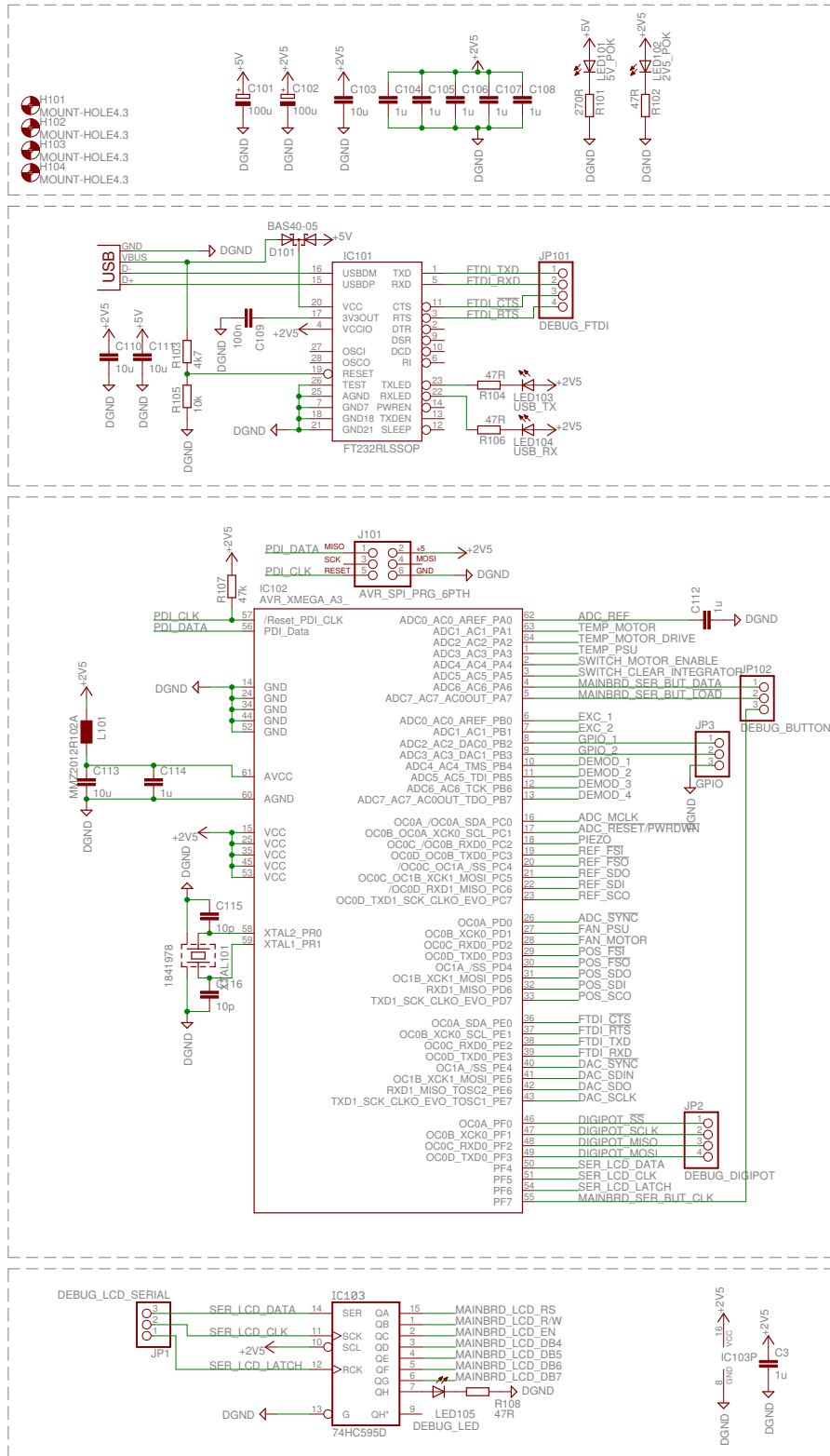


Figure 90: Schematic for sheet 3 of digital board.

note: set "2.5V" rail to 2.6V±20mv



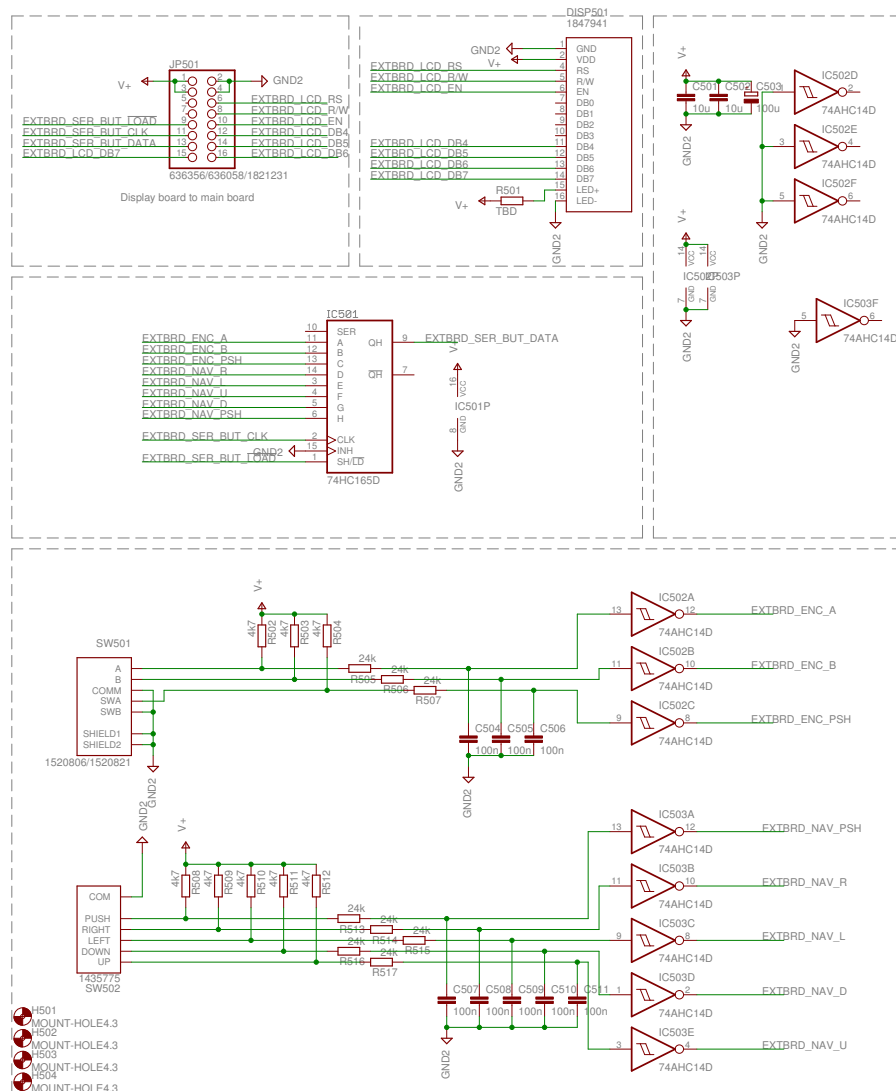


Figure 93: Schematic for sheet 5 of digital board.

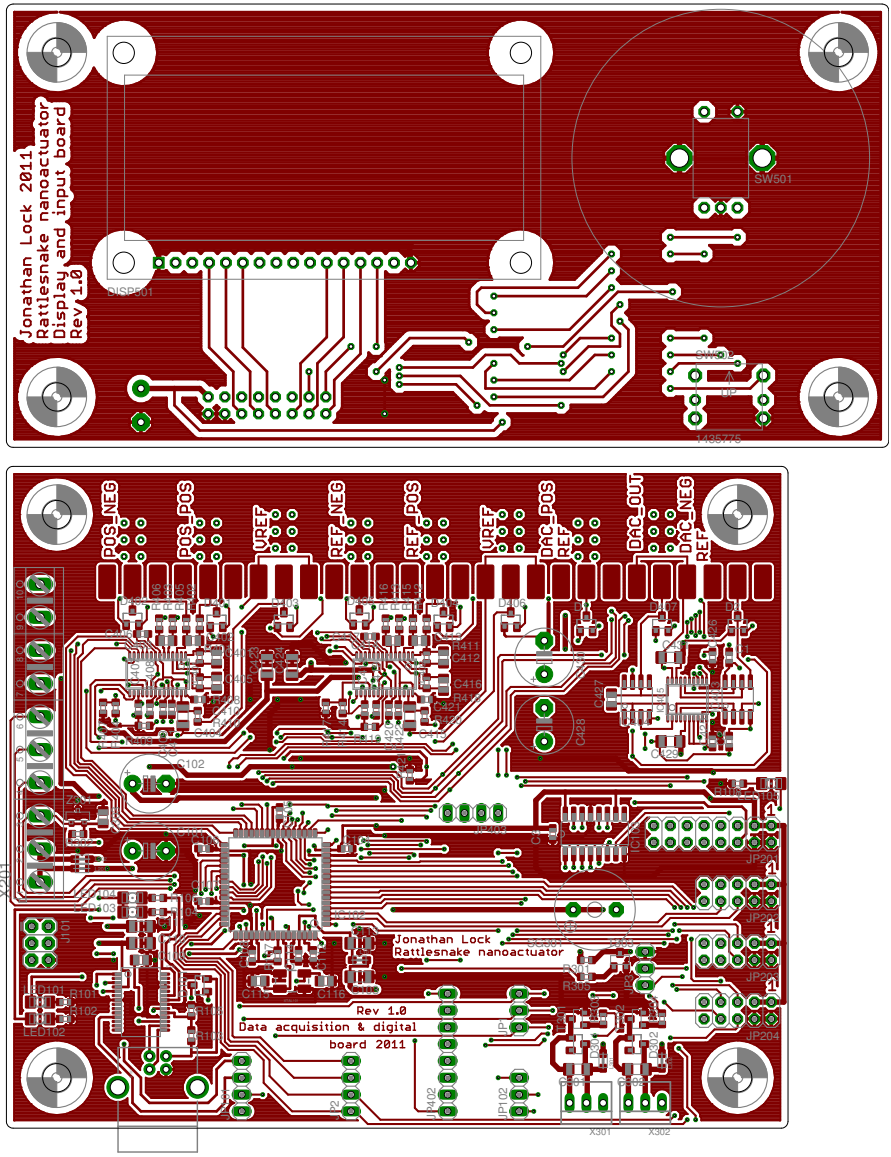


Figure 94: Top layer of PCB for digital board.

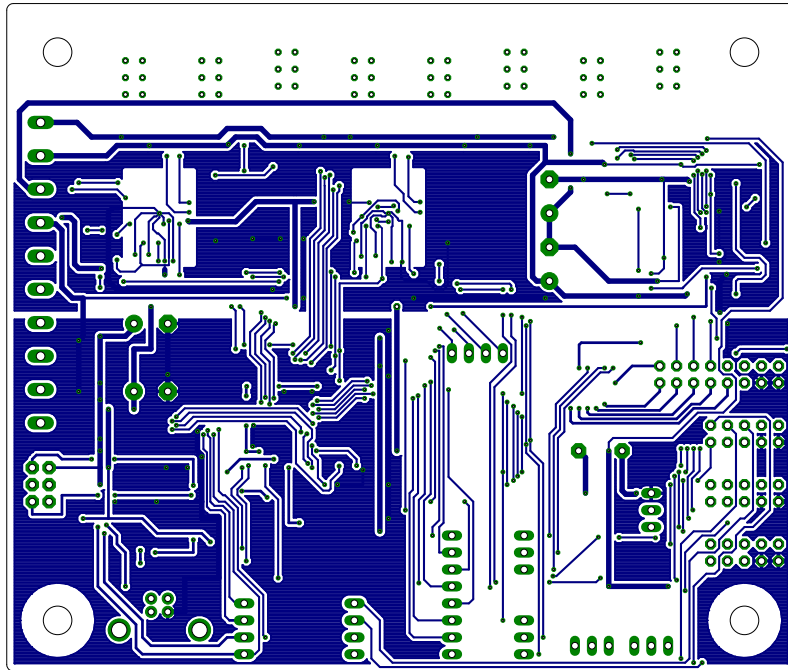
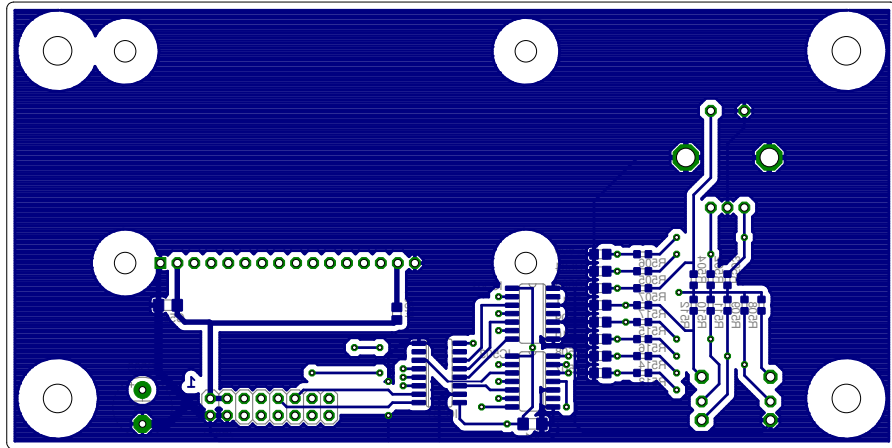


Figure 95: Bottom layer of PCB for digital board.

AFFECTED COMPONENT	DESCRIPTION	WORKAROUND
<i>DISP501</i>	2.6V is not enough for LCD R/W pin can be changed by software, setting R/W high sets LCD data pins to output which could destroy hardware	Cut trace for power, drive from 5V with a red LED to drop voltage to roughly 3.3V Cut trace from shift register to LCD and tie LCD R/W pin to ground
<i>IC102</i>	No decoupling on temperature inputs	Place 1u on nets <i>TEMP_MOTOR</i> <i>TEMP_MOTOR_DRIVE</i> and <i>TEMP_PSU</i>

Table 7: Errata for digital board PCB and schematic.

1	Partlist			
	Exported from digital_board.sch at 7/3/11 1:17 PM			
	EAGLE Version 5.10.0 Copyright (c) 1988-2010 CadSoft			
6	Part	Value Library	Device Sheet	Package
	C1	1u rcl	C-EUC0603 4	C0603
	C2	1u rcl	C-EUC0603 4	C0603
11	C3	1u rcl	C-EUC0603 1	C0603
	C101	100u rcl	CP0L-EUE5-8.5 1	E5-8,5
	C102	100u rcl	CP0L-EUE5-8.5 1	E5-8,5
	C103	10u rcl	C-EUC1206 1	C1206
	C104	1u rcl	C-EUC0603 1	C0603
16	C105	1u rcl	C-EUC0603 1	C0603
	C106	1u rcl	C-EUC0603 1	C0603
	C107	1u rcl	C-EUC0603 1	C0603
	C108	1u rcl	C-EUC0603 1	C0603
	C109	100n rcl	C-EUC0805 1	C0805
21	C110	10u rcl	C-EUC1206 1	C1206
	C111	10u rcl	C-EUC1206 1	C1206
	C112	1u rcl	C-EUC0603 1	C0603

	C113	10u		C-EUC1206	C1206
			rcl	1	
	C114	1u		C-EUC0603	C0603
			rcl	1	
26	C115	10p		C-EUC0805	C0805
			rcl	1	
	C116	10p		C-EUC0805	C0805
			rcl	1	
	C301	10u		C-EUC1206	C1206
			rcl	3	
	C302	10u		C-EUC1206	C1206
			rcl	3	
	C303	1u		C-EUC0805	C0805
			rcl	3	
31	C401	47p		C-EUC0805	C0805
			rcl	4	
	C402	8p2		C-EUC0805	C0805
			rcl	4	
	C403	56p		C-EUC0805	C0805
			rcl	4	
	C404	10u		C-EUC1206	C1206
			rcl	4	
	C405	47p		C-EUC0805	C0805
			rcl	4	
36	C406	1u		C-EUC0603	C0603
			rcl	4	
	C407	1u		C-EUC0603	C0603
			rcl	4	
	C408	1u		C-EUC0603	C0603
			rcl	4	
	C409	1u		C-EUC0603	C0603
			rcl	4	
	C410	1u		C-EUC0603	C0603
			rcl	4	
41	C411	1u		C-EUC0603	C0603
			rcl	4	
	C412	47p		C-EUC0805	C0805
			rcl	4	
	C413	8p2		C-EUC0805	C0805
			rcl	4	
	C414	56p		C-EUC0805	C0805
			rcl	4	
	C415	10u		C-EUC1206	C1206
			rcl	4	
46	C416	47p		C-EUC0805	C0805
			rcl	4	
	C417	1u		C-EUC0603	C0603
			rcl	4	
	C418	1u		C-EUC0603	C0603
			rcl	4	
	C419	1u		C-EUC0603	C0603
			rcl	4	
	C420	1u		C-EUC0603	C0603
			rcl	4	
51	C421	1u		C-EUC0603	C0603
			rcl	4	
	C422	1u		C-EUC0603	C0603
			rcl	4	
	C423	10u		C-EUC1206	C1206
			rcl	4	
	C424	10u		C-EUC1206	C1206
			rcl	4	
	C425	1u		C-EUC0603	C0603
			rcl	4	
56	C426	1u		C-EUC0603	C0603
			rcl	4	

	C427	10p		C - EUC0805	C0805
			rcl	4	
	C428	100u		CPOL - EUE5 - 8.5	E5 - 8,5
			rcl	4	
	C429	10u		C - EUC1206	C1206
			rcl	4	
	C430	100u		CPOL - EUE5 - 8.5	E5 - 8,5
			rcl	4	
61	C431	10u		C - EUC1206	C1206
			rcl	4	
	C501	10u		C - EUC1206	C1206
			rcl	5	
	C502	10u		C - EUC1206	C1206
			rcl	5	
	C503	100u		CPOL - EUE5 - 8.5	E5 - 8,5
			rcl	5	
	C504	100n		C - EUC0805	C0805
			rcl	5	
66	C505	100n		C - EUC0805	C0805
			rcl	5	
	C506	100n		C - EUC0805	C0805
			rcl	5	
	C507	100n		C - EUC0805	C0805
			rcl	5	
	C508	100n		C - EUC0805	C0805
			rcl	5	
	C509	100n		C - EUC0805	C0805
			rcl	5	
71	C510	100n		C - EUC0805	C0805
			rcl	5	
	C511	100n		C - EUC0805	C0805
			rcl	5	
	D1	BAV199		BAV199	SOT23
			diode	4	
	D2	BAV199		BAV199	SOT23
			diode	4	
	D101	BAS40-05		BAS40-05	SOT23
			diode	1	
76	D301	BAS70		BAS70	SOT23
			diode	3	
	D302	BAS70		BAS70	SOT23
			diode	3	
	D401	BAV199		BAV199	SOT23
			diode	4	
	D402	BAV199		BAV199	SOT23
			diode	4	
	D403	BAV199		BAV199	SOT23
			diode	4	
81	D404	BAV199		BAV199	SOT23
			diode	4	
	D405	BAV199		BAV199	SOT23
			diode	4	
	D406	BAV199		BAV199	SOT23
			diode	4	
	D407	BAV199		BAV199	SOT23
			diode	4	
	DISP501	1847941		16X2 - LCD	LCD16X2
			16x2_lcd	5	
86	IC101	FT232RLSS0P		FT232RLSS0P	SS0P28DB
			SparkFun	1	
	IC102	AVR_XMEGA_A3_		AVR_XMEGA_A3_	TQFP64
			xmega	1	
	IC103	74HC595D		74HC595D	S016
			74xx - eu	1	
	IC401	AD7764		AD7764	TSS0P28
			ad7764	4	

	IC402	AD7764 ad7764	AD7764 4	TSS0P28
91	IC403	AD8676ARZ* burr-brown	OPA2134U 4	S008
	IC404	AD8675 burr-brown	OPA134U 4	S008
	IC405	AD5791 ad5791	AD5791 4	TSS0P20
	IC501	74HC165D 74xx-eu	74HC165D 5	S016
	IC502	74AHC14D 74xx-eu	74HC14D 5	S014
96	IC503	74AHC14D 74xx-eu	74HC14D 5	S014
	J101	AVR_SPI_PRG_6PTH SparkFun	AVR_SPI_PRG_6PTH 1	2X3
	JP1	DEBUG_LCD_SERIAL pinhead	PINHD-1X3 1	1X03
	JP2	DEBUG_DIGIP0T pinhead	PINHD-1X4 1	1X04
	JP3	GPIO pinhead	PINHD-1X3 1	1X03
101	JP101	DEBUG_FTDI pinhead	PINHD-1X4 1	1X04
	JP102	DEBUG_BUTTON pinhead	PINHD-1X3 1	1X03
	JP201	636356/636058/1821231 pinhead	PINHD-2X8 2	2X08
	JP202	636332/635935/1207436 pinhead	PINHD-2X5 2	2X05
	JP203	636332/635935/1207436 pinhead	PINHD-2X5 2	2X05
106	JP204	636332/635935/1207436 pinhead	PINHD-2X5 2	2X05
	JP402	ADC_DEBUG pinhead	PINHD-1X8 4	1X08
	JP403	DEBUG_DAC pinhead	PINHD-1X4 4	1X04
	JP501	636356/636058/1821231 pinhead	PINHD-2X8 5	2X08
	L101	MMZ2012R102A wuerth-elektronik	WE-CBF_0805 1	0805
111	L201	1635738 wuerth-elektronik	WE-CBF_0805 2	0805
	L202	1635738 wuerth-elektronik	WE-CBF_0805 2	0805
	L301	MMZ2012R102A wuerth-elektronik	WE-CBF_0805 3	0805
	L302	MMZ2012R102A wuerth-elektronik	WE-CBF_0805 3	0805
	LED101	5V_POK led	LEDSMT1206 1	1206
116	LED102	2V5_POK led	LEDSMT1206 1	1206
	LED103	USB_TX led	LEDSMT1206 1	1206
	LED104	USB_RX led	LEDSMT1206 1	1206
	LED105	DEBUG_LED led	LEDSMT1206 1	1206
	PAD401	GND_ADC_SIG wirepad	SMD5 4	SMD2,54-5,08
121	PAD402	POS_POS wirepad	SMD5 4	SMD2,54-5,08
	PAD403	GND_ADC_SIG wirepad	SMD5 4	SMD2,54-5,08

	PAD404	GND_ADC_SIG		SMD5	SMD2,54-5,08
		wirepad	4		
	PAD405	POS_NEG		SMD5	SMD2,54-5,08
		wirepad	4		
	PAD406	GND_ADC_SIG		SMD5	SMD2,54-5,08
		wirepad	4		
126	PAD407	GND_VREF_ADC		SMD5	SMD2,54-5,08
		wirepad	4		
	PAD408	VREF_ADC		SMD5	SMD2,54-5,08
		wirepad	4		
	PAD409	GND_VREF_ADC		SMD5	SMD2,54-5,08
		wirepad	4		
	PAD410	GND_ADC_SIG		SMD5	SMD2,54-5,08
		wirepad	4		
	PAD411	REF_POS		SMD5	SMD2,54-5,08
		wirepad	4		
131	PAD412	GND_ADC_SIG		SMD5	SMD2,54-5,08
		wirepad	4		
	PAD413	GND_ADC_SIG		SMD5	SMD2,54-5,08
		wirepad	4		
	PAD414	REF_NEG		SMD5	SMD2,54-5,08
		wirepad	4		
	PAD415	GND_ADC_SIG		SMD5	SMD2,54-5,08
		wirepad	4		
	PAD416	GND_VREF_ADC		SMD5	SMD2,54-5,08
		wirepad	4		
136	PAD417	VREF_ADC		SMD5	SMD2,54-5,08
		wirepad	4		
	PAD418	GND_VREF_ADC		SMD5	SMD2,54-5,08
		wirepad	4		
	PAD419	DAC_REF_GND		SMD5	SMD2,54-5,08
		wirepad	4		
	PAD420	DAC_POS_REF		SMD5	SMD2,54-5,08
		wirepad	4		
	PAD421	DAC_REF_GND		SMD5	SMD2,54-5,08
		wirepad	4		
141	PAD422	DAC_OUT_GND		SMD5	SMD2,54-5,08
		wirepad	4		
	PAD423	DAC_OUT		SMD5	SMD2,54-5,08
		wirepad	4		
	PAD424	DAC_OUT_GND		SMD5	SMD2,54-5,08
		wirepad	4		
	PAD425	DAC_REF_GND		SMD5	SMD2,54-5,08
		wirepad	4		
	PAD426	DAC_NEG_REF		SMD5	SMD2,54-5,08
		wirepad	4		
146	PAD427	DAC_REF_GND		SMD5	SMD2,54-5,08
		wirepad	4		
	R101	270R		R-EU_R0603	R0603
		rcl		1	
	R102	47R		R-EU_R0603	R0603
		rcl		1	
	R103	4k7		R-EU_R0603	R0603
		rcl		1	
	R104	47R		R-EU_R0603	R0603
		rcl		1	
151	R105	10k		R-EU_R0603	R0603
		rcl		1	
	R106	47R		R-EU_R0603	R0603
		rcl		1	
	R107	47k		R-EU_R0603	R0603
		rcl		1	
	R108	47R		R-EU_R0603	R0603
		rcl		1	
	R301	1k		R-EU_R0603	R0603
		rcl		3	

156	R302	4k7 rcl	R-EU_R0603 3	R0603
	R303	470R rcl	R-EU_R0603 3	R0603
	R304	470R rcl	R-EU_R0603 3	R0603
	R305	470R rcl	R-EU_R0603 3	R0603
	R401	3k01_0P1 rcl	R-EU_R0603 4	R0603
161	R402	4k75_0P1 rcl	R-EU_R0603 4	R0603
	R403	43R rcl	R-EU_R0603 4	R0603
	R404	0R_OPTIONAL rcl	R-EU_R0603 4	R0603
	R405	4k75_0P1 rcl	R-EU_R0603 4	R0603
	R406	43R rcl	R-EU_R0603 4	R0603
166	R407	0R_OPTIONAL rcl	R-EU_R0603 4	R0603
	R408	3k01_0P1 rcl	R-EU_R0603 4	R0603
	R409	160k rcl	R-EU_R0603 4	R0603
	R410	100R rcl	R-EU_R0603 4	R0603
	R411	3k01_0P1 rcl	R-EU_R0603 4	R0603
171	R412	4k75_0P1 rcl	R-EU_R0603 4	R0603
	R413	43R rcl	R-EU_R0603 4	R0603
	R414	0R_OPTIONAL rcl	R-EU_R0603 4	R0603
	R415	4k75_0P1 rcl	R-EU_R0603 4	R0603
	R416	43R rcl	R-EU_R0603 4	R0603
176	R417	0R_OPTIONAL rcl	R-EU_R0603 4	R0603
	R418	3k01_0P1 rcl	R-EU_R0603 4	R0603
	R419	160k rcl	R-EU_R0603 4	R0603
	R420	100R rcl	R-EU_R0603 4	R0603
	R421	0R rcl	R-EU_R0603 4	R0603
181	R501	TBD rcl	R-EU_R0805 5	R0805
	R502	4k7 rcl	R-EU_R0603 5	R0603
	R503	4k7 rcl	R-EU_R0603 5	R0603
	R504	4k7 rcl	R-EU_R0603 5	R0603
	R505	24k rcl	R-EU_R0603 5	R0603
186	R506	24k rcl	R-EU_R0603 5	R0603
	R507	24k rcl	R-EU_R0603 5	R0603
	R508	4k7 rcl	R-EU_R0603 5	R0603

	R509	4k7		R-EU_R0603	R0603
			rcl	5	
	R510	4k7		R-EU_R0603	R0603
			rcl	5	
191	R511	4k7		R-EU_R0603	R0603
			rcl	5	
	R512	4k7		R-EU_R0603	R0603
			rcl	5	
	R513	24k		R-EU_R0603	R0603
			rcl	5	
	R514	24k		R-EU_R0603	R0603
			rcl	5	
	R515	24k		R-EU_R0603	R0603
			rcl	5	
196	R516	24k		R-EU_R0603	R0603
			rcl	5	
	R517	24k		R-EU_R0603	R0603
			rcl	5	
	SG301	1669967		F/QMX	F/QMX
		buzzer		3	
	SW501	1520806/1520821		EC11E15244C0	TYPE8
		EC11E15244C0		5	
	SW502	1435775		SKQU_MULTIDIRECTION_BUTTON	SKQU
		skqu_multidirectional_button		5	
201	T301	2STR1160		BC817-16-NPN-SOT23-BEC	SOT23-BEC
		transistor		3	
	T302	2STR1160		BC817-16-NPN-SOT23-BEC	SOT23-BEC
		transistor		3	
	T303	2STR1160		BC817-16-NPN-SOT23-BEC	SOT23-BEC
		transistor		3	
	X101	1308876		USBPTH	USB-B-PTH
		SparkFun		1	
	X201	POWER,TEMP_IN		AK500/10	AK500/10
		con-ptr500		2	
206	X301	1675765/1675755/1675781/1568469		22-23-2031	22-23-2031
		con-molex		3	
	X302	1675765/1675755/1675781/1568469		22-23-2031	22-23-2031
		con-molex		3	
	XTAL101	1841978		5X3_SMD_CRYSTAL	CRYSTAL-SMD-5
		X3 smd_crystal		1	
	Z301	LMV431AIMF		LMV431	SOT-23
		LM431		3	

B.5 EXCITATION CONTROL

All schematics, PCB artwork and part lists follow.

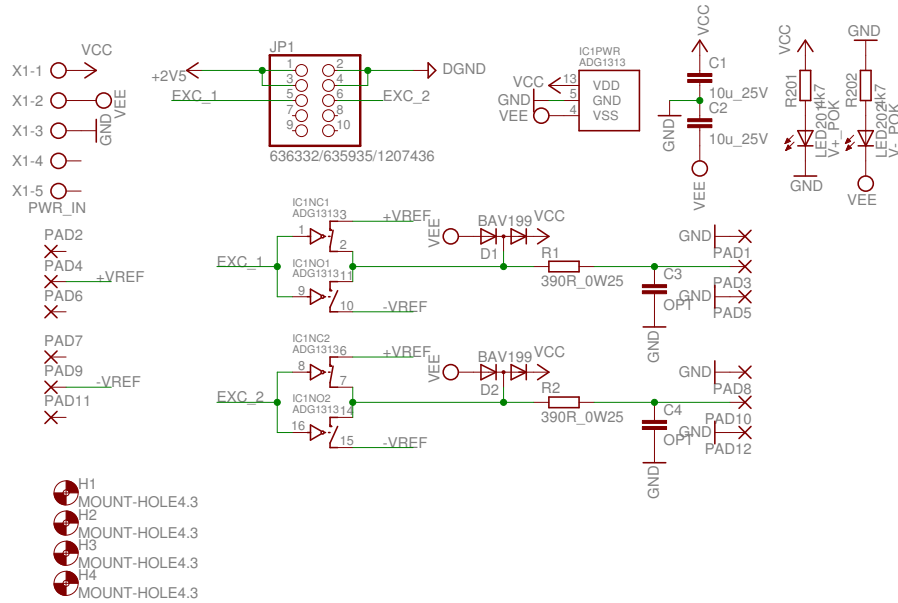


Figure 96: Schematic for excitation control.

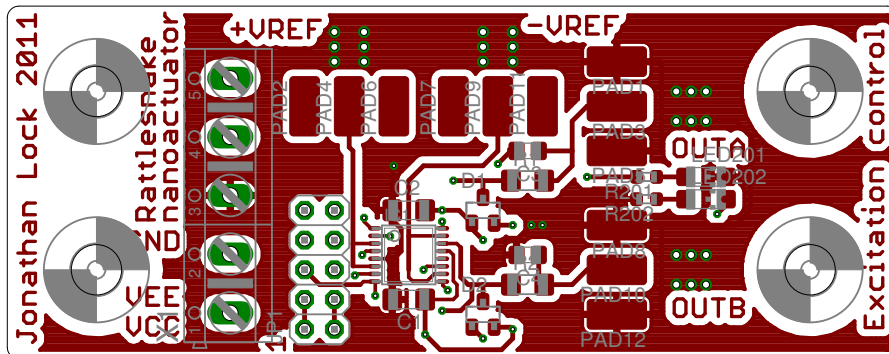


Figure 97: Top layer of PCB for excitation control.

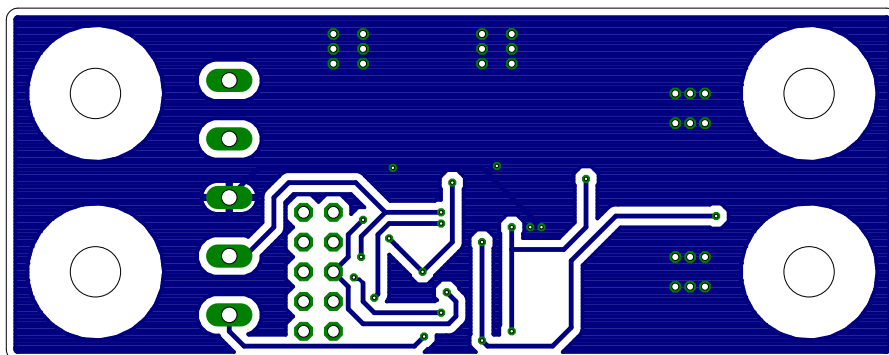


Figure 98: Bottom layer of PCB for excitation.

Partlist

Exported from excitation.sch at 7/3/11 1:17 PM

5 EAGLE Version 5.10.0 Copyright (c) 1988-2010 CadSoft

	Part	Value	Device	Package	Library	Sheet
	C1	10u_25V	C-EUC1206	C1206	rcl	1
10	C2	10u_25V	C-EUC1206	C1206	rcl	1
	C3	OPT	C-EUC0805	C0805	rcl	1
	C4	OPT	C-EUC0805	C0805	rcl	1
	D1	BAV199	BAV199	SOT23	diode	1
	D2	BAV199	BAV199	SOT23	diode	1
15	IC1	ADG1313	ADG1313YRUZ	TSSOP16	adg131x	1
	JP1	636332/635935/1207436	PINH-2X5	2X05	pinhead	1
	LED201	V+_POK	LEDCHIPLED_1206	CHIPLED_1206	led	1
	LED202	V-_POK	LEDCHIPLED_1206	CHIPLED_1206	led	1
	PAD1		SMD5	SMD2,54-5,08	wirepad	1
20	PAD2		SMD5	SMD2,54-5,08	wirepad	1
	PAD3		SMD5	SMD2,54-5,08	wirepad	1
	PAD4		SMD5	SMD2,54-5,08	wirepad	1
	PAD5		SMD5	SMD2,54-5,08	wirepad	1
	PAD6		SMD5	SMD2,54-5,08	wirepad	1
25	PAD7		SMD5	SMD2,54-5,08	wirepad	1
	PAD8		SMD5	SMD2,54-5,08	wirepad	1
	PAD9		SMD5	SMD2,54-5,08	wirepad	1
	PAD10		SMD5	SMD2,54-5,08	wirepad	1
	PAD11		SMD5	SMD2,54-5,08	wirepad	1
30	PAD12		SMD5	SMD2,54-5,08	wirepad	1
	R1	390R_0W25	R-EU_R1206	R1206	rcl	1
	R2	390R_0W25	R-EU_R1206	R1206	rcl	1
	R201	4k7	R-EU_R0603	R0603	rcl	1
	R202	4k7	R-EU_R0603	R0603	rcl	1
35	X1	PWR_IN	AK500/5	AK500/5	con-ptr500	1

B.6 MOTOR DRIVE

All schematics, [PCB artwork](#), part lists and an errata follow.

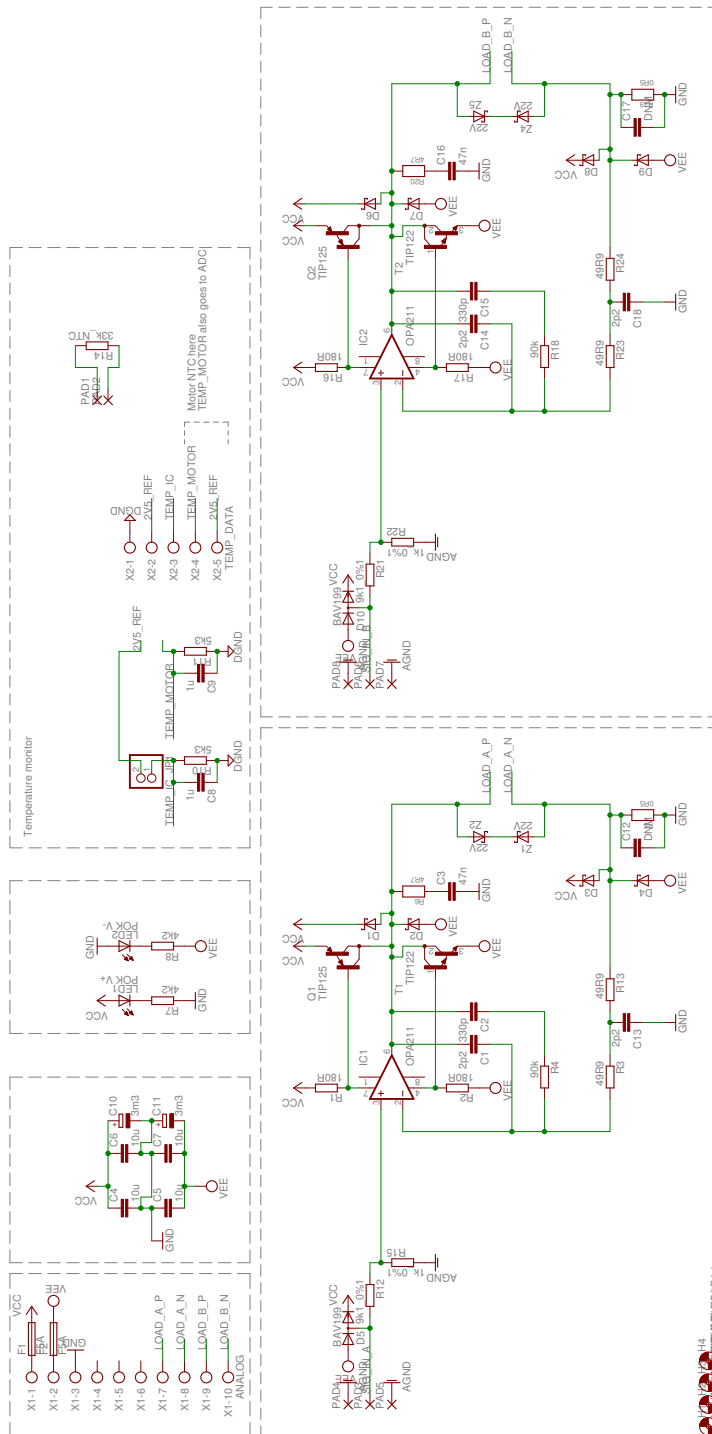


Figure 99: Schematic for motor drive.

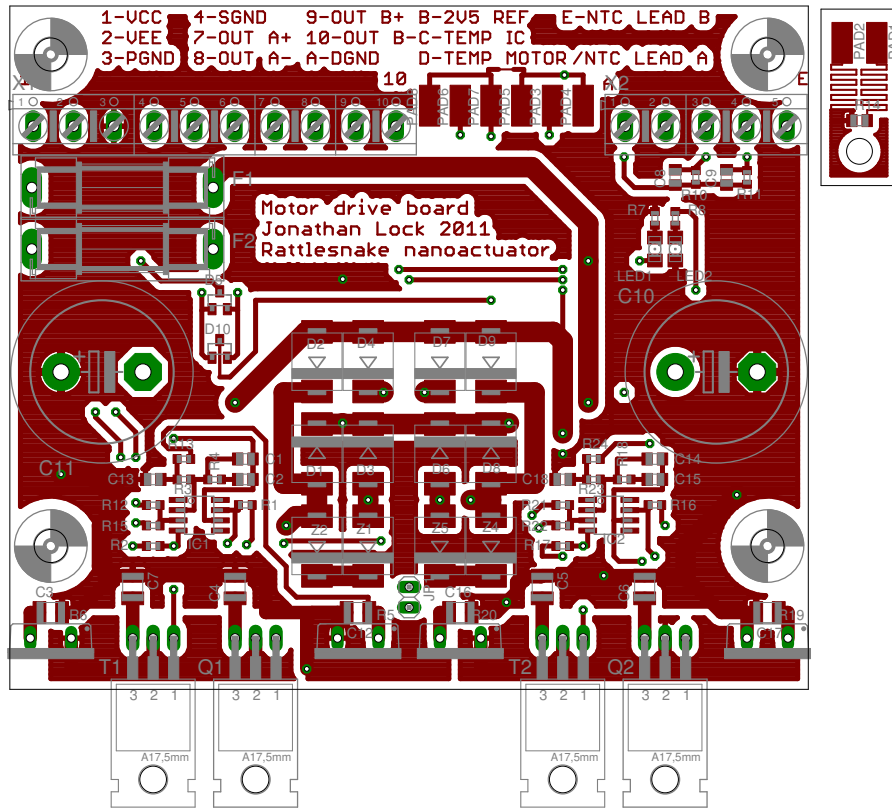


Figure 100: Top layer of PCB for motor drive.

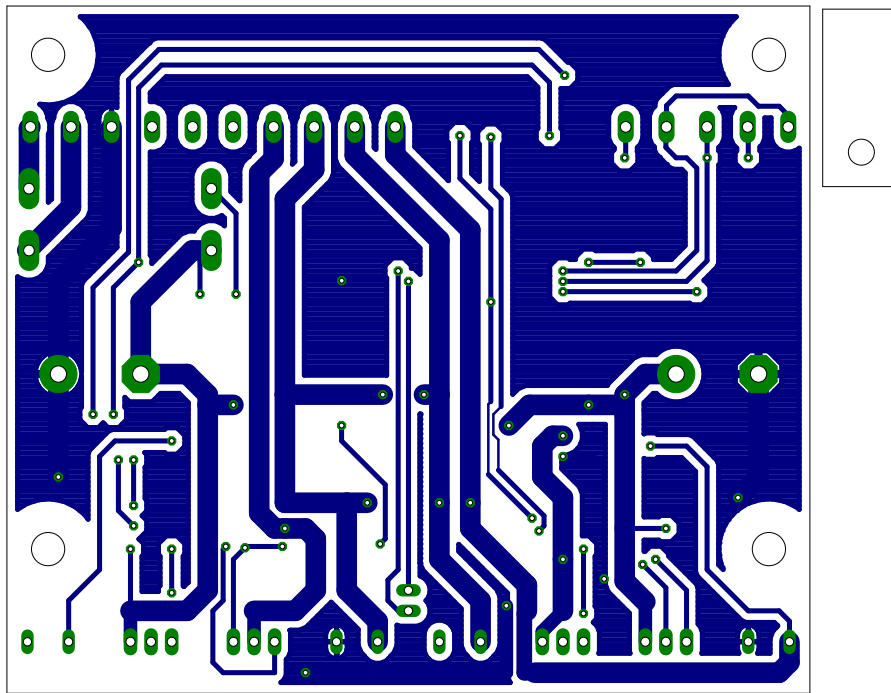


Figure 101: Bottom layer of PCB for motor drive.

AFFECTED COMPONENT	DESCRIPTION	WORKAROUND
PAD5, PAD7	Inputs are not connected by default	Connect pads

Table 8: Errata for motor drive PCB and schematic.

Partlist					
Exported from motor_drive.sch at 7/3/11 1:17 PM					
5 EAGLE Version 5.10.0 Copyright (c) 1988-2010 CadSoft					
Part	Value	Device	Package	Library	Sheet
C1	2p2	C-EUC0805	C0805	rcl	1
10 C2	330p	C-EUC0805	C0805	rcl	1
C3	47n	C-EUC1210	C1210	rcl	1
C4	10u	C-EUC1210	C1210	rcl	1
C5	10u	C-EUC1210	C1210	rcl	1
C6	10u	C-EUC1210	C1210	rcl	1
15 C7	10u	C-EUC1210	C1210	rcl	1
C8	1u	C-EUC0805	C0805	rcl	1
C9	1u	C-EUC0805	C0805	rcl	1
C10	3m3	CPOL-EUE10-22.5	EB22,5D	rcl	1
C11	3m3	CPOL-EUE10-22.5	EB22,5D	rcl	1
20 C12	DNM	C-EUC1210	C1210	rcl	1
C13	2p2	C-EUC0805	C0805	rcl	1

	C14	2p2	C-EUC0805	C0805	rcl	1
	C15	330p	C-EUC0805	C0805	rcl	1
	C16	47n	C-EUC1210	C1210	rcl	1
25	C17	DNM	C-EUC1210	C1210	rcl	1
	C18	2p2	C-EUC0805	C0805	rcl	1
	D1		SCHOTTKY-DIODESMC	SMC	diode	1
	D2		SCHOTTKY-DIODESMC	SMC	diode	1
	D3		SCHOTTKY-DIODESMC	SMC	diode	1
30	D4		SCHOTTKY-DIODESMC	SMC	diode	1
	D5	BAV199	BAV199	SOT23	diode	1
	D6		SCHOTTKY-DIODESMC	SMC	diode	1
	D7		SCHOTTKY-DIODESMC	SMC	diode	1
	D8		SCHOTTKY-DIODESMC	SMC	diode	1
35	D9		SCHOTTKY-DIODESMC	SMC	diode	1
	D10	BAV199	BAV199	SOT23	diode	1
	F1	F5A	SH22,5	SH22,5	fuse	1
	F2	F5A	SH22,5	SH22,5	fuse	1
	IC1	OPA211	OPA134U	S008	burr-brown	1
40	IC2	OPA211	OPA134U	S008	burr-brown	1
	JP1		PINHD-1X2	1X02	pinhead	1
	LED1	POK V+	LEDSMT1206	1206	led	1
	LED2	POK V-	LEDSMT1206	1206	led	1
	PAD1		SMD5	SMD2,54-5,08	wirepad	1
45	PAD2		SMD5	SMD2,54-5,08	wirepad	1
	PAD3		SMD5	SMD2,54-5,08	wirepad	1
	PAD4		SMD5	SMD2,54-5,08	wirepad	1
	PAD5		SMD5	SMD2,54-5,08	wirepad	1
	PAD6		SMD5	SMD2,54-5,08	wirepad	1
50	PAD7		SMD5	SMD2,54-5,08	wirepad	1
	PAD8		SMD5	SMD2,54-5,08	wirepad	1
	Q1	TIP125	TIP125	T0220	transistor-pnp	1
	Q2	TIP125	TIP125	T0220	transistor-pnp	1
	R1	180R	R-EU_R0603	R0603	rcl	1
55	R2	180R	R-EU_R0603	R0603	rcl	1
	R3	49R9	R-EU_R0603	R0603	rcl	1
	R4	90k	R-EU_R0603	R0603	rcl	1
	R5	0R5	R	D0220S	power_resistor	1
	R6	4R7	R	D0220S	power_resistor	1
60	R7	4k2	R-EU_R0603	R0603	rcl	1
	R8	4k2	R-EU_R0603	R0603	rcl	1
	R10	5k3	R-EU_R0603	R0603	rcl	1
	R11	5k3	R-EU_R0603	R0603	rcl	1
	R12	9k1_0R-EU_R0603		R0603	rcl	1 %6
65	R13	49R9	R-EU_R0603	R0603	rcl	1
	R14	33k_NTC	R-EU_R0805	R0805	rcl	1
	R15	1k_0R-EU_R0603		R0603	rcl	1 %6
	R16	180R	R-EU_R0603	R0603	rcl	1
	R17	180R	R-EU_R0603	R0603	rcl	1
70	R18	90k	R-EU_R0603	R0603	rcl	1
	R19	0R5	R	D0220S	power_resistor	1
	R20	4R7	R	D0220S	power_resistor	1
	R21	9k1_0R-EU_R0603		R0603	rcl	1 %6
	R22	1k_0R-EU_R0603		R0603	rcl	1 %6
75	R23	49R9	R-EU_R0603	R0603	rcl	1
	R24	49R9	R-EU_R0603	R0603	rcl	1
	T1	TIP122	TIP122	T0220	transistor	1
	T2	TIP122	TIP122	T0220	transistor	1
	X1	ANALOG	AK500/10	AK500/10	con-ptr500	1
80	X2	TEMP_DATA	AK500/5	AK500/5	con-ptr500	1
	Z1	22V	SCHOTTKY-DIODESMC	SMC	diode	1
	Z2	22V	SCHOTTKY-DIODESMC	SMC	diode	1
	Z4	22V	SCHOTTKY-DIODESMC	SMC	diode	1
	Z5	22V	SCHOTTKY-DIODESMC	SMC	diode	1

B.7 POWER SUPPLY

All schematics, PCB artwork, part lists and an errata follow.

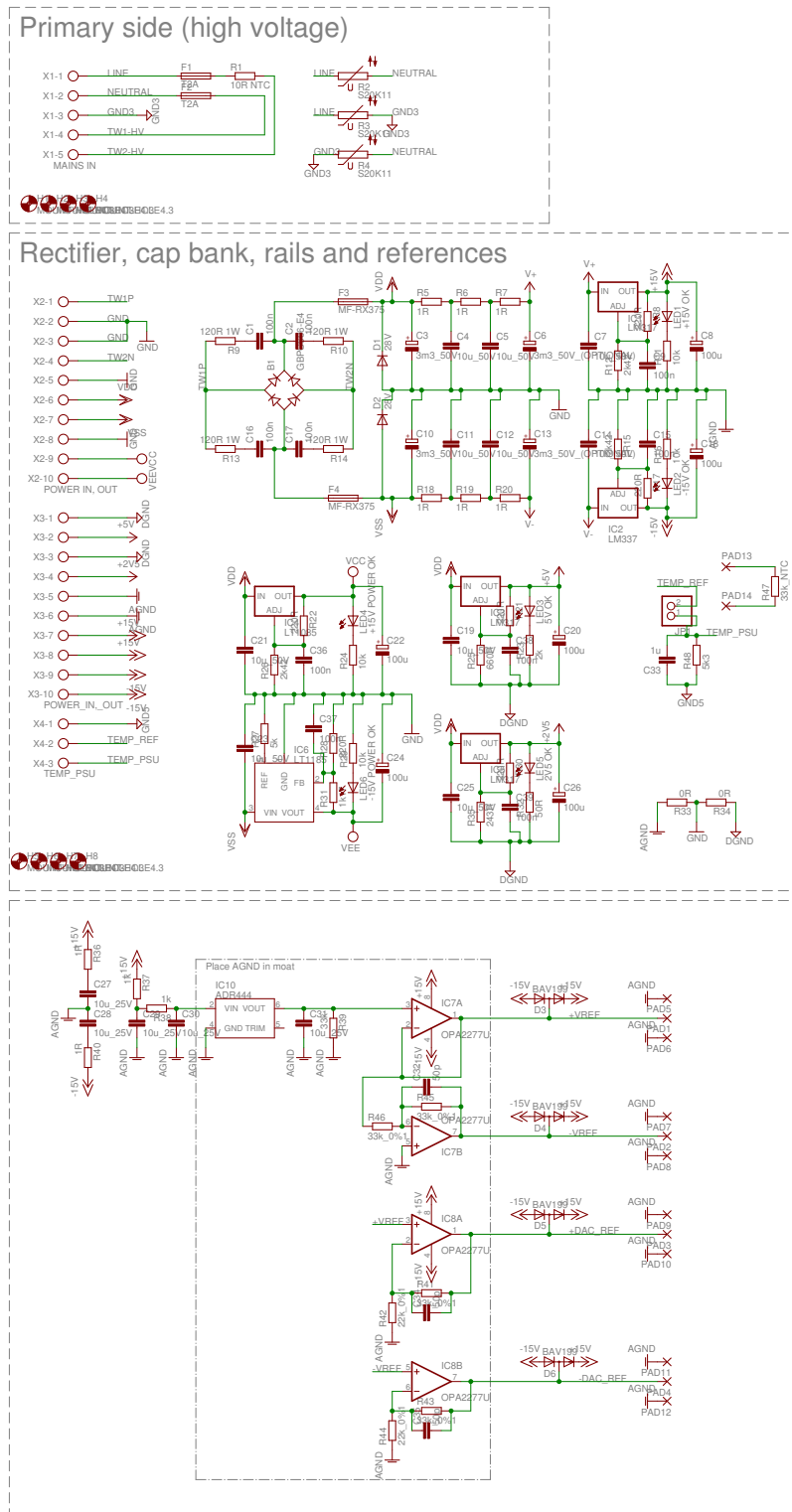


Figure 102: Schematic for power supply.

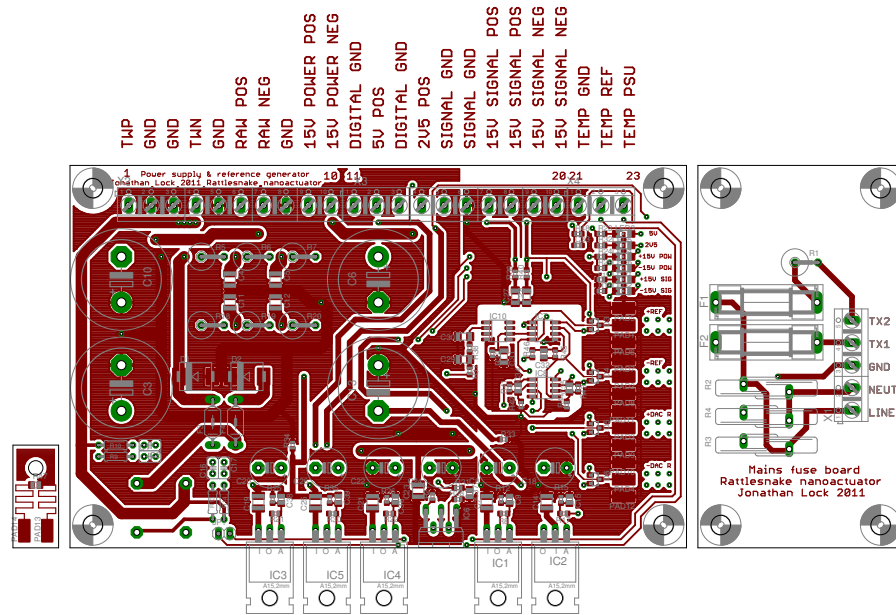


Figure 103: Top layer of PCB for power supply.

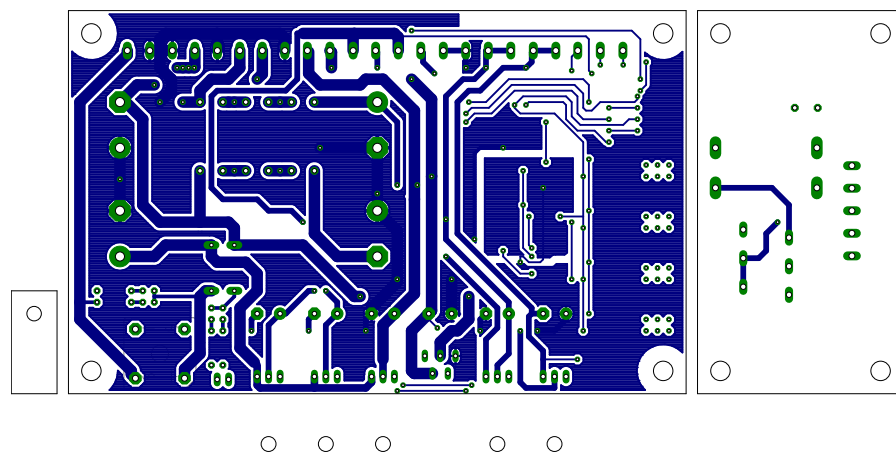


Figure 104: Bottom layer of PCB for power supply.

AFFECTED COMPONENT	DESCRIPTION	WORKAROUND
R35	Output 2.5V rail should be 2.65V±0.05V to lie in safe range	Trim value to give correct output voltage

Table 9: Errata for motor drive PCB and schematic.

1 Partlist
 Exported from psu.sch at 7/3/11 1:17 PM
 EAGLE Version 5.10.0 Copyright (c) 1988-2010 CadSoft

6	Part	Value	Device	Package	Library	Sheet
	B1	GBPC606-E4	RECTIFIER-GBP6	GBPC6	rectifier	1
	C1	100n	C-EU025-025X050	C025-025X050	rc1	1
11	C2	100n	C-EU025-025X050	C025-025X050	rc1	1
	C3	3m3_50V	CPOL-EUE10-22.5	EB22,5D	rc1	1
	C4	10u_50V	C-EUC1210	C1210	rc1	1
	C5	10u_50V	C-EUC1210	C1210	rc1	1
	C6	3m3_50V_ (OPTIONAL)	CPOL-EUE10-22.5	EB22,5D	rc1	1
16	C7	10u_50V	C-EUC1210	C1210	rc1	1
	C8	100u	CPOL-EUE5-8.5	E5-8,5	rc1	1
	C9	100n	C-EUC0805	C0805	rc1	1
	C10	3m3_50V	CPOL-EUE10-22.5	EB22,5D	rc1	1
	C11	10u_50V	C-EUC1210	C1210	rc1	1
21	C12	10u_50V	C-EUC1210	C1210	rc1	1
	C13	3m3_50V_ (OPTIONAL)	CPOL-EUE10-22.5	EB22,5D	rc1	1
	C14	10u_50V	C-EUC1210	C1210	rc1	1
	C15	100n	C-EUC0805	C0805	rc1	1
	C16	100n	C-EU025-025X050	C025-025X050	rc1	1
26	C17	100n	C-EU025-025X050	C025-025X050	rc1	1
	C18	100u	CPOL-EUE5-8.5	E5-8,5	rc1	1
	C19	10u_50V	C-EUC1210	C1210	rc1	1
	C20	100u	CPOL-EUE5-8.5	E5-8,5	rc1	1
	C21	10u_50V	C-EUC1210	C1210	rc1	1
31	C22	100u	CPOL-EUE5-8.5	E5-8,5	rc1	1
	C23	10u_50V	C-EUC1210	C1210	rc1	1
	C24	100u	CPOL-EUE5-8.5	E5-8,5	rc1	1
	C25	10u_50V	C-EUC1210	C1210	rc1	1
	C26	100u	CPOL-EUE5-8.5	E5-8,5	rc1	1
36	C27	10u_25V	C-EUC1206	C1206	rc1	1
	C28	10u_25V	C-EUC1206	C1206	rc1	1
	C29	10u_25V	C-EUC1206	C1206	rc1	1
	C30	10u_25V	C-EUC1206	C1206	rc1	1
	C31	10u_25V	C-EUC1206	C1206	rc1	1
41	C32	50p	C-EUC0805	C0805	rc1	1
	C33	1u	C-EUC0603	C0603	rc1	1
	C34	50p	C-EUC0805	C0805	rc1	1
	C35	50p	C-EUC0805	C0805	rc1	1
	C36	100n	C-EUC0805	C0805	rc1	1
46	C37	100n	C-EUC0805	C0805	rc1	1
	C38	100n	C-EUC0805	C0805	rc1	1
	C39	100n	C-EUC0805	C0805	rc1	1
	D1	28V	DIODE-SMC	SMC	diode	1
	D2	28V	DIODE-SMC	SMC	diode	1
51	D3	BAV199	BAV199	SOT23	diode	1
	D4	BAV199	BAV199	SOT23	diode	1
	D5	BAV199	BAV199	SOT23	diode	1
	D6	BAV199	BAV199	SOT23	diode	1
	F1	T2A	SH22,5	SH22,5	fuse	1
56	F2	T2A	SH22,5	SH22,5	fuse	1
	F3	MF-RX375	FUSELITTLEFUSE	LITTLEFUSE	fuse	1
	F4	MF-RX375	FUSELITTLEFUSE	LITTLEFUSE	fuse	1
	IC1	LM317	LM317TL	317TL	v-reg	1
	IC2	LM337	LM337TL	337TL	v-reg	1
61	IC3	LM317	LM317TL	317TL	v-reg	1
	IC4	LT1085	LM317TL	317TL	v-reg	1
	IC5	LM317	LM317TL	317TL	v-reg	1
	IC6	LT1185	LT1185	T0220-51	lt1185	1
	IC7	OPA2277U	OPA2277U	S008	linear	1
66	IC8	OPA2277U	OPA2277U	S008	linear	1
	IC10	ADR444	ADR444	S0IC8	adr444	1
	JP1		PINHD-1X2	1X02	pinhead	1
	LED1	+15V OK	LEDCHIPLD_1206	CHIPLD_1206	led	1
	LED2	-15V OK	LEDCHIPLD_1206	CHIPLD_1206	led	1
71	LED3	5V OK	LEDCHIPLD_1206	CHIPLD_1206	led	1

	LED4	+15V POWER OK	LEDCHIPLD_1206	CHIPLD_1206	led	1
	LED5	2V5 OK	LEDCHIPLD_1206	CHIPLD_1206	led	1
	LED6	-15V POWER OK	LEDCHIPLD_1206	CHIPLD_1206	led	1
76	PAD1		SMD5	SMD2,54-5,08	wirepad	1
	PAD2		SMD5	SMD2,54-5,08	wirepad	1
	PAD3		SMD5	SMD2,54-5,08	wirepad	1
	PAD4		SMD5	SMD2,54-5,08	wirepad	1
	PAD5		SMD5	SMD2,54-5,08	wirepad	1
	PAD6		SMD5	SMD2,54-5,08	wirepad	1
81	PAD7		SMD5	SMD2,54-5,08	wirepad	1
	PAD8		SMD5	SMD2,54-5,08	wirepad	1
	PAD9		SMD5	SMD2,54-5,08	wirepad	1
	PAD10		SMD5	SMD2,54-5,08	wirepad	1
	PAD11		SMD5	SMD2,54-5,08	wirepad	1
86	PAD12		SMD5	SMD2,54-5,08	wirepad	1
	PAD13		SMD5	SMD2,54-5,08	wirepad	1
	PAD14		SMD5	SMD2,54-5,08	wirepad	1
	R1	10R NTC	R-EU_0617/5V	0617V	rcl	1
	R2	S20K11	S20K11	S20K11	varistor	1
91	R3	S20K11	S20K11	S20K11	varistor	1
	R4	S20K11	S20K11	S20K11	varistor	1
	R5	1R	R-EU_0617/5V	0617V	rcl	1
	R6	1R	R-EU_0617/5V	0617V	rcl	1
	R7	1R	R-EU_0617/5V	0617V	rcl	1
96	R8	220R	R-EU_R0603	R0603	rcl	1
	R9	120R 1W	R-EU_0204/7	0204/7	rcl	1
	R10	120R 1W	R-EU_0204/7	0204/7	rcl	1
	R11	10k	R-EU_R0603	R0603	rcl	1
	R12	2k42	R-EU_R0603	R0603	rcl	1
101	R13	120R 1W	R-EU_0204/7	0204/7	rcl	1
	R14	120R 1W	R-EU_0204/7	0204/7	rcl	1
	R15	2k42	R-EU_R0603	R0603	rcl	1
	R16	10k	R-EU_R0603	R0603	rcl	1
	R17	220R	R-EU_R0603	R0603	rcl	1
106	R18	1R	R-EU_0617/5V	0617V	rcl	1
	R19	1R	R-EU_0617/5V	0617V	rcl	1
	R20	1R	R-EU_0617/5V	0617V	rcl	1
	R21	220R	R-EU_R0603	R0603	rcl	1
	R22	220R	R-EU_R0603	R0603	rcl	1
111	R23	2k	R-EU_R0603	R0603	rcl	1
	R24	10k	R-EU_R0603	R0603	rcl	1
	R25	660R	R-EU_R0603	R0603	rcl	1
	R26	2k42	R-EU_R0603	R0603	rcl	1
	R27	5k	R-EU_R0603	R0603	rcl	1
116	R28	220R	R-EU_R0603	R0603	rcl	1
	R29	10k	R-EU_R0603	R0603	rcl	1
	R30	220R	R-EU_R0603	R0603	rcl	1
	R31	1k17	R-EU_R0603	R0603	rcl	1
	R32	50R	R-EU_R0603	R0603	rcl	1
121	R33	0R	R-EU_R0603	R0603	rcl	1
	R34	0R	R-EU_R0603	R0603	rcl	1
	R35	243R	R-EU_R0603	R0603	rcl	1
	R36	1R	R-EU_R0603	R0603	rcl	1
	R37	1k	R-EU_R0603	R0603	rcl	1
126	R38	1k	R-EU_R0603	R0603	rcl	1
	R39	33k	R-EU_R0603	R0603	rcl	1
	R40	1R	R-EU_R0603	R0603	rcl	1
	R41	33k_0R-EU_R0603		R0603	rcl	1 %6
	R42	22k_0R-EU_R0603		R0603	rcl	1 %6
131	R43	33k_0R-EU_R0603		R0603	rcl	1 %6
	R44	22k_0R-EU_R0603		R0603	rcl	1 %6
	R45	33k_0R-EU_R0603		R0603	rcl	1 %6
	R46	33k_0R-EU_R0603		R0603	rcl	1 %6
	R47	33k_NTC	R-EU_R0805	R0805	rcl	1
136	R48	5k3	R-EU_R0603	R0603	rcl	1
	X1	MAINS IN	AK500/5	AK500/5	con-pt500	1

X2	POWER_IN, OUT	AK500/10	AK500/10	con-ptr500 1
X3	POWER_IN,_OUT	AK500/10	AK500/10	con-ptr500 1
X4	TEMP_PSU	AK500/3	AK500/3	con-ptr500 1

SOFTWARE

C.1 MICROPROCESSOR SOFTWARE

The software used in the actuator is programmed in C, compiled with GNU C compiler ([GCC](#)) and transferred to the microprocessor with AVR downloader/uploader ([AVRDUDE](#)) over an in-system programmer mark ii ([ISPMKii](#)).

The software source code is divided into several logical blocks, each performing a set range of tasks. These blocks are;

MAIN The main loop handles all initialization on startup and then enters an infinite loop that draws the user interface to the LCD.

BASE The base loop (base-thread) block contains everything to do with the base thread, which runs continuously and shifts data in and out of the transfer buffers, runs a finite state machine for the external control interface, checks the current position and turns the motor off if limits are exceeded and so on.

BOARD Contains all I/O definitions, timer register use and pin name declarations.

BUTTON All button (joystick and rotary dial) functionality. Offers an interface to check the current button status, if a flank has occurred and how many increments the rotary dial has rotated since last checked.

CONTROL All DAC and digital potentiometer control routines. Offers interface can set the DAC and digital potentiometer positions, write and read digital potentiometer positions to EEPROM.

EXT_COM External communications module, handles RS232/USB communications. Gives a function to queue a message to be transmitted and to check for received messages.

LCD All LCD routines, allows for initializing the LCD display, writing a string, setting the current line and position and writing a character.

SENSOR All functionality related to the capacitive sensor, writes to the POS and REF buffers and convert POS and REF to position.

TEMP_MEAS Temperature measurement routines, measures the NTC resistors attached to the motor, motor drive and power supply and controls the fans accordingly. A look-up-table converts the nonlinear voltage/temperature relationship to degrees Celsius.

UI All user-interface related routines, including menu structure and navigation.

UTIL Various utility functions that span several modules such as the buffer implementation and small delays.

All files are separated into a source (.c) and header (.h) file according to commonly used C programming conventions. Generally upper case names are used for `#define`'s and lower case for variables. The code is commented and documented using Doxygen, an open-source documentation generator. See the unpublished document appended to this document for full source code and more detailed explanations (Lock [11]).

C.2 MATLAB DEMO APPLICATION

In order to test the actuator and as a demo application a simple Matlab program was developed (the same program is used to generate most of the plots). The source code for the demo application follow with the filenames in the first line;

```

%decodePackets.m
%Decodes length(packets) packets and converts them to an array of headers
%and payload.

5 function [header,payload] = decodePackets(packets)

if(~isempty(packets))
    data=uint8(packets);
    i=0;    %current byte (0->packet has been decoded, 1-> header, 2,3,4 ->
           payload)
10    header_raw=0;
    payload_raw=0;
    header_i=0;
    payload_i=zeros(1,3,'uint8');
    for j=1:length(data)
15        if(i==0 && isHeader(data(j)))    %if a previous packet has been decoded,
            check if the next byte is a valid header
            i=1;                            %if so reset the counter state machine
            header_i=data(j);                %and store the current value.
            elseif(i~=0)                    %otherwise we are currently decoding a
                packet if i!=0
                payload_i(i)=data(j);        %store the 1-3rd byte in payload_i
                temp variable
20            i=i+1;                          %increment the byte marker variable
            if(i>=4)                          %if a packet has been completely
                decoded
                %store the current header in the
                output array
                header_raw=[header_raw;header_i];
                %and the current payload
25            payload_raw=[payload_raw;bin2dec([dec2bin(payload_i(1),8),dec2bin(
                payload_i(2),8),dec2bin(payload_i(3),8))]);    %super ugly
                uint8->string->uint8 conversion needed for concatentaion!
                i=0;                            %reset state machine
            end;
        end
    end
30    header_raw(1)=[];                        %remove top element (was created
        before decoding loop)
    payload_raw(1)=[];
    header=header_raw;
    payload=fi(payload_raw, 1, 24, 0, ...
35        'RoundMode', 'Nearest', ...
        'OverflowMode', 'Wrap', ...
        'ProductMode', 'FullPrecision', ...
        'MaxProductWordLength', 24, ...
        'SumMode', 'FullPrecision', ...
40        'MaxSumWordLength', 24, ...
        'CastBeforeSum', true);
end

```

```
%defs_header.m
%Header definitions used for writing and decoding packets
3  HEX_POSREF='fo';
   HEX_POS='f1';
   HEX_REF='f2';
   HEX_SETPT='f3';
8  HEX_TEMP_MOTOR='f8';
   HEX_TEMP_DRIVE='f9';
   HEX_TEMP_PSU='fa';
   HEX_ADC_K='fb';
   HEX_SETPT_K='fc';
13 HEX_SETPT_BUFFER_READY='fd';
   HEX_EOC='fe';
   HEX_BUSY='ff';
```

```

% demo.m
% Demo program to interface Rattlesnake Nanoactuator
% Output a couple setpoint waveforms as defined below, plot setpoint and process
% variable in a chart. Also display system temperatures
5
%% Startup init

ins=instrfind;
if(~isempty(ins))
10     fclose(ins);
        delete(ins);
end
clc
clear all
15 close all
format short eng

port = '/dev/ttyUSB1';
tx_buff=1000000;
20 rx_buff=1000000;
rattlesnake = initInstrument(port,tx_buff,rx_buff);

%Get ADC_k and SETPOINT_k values
scale_packets=[generatePackets('adc_k',0),generatePackets('setpt_k',0)];
25

%clear data in input buffer
if(rattlesnake.BytesAvailable)
    disp('Bytes found in input buffer when none should be there, clearing...');
    fread(rattlesnake, rattlesnake.BytesAvailable);
30 end

sendPackets(rattlesnake,scale_packets);
pause(1);
data=readPackets(rattlesnake);
35

%use adc_k such that: position=adc_k*pos/ref [nanometers]
%use setpt_k such that dac_code=setpt_k*setpoint [nanometers]
adc_k=2^39/double(extractPackets(data,'adc_k')); %scale ADC_k from the
        transmitted, fixed point, format
setpt_k=double(extractPackets(data,'setpt_k'))/2^25; %scale SETPT_k similarly
40

%% Run on change
close all

%System definitions
45 fs_setpt=1/(500e-6); %sample rate for setpoint output [Hz]
fs_pv=(500e3/256)/2; %sample rate for process variable input [Hz]
prop_delay=40e-3; %amount of delay in system (add this much extra time to
        the posref sampling) [s]

%Setpoint global defs
50 setpt_stoptime=.4; %time for waveform [s]
setpt_samples=ceil(setpt_stoptime*fs_setpt); %number of desired setpoint samples
setpt_ampl=500e3; %desired amplitude [nm]
setpt_offset=0; %setpoint DC offset [nm]

55 %Various setpoint wave definitions
setpt_square=[zeros(1,round(.1*setpt_samples)),setpt_ampl*ones(1,round(.45*
        setpt_samples)),zeros(1,round(.45*setpt_samples))];
setpt_triangle=[zeros(1,round(.1*setpt_samples)),setpt_ampl*(.5+sawtooth(linspace
        (0,2*pi,round(.8*setpt_samples)),.5)/2),zeros(1,round(.1*setpt_samples))];
setpt_sine=[zeros(1,round(.1*setpt_samples)),setpt_ampl*(.5-cos(linspace(0,2*pi,
        round(.8*setpt_samples)))/2),zeros(1,round(.1*setpt_samples))];
setpt_zero=zeros(1,setpt_samples);

```

```

60 setpt_2deriv=[zeros(1,round(.1*setpt_samples)),setpt_ampl*quintic_traj(round(.8*
    setpt_samples),zeros(1,round(.1*setpt_samples))];
setpt_1deriv=[0,setpt_ampl*diff(setpt_2deriv)/max(abs(diff(setpt_2deriv)))]];
setpt_0deriv=[0,setpt_ampl*diff(setpt_1deriv)/max(abs(diff(setpt_1deriv)))]];

%change here to choose which setpoint to use
65 setpt_sel='setpt_0deriv';
setpt=setpt_offset+eval(setpt_sel);
outputdir='./large_scale/';
name_suffix='';

70

%Generate packets to send to instrument
%Temperature request
packets_temp=[generatePackets('temp_motor',0),generatePackets('temp_drive',0),
    generatePackets('temp_psu',0)];
75 %POS and REF request of n values
posref_samples=ceil(setpt_stoptime*fs_pv+prop_delay*fs_pv);
packets_posref=generatePackets('posref',posref_samples);
%Setpoint values
packets_setpt=generatePackets('setpt',setpt2code(setpt,setpt_k));
80 packets_concat=[packets_temp,packets_posref,packets_setpt];

% Perform measurement

%clear data in input buffer
85 if(rattlesnake.BytesAvailable)
    disp('Bytes found in input buffer when none should be there, clearing...');
    fread(rattlesnake, rattlesnake.BytesAvailable);
end

90 %Send packets to instrument
sendPackets(rattlesnake,packets_concat);
pause(2*setpt_stoptime+2);
%Read measurement data from instrument
data=readPackets(rattlesnake);

95 % Filter the data

temp=double([extractPackets(data,'temp_motor'),extractPackets(data,'temp_drive'),
    extractPackets(data,'temp_psu')]);
[pos_fi posindex]=extractPackets(data,'pos');
100 [ref_fi refindex]=extractPackets(data,'ref');
pos=double(pos_fi);
ref=double(ref_fi);
foo=mod(posindex,2); %all values of posindex should be either even or odd,
    check for this
if(foo(1)~=mean(foo))
105     error('Error in receiving POS data')
end
foo=mod(refindex,2); %similarly for refindex
if(foo(1)~=mean(foo))
    error('Error in receiving REF data')
110 end
position=posref2position(pos,ref,adc_k);

% Display settings

115 %set the display sample rate to be the lowest common multiple of the
%setpoint and ADC sample rates. Use ugly workaround to bypass the
%limitation of lcm only working with integers.
output_samplerate=lcm(fs_setpt*2^16, fs_pv*2^16)/2^16;

120 position_rs=resample(position,output_samplerate/fs_pv,1);
setpt_rs=resample(setpt,output_samplerate/fs_setpt,1);

```

```

time=linspace(0,setpt_stoptime,setpt_stoptime*output_samplerate);

%shift pos and setpt to the same time (remove system delay)
125 if(max(setpt)==0 && min(setpt)==0)
    position_temp=position_rs;
    clear position_rs;
    position_rs=position_temp(1:length(setpt_rs));
    disp('Zero setpoint detected, no shifting performed')
130 else
    shift=finddelay(setpt_rs,position_rs);
    if(shift<0)
        error('Negative shift found, some measurement error must have occurred')
    end
135 position_temp=position_rs;
    clear position_rs;
    position_rs=position_temp(shift:end);
    if(length(position_rs)>length(setpt_rs))
140 position_temp=position_rs;
        clear position_rs;
        position_rs=position_temp(1:length(setpt_rs));
        disp('Position was longer than setpoint, truncating');
    end
    if(length(position_rs)<length(setpt_rs))
145 position_temp=[position_temp;zeros(1,length(setpt_rs)-length(position_rs))
        ];
        disp('Position was shorter than setpoint, zero-padding');
    end
end

150 % calculate filtered velocity data
vel_decimation=10; %decimation rate of signal for velocity calculation
dh=1/(output_samplerate/vel_decimation); %time between each decimated sample

position_filt=sgolayfilt(resample(position_rs,1,vel_decimation),1,21);
155 setpt_d_filt=diff(resample(setpt,output_samplerate/fs_setpt,vel_decimation,10,30))
    /dh;
vel_filt=diff(position_filt)/dh;
time_vel=decimate(time,vel_decimation);
time_vel=time_vel(1:end-1);

160 %calculate filtered acceleration data
accel_filt=sgolayfilt(diff(vel_filt),3,101);
setpt_dd_filt=sgolayfilt(diff(setpt_d_filt),3,101);
time_accel=time_vel(1:end-1);

165 % Display data
figure(1)

subplot(2,1,1)
170 plot(time,[position_rs';setpt_rs])
title('Setpoint and measured position')
xlabel('Time [s]')
ylabel('Position [mm]')
legend('Position','Setpoint')
175 xlim([min(time),max(time)]);
grid on

subplot(2,1,2)
180 plot(time,setpt_rs-position_rs');
title('Measured position error (setpoint - measured)')
xlabel('Time [s]')
ylabel('Position error [mm]')
xlim([min(time),max(time)]);
grid on
185

```

```

h = axes('Position',[.15,.01,.8,.1]);
axis off
text(.75,0, strcat('Motor temp:', num2str(temp(1)/10), ' [degC]'), 'FontSize', 8);
text(.50,0, strcat('Drive temp:', num2str(temp(2)/10), ' [degC]'), 'FontSize', 8);
190 text(.25,0, strcat('PSU temp:', num2str(temp(3)/10), ' [degC]'), 'FontSize', 8);
text(0,0, strcat('RMS error:', num2str(std(setpt_rs-position_rs'-mean(setpt_rs-
position_rs'))), ' [nm]'), 'FontSize', 8);

foo=strcat(outputdir, 'position_', setpt_sel, name_suffix);
print('-depsec', foo)
195
figure(2)

subplot(2,1,1)
plot(time_vel, [vel_filt'; setpt_d_filt]);
200 title('Setpoint and measured velocity (filtered)')
xlabel('Time [s]')
ylabel('Velocity [nm/s] (filtered)')
legend('Velocity', 'Setpoint')
xlim([min(time), max(time)]);
205 grid on

subplot(2,1,2)
plot(time_vel, setpt_d_filt-vel_filt');
title('Measured velocity error (setpoint - measured) (filtered)')
210 xlabel('Time [s]')
ylabel('Velocity error [nm/s] (filtered)')
xlim([min(time), max(time)]);
grid on

215 h = axes('Position',[.15,.01,.8,.1]);
axis off
text(.75,0, strcat('Motor temp:', num2str(temp(1)/10), ' [degC]'), 'FontSize', 8);
text(.50,0, strcat('Drive temp:', num2str(temp(2)/10), ' [degC]'), 'FontSize', 8);
text(.25,0, strcat('PSU temp:', num2str(temp(3)/10), ' [degC]'), 'FontSize', 8);
220
foo=strcat(outputdir, 'velocity_', setpt_sel, name_suffix);
print('-depsec', foo)

figure(3)
225
subplot(2,1,1)
plot(time_accel, [accel_filt'; setpt_dd_filt]);
title('Setpoint and measured acceleration (filtered)')
xlabel('Time [s]')
230 ylabel('Acceleration [nm/s^2] (filtered)')
legend('Acceleration', 'Setpoint')
xlim([min(time), max(time)]);
grid on

235 subplot(2,1,2)
plot(time_accel, setpt_dd_filt-accel_filt');
title('Measured acceleraion error (setpoint - measured) (filtered)')
xlabel('Time [s]')
ylabel('Acceleration error [nm/s^2] (filtered)')
240 xlim([min(time), max(time)]);
grid on

h = axes('Position',[.15,.01,.8,.1]);
axis off
245 text(.75,0, strcat('Motor temp:', num2str(temp(1)/10), ' [degC]'), 'FontSize', 8);
text(.50,0, strcat('Drive temp:', num2str(temp(2)/10), ' [degC]'), 'FontSize', 8);
text(.25,0, strcat('PSU temp:', num2str(temp(3)/10), ' [degC]'), 'FontSize', 8);

foo=strcat(outputdir, 'acceleration_', setpt_sel, name_suffix);
250 print('-depsec', foo)

```

```

%extractPackets.m
%This function extracts the specified packet types from the input raw data
%and outputs the payload of the specified packet types and their position
%in the input data array
5
function [filteredData index] = extractPackets(rawData, type)
    [header payload]=decodePackets(rawData);
    defs_header
    dataraw=0;
10    posraw=0;
    switch(type)
        case 'pos'
            desiredHeader=HEX_POS;
        case 'ref'
15            desiredHeader=HEX_REF;
        case 'setpt'
            desiredHeader=HEX_SETPT;
        case 'temp_motor'
            desiredHeader=HEX_TEMP_MOTOR;
20        case 'temp_drive'
            desiredHeader=HEX_TEMP_DRIVE;
        case 'temp_psu'
            desiredHeader=HEX_TEMP_PSU;
        case 'adc_k'
25            desiredHeader=HEX_ADC_K;
        case 'setpt_k'
            desiredHeader=HEX_SETPT_K;
        case 'setpt_buffer_ready'
            desiredHeader=HEX_SETPT_BUFFER_READY;
30        case 'eoc'
            desiredHeader=HEX_EOC;
        case 'busy'
            desiredHeader=HEX_BUSY;
        otherwise
35            error('Packet type must be valid');
    end
    for i=1:length(header)
        if(header(i) == hex2dec(desiredHeader))
            dataraw=[dataraw;payload(i)];
40            posraw=[posraw;i];
        end
    end
    dataraw(1)=[];
    posraw(1)=[];
45    filteredData=dataraw;
    index=posraw;
end

```

```

%generatePackets.m
%Generates n packets with the same header and specified payload, outputs an
3 %array with the formatted output (ready to write to device)

function packets = generatePackets(header,payload)

%Internal block size to use when generating raw data. (Number of packets to
8 %convert per for loop iteration). Hand trim value!
BLOCKSIZE=1000;

%Limits for range of data input
MAXVAL_DATA=2^(24-1)-1;
13 MINVAL_DATA=2^(24-1);

defs_header

%Generate packet header based on input
18 switch header
    case 'posref'
        header=uint8(hex2dec(HEX_POSREF));
    case 'pos'
        header=uint8(hex2dec(HEX_POS));
23    case 'ref'
        header=uint8(hex2dec(HEX_REF));
    case 'setpt'
        header=uint8(hex2dec(HEX_SETPT));
    case 'temp_motor'
28    case 'temp_drive'
        header=uint8(hex2dec(HEX_TEMP_DRIVE));
    case 'temp_psu'
        header=uint8(hex2dec(HEX_TEMP_PSU));
33    case 'adc_k'
        header=uint8(hex2dec(HEX_ADC_K));
    case 'setpt_k'
        header=uint8(hex2dec(HEX_SETPT_K));
    case 'setpt_buffer_rdy'
38    case 'eoc'
        header=uint8(hex2dec(HEX_EOC));
    case 'busy'
        header=uint8(hex2dec(HEX_BUSY));
43    otherwise
        error('Invalid packet header type')
end

%Generate error if payload is outside of valid range
48 assert(max(payload>MAXVAL_DATA) || max(payload<MINVAL_DATA), 'Message payload must
    fit in 24 bit word length.');
```

```

data_cat_fi=fi(zeros(1,length(payload)), ...
    0, 32, 0, ...
    'RoundMode', 'Nearest', ...
53    'OverflowMode', 'Saturate', ...
    'ProductMode', 'FullPrecision', ...
    'MaxProductWordLength', 32, ...
    'SumMode', 'FullPrecision', ...
58    'MaxSumWordLength', 32, ...
    'CastBeforeSum', true);

%run parts of code that run slower than O(n) after a certain size in a loop
for n=0:ceil(length(payload)/BLOCKSIZE)-1
    %Generate finite precision data for payload
63    %Desire to look at certain part of payload only per value of n

```

```

payload_fi=fi(payload(:,1+n*BLOCKSIZE:min(length(payload),(n+1)*BLOCKSIZE)),
...
1, 24, 0, ...
'RoundMode', 'Nearest', ...
'OverflowMode', 'Saturate', ...
68 'ProductMode', 'FullPrecision', ...
'MaxProductWordLength', 24, ...
'SumMode', 'FullPrecision', ...
'MaxSumWordLength', 24, ...
'CastBeforeSum', true);
73
%Generate finite precision data for header
header_fi=fi(header, 0, 8, 0, ...
'RoundMode', 'Nearest', ...
'OverflowMode', 'Saturate', ...
78 'ProductMode', 'FullPrecision', ...
'MaxProductWordLength', 8, ...
'SumMode', 'FullPrecision', ...
'MaxSumWordLength', 8, ...
'CastBeforeSum', true);
83
%Concatenate header and payload
data_int=bitconcat(header_fi,payload_fi);
data_cat_fi(1,1+n*BLOCKSIZE:min(length(payload),(n+1)*BLOCKSIZE))=data_int;
end
88 packets=data_cat_fi;

```

```
% initInstrument.m
2 % Initialize instrument (set up port, baud rate, buffer size (bytes), etc)
function [ins] = initInstrument(port,tx_buff,rx_buff)

ins=serial(port);
ins.BaudRate=230400;
7 ins.DataBits=8;
ins.StopBits=1;
ins.Parity='none';
ins.FlowControl='hardware';
%ins.FlowControl='none';
12 ins.ByteOrder='bigEndian';
ins.OutputBufferSize=tx_buff;
ins.InputBufferSize=rx_buff;
ins.Timeout=5.0;
fopen(ins); %open in read/write mode, big endian byte order
```

```

%isheader.m
%Checks if an input byte is a header type or not
%
4 %byte - the input byte to check
%
%bool - nonzero if the input byte was a header, zero otherwise

function bool = isHeader(byte)
9     defns_header
    switch(byte)
        case hex2dec(HEX_POSREF)
            retval=1;
        case hex2dec(HEX_POS)
14            retval=1;
        case hex2dec(HEX_REF)
            retval=1;
        case hex2dec(HEX_SETPT)
            retval=1;
19        case hex2dec(HEX_TEMP_MOTOR)
            retval=1;
        case hex2dec(HEX_TEMP_DRIVE)
            retval=1;
        case hex2dec(HEX_TEMP_PSU)
24            retval=1;
        case hex2dec(HEX_ADC_K)
            retval=1;
        case hex2dec(HEX_SETPT_K)
            retval=1;
29        case hex2dec(HEX_SETPT_BUFFER_READY)
            retval=1;
        case hex2dec(HEX_EOC)
            retval=1;
        case hex2dec(HEX_BUSY)
34            retval=1;
        otherwise
            retval=0;
    end
    bool=retval;
39 end

```

```
1 %posref2position.m
  %converts POS and REF ADC codewords to position [nm]

  function position=posref2position(pos,ref,adc_k)
  position=adc_k*double(pos)./double(ref);
```

```

%quintic_traj.m
%Ugly code to generate a nice smooth test function
function traj=quintic_traj(len)
P=[
5   1  -1  1  -1  1  -1  1  -1;
   1  1  1  1  1  1  1  1  1;
   0  1  -2  3  -4  5  -6  7;
   0  1  2  3  4  5  6  7;
  10  0  0  2  -6  12  -20  30  -42;
   0  0  2  6  12  20  30  42;
   0  0  0  12  72  240  600  1260;
   0  0  0  12  -72  240  -600  1260;
   ]; %contains the coefficients of a_n*x^n+...+a_0*x and its derivatives

15 b=zeros(size(P,1),1);
   b(end)=1;
   b(end-1)=1;
   a=flipdim(P\b,1);
   x=linspace(-1,1,len);
20 traj=polyval(a,x);
   traj=traj./max(abs(traj));
   %plot(traj);

```

```
3 %readPackets.m
  %Reads the data currently in the input buffer
  %
  %device is the serial device to read from
  %
  %data is the data found in the read buffer
8
function data=readPackets(device)

bytes=device.BytesAvailable;
data=fread(device,bytes,'uint8');
```

```
%sendPackets.m
%Sends packets to the instrument. Packets are to be assumed sorted as an
3 %nx32 array with n packets to write.
%device: The serial device to output to
%
%packets: The packets to send
8 function sendPackets(device, data)
    fwrite(device,uint32(data),'uint32','sync');
end
```

```
%setpt2code.m
%converts desired setpoint [nm] to DAC codeword

function code=setpt2code(setpt,dac_k)
5 code=round(setpt*dac_k);
```

GNU FREE DOCUMENTATION LICENSE

GNU FREE DOCUMENTATION LICENSE

Version 1.3.3, November 2008

Copyright © 2000,2001,2002,2007,2008 Free Software Foundation, Inc.

<<http://fsf.org>>

Everyone is permitted to copy and distribute verbatim copies of this license document, but changing it is not allowed.

D.1 PREAMBLE

The purpose of this License is to make a manual, textbook, or other functional and useful document “free” in the sense of freedom: to assure everyone the effective freedom to copy and redistribute it, with or without modifying it, either commercially or noncommercially. Secondly, this License preserves for the author and publisher a way to get credit for their work, while not being considered responsible for modifications made by others.

This License is a kind of “copyleft”, which means that derivative works of the document must themselves be free in the same sense. It complements the GNU General Public License, which is a copyleft license designed for free software.

We have designed this License in order to use it for manuals for free software, because free software needs free documentation: a free program should come with manuals providing the same freedoms that the software does. But this License is not limited to software manuals; it can be used for any textual work, regardless of subject matter or whether it is published as a printed book. We recommend this License principally for works whose purpose is instruction or reference.

D.2 APPLICABILITY AND DEFINITIONS

This License applies to any manual or other work, in any medium, that contains a notice placed by the copyright holder saying it can be distributed under the terms of this License. Such a notice grants a world-wide, royalty-free license, unlimited in duration, to use that work under the conditions stated herein. The “Document”, below, refers to any such manual or work. Any member of the public is a licensee, and is addressed as “you”. You accept the license if you copy,

modify or distribute the work in a way requiring permission under copyright law.

A “Modified Version” of the Document means any work containing the Document or a portion of it, either copied verbatim, or with modifications and/or translated into another language.

A “Secondary Section” is a named appendix or a front-matter section of the Document that deals exclusively with the relationship of the publishers or authors of the Document to the Document’s overall subject (or to related matters) and contains nothing that could fall directly within that overall subject. (Thus, if the Document is in part a textbook of mathematics, a Secondary Section may not explain any mathematics.) The relationship could be a matter of historical connection with the subject or with related matters, or of legal, commercial, philosophical, ethical or political position regarding them.

The “Invariant Sections” are certain Secondary Sections whose titles are designated, as being those of Invariant Sections, in the notice that says that the Document is released under this License. If a section does not fit the above definition of Secondary then it is not allowed to be designated as Invariant. The Document may contain zero Invariant Sections. If the Document does not identify any Invariant Sections then there are none.

The “Cover Texts” are certain short passages of text that are listed, as Front-Cover Texts or Back-Cover Texts, in the notice that says that the Document is released under this License. A Front-Cover Text may be at most 5 words, and a Back-Cover Text may be at most 25 words.

A “Transparent” copy of the Document means a machine-readable copy, represented in a format whose specification is available to the general public, that is suitable for revising the document straightforwardly with generic text editors or (for images composed of pixels) generic paint programs or (for drawings) some widely available drawing editor, and that is suitable for input to text formatters or for automatic translation to a variety of formats suitable for input to text formatters. A copy made in an otherwise Transparent file format whose markup, or absence of markup, has been arranged to thwart or discourage subsequent modification by readers is not Transparent. An image format is not Transparent if used for any substantial amount of text. A copy that is not “Transparent” is called “Opaque”.

Examples of suitable formats for Transparent copies include plain ASCII without markup, Texinfo input format, \LaTeX input format, SGML or XML using a publicly available DTD, and standard-conforming simple HTML, PostScript or PDF designed for human modification. Examples of transparent image formats include PNG, XCF and JPG. Opaque formats include proprietary formats that can be read and edited only by proprietary word processors, SGML or XML for which the DTD and/or processing tools are not generally available, and the

machine-generated HTML, PostScript or PDF produced by some word processors for output purposes only.

The “Title Page” means, for a printed book, the title page itself, plus such following pages as are needed to hold, legibly, the material this License requires to appear in the title page. For works in formats which do not have any title page as such, “Title Page” means the text near the most prominent appearance of the work’s title, preceding the beginning of the body of the text.

The “publisher” means any person or entity that distributes copies of the Document to the public.

A section “Entitled XYZ” means a named subunit of the Document whose title either is precisely XYZ or contains XYZ in parentheses following text that translates XYZ in another language. (Here XYZ stands for a specific section name mentioned below, such as “Acknowledgements”, “Dedications”, “Endorsements”, or “History”.) To “Preserve the Title” of such a section when you modify the Document means that it remains a section “Entitled XYZ” according to this definition.

The Document may include Warranty Disclaimers next to the notice which states that this License applies to the Document. These Warranty Disclaimers are considered to be included by reference in this License, but only as regards disclaiming warranties: any other implication that these Warranty Disclaimers may have is void and has no effect on the meaning of this License.

D.3 VERBATIM COPYING

You may copy and distribute the Document in any medium, either commercially or noncommercially, provided that this License, the copyright notices, and the license notice saying this License applies to the Document are reproduced in all copies, and that you add no other conditions whatsoever to those of this License. You may not use technical measures to obstruct or control the reading or further copying of the copies you make or distribute. However, you may accept compensation in exchange for copies. If you distribute a large enough number of copies you must also follow the conditions in section [D.4](#).

You may also lend copies, under the same conditions stated above, and you may publicly display copies.

D.4 COPYING IN QUANTITY

If you publish printed copies (or copies in media that commonly have printed covers) of the Document, numbering more than 100, and the Document’s license notice requires Cover Texts, you must enclose the copies in covers that carry, clearly and legibly, all these Cover Texts: Front-Cover Texts on the front cover, and Back-Cover Texts on the back

cover. Both covers must also clearly and legibly identify you as the publisher of these copies. The front cover must present the full title with all words of the title equally prominent and visible. You may add other material on the covers in addition. Copying with changes limited to the covers, as long as they preserve the title of the Document and satisfy these conditions, can be treated as verbatim copying in other respects.

If the required texts for either cover are too voluminous to fit legibly, you should put the first ones listed (as many as fit reasonably) on the actual cover, and continue the rest onto adjacent pages.

If you publish or distribute Opaque copies of the Document numbering more than 100, you must either include a machine-readable Transparent copy along with each Opaque copy, or state in or with each Opaque copy a computer-network location from which the general network-using public has access to download using public-standard network protocols a complete Transparent copy of the Document, free of added material. If you use the latter option, you must take reasonably prudent steps, when you begin distribution of Opaque copies in quantity, to ensure that this Transparent copy will remain thus accessible at the stated location until at least one year after the last time you distribute an Opaque copy (directly or through your agents or retailers) of that edition to the public.

It is requested, but not required, that you contact the authors of the Document well before redistributing any large number of copies, to give them a chance to provide you with an updated version of the Document.

D.5 MODIFICATIONS

You may copy and distribute a Modified Version of the Document under the conditions of sections [D.3](#) and [D.4](#) above, provided that you release the Modified Version under precisely this License, with the Modified Version filling the role of the Document, thus licensing distribution and modification of the Modified Version to whoever possesses a copy of it. In addition, you must do these things in the Modified Version:

1. Use in the Title Page (and on the covers, if any) a title distinct from that of the Document, and from those of previous versions (which should, if there were any, be listed in the History section of the Document). You may use the same title as a previous version if the original publisher of that version gives permission.
2. List on the Title Page, as authors, one or more persons or entities responsible for authorship of the modifications in the Modified Version, together with at least five of the principal authors of the

Document (all of its principal authors, if it has fewer than five), unless they release you from this requirement.

3. State on the Title page the name of the publisher of the Modified Version, as the publisher.
4. Preserve all the copyright notices of the Document.
5. Add an appropriate copyright notice for your modifications adjacent to the other copyright notices.
6. Include, immediately after the copyright notices, a license notice giving the public permission to use the Modified Version under the terms of this License, in the form shown in the Addendum below.
7. Preserve in that license notice the full lists of Invariant Sections and required Cover Texts given in the Document's license notice.
8. Include an unaltered copy of this License.
9. Preserve the section Entitled "History", Preserve its Title, and add to it an item stating at least the title, year, new authors, and publisher of the Modified Version as given on the Title Page. If there is no section Entitled "History" in the Document, create one stating the title, year, authors, and publisher of the Document as given on its Title Page, then add an item describing the Modified Version as stated in the previous sentence.
10. Preserve the network location, if any, given in the Document for public access to a Transparent copy of the Document, and likewise the network locations given in the Document for previous versions it was based on. These may be placed in the "History" section. You may omit a network location for a work that was published at least four years before the Document itself, or if the original publisher of the version it refers to gives permission.
11. For any section Entitled "Acknowledgements" or "Dedications", Preserve the Title of the section, and preserve in the section all the substance and tone of each of the contributor acknowledgements and/or dedications given therein.
12. Preserve all the Invariant Sections of the Document, unaltered in their text and in their titles. Section numbers or the equivalent are not considered part of the section titles.
13. Delete any section Entitled "Endorsements". Such a section may not be included in the Modified Version.
14. Do not retitle any existing section to be Entitled "Endorsements" or to conflict in title with any Invariant Section.

15. Preserve any Warranty Disclaimers.

If the Modified Version includes new front-matter sections or appendices that qualify as Secondary Sections and contain no material copied from the Document, you may at your option designate some or all of these sections as invariant. To do this, add their titles to the list of Invariant Sections in the Modified Version's license notice. These titles must be distinct from any other section titles.

You may add a section Entitled "Endorsements", provided it contains nothing but endorsements of your Modified Version by various parties—for example, statements of peer review or that the text has been approved by an organization as the authoritative definition of a standard.

You may add a passage of up to five words as a Front-Cover Text, and a passage of up to 25 words as a Back-Cover Text, to the end of the list of Cover Texts in the Modified Version. Only one passage of Front-Cover Text and one of Back-Cover Text may be added by (or through arrangements made by) any one entity. If the Document already includes a cover text for the same cover, previously added by you or by arrangement made by the same entity you are acting on behalf of, you may not add another; but you may replace the old one, on explicit permission from the previous publisher that added the old one.

The author(s) and publisher(s) of the Document do not by this License give permission to use their names for publicity for or to assert or imply endorsement of any Modified Version.

D.6 COMBINING DOCUMENTS

You may combine the Document with other documents released under this License, under the terms defined in section [D.5](#) above for modified versions, provided that you include in the combination all of the Invariant Sections of all of the original documents, unmodified, and list them all as Invariant Sections of your combined work in its license notice, and that you preserve all their Warranty Disclaimers.

The combined work need only contain one copy of this License, and multiple identical Invariant Sections may be replaced with a single copy. If there are multiple Invariant Sections with the same name but different contents, make the title of each such section unique by adding at the end of it, in parentheses, the name of the original author or publisher of that section if known, or else a unique number. Make the same adjustment to the section titles in the list of Invariant Sections in the license notice of the combined work.

In the combination, you must combine any sections Entitled "History" in the various original documents, forming one section Entitled "History"; likewise combine any sections Entitled "Acknowledge-

ments”, and any sections Entitled “Dedications”. You must delete all sections Entitled “Endorsements”.

D.7 COLLECTIONS OF DOCUMENTS

You may make a collection consisting of the Document and other documents released under this License, and replace the individual copies of this License in the various documents with a single copy that is included in the collection, provided that you follow the rules of this License for verbatim copying of each of the documents in all other respects.

You may extract a single document from such a collection, and distribute it individually under this License, provided you insert a copy of this License into the extracted document, and follow this License in all other respects regarding verbatim copying of that document.

D.8 AGGREGATION WITH INDEPENDENT WORKS

A compilation of the Document or its derivatives with other separate and independent documents or works, in or on a volume of a storage or distribution medium, is called an “aggregate” if the copyright resulting from the compilation is not used to limit the legal rights of the compilation’s users beyond what the individual works permit. When the Document is included in an aggregate, this License does not apply to the other works in the aggregate which are not themselves derivative works of the Document.

If the Cover Text requirement of section [D.4](#) is applicable to these copies of the Document, then if the Document is less than one half of the entire aggregate, the Document’s Cover Texts may be placed on covers that bracket the Document within the aggregate, or the electronic equivalent of covers if the Document is in electronic form. Otherwise they must appear on printed covers that bracket the whole aggregate.

D.9 TRANSLATION

Translation is considered a kind of modification, so you may distribute translations of the Document under the terms of section [D.5](#). Replacing Invariant Sections with translations requires special permission from their copyright holders, but you may include translations of some or all Invariant Sections in addition to the original versions of these Invariant Sections. You may include a translation of this License, and all the license notices in the Document, and any Warranty Disclaimers, provided that you also include the original English version of this License and the original versions of those notices and disclaimers. In case of a disagreement between the translation and the original

version of this License or a notice or disclaimer, the original version will prevail.

If a section in the Document is Entitled “Acknowledgements”, “Dedications”, or “History”, the requirement (section D.5) to Preserve its Title (section D.2) will typically require changing the actual title.

D.10 TERMINATION

You may not copy, modify, sublicense, or distribute the Document except as expressly provided under this License. Any attempt otherwise to copy, modify, sublicense, or distribute it is void, and will automatically terminate your rights under this License.

However, if you cease all violation of this License, then your license from a particular copyright holder is reinstated (a) provisionally, unless and until the copyright holder explicitly and finally terminates your license, and (b) permanently, if the copyright holder fails to notify you of the violation by some reasonable means prior to 60 days after the cessation.

Moreover, your license from a particular copyright holder is reinstated permanently if the copyright holder notifies you of the violation by some reasonable means, this is the first time you have received notice of violation of this License (for any work) from that copyright holder, and you cure the violation prior to 30 days after your receipt of the notice.

Termination of your rights under this section does not terminate the licenses of parties who have received copies or rights from you under this License. If your rights have been terminated and not permanently reinstated, receipt of a copy of some or all of the same material does not give you any rights to use it.

D.11 FUTURE REVISIONS OF THIS LICENSE

The Free Software Foundation may publish new, revised versions of the GNU Free Documentation License from time to time. Such new versions will be similar in spirit to the present version, but may differ in detail to address new problems or concerns. See <http://www.gnu.org/copyleft/>.

Each version of the License is given a distinguishing version number. If the Document specifies that a particular numbered version of this License “or any later version” applies to it, you have the option of following the terms and conditions either of that specified version or of any later version that has been published (not as a draft) by the Free Software Foundation. If the Document does not specify a version number of this License, you may choose any version ever published (not as a draft) by the Free Software Foundation. If the Document specifies that a proxy can decide which future versions of this License

can be used, that proxy's public statement of acceptance of a version permanently authorizes you to choose that version for the Document.

D.12 RELICENSING

"Massive Multiauthor Collaboration Site" (or "MMC Site") means any World Wide Web server that publishes copyrightable works and also provides prominent facilities for anybody to edit those works. A public wiki that anybody can edit is an example of such a server. A "Massive Multiauthor Collaboration" (or "MMC") contained in the site means any set of copyrightable works thus published on the MMC site.

"CC-BY-SA" means the Creative Commons Attribution-Share Alike 3.0 license published by Creative Commons Corporation, a not-for-profit corporation with a principal place of business in San Francisco, California, as well as future copyleft versions of that license published by that same organization.

"Incorporate" means to publish or republish a Document, in whole or in part, as part of another Document.

An MMC is "eligible for relicensing" if it is licensed under this License, and if all works that were first published under this License somewhere other than this MMC, and subsequently incorporated in whole or in part into the MMC, (1) had no cover texts or invariant sections, and (2) were thus incorporated prior to November 1, 2008.

The operator of an MMC Site may republish an MMC contained in the site under CC-BY-SA on the same site at any time before August 1, 2009, provided the MMC is eligible for relicensing.

D.13 ADDENDUM: HOW TO USE THIS LICENSE FOR YOUR DOCUMENTS

To use this License in a document you have written, include a copy of the License in the document and put the following copyright and license notices just after the title page:

Copyright © YEAR YOUR NAME. Permission is granted to copy, distribute and/or modify this document under the terms of the GNU Free Documentation License, Version 1.2 or any later version published by the Free Software Foundation; with no Invariant Sections, no Front-Cover Texts, and no Back-Cover Texts. A copy of the license is included in the section entitled "GNU Free Documentation License".

If you have Invariant Sections, Front-Cover Texts and Back-Cover Texts, replace the "with...Texts." line with this:

with the Invariant Sections being LIST THEIR TITLES, with the Front-Cover Texts being LIST, and with the Back-Cover Texts being LIST.

If you have Invariant Sections without Cover Texts, or some other combination of the three, merge those two alternatives to suit the situation.

If your document contains nontrivial examples of program code, we recommend releasing these examples in parallel under your choice of free software license, such as the GNU General Public License, to permit their use in free software.

